1993

Computer simulation of air to water reversed heat engines.

Joseph R. Emersberger
University of Windsor

National Library of Canada
Acquisitions and Bibliographic Services Branch
395 Wellington Street
Ottawa, Ontario
K1A 0N4

Bibliothèque nationale du Canada
Direction des acquisitions et des services bibliographiques
395, rue Wellington
Ottawa (Ontario)
K1A 0N4

Your file Votre référence

Our file Notre référence

NOTICE

The quality of this microform is heavily dependent upon the quality of the original thesis submitted for microfilming. Every effort has been made to ensure the highest quality of reproduction possible.

If pages are missing, contact the university which granted the degree.

Some pages may have indistinct print especially if the original pages were typed with a poor typewriter ribbon or if the university sent us an inferior photocopy.

Reproduction in full or in part of this microform is governed by the Canadian Copyright Act, R.S.C. 1970, c. C-30, and subsequent amendments.

AVIS

La qualité de cette microforme dépend grandement de la qualité de la thèse soumise au microfilmage. Nous avons tout fait pour assurer une qualité supérieure de reproduction.

S'il manque des pages, veuillez communiquer avec l'université qui a conféré le grade.

La qualité d'impression de certaines pages peut laisser à désirer, surtout si les pages originales ont été dactylographiées à l'aide d'un ruban usé ou si l'université nous a fait parvenir une photocopie de qualité inférieure.

La reproduction, même partielle, de cette microforme est soumise à la Loi canadienne sur le droit d'auteur, SRC 1970, c. C-30, et ses amendements subséquents.

Canada

COMPUTER SIMULATION OF AIR TO WATER REVERSED HEAT ENGINES

by

Joseph R. Emersberger

A thesis

Submitted to the Faculty of Graduate Studies through the

Department of Mechanical Engineering in Partial Fulfilment

of the Requirements for the Degree of

Master of Applied Science at the

University of Windsor

Windsor, Ontario, CANADA

1992

ISBN 0-315-83049-2

Name _____

Dissertation Abstracts International is arranged by broad, general subject categories. Please select the one subject which most nearly describes the content of your dissertation. Enter the corresponding four-digit code in the spaces provided.

SUBJECT TERM

SUBJECT CODE 0348

U·M·I

Subject Categories

THE HUMANITIES AND SOCIAL SCIENCES

COMMUNICATIONS AND THE ARTS
Architecture 0729
Art History 0377
Cinema 0900
Dance 0378
Fine Arts 0357
Information Science 0723
Journalism 0391
Library Science 0399
Mass Communications 0708
Music 0413
Speech Communication 0459
Theater 0465

EDUCATION
General 0515
Administration 0514
Adult and Continuing 0516
Agricultural 0517
Art 0273
Bilingual and Multicultural 0282
Business 0688
Community College 0275
Curriculum and Instruction 0727
Early Childhood 0518
Elementary 0524
Finance 0277
Guidance and Counseling 0519
Health 0680
Higher 0745
History of 0520
Home Economics 0278
Industrial 0521
Language and Literature 0279
Mathematics 0280
Music 0522
Philosophy of 0998
Physical 0523
Psychology 0525
Reading 0535
Religious 0527
Sciences 0714
Secondary 0533
Social Sciences 0534
Sociology of 0340
Special 0529
Teacher Training 0530
Technology 0710
Tests and Measurements 0288
Vocational 0747

LANGUAGE, LITERATURE AND LINGUISTICS
Language
- General 0679
- Ancient 0289
- Linguistics 0290
- Modern 0291

Literature
- General 0401
- Classical 0294
- Comparative 0295
- Medieval 0297
- Modern 0298
- African 0316
- American 0591
- Asian 0305
- Canadian (English) 0352
- Canadian (French) 0355
- English 0593
- Germanic 0311
- Latin American 0312
- Middle Eastern 0315
- Romance 0313
- Slavic and East European 0314

PHILOSOPHY, RELIGION AND THEOLOGY
Philosophy 0422
Religion
- General 0318
- Biblical Studies 0321
- Clergy 0319
- History of 0320
- Philosophy of 0322

Theology 0469

SOCIAL SCIENCES
American Studies 0323
Anthropology
- Archaeology 0324
- Cultural 0326
- Physical 0327

Business Administration
- General 0310
- Accounting 0272
- Banking 0770
- Management 0454
- Marketing 0338

Canadian Studies 0385
Economics
- General 0501
- Agricultural 0503
- Commerce-Business 0505
- Finance 0508
- History 0509
- Labor 0510
- Theory 0511

Folklore 0358
Geography 0366
Gerontology 0351
History
- General 0578
- Ancient 0579
- Medieval 0581
- Modern 0582
- Black 0328
- African 0331
- Asia, Australia and Oceania 0332
- Canadian 0334
- European 0335
- Latin American 0336
- Middle Eastern 0333
- United States 0337

History of Science 0585
Law 0398
Political Science
- General 0615
- International Law and Relations 0616
- Public Administration 0617

Recreation 0814
Social Work 0452
Sociology
- General 0626
- Criminology and Penology 0627
- Demography 0938
- Ethnic and Racial Studies 0631
- Individual and Family Studies 0628
- Industrial and Labor Relations 0629
- Public and Social Welfare 0630
- Social Structure and Development 0700
- Theory and Methods 0344

Transportation 0709
Urban and Regional Planning 0999
Women's Studies 0453

THE SCIENCES AND ENGINEERING

BIOLOGICAL SCIENCES
Agriculture
- General 0473
- Agronomy 0285
- Animal Culture and Nutrition 0475
- Animal Pathology 0476
- Food Science and Technology 0359
- Forestry and Wildlife 0478
- Plant Culture 0479
- Plant Pathology 0480
- Plant Physiology 0817
- Range Management 0777
- Wood Technology 0746

Biology
- General 0306
- Anatomy 0287
- Biostatistics 0308
- Botany 0309
- Cell 0379
- Ecology 0329
- Entomology 0353
- Genetics 0369
- Limnology 0793
- Microbiology 0410
- Molecular 0307
- Neuroscience 0317
- Oceanography 0416
- Physiology 0433
- Radiation 0821
- Veterinary Science 0778
- Zoology 0472

Biophysics
- General 0786
- Medical 0760

EARTH SCIENCES
Biogeochemistry 0425
Geochemistry 0996
Geodesy 0370
Geology 0372
Geophysics 0373
Hydrology 0388
Mineralogy 0411
Paleobotany 0345
Paleoecology 0426
Paleontology 0418
Paleozoology 0985
Palynology 0427
Physical Geography 0368
Physical Oceanography 0415

HEALTH AND ENVIRONMENTAL SCIENCES
Environmental Sciences 0768
Health Sciences
- General 0566
- Audiology 0300
- Chemotherapy 0992
- Dentistry 0567
- Education 0350
- Hospital Management 0769
- Human Development 0758
- Immunology 0982
- Medicine and Surgery 0564
- Mental Health 0347
- Nursing 0569
- Nutrition 0570
- Obstetrics and Gynecology 0380
- Occupational Health and Therapy 0354
- Ophthalmology 0381
- Pathology 0571
- Pharmacology 0419
- Pharmacy 0572
- Physical Therapy 0382
- Public Health 0573
- Radiology 0574
- Recreation 0575
- Speech Pathology 0460
- Toxicology 0383

Home Economics 0386

PHYSICAL SCIENCES
Pure Sciences
Chemistry
- General 0485
- Agricultural 0749
- Analytical 0486
- Biochemistry 0487
- Inorganic 0488
- Nuclear 0738
- Organic 0490
- Pharmaceutical 0491
- Physical 0494
- Polymer 0495
- Radiation 0754

Mathematics 0405
Physics
- General 0605
- Acoustics 0986
- Astronomy and Astrophysics 0606
- Atmospheric Science 0608
- Atomic 0748
- Electronics and Electricity 0607
- Elementary Particles and High Energy 0798
- Fluid and Plasma 0759
- Molecular 0609
- Nuclear 0610
- Optics 0752
- Radiation 0756
- Solid State 0611

Statistics 0463

Applied Sciences
Applied Mechanics 0346
Computer Science 0984
Engineering
- General 0537
- Aerospace 0538
- Agricultural 0539
- Automotive 0540
- Biomedical 0541
- Chemical 0542
- Civil 0543
- Electronics and Electrical 0544
- Heat and Thermodynamics 0348
- Hydraulic 0545
- Industrial 0546
- Marine 0547
- Materials Science 0794
- Mechanical 0548
- Metallurgy 0743
- Mining 0551
- Nuclear 0552
- Packaging 0549
- Petroleum 0765
- Sanitary and Municipal 0554
- System Science 0790

Geotechnology 0428
Operations Research 0796
Plastics Technology 0795
Textile Technology 0994

PSYCHOLOGY
General 0621
Behavioral 0384
Clinical 0622
Developmental 0620
Experimental 0623
Industrial 0624
Personality 0625
Physiological 0989
Psychobiology 0349
Psychometrics 0632
Social 0451

ABSTRACT

In order to investigate the use of air-to-water vapour compression reversed heat engines for heating domestic hot water supplies, a user friendly computer program was developed to simulate such systems operating under steady state conditions. An experimental study was also carried out so that simulation results could be compared to actual data. The comparison revealed that the program accurately predicts trends in system performance.

The program simulates systems that consist of a compact heat exchanger evaporator, a reciprocating compressor, a throttle valve, and a condenser that may be either a coil immersed in a water tank or a concentric tube heat exchanger. The user may optionally specify a regenerator and must specify either R-12 or R-22 as the refrigerant. The user must also specify

1) the inlet air temperature, relative humidity and face velocity and the water temperature (and mass flow rate for concentric tube heat exchangers),
2) the compressor outlet to inlet pressure ratio,
3) performance data for the compressor,
4) physical dimensions and thermal conductance of the evaporator,
5) physical dimensions of the condenser
6) whether the system has a receiver at the condenser outlet or an accumulator at the evaporator outlet
7) whether or not to consider frictional pressure drop and

secondary heat transfer in the interconnecting piping (in order to speed up simulation during preliminary studies).

The program determined the condenser capacity, evaporator capacity, power input to the compressor, and coefficient of performance all within 10 percent of experimental data. The predictions of the compressor inlet and outlet pressures differed by less than 5 percent from the experimental data (usually less than 2 percent). The program successfully predicted system performance trends when the compressor crank shaft speed, throttle valve setting, condenser cooling water temperature, and cooling water mass flow rate were independently varied.

The program achieves convergence within 100 seconds on an IBM 386SX/25 PC with a math coprocessor.

An improvement to the program would be the addition of property subroutines which would provide the capability to simulate systems that operate with the proposed alternative to R-12.

ACKNOWLEDGMENTS

Without the assistance of Dr. T.W. McDonald this project would never have been completed. I am especially grateful to him for his willingness to make available to me his considerable insight into both the practical and theoretical aspects of this project.

The author is also indebted to W. Beck, R. Tattersall, and Marko Jovanovic for the substantial assistance they provided with the experimental work.

My fellow graduate student, Ignacio Martin Dominguez, was generous in providing technical advice as well as friendship. I am grateful to him for both.

I also acknowledge the Natural Sciences and Engineering Research Council of Canada for the financial assistance provided through Grant 877.

My final expression of gratitude is made to my parents for the patience they displayed while this project was being completed.

to my parents, my brother, and Mónica

TABLE OF CONTENTS

LIST OF FIGURES

LIST OF TABLES

NOMENCLATURE

A	Area (m^2/s)
A1	Constant in equation (50)
A2	Constant in equation (50)
A3	Constant in equation (50)
A4	Constant in equation (50)
A5	Constant in equation (50)
AIRcp	Specific heat capacity of air (kJ/(kg K))
AIRmdot	Mass flow rate of air (kg/s)
B	Minor axis of horizontal elliptical tube (m)
C	Major axis of horizontal elliptical tube (m)
C1	A function of C/B
C2	A function of C/B
CF	Clearance Fraction
Check_Q_HTnew	Difference between Q_HTtot
$\overline{C}_L$	Function of Pr required in natural convection heat transfer correlation for elliptical tubes
CnD.check_Q	Difference between CnD.Q_HTtot and CnD.Q_thermo as a percentage of CnD.Q_thermo
CnD.Q_HTtot	Heat transferred in condenser as determined from heat transfer correlations (kW)
CnD.Q_thermo	Heat transferred in condenser as determined from first law of thermodynamics (kW)
Cp	Specific Heat Capacity (kJ/(kg K))
$\overline{C}_t$	Function of Pr and C/B required in the natural convection heat transfer correlation for elliptical tubes

Cv	Specific heat at constant volume (kJ/kg)
D	Diameter (m)
D1,D3	Inner Diameters of tubing (m)
D2	Outer Diameter of tubing (m)
Dins	Combined diameter of tubing and insulation (m)
Ecomp	Total energy inputed to refrigerant in compressor (kW)
Eff	Effectiveness of liquid portion of concentric tube condenser
EFF_allwet	Effectiveness of entire evaporator when refrigerant exits as saturated vapour
EFFreg	Effectiveness of regenerator
error	Difference between CnD.Q_HTtot and CnD.Q_thermo or between EvP.Q_HTtot and EvP.Q_thermo (kW).
error_n	Value of error corresponding to t3_n or t5_n (kW)
error_p	Value of error corresponding to t3_p or t5_p (kW)
error_Twallx	Difference between twallx and tsat2 (K)
error_Twallx_n	Value of error_Twallx corresponding to tx_n
error_Twallx_p	Value of error_Twallx corresponding to tx_p
EvP.Q_HTtot	Heat transferred in evaporator as determined from heat transfer correlations (kW)
EvP.Q_thermo	Heat transferred in evaporator as determined from first law of thermodynamics (kW)
f	Friction factor
fsmooth	Friction factor for smooth wall
g	Gravitational acceleration (m/s^2)
h	Enthalpy (kJ/kg)

h1	Refrigerant enthalpy at regenerator outlet (kJ/kg)
h1′	Refrigerant enthalpy at compressor inlet (kJ/kg)
h2	Refrigerant enthalpy at compressor outlet (kJ/kg)
h2′	Refrigerant enthalpy at condenser inlet (kJ/kg)
h3	Refrigerant enthalpy at condenser outlet (kJ/kg)
h3′	Refrigerant enthalpy at regenerator high pressure inlet (kJ/kg)
h4	Refrigerant enthalpy at regenerator high pressure outlet (kJ/kg)
h4′	Refrigerant enthalpy at throttle valve inlet (kJ/kg)
h5	Refrigerant enthalpy at throttle valve outlet (kJ/kg)
h5′	Refrigerant enthalpy at evaporator inlet (kJ/kg)
h6	Refrigerant enthalpy at evaporator outlet (kJ/kg)
h6′	Refrigerant enthalpy at regenerator low pressure inlet (kJ/kg)
H2Ocpf	Specific heat capacity of water (kJ/(kg K))
H2Omdot	Water mass flow rate (kg/s)
hf_cond	Enthalpy of refrigerant liquid at condenser outlet pressure (kJ/kg)
hfg	Latent heat of vaporization (kJ/kg)
$\bar{h}$	Heat transfer coefficient ($kW/(m^2 K)$)
$\bar{h}_z$	Local heat transfer coefficient ($kW/(m^2 K)$)

isen_ratio	Ratio of enthalpy rise in compressor during an isentropic process to the actual enthalpy rise
k	Thermal conductivity (kW/(m K))
L	Tube length (m)
Lcond	Total length of condenser tubing (m)
Lcond_dry	Length of dry portion of condenser (m)
Lcond_liq	Length of liquid portion of condenser (m)
Lcond_wet	Length of wet portion of condenser (m)
Levap	Total length of evaporator tubing (m)
LMTD	Log mean temperature difference (K)
LMTD_dry	Log mean temperature difference for dry portion of condenser (K)
LMTD_e	Log mean temperature difference for wet portion of evaporator (K)
LMTD_liq	Log mean temperature difference for liquid portion of condenser (K)
LMTD_wet	Log mean temperature difference for wet portion of condenser
MCp_max	Minimum heat capacity (kW/K)
MCp_min	Maximum heat capacity (kW/K)
NTU	Number of transfer units
Nu	Nusselt number ($\bar{h}D/k$)
N_u^T	Thin layer Nusselt number for laminar natural convection
N_{u_t}	Thick layer Nusselt number for laminar natural convection

N_{u_t}	Nusselt number for turbulent natural convection
n	Polytropic index
ovrl_ratio	Ratio of Wcomp_mec to Ecomp
p	Pressure (MPa)
p1	Refrigerant pressure at regenerator outlet (MPa)
p1'	Refrigerant pressure at compressor inlet (MPa)
p2	Refrigerant pressure at compressor outlet (MPa)
p2'	Refrigerant pressure at condenser inlet (MPa)
p3	Refrigerant pressure at condenser outlet (MPa)
p3'	Refrigerant pressure at regenerator high pressure inlet (MPa)
p4	Refrigerant pressure at regenerator high pressure outlet (MPa)
p4'	Refrigerant pressure at throttle valve inlet (MPa)
p5	Refrigerant pressure at throttle valve outlet (MPa)
p5'	Refrigerant pressure at evaporator inlet (MPa)
p6	Refrigerant pressure at evaporator outlet (MPa)
p6'	Refrigerant pressure at regenerator low pressure inlet (MPa)
Pr	Prandtl number
PRATIO	Compressor outlet to inlet pressure ratio
Qac	Heat lost by air in process a to c of figure 69

Qevap_a	Heat transfered in evaporator calculated through energy balance on air (KW)
Qevap_r	Heat transfer in evaporator calculated through an energy balance on the refrigerant (kW)
Qevap_wet	Heat transfered in portion of evaporator containing wet mixture (kW)
Q_HTdry	Heat transferred in dry portion of condenser or evaporator as calculated by heat transfer correlations (kW)
Q_HTliq	Heat transferred in liquid portion of condenser as calculated by heat transfer correlations (kW)
Q_HTtot	Total heat transferred in either condenser or evaporator as calculated by heat transfer correlations (kW)
Q_HTwet	Heat transferred in either condenser or evaporator as calculated by heat transfer correlations (kW)
Qmax	Maximum amount of heat that can be transferred between two fluids (kW)
q_{los}	Heat loss in piping (kW)
Qreg_liq	Heat transferred to liquid side of regenerator
Qreg_vap	Heat transfered to gas portion of regenerator
R	Ideal gas constant (kJ/(kg K))
Ra	Rayleigh number
Radius_cond	Inside radius of condenser coil (m)
Radius_curv	Radius of curvature of condenser coil (m)
REFmdot	Refrigerant mass flow rate (kg/s)
REFmdot_c	Refrigerant mass flow rate obtained through energy balance on condenser (kg/s)
REFmdot_e	Refrigerant mass flow rate obtained through energy balance on evaporator (kg/s)

REFmdot_f	Refrigerant mass flow rate obtained from rotameter reading (kg/s)
Rin'	Thermal resistance due to convection on inside of tube (m K / kW)
Rout'	Thermal resistance due to convection on outside of tube (m K / kW)
Rtot'	Thermal resistance (m K/ kW)
Rwall'	Thermal resistance of tube wall (m K / kW)
s	Entropy (kJ/(kg K))
t	Temperature (K)
Tao	Evaporator outlet air temperature (K)
t1	Refrigerant temperature at regenerator low pressure outlet (K)
t1'	Refrigerant temperature at compressor inlet (K)
t2	Refrigerant temperature at compressor outlet (K)
t2'	Refrigerant temperature at condenser inlet (K)
t3	Refrigerant temperature at condenser outlet (K)
t3'	Refrigerant temperature at regenerator high pressure inlet (K)
t3_n	The most recent value of t3 that yielded a negative value for error in an iterative procedure
t3_new	New value for t3 in an iterative procedure
t3_p	The most recent value of t3 that yielded a positive value for error in an iterative procedure
t4	Refrigerant temperature at regenerator high pressure outlet (K)
t4'	Refrigerant temperature at throttle valve inlet (K)

t5	Refrigerant temperature at throttle valve outlet (K)
t5'	Refrigerant temperature at evaporator inlet (K)
t5''	Refrigerant temperature at evaporator inlet (K)
t5_n	The most recent value of t5 that yielded a negative value for error in an iterative procedure
t5_p	The most recent value of t5 that yielded a positive value for error in an iterative procedure
t6	Refrigerant temperature at evaporator outlet (K)
t6'	Refrigerant temperature at regenerator low pressure inlet (K)
T16,...T24	Evaporator outlet air grid temperatures
Ta	Temperature at point A on figure 52 (K)
Tair_i	Evaporator inlet air temperature (K)
Tb	Temperature at point B on figure 52 (K)
Te	Temperature at point E on figure 52 (K)
Td	Temperature at point D on figure 52 (K)
Tdew	Dew Point Temperature
Twb	Wet bulb temperature of evaporator outlet air (K)
tcond	Average temperature of refrigerant condensate
thick	Tube thickness
tsat2	Saturation temperature at p2 (K)
tsat3	Saturation temperature at p3 (K)
tsat6	Saturation pressure at p6 (K)
twallo	Refrigerant side wall temperature at condenser refrigerant inlet (K)

twallx	Refrigerant side wall temperature at the end of condenser dry portion (K)
twallx1	Refrigerant side wall temperature at the end of condenser wet portion (K)
twall_L	Refrigerant side wall temperature at the condenser refrigerant outlet (K)
twi	Condenser cooling water inlet temperature (K)
two	Condenser cooling water outlet temperature (K)
twx	Condenser cooling water temperature at end of condenser dry portion (K)
twx1	Condenser cooling water temperature at end of condenser wet portion (K)
tx	Refrigerant temperature at end of condenser dry portion (K)
tx_n	Most recent value of tx that yields negative value of error_Twallx in iterative procedure
tx_p	Most recent value of tx that yields positive value of error_Twallx in iterative procedure
UA	Thermal conductance in (kW/K)
UA_allwet	Thermal conductance of evaporator when the entire process the refrigerant undergoes is is in the wet region (kW/K)
UA_dry	Thermal conductance of dry portion of condenser or evaporator (kW/K)
UA_dry'	Thermal conductance per unit length of dry portion of condenser or evaporator (kW/(mK))
UA_liq	Thermal conductance of liquid portion of condenser or evaporator (kW/K)
UA_liq'	Thermal conductance per unit length of liquid portion of condenser or evaporator (kW(mK))
UA_wet	Thermal conductance of wet portion of condenser or evaporator (kW/K)
UA_wet'	Thermal conductance per unit length of wet portion of condenser or evaporator (kW/(mK))

u_ice	Specific internal energy of ice (kJ/kg)
v	Specific volume (m^3/kg)
v1	Specific volume at compressor inlet (m^3/kg)
Vel16,..Vel24	Velocity of evaporator outlet air (m/s)
volum_eff	Volumetric efficiency
Vs	Swept volume
Wcomp_mec	Mechanical work applied to compressor crank shaft (kW)
Wcomp_rev	Work done on refrigerant if process in Compressor were reversible
Wfan	Electrical power supplied to fan
Wi	Evaporator inlet air humidity ratio
Wo	Evaporator outlet air humidity ratio
x	Quality
x5	Quality at evaporator inlet
x6	Quality at evaporator outlet
X	Martinelli parameter

Greek Symbols

α	Thermal diffusivity (m^2/s)
β	Coefficient of thermal expansion (1/K)
Δ	Difference
μ	Absolute viscosity ($Pa\,s$)
θ	Temperature difference (K)

ρ	Density (kg/m^3)
ν	Kinematic viscosity (m^2/s)
τ	time (s)

Superscripts

1rst	First approximation
2nd	Second approximation
o	Ideal gas state

Subscript

air	Air
avg	Average
cond	Condenser
dry	Refers to dry portion of evaporator or condenser
evap	Evaporator
f	Liquid
g	Gas
i	Inlet
j	Term in a summation
in	Inside
ins	Insulation
liq	Refers to liquid portion of evaporator or condenser
lng	Longitudinal heat conduction
new	New value obtained in iterative procedure
o	Outlet
out	Outside

pipe	Pipe
q	Reference State
r	Reduced property
rad	Radial heat conduction
s	Insentropically reached state point
sat	Saturation
sink	Sink conditions
source	Source conditions
x	Reference State
y	Reference State
w	Water
wet	Refers to wet portion of evaporator or condenser

I. INTRODUCTION

A. Background

Reversed heat engines are used as refrigerators, air conditioners and heat pumps. A reversed heat engine, shown schematically in figure 1, is a cyclically operating thermodynamic system that makes use of mechanical work input to extract heat from a low temperature source and deliver heat to a high temperature sink.

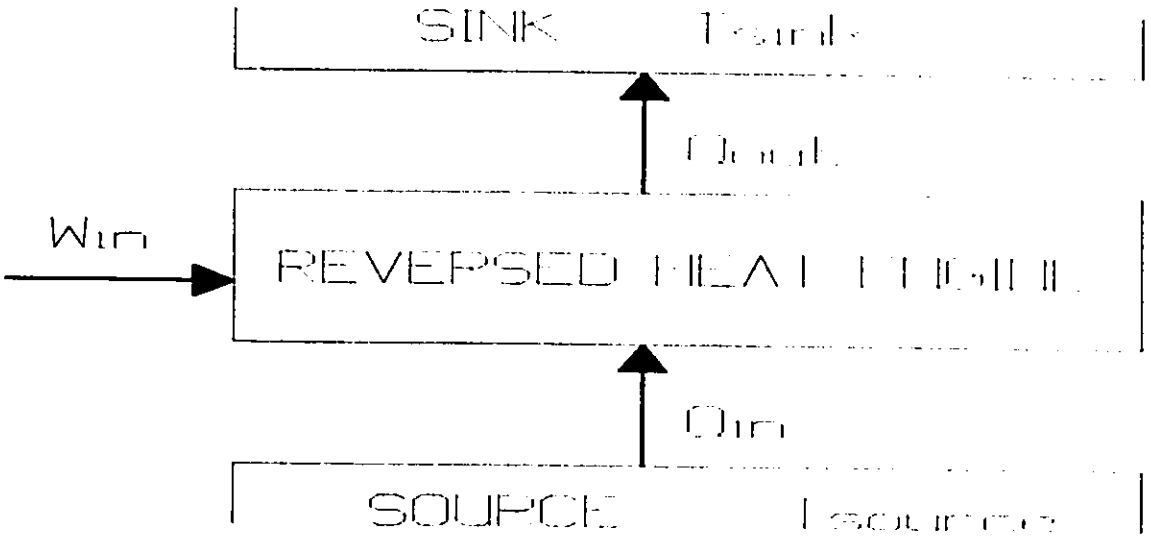

Figure 1: The Reversed Heat Engine

The three main types of reversed heat engines are the vapour compression, absorption, and thermoelectric types. In both vapour compression and absorption type systems a working fluid (the refrigerant) is made to repeatedly undergo a thermodynamic cycle which consists, essentially, of the four processes depicted in figure 2: process 4 to 1, in which the refrigerant extracts heat

from the source; process 1 to 2, in which the temperature and pressure of the refrigerant are increased; process 2 to 3 in which the refrigerant delivers heat to the sink; and process 3 to 4, in which the pressure of the refrigerant is reduced at constant enthalpy. The basic difference between vapour compression and absorption systems is in the method used to produce the temperature and pressure rise that takes place in process 1 to 2. In vapour compression systems a compressor is used to increase the temperature and pressure of refrigerant vapour. In absorption systems a second fluid (the absorbent) is made to react with the refrigerant to produce a liquid solution which is then heated so that refrigerant vapour can be separated out of the solution at an increased temperature and pressure.

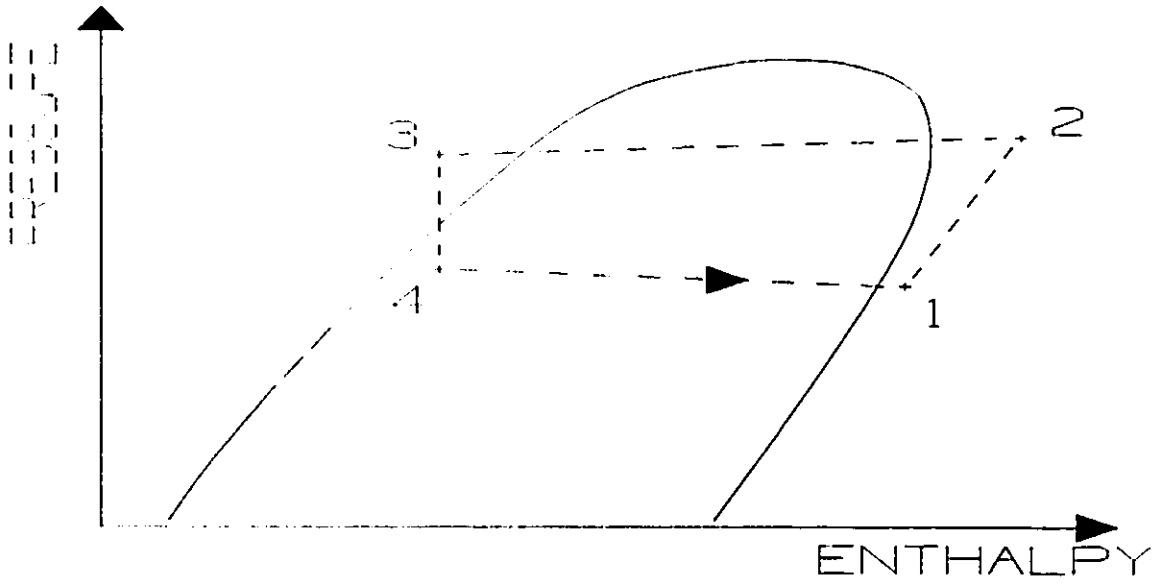

Figure 2: The Refrigeration Cycle

Reversed heat engines are also classified by the source and sink between which they operate. A reversed heat engine operating

between an air source and a water sink, for example, is referred to as an air to water reversed heat engine.

Figure 3 depicts the main components of a vapour compression reversed heat engine: an evaporator, in which heat is absorbed by the refrigerant from the source; a compressor, which circulates the refrigerant through the system; a condenser, in which refrigerant delivers heat to the sink; and a throttle valve, in which the pressure of the refrigerant is reduced in an isenthalpic process. Also shown in figure 3 is a receiver, a container for excess refrigerant; an accumulator, another container for refrigerant liquid storage; and a regenerator, a heat exchanger which helps to ensure that slightly superheated vapour enters the compressor.

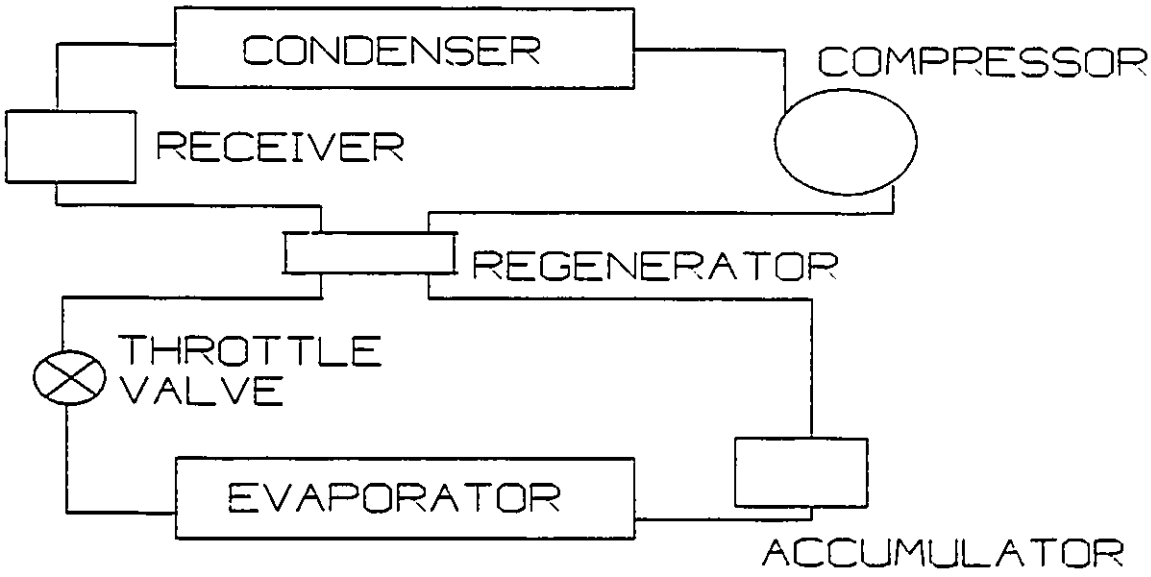

Figure 3: Components of Vapour Compression Reversed Heat Engine

B. Motivation For Carrying Out Study

Because of their excessive reliance on the burning of fossil fuels for the production of energy, the wealthy nations of the world produce the highest emissions of gases responsible for global warming. Increased awareness and concern about the potential effects of global warming have therefore focused a great deal of attention on energy conservation as a means of reducing such gas emissions. One outcome of the implementation of energy conservation measures will be that vapour compression reversed heat engines will be much more frequently used in the following ways: to heat domestic hot water by recovering heat from ventilation air, and to heat water in swimming pools while at the same time dehumidifying the air entering the pool area.

1. Heating of Domestic Hot water

As pointed out by Peterson [31], as new houses become more energy efficient a higher percentage of domestic energy consumption will be allocated to the heating of water. Additionally, as more houses of tighter construction (less air infiltration) appear on the market, the heating of water by recovering heat from ventilation air will become more economic.

2. Heating of Indoor Pool Water and Dehumidification of Air

An air to water heat pump system is among the recommendations made in a 1987 Ontario government report on energy conservation measures for indoor swimming pools and arenas [25]. To heat the water in an indoor pool, the system makes use the heat extracted from incoming air during the process of

dehumidification. Such systems conserve energy and help to prevent corrosion problems that could result from excessively high relative humidity.

3. The Need For Computer Simulation

A slight change in operating conditions (the air and water temperatures) can have a significant effect on the performance of air to water heat pumps [24,33]. To properly evaluate a design of an air to water heat pump, its performance for a broad range of operating conditions must therefore be known. Such information is more quickly and easily obtained from a computer simulation program than from experimental studies: it is easier to change the value of an input to a computer program than to alter an existing system.

C. Objectives

The objectives of the research project described in this report were to develop and verify a computer program capable of simulating air to water vapour compression reversed heat engines operating under steady state conditions. The program was to be easy to use and accurate enough to predict trends in system performance.

1. Approach Taken To Achieve Objectives

The problem of developing a program to simulate a reversed heat engine operating under steady state conditions is ultimately one of setting up and solving a system of non-linear algebraic equations which describe the reversed heat engine behaviour. The equations must be solved simultaneously and

consist of the conservation equations for mass and energy, the characteristic equations for each component, and equations which correlate refrigerant, air and water properties.

A literature survey was carried out in order to determine the equations which describe the system behaviour and the solution technique that most efficiently solves the equations.

The required property correlations were found in the literature and, in some cases, developed by curve fitting published data. Heat exchanger modelling equations, apart from those based directly on mass and energy conservation, were derived based on heat transfer correlations found in the literature. The solution technique used to solve the system of equations was unique to this work. One reason why a lot of the work done on the program was original was because only one paper was found which dealt specifically with the simulation of air to water reversed heat engines through mathematical modelling of the components [36]: most of the literature dealt with air to air systems. Another reason was that none of the programs found in the literature required compressor outlet to inlet pressure ratio as an input.

Experimental data was collected to verify that the computer program could predict trends in system performance.

II. LITERATURE SURVEY

A. Reversed Heat Engine Simulation Programs

The computer simulations developed by previous workers can be divided into two broad types: "first principle" type simulations, and "functional fit" type simulations. In functional fit type simulations, the equations used to model the components are curve fits of experimental data. In first principle simulations, the equations used to model the components are derived from the fundamental principles of thermodynamics, heat transfer, and fluid mechanics. It should be noted, however, that even the first principle type simulations require that the user provide some experimental performance data as input. Performance data is always required for the compressor since a completely theoretical simulation of the compressor that accounted for valve dynamics and heat loss would slow down the simulation of the entire system. The computer simulation program discussed in this report is a first principle type.

1. First Principle Simulations

The earliest computer simulation of a reversed heat engine that was found in the literature was the one developed by Davis et al. [10]. The program was created to simulate automotive air conditioning systems (i.e. air to air reversed heat engines). The program required the user to input the amount of evaporator superheat. The program simulated the case in which a receiver is

located at the condenser outlet forcing the refrigerant at the condenser outlet to be saturated liquid. Systems with regenerators were not simulated.

Parise [30] developed a computer simulation program for water to water reversed heat engine. The way in which he modelled the evaporator and condenser required that extensive test data be collected by the user. His program required the user to input the amount of superheat at the evaporator outlet and the amount of subcooling at the condenser outlet. Frictional pressure drops and secondary heat transfer were not taken into account. Systems with regenerators were not simulated.

Jeter et al. [19] developed a computer simulation for air to air systems. Their simulation program was developed to obtain qualitative information on the effect of variable speed compressors on the system's coefficient of performance (as a heat pump). The user was required to input the overall conductance of both the evaporator and the condenser (heat transfer correlations were not used). The throttle valve was modelled as a capillary tube for which the user must input the valve coefficient. Because the throttle valve was modelled, the amount of refrigerant superheat and subcooling at the evaporator and condenser outlets respectively were not required as inputs to the program. Frictional pressure and secondary heat transfer were not taken into account. Systems with regenerators were not simulated.

The most detailed first principle type simulations that have been developed to date were for air to air systems. They are

the HPSIM program by Domanski and Didion [11]; the Mark III program by Fischer and Rice [14,15]; and the HN program by Damasceno and Goldschmidt [8]. In all three programs the throttle valve is modelled. In a review of these three programs which was published by Damasceno an Goldschmidt [9] it was concluded that the HPSIM was the most accurate. However, Damasceno and Goldschmidt also concluded that "while the prediction of C.O.P. and Capacity might be acceptable for all programs, they all fail in adequately predicting detailed refrigerant pressure and temperature distributions". For example, a typical error in the output of HPSIM is 11 degrees Celsius for compressor discharge temperature and 4 bars for compressor discharge pressure [9]. Damasceno and Goldschmidt found that the predictions of compressor discharge temperature produced by MARK III and HN were in error by as much as 110 degrees Celsius under certain conditions. Although HPSIM was found to be the most accurate of the programs, it was also found to be the slowest: even with excellent initial guesses inputed, HPSIM it took 48.7 seconds to converge on a mainframe computer which had a floating point accelerator [9].

Since the publication of Domasceno and Goldschmidt's review, HPSIM2, an more accurate version of HPSIM, has been developed [9]. However, its accuracy is highly dependent upon the user inputting accurate estimates of all the system's internal volumes. Moreover, much of the input to the program must be entered by the user through data files, not interactively.

Tassou et al. developed a computer simulation program for air to water heat pumps [36]. The user was required to specify the amount of subcooling at the condenser outlet and the amount of superheat at the evaporator outlet. The amount of heat transferred to the water was also required as input. Frictional pressure drops were taken into account but not secondary heat transfer in the interconnecting piping. Systems with regenerators were not modelled.

2. Functional Fit Simulations

The functional fit type simulations can be divided into two types: the type developed by D'Valentine and Goldschmidt [13], McMullen et al. [24], and Rosell et al. [33] in which the experimental data must be obtained from the components when they are all interconnected; and the type developed by Hamilton and Miller [16] in which the experimental data for each component is obtained from the manufacturer of the component.

The program developed by Hamilton and Miller required that the user specify the amount of refrigerant subcooling at the condenser outlet and the amount of refrigerant superheat at the compressor inlet. An important difficulty encountered by Hamilton and Miller was that manufacturer's data for the components is based on specific test conditions. No method of correcting the data for non-test conditions is provided by manufacturers. The same problem was encountered by D'Valentine and Goldschmidt in their simulation program.

3. Advantages and Disadvantages of First Principle And Functional Fit Simulations

From the point of view of the user, the main advantages of first principle simulations are the following:

1) The user is not required to input and therefore to collect as much experimental data.

2) The user can easily obtain insight into how the system design can be improved by merely changing an input to the simulation program. The user can study the effect that specific system parameters, such as condenser tube size or evaporator tube diameter, have on system performance. Performing such a study with a functional fit type program would require that the system be altered and then that experimental data be collected and curve fitted to provide the new modelling equations for the program, a time consuming and expensive undertaking.

From the stand point of the developer of a simulation program, the first principle approach has two main advantages over the functional fit approach: the first principle approach provides more insight into the processes that occur inside the reversed heat engine; and, as Sauer and Howell [35] pointed out, the first principle approach identifies "...processes for which more or better technical information is needed".

To summarize, the most detailed first principle simulation programs require input for a great many design parameters which the user may find difficult to obtain (i.e. accurate estimates of internal volumes). For the functional fit simulations based on manufacturer's data (such as Hamilton and

Miller's) the difficulty of obtaining manufacturer's data is not substantial for the conditions of condenser outlet subcooling and evaporator outlet superheat under which the manufacturers carried out tests. Difficulty is encountered because the data must be correlated in specific form before it can be used in the simulation program and because manufactures do not provide subcooling and superheat correction factors for condenser and evaporator data. Furthermore, to study system performance with components which are not commercially available the components would have to be built and tested in order to generate the appropriate modelling equations.

B. Property Correlations and Data

The thermodynamic property correlations used for R-12 were those available in ASHRAE's Thermodynamic Properties of Refrigerants [3] and those provided by R.C. Downing [12]. The thermophysical property correlations used for R-12 were taken from ASHRAE's Thermophysical Properties of Refrigerants [2].

The sources for the property correlations for R-22 were the same as for R-12 with one exception: the correlation for the specific heat capacity of superheated vapour was taken from Kletskii's Thermophysical Properties of R-22 [22].

The property correlations used for the refrigerant properties were checked against the values tabulated in ASHRAE Handbook: 1985 Fundamentals [4] and Vargaftik's Tables on the Thermophysical Properties of Liquids and Gases [23].

At certain points in the simulation program algorithm the

refrigerant correlations must be evaluated through numerical methods which require initial estimates. The methods used to obtain initial guesses in these cases were based on the work done by Hill and Jeter [17].

Correlations for the properties of water were obtained by curve fitting the data tabulated in Incropera and Dewit's Fundamentals of Heat and Mass Transfer [18].

C. Heat Transfer and Pressure Drop Correlations

Many of the heat transfer correlations used in the program were taken from or developed based on data provided by Handbook of Heat Transfer Fundamentals [32]. Incropera and Dewit's Fundamentals of Heat and Mass Transfer [18] provided useful information on the proper use of heat transfer correlations.

To model the condenser the correlation developed by Traviss et al. [37] for forced convection condensation inside horizontal tubes was used.

To model the evaporator the correlation developed by Chen [7] and used by Jung and Radermacher [20] for forced convection evaporation of refrigerants in horizontal tubes was used.

The pressure drop correlations and data used in the program for single phase flow were those available in White's Fluid Mechanics [39]. Pressure drop in the condenser was calculated using the correlation derived by Traviss et al. [37]. Pressure drop in the evaporator was calculated by using Bo Pierre's correlation [6].

D. Applications of Reversed Heat Engines

Kew [21] and Berghman [5] published papers which provide, respectively, detailed discussions of the industrial and domestic applications of reversed heat engines. Peterson [31] published a paper in 1989 in which the future applications and economic feasibility of air source heat pumps for space and water heating were discussed. He concluded that the use of air to water heat pumps for heating domestic hot water is a very promising application.

III. SIMULATION ALGORITHMS AND PROGRAM

The general approach taken in the simulation program in shown symbolically in figure 4. The system specified by the user is first simulated neglecting frictional pressure drop and secondary heat transfer. The results obtained by neglecting frictional pressure drop and secondary heat transfer are then used as initial estimates for the program modules which take these effects into account. Most systems, refrigeration units for example, are designed so that frictional pressure drop and secondary heat transfer have little effect on performance.

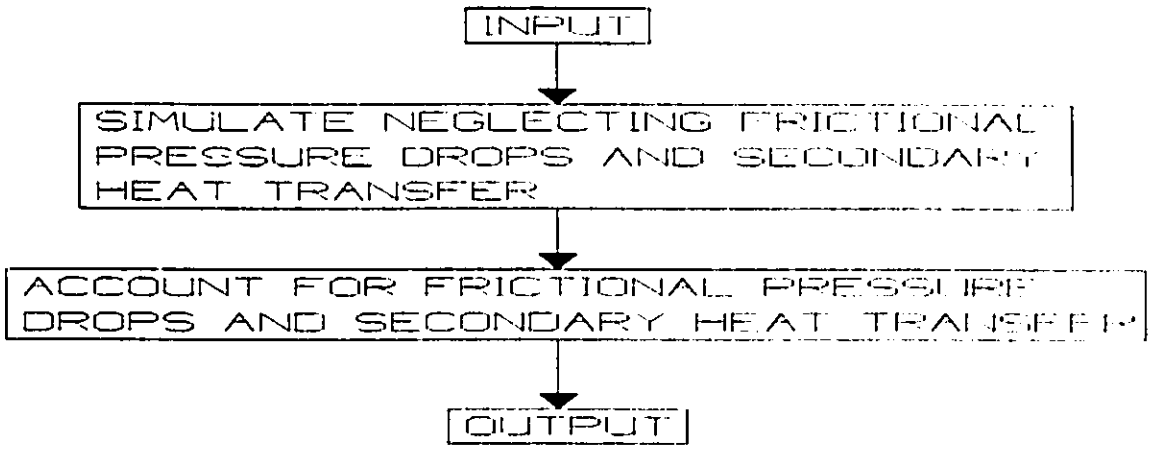

Figure 4: General Approach of Simulation Program

The simulation program consists of the six modules shown symbolically in figure 5. The MAINinput module accepts input from the user. HPunit is the module that simulates systems for the case in which a receiver is located at the condenser outlet. The

HP2unit module simulates the case in which an accumulator is located at the evaporator outlet. Neither HPunit nor HP2unit considers the effect of frictional pressure drop and secondary heat transfer. The HPmodfy and HP2modfy modules, which are modified versions of HPunit and HP2unit respectively, take into account the effects of frictional pressure drop and secondary heat transfer.

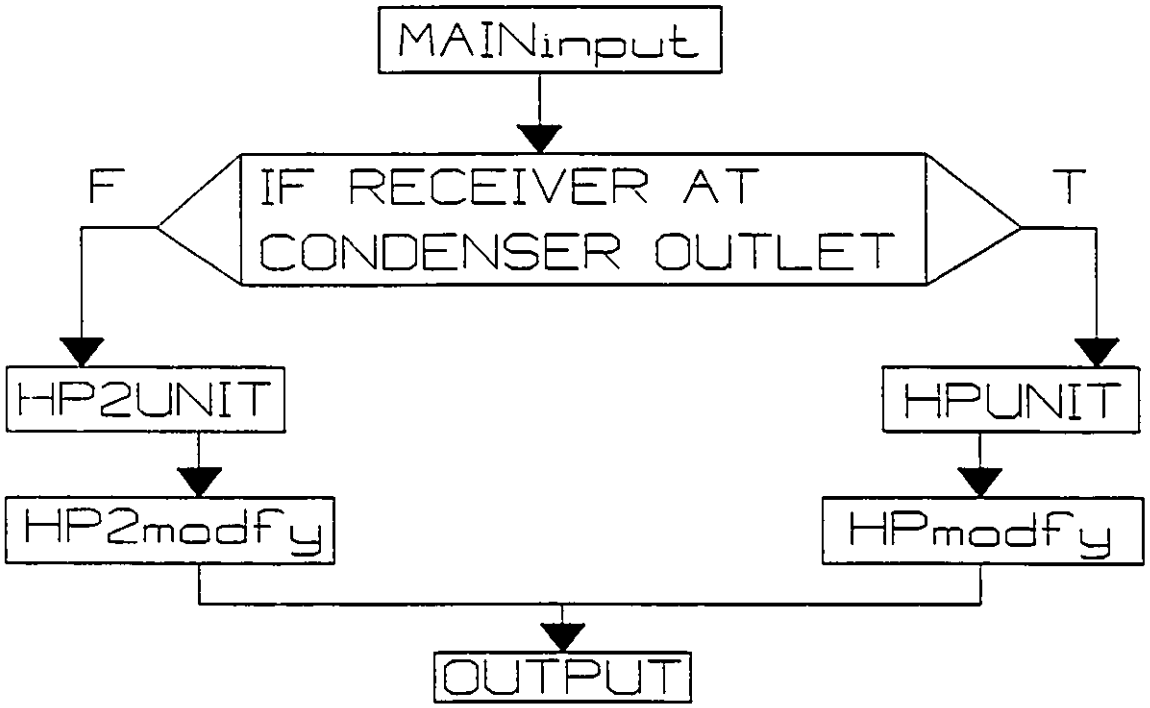

Figure 5: The Main Modules of the Simulation

A. Procedure Used to Obtain Initial Estimates

The procedure used to obtain the initial estimates for HPunit and HP2unit was based on the following three assumptions:

(1) The refrigerant leaves the evaporator as saturated vapour

(2) The refrigerant leaves the condenser as saturated

liquid

(3) The moisture content of the source air is negligible.

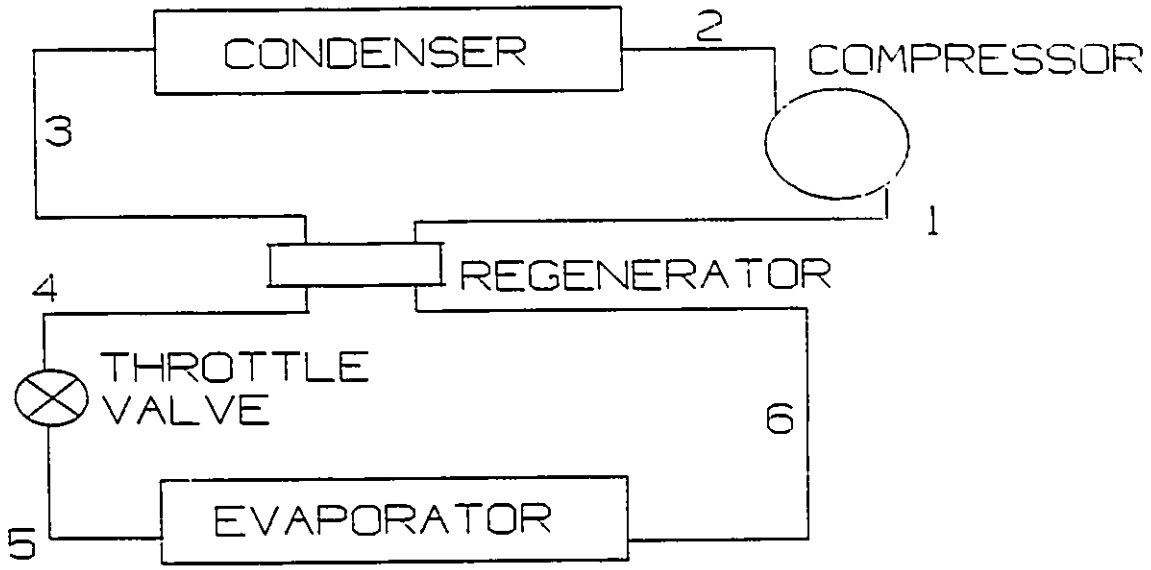

Figure 6: Locations on Reversed Heat Engine Corresponding To State Points on Figure 7

Figure 6 indicates the locations on the reversed heat engine to which the state points shown in figure 7 correspond. Note that, because frictional pressure drops and secondary heat transfer are neglected, p2 and p1 are equal to the saturation pressures at t3 and t5 respectively. Therefore, if t5 is known, then p1 can be found since p1 is the saturation pressure at t5. Once p1 is known, p2 is easily determined since the pressure ratio, PRATIO, is an input parameter in the program. After p2 is found, the condenser outlet temperature, t3, can be found since t3 is the saturation temperature at p2.

Figure 8 is a flow diagram of the iterative procedure used to obtain the initial estimates for HPunit and HP2unit. The first

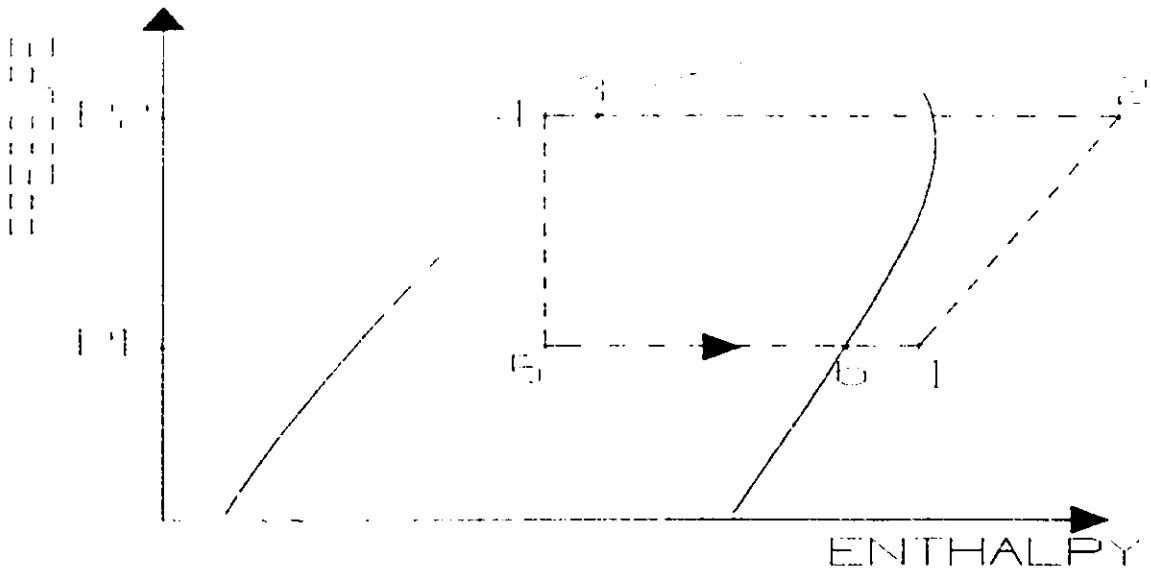

Figure 7: Thermodynamic Cycle - Neglecting Frictional Pressure Drop And Secondary Heat Transfer

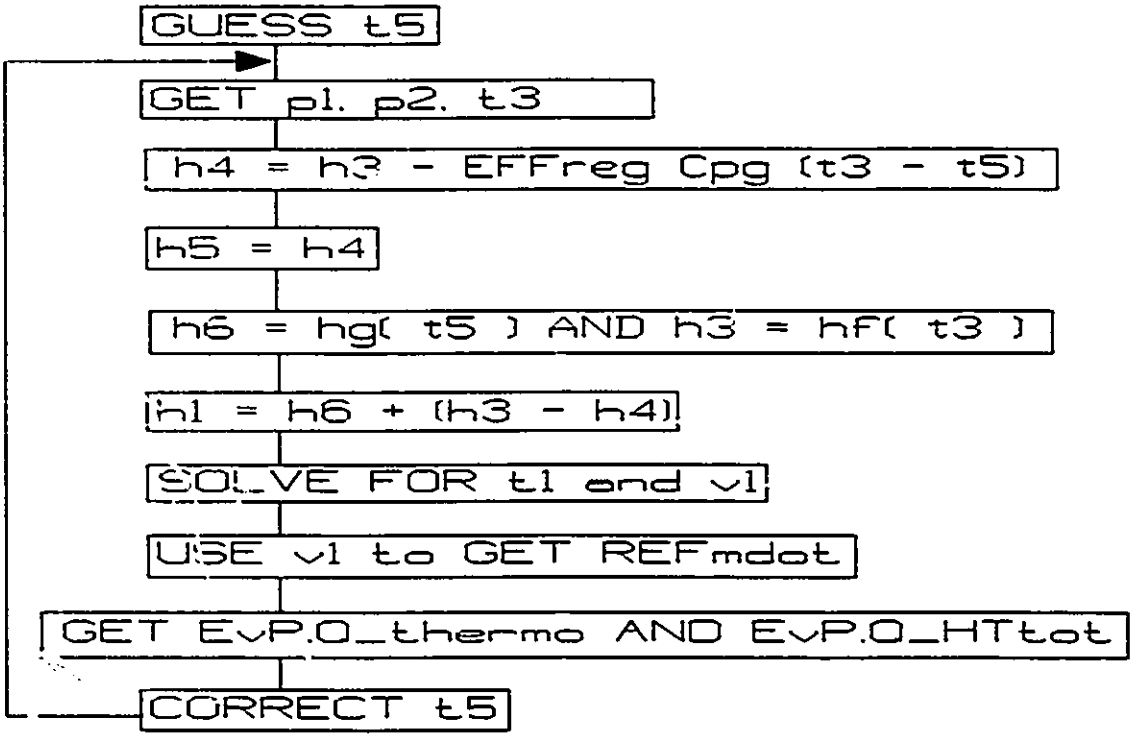

Figure 8: Flow Diagram For Initial Guess Routine

part of the procedure is to make a guess for t5. The guess is made by first establishing the limits for t5. The highest value that t5 can have corresponds to the condition where t3 equals the critical temperature of the refrigerant. The lowest value that t5 can have corresponds to the case where t3 is equal to the sink temperature. The initial guess for t5 is then taken as the average of these highest and lowest possible values. The enthalpy correlation and equation of state for refrigerant vapour must be solved simultaneously so that v1 can be found. After v1 is determined, the refrigerant mass flow rate can be calculated using the compressor volumetric efficiency, size, and rotational speed (for details see chapter VI). The quantity EvP.Q_thermo is the rate of heat transfer in the evaporator as calculated by applying the energy equation to the refrigerant space in the evaporator; EvP.Q_HTtot is the rate of heat transfer in the evaporator as calculated by the following equation:

$$EvP.Q\_HTtot = EFF\_allwet\,(AIRmdot\,AIRcp)\,(t_{source}-t5) \qquad (1)$$

where EFF_allwet is given by

$$EFF\_allwet = 1-EXP(-UA\_allwet/(AIRmdot\,AIRcp)) \qquad (2)$$

which is consistent with the assumptions that the moisture in the air can be neglected and that the refrigerant leaves the evaporator as a saturated vapour. Recall that UA_allwet is an input to the program. The value of t5 is then corrected as described in section C.4 of this chapter.

B. Logic of HPunit

Figure 9 is a flow diagram which outlines the solution technique employed by HPunit. Each step in figure 9 will now be elaborated.

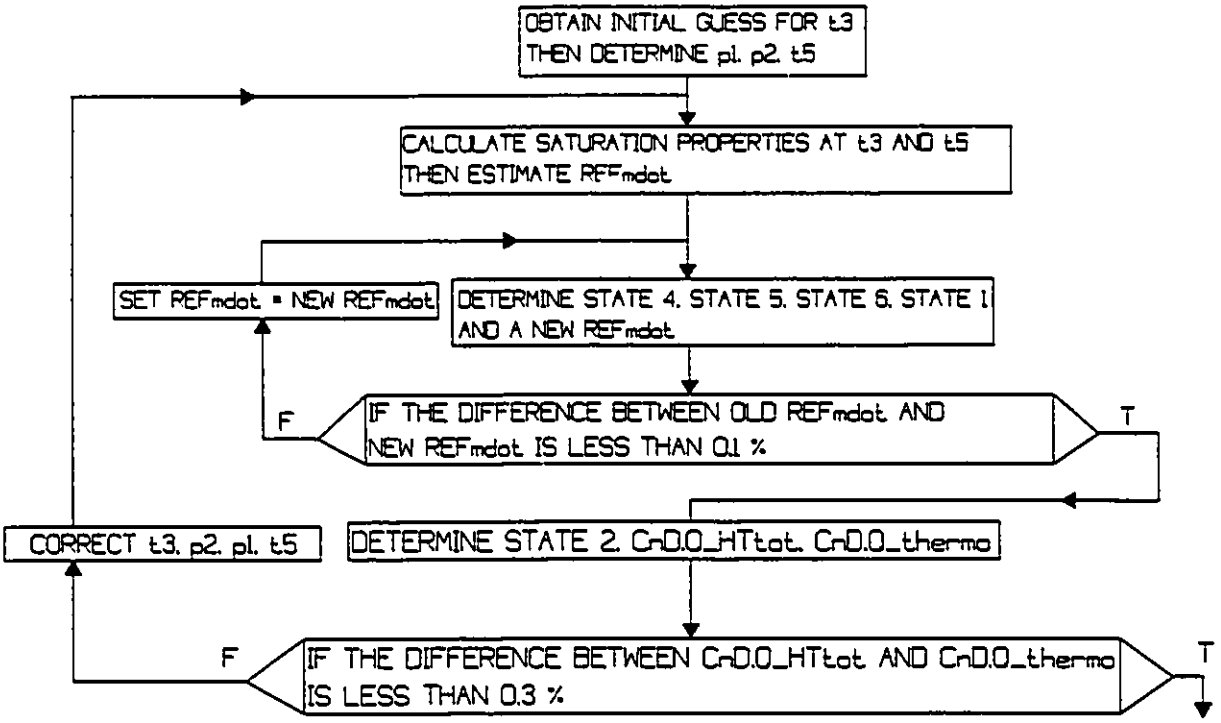

Figure 9: Outline of Solution Technique Executed in HPUNIT module

1. Initial Estimate of Refrigerant Mass Flow Rate

Saturation properties (specifically vf, vg, hg, hfg, cpf, cpg) evaluated at t3 and at t5 are required at various points in the module. They are determined through calls to the appropriate procedures.

In order to calculate the refrigerant mass flow rate, REFmdot, the compressor inlet specific volume, v1, is required as explained in the chapter dealing with the modelling of the compressor (chapter VI).

2. Determine Refrigerant Mass Flow Rate For Estimated Condenser Outlet Temperature

If state 1 is in the superheated vapour region, h4 is determined from

$$h3-h4 = EFFreg\, cpg_5\, (t3-t5) \qquad (3)$$

because the specific heat capacity of refrigerant vapour is lower than the specific heat capacity of refrigerant liquid. If state 1 is in the wet region then h4 is determined from

$$h3-h4 = EFFreg\, cpf_3\, (t3-t6) \qquad (4)$$

because the specific heat capacity of boiling refrigerant is infinite. If no regenerator is present then h4 is forced to be equal to h3 by setting EFFreg equal to zero. The temperature, t4, is found through a call to a subroutine (explained in chapter VII) that finds the temperature of saturated liquid given enthalpy. If at state 4 the refrigerant is a subcooled liquid then it is assumed that the properties of subcooled liquid are equal to the properties of a saturated liquid at the same temperature.

In going from state 4 to state 5, the refrigerant undergoes an adiabatic throttling process. The first law of thermodynamics, provided there is no significant kinetic energy change, requires that h5 equals h4. The quality at state 5,"x5", is therefore found from

$$h5 = hg5 - (1-x5)\, hfg5 \qquad (5)$$

To find h6 requires modelling of the evaporator. The modelling of the evaporator is explained in detail in chapter V. If h6 is found to be greater than hg5, the enthalpy of saturated vapour at t5, then state 6 is in the superheated vapour region. The temperature of state 6 is then found through a call to a subroutine (explained in chapter VII) which calculates the temperature of superheated vapour given enthalpy and pressure. If state 6 is found to be in the wet region (h6 is less than hg5) then t6 is set equal to t5 and x6 is determined from

$$h6 = hg5 + (1-x6)\, hfg5 \qquad (6)$$

The enthalpy at state 1, h1, is then found by applying the first law of thermodynamics to the regenerator:

$$h1-h6 = h3-h4 \qquad (7)$$

The values of t1 and v1 are found the same way the values were found for state 6.

3. Determination of Heat Transfer Rate in The Condenser

To obtain state 2 modelling of the compressor is required. Modelling of the condenser is required to obtain CnD.Q_HTtot, the rate of heat transfer in the condenser determined from heat transfer equations. The value of CnD.Q_thermo is obtained by applying the first law to the refrigerant space in the condenser. The "CnD" prefix to variable names indicates that they denote quantities calculated in the condenser module of the program.

4. Correct Condenser Outlet Temperature

The variable CnD.check_Q was defined as

$$CnD.check\_Q = \frac{(CnD.Q\_HTtot - CnD.Q\_thermo) * 100}{CnD.Q\_thermo} \qquad (8)$$

If the absolute value of CnD.check_Q is less than 0.3 then the HPunit module is exited; otherwise, the condenser outlet temperature, t3, is corrected. Figure 10 is a flow diagram illustrating the procedure to correct t3.

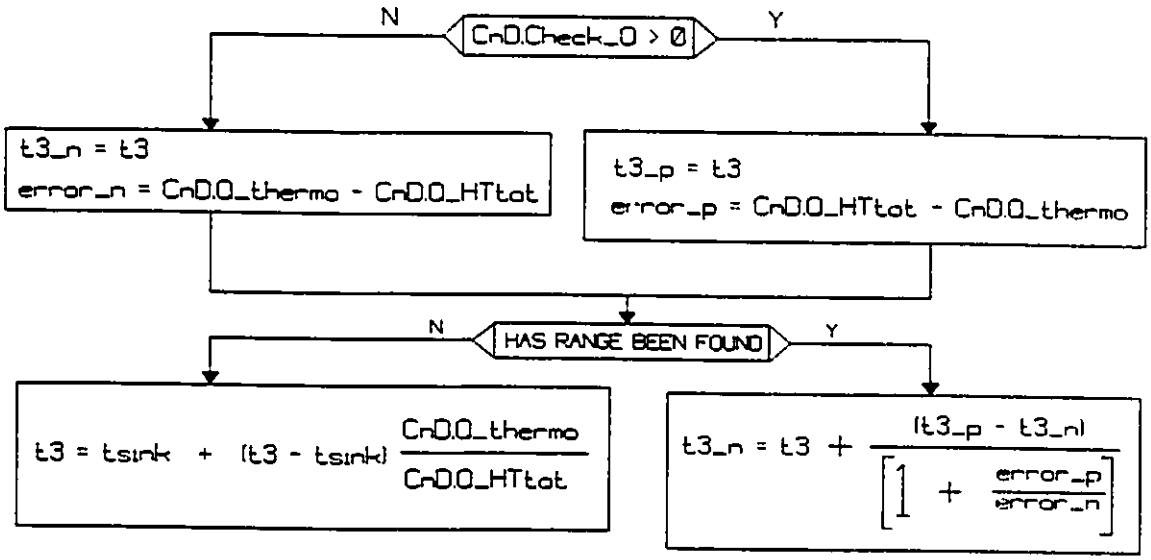

Figure 10: Procedure to Correct Condenser Outlet Temperature

If and upper and lower bounds for t3 (t3_p and t3_n respectively) are not yet established then t3 is corrected by assuming that the following equation is valid:

$$t3_{new} = t_{sink} + \frac{CnD.Q\_thermo}{CnD.Q\_HTtot} (t3 - t_{sink}) \qquad (9)$$

After t3_p and t3_n have been established, the following expression is used:

$$t3_{new} = t3\_n + \frac{t3\_p - t3\_n}{1 + \frac{error\_p}{error\_n}} \qquad (10)$$

Figure 11 illustrates the rational behind the use of (10) to correct t3 after the values of t3_p and t3_n. Note that error_n and error_p are both positive quantities. The quantity on

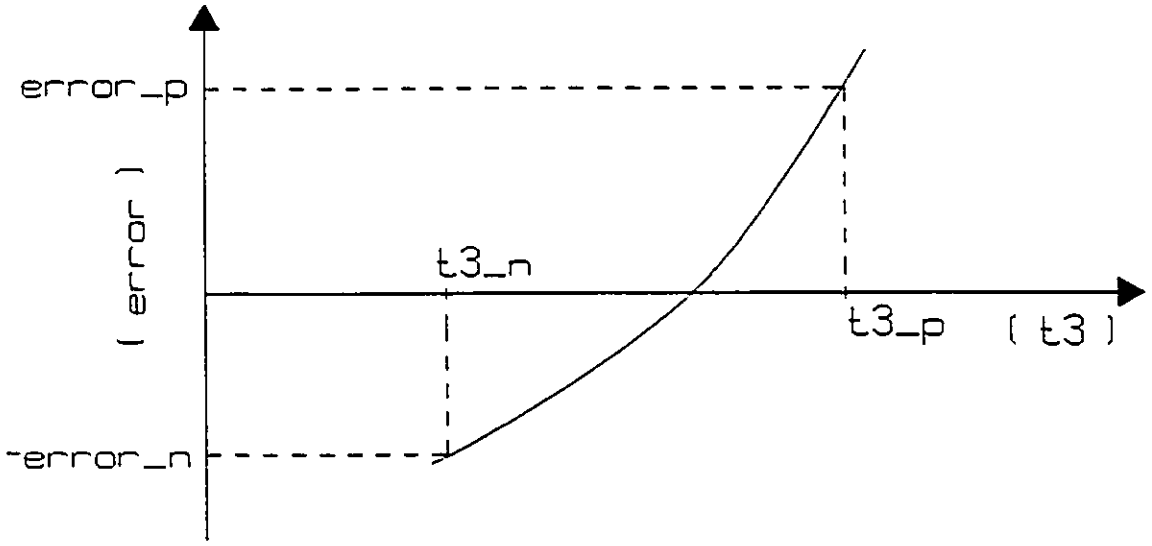

Figure 11: error VS Guesses For Condenser Outlet Temperature

the vertical axis, error, is defined as CnD.Q_HTtot minus CnD.Q_thermo. If error_n is much smaller than error_p then the new value for t3 yielded by (10) is much closer to t3_n. Similarly if error_p is much smaller than error_n then the new value for t3 is much closer to t3_p. In the case in which error_n equals error_p the new value of t3 is equal to the average of t3_n and t3_p. If error varied linearly with the estimates of t3 then the exact value of t3 would be found the first time (10) was used.

C. Logic of HP2UNIT

Figure 12 is a flow diagram which outlines the solution technique executed by the program for systems in which an accumulator is located at the evaporator outlet.

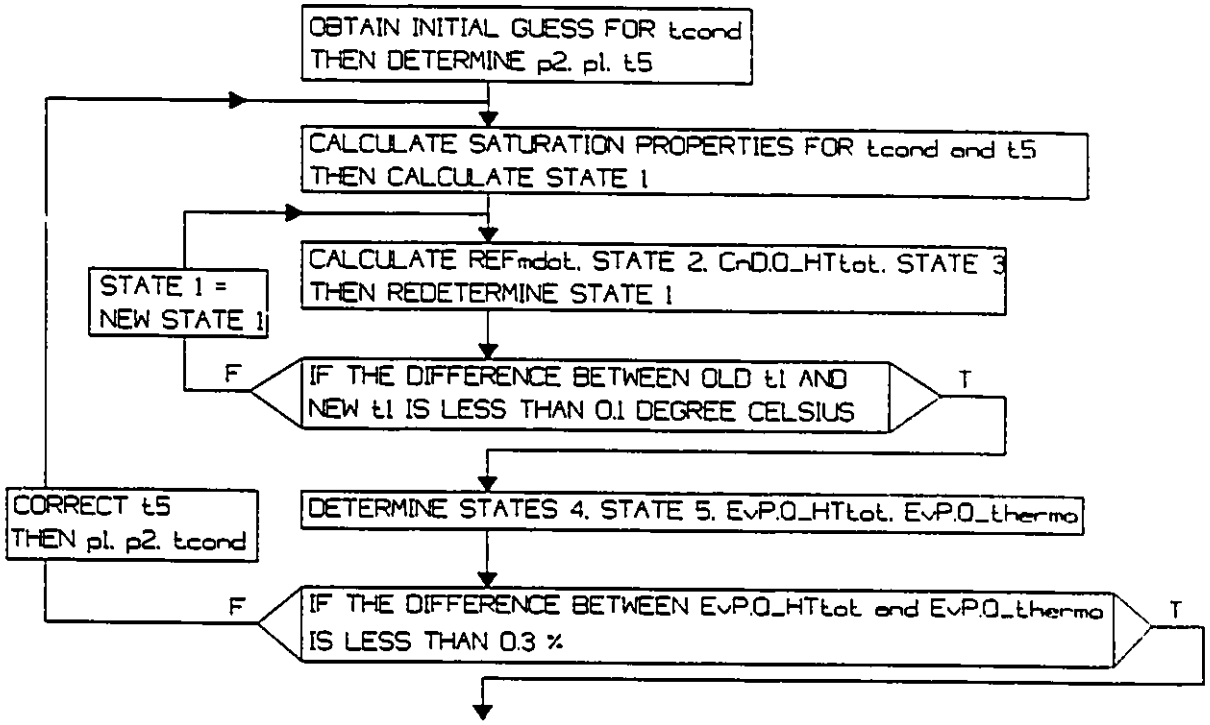

Figure 12: Outline of Solution Technique Executed in HP2UNIT module

1. Estimate Compressor Inlet State

The temperature at which refrigerant condenses inside the condenser is denoted by tcond. Saturation properties (specifically vf, vg, hg, hfg, cpf, cpg) evaluated at tcond and at t5 are required at various points in the module. They are determined through calls to the appropriate subroutines.

State 1 is always superheated vapour since state 6 is always saturated vapour. State 3, however, may be a wet mixture or subcooled liquid. Initially the enthalpy at state 1, h1 is

determined based on the assumption that state 3 is a wet mixture (i.e. t3 equals tcond):

$$h1 = h6 + EFFreg\, C_{pg}\, (t3-t5) \qquad (11)$$

The values of t1 and v1 are then calculated through a call to the subroutine that determines the temperature and specific volume of saturated vapour given enthalpy and pressure.

If no regenerator is present then h1 is forced to be equal to h6 by setting EFFreg equal to zero in (11).

2. Redetermine Compressor Inlet State

The refrigerant mass flow rate is then calculated using v1 as described in chapter VI, in which the modelling of the compressor is explained. State 2 is also determined by modelling the compressor.

The amount of heat transferred in the condenser, CnD.Q_HTtot, and state 3 are determined by modelling the condenser as described in chapter IV. Note that for the case in which the accumulator is located at the evaporator outlet CnD.Q_HTtot is equal to CnD.Q_thermo.

Once a new state 3 is determined, state 1 may be redetermined. The enthalpy at state 1 is re-evaluated from (11). Again t1 and v1 are calculated in the subroutine which determines temperature and specific volume of saturated vapour given enthalpy and pressure.

3. Determine The Rate of Heat Transfer in Evaporator

Once convergence has been achieved for state 1, state 4 may be calculated. The enthalpy at state 4, h4, is determined

from the equation derived by applying the first law to the regenerator:

$$h3-h4 = h1-h6 \qquad (12)$$

If no regenerator is present then h1 equals h6 therefore h4 equals h3. Since state 4 is subcooled liquid, t4 is calculated in the procedure which determines temperature of saturated liquid given its enthalpy: the assumption is made that the properties of subcooled liquid are equal to the properties of saturated liquid at the same temperature.

The process undergone between states 4 and 5 is a throttling process. Therefore, h5 equals h4.

The heat transferred from the air to the refrigerant in the evaporator is then calculated from heat transfer relationships, which yield EvP.Q_HTtot, and from application of the first law, yields EvP.Q_thermo. The details are described in chapter V, in which the modelling of the evaporator is explained.

4. Correct Evaporator Inlet Temperature

Essentially the same method that was used to correct t3 in the HPunit module was used to correct t5 in the HP2unit module. New values of t5 were found using the following equation:

$$\frac{t_{source}-t5_{new}}{t_{source}-t5} = \frac{EvP.Q\_thermo}{EvP.Q\_HTtot} \qquad (13)$$

After upper and lower bounds for t5 are established, t5_n and t5_p respectively, the following equation was used to obtain improved estimates of t5:

$$t5_{new} = t5\_n + \frac{t5\_p - t5\_n}{1 + \frac{error\_p}{error\_n}} \qquad (14)$$

D. Logic of HPmodify And HP2modfy

Figure 13 is a pressure versus enthalpy diagram showing the cycle that the refrigerant undergoes when frictional pressure drops and secondary heat transfer are not negligible. Figure 14 is a schematic of a reversed heat engine. The labelling of the schematic corresponds to the state points on figure 13. On

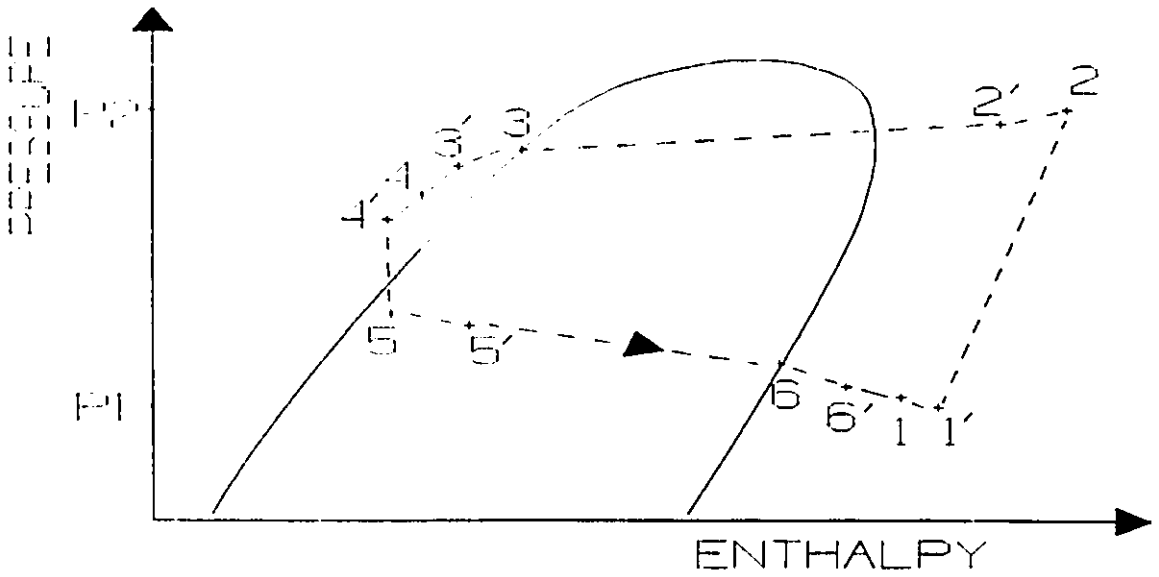

Figure 13: Process Diagram System With Frictional Pressure Drops And Secondary Heat Transfer

figure 13, h6′ is shown as being greater than h6 and h1′ as being greater than h1 because the air surrounding the interconnecting piping will usually be warmer than the refrigerant leaving the evaporator and entering the compressor. Similarly, h2′ is shown as being less than h2 because the surrounding air temperature

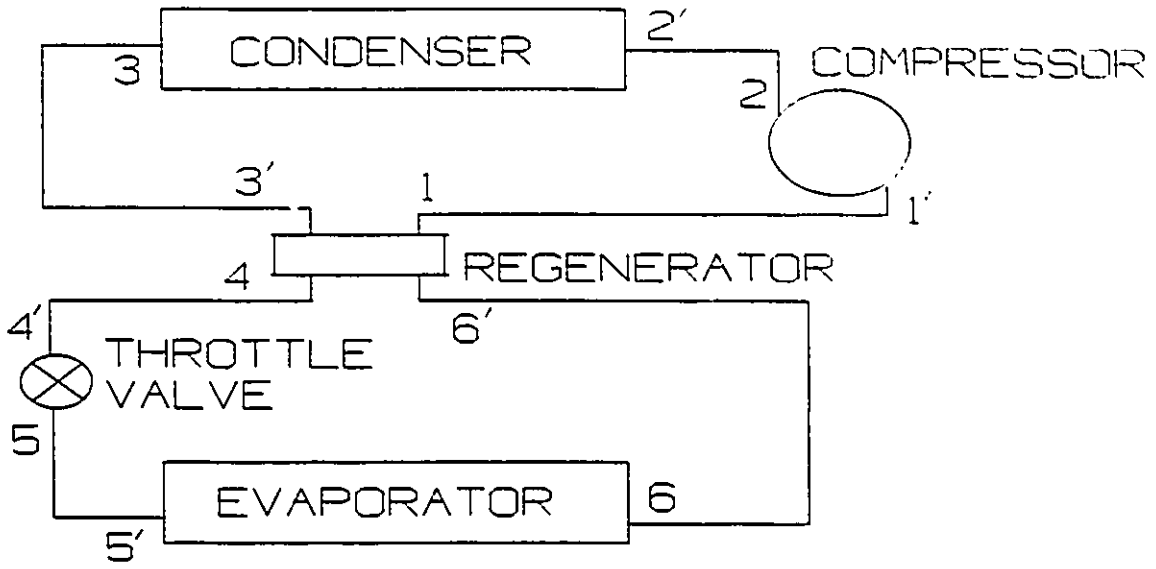

Figure 14: Locations on Reversed Heat Engine Corresponding To Refrigerant State Points of Figure 10

will usually be lower than the refrigerant leaving the condenser.

Figure 15 is a flow diagram that outlines the logic of the HPmodfy module. The logic is very similar to that of HPunit. The pressure at state 3 is equal to the saturation pressure at t3. Once p3 is found from the appropriate correlation for refrigerant saturation pressure, all the other pressures are determined from frictional pressure drop correlations that are discussed in chapter VIII.

Figure 16 is a flow diagram of the logic used in the HP2modfy module. Again, note the close similarity with the logic of HPunit. The refrigerant pressure at state 6 is equal to the saturation pressure at t6. The other pressures are determined from frictional pressure drop correlations (see chapter VIII for more details).

In calculating secondary heat transfer that occurs in

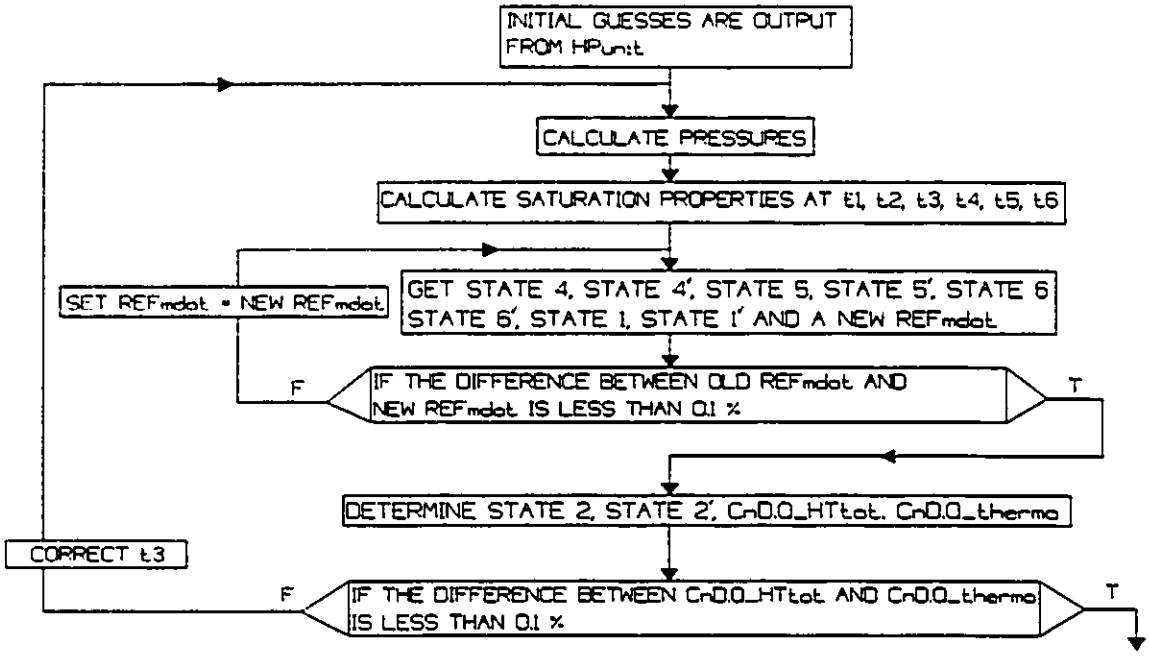

Figure 15: Logic of HPmodfy Module

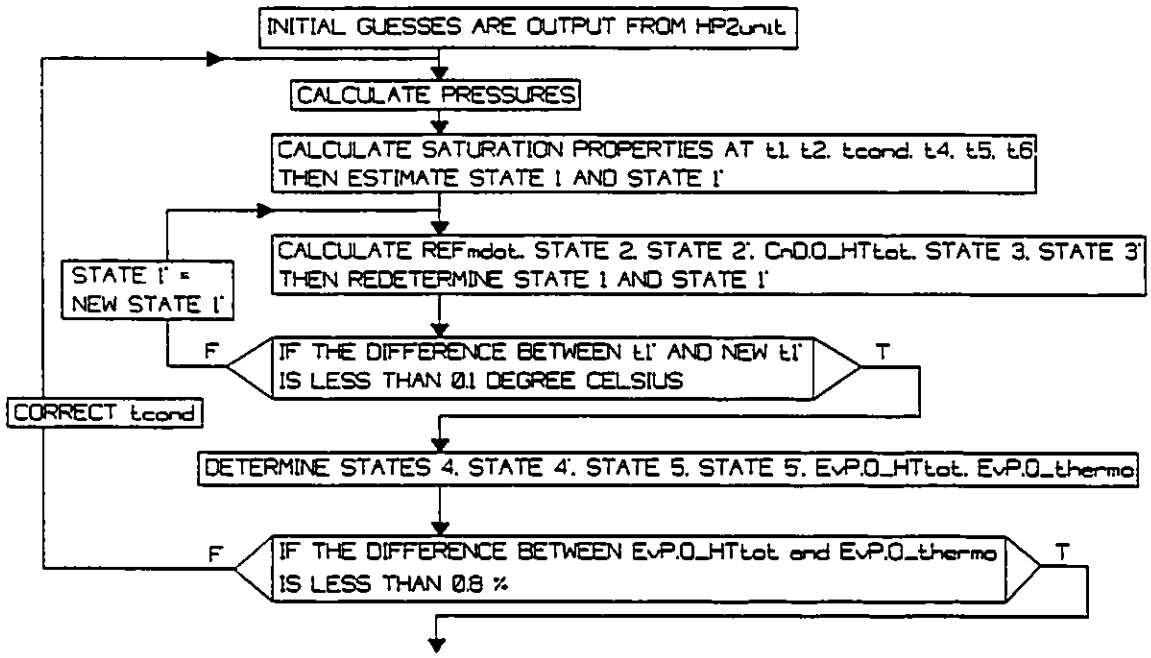

Figure 16: Logic of HP2modfy Module

the interconnecting piping it was assumed that total thermal resistance between the refrigerant and the air surrounding tubes was due to the following:

1) natural convection with the air on the outside of the tubing insulation
2) conduction through the insulation
3) conduction through the tube wall

The thermal resistance due to forced convection with refrigerant inside the tube was neglected. This assumption speeds up the calculation of secondary heat transfer and is reasonable because in most systems insulation is used to minimize secondary heat transfer. One dimensional steady state heat transmission was assumed. The temperature of the air surrounding each portion of the interconnecting piping was inputed by the user.

Each portion of interconnecting tubing was modeled as a straight, horizontal tube. By applying the first law of thermodynamics to the refrigerant space in the tube and making use of the assumptions previously stated, the following expression was derived:

$$REFmdot(h_i - h_o) = \frac{length}{R'_{tot}} LMTD \qquad (15)$$

where hi is the enthalpy of the refrigerant at the tube inlet, ho is the enthalpy of the refrigerant at the tube outlet, LMTD is the log mean temperature difference between the refrigerant and the air surrounding the tube, and Rtot' is the total thermal resistance:

$$R'_{tot} = \frac{1}{\bar{h}_{air}\pi(D_{out}+2thick_{ins})} + \frac{\ln\left(\frac{D_{out}+2thick_{ins}}{D_{out}}\right)}{k_{ins}} + \frac{\ln\left(\frac{D_{out}}{D_{out}-2thick_{pipe}}\right)}{k_{pipe}} \quad (16)$$

where the air side natural convection heat transfer coefficient was calculated by using equation 17 [18]:

$$\frac{\bar{h}_{air}(D_{out}+2thick_{ins})}{k_{air}} = \left\{0.60 + \frac{0.378R_a^{1/6}}{[1+(0.559/Pr)^{9/16}]^{8/27}}\right\}^2 \quad (17)$$

1. Secondary Heat Transfer Between Condenser Outlet And Throttle Valve

Between the condenser outlet and throttle valve inlet, seven possible conditions must be considered for the proper determination of secondary heat transfer. All seven of these conditions are shown on figure 17 where "i" and "o" refer to the inlet and outlet states, respectively, of the refrigerant inside the interconnecting tubing. When the temperature of the air surrounding the interconnecting tubing is greater than the temperature of the refrigerant inside the tubing then ho is greater than hi. Otherwise ho is less than hi.

2. Secondary Heat Transfer Between Throttle Valve And Evaporator Inlet

Inside the interconnecting piping joining the throttle valve and the evaporator, the processes shown in figure 18 are possible and were therefore taken into account.

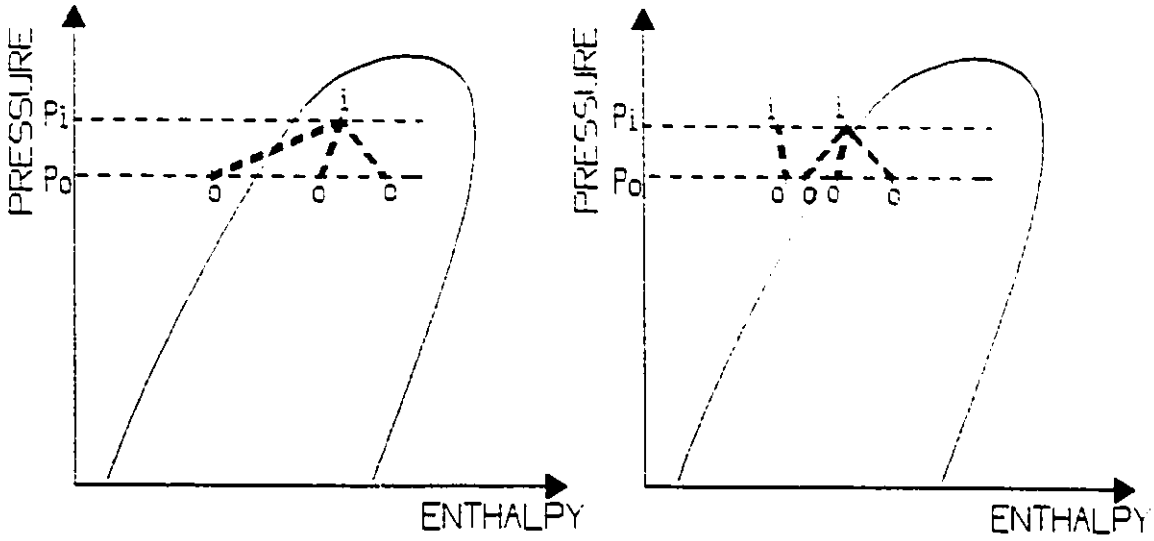

Figure 17: Processes Possible Inside Interconnecting Piping Between Condenser And Throttle Valve

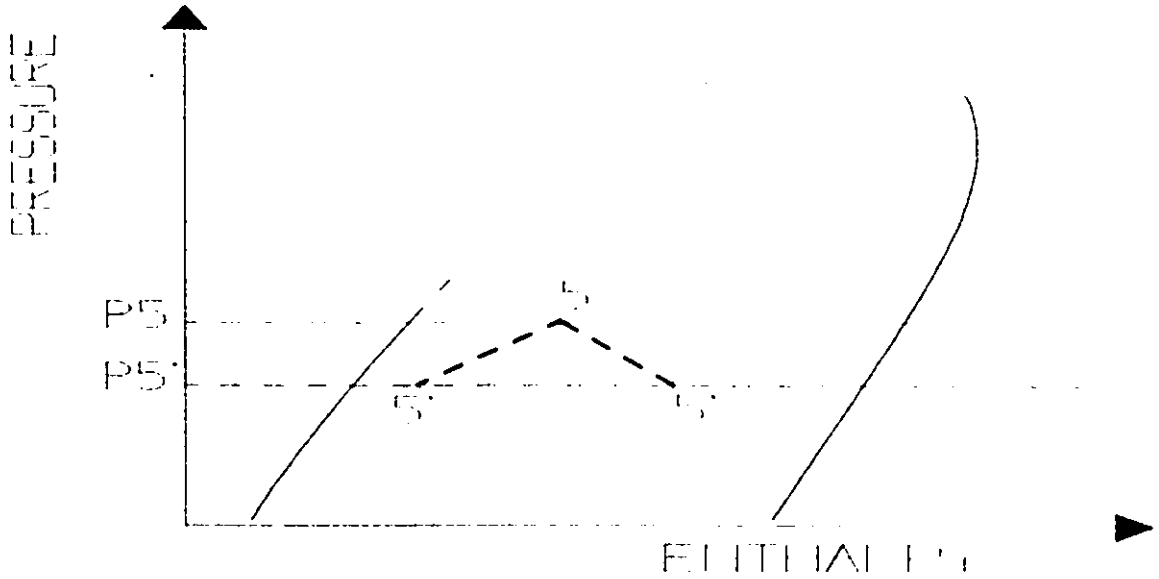

Figure 18: Processes Possible Inside Interconnecting Piping Between Throttle Valve And Evaporator

3. <u>Secondary Heat Transfer Between Evaporator Outlet And Compressor Inlet</u>

Between the evaporator outlet and the compressor inlet, six possible processes were taken into account that could occur

inside the interconnecting tubing. The processes are shown in

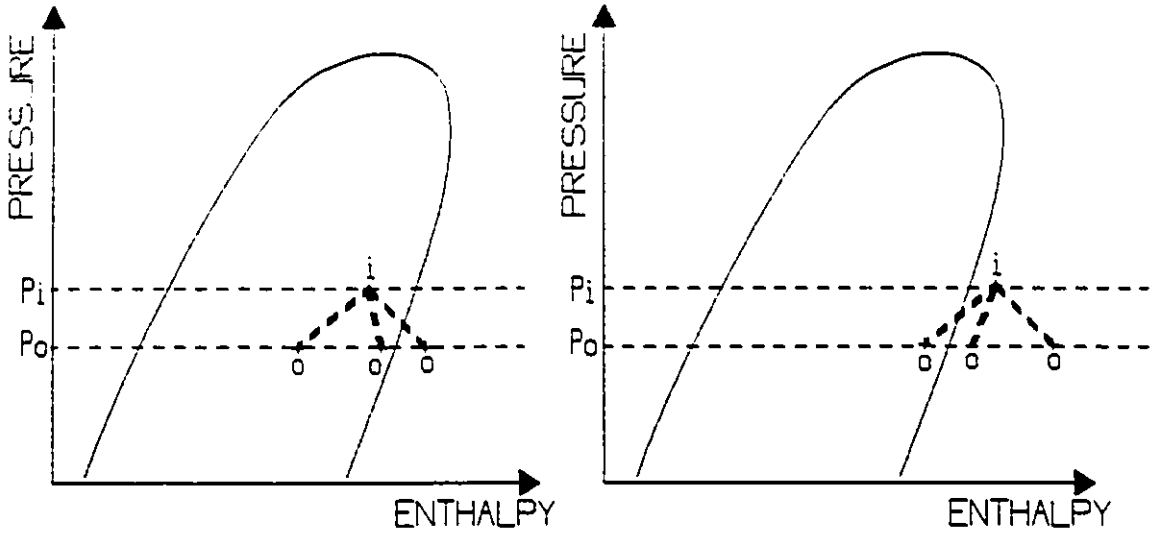

Figure 19: Processes Possible in The Interconnecting Tubing Between Evaporator And Compressor

figure 19.

4. Secondary Heat Transfer Between Condenser Outlet And Condenser Inlet

Inside the interconnecting tubing joining the compressor to the condenser the six processes shown in figure 20 are possible

E. Use of Approximation to Accelerate Convergence

Iterative procedures are required for the evaluation of refrigerant properties at various stages within the program. Based on the ideas of Hill and Jeter [17], routines were developed to obtain initial estimates for the refrigerant properties which are evaluated using iterative methods (for a detailed discussion of these methods see chapter VII). It was found that if the program is made to converge by using only the

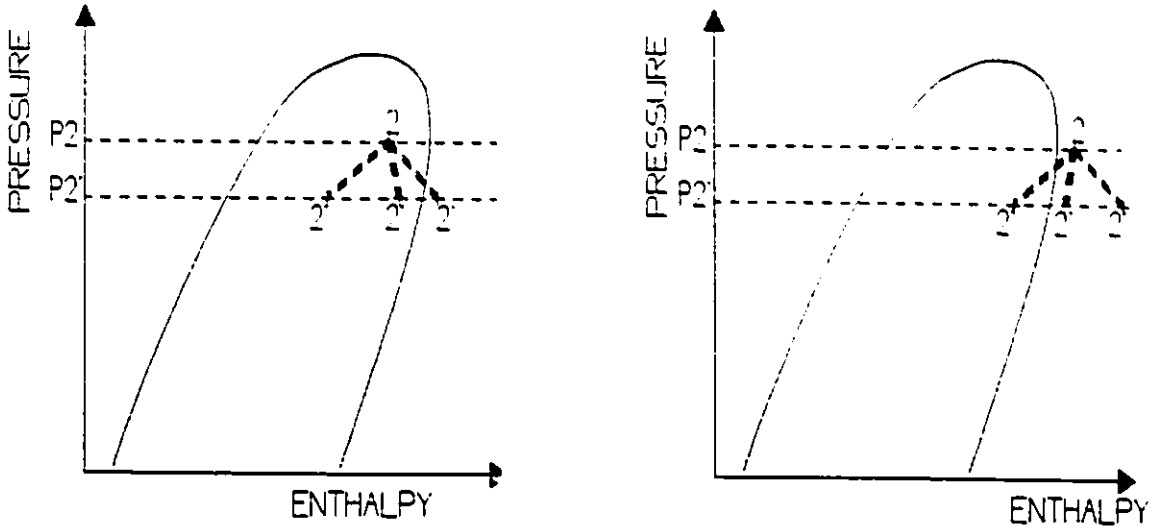

Figure 20: Processes Possible Inside Interconnecting Tubing Between Compressor And Condenser

initial guesses for refrigerant properties in cases where iterative procedures are required then the program converges in less than half the time. Furthermore, the simulation results do not differ significantly from the results that are produced when the iterative procedures for property evaluation are used.

It was found that the time required for convergence of the program is reduced by at least a factor of two, in most cases, if the following procedure is used: the program is first made to converge with only the initial estimates of refrigerant properties used (when iterative procedures are required) so that approximate simulation results are obtained; the program is then made to converge by carrying out the iterative routines for property evaluation when required. The second time the program is made to converge, the approximate simulation results are used as initial guesses. Usually, only two additional iterations are

required to make the program converge.

F. Description of Program

The program was named RHEsim92 and was written in Turbo Pascal (version 6.0). The executable file and the accompanying files required for the generation of menu and data entry screens can all be stored on one high density, 5.25 inch floppy disk (see Appendix VI).

Because the program was designed to be menu driven, it is very easy to use. In Appendix VII, some of the menu screens are shown. The user is not allowed access to the menu items that run the program and output the results until all the required input is provided. The user is also denied access to the menu item that outputs results if the input from a previous run has been altered: the user must run the program again in order to output results. The data entry screens do not allow the user to enter non-numeric characters. For each numeric input an allowable range is specified by the program; the user is not allowed to enter values out of range.

IV. CONDENSER MODELLING AND SIMULATION

Two types of condensers are modeled in the simulation program: a coil immersed in a water tank and a concentric-tube type. Figures 21 and 22 illustrate these two types.

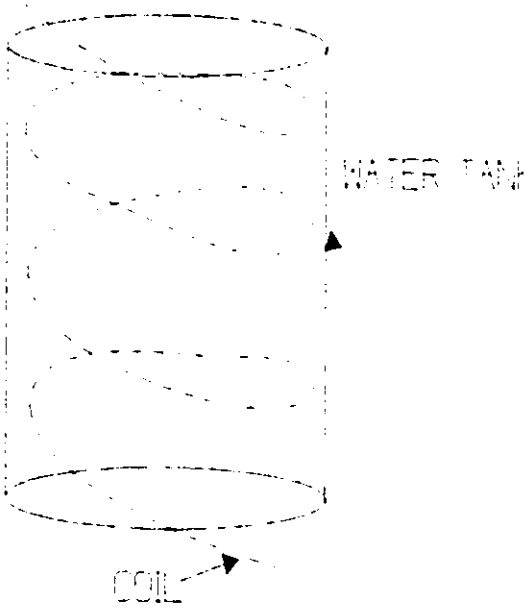

Figure 21: Coil in Tank Condenser

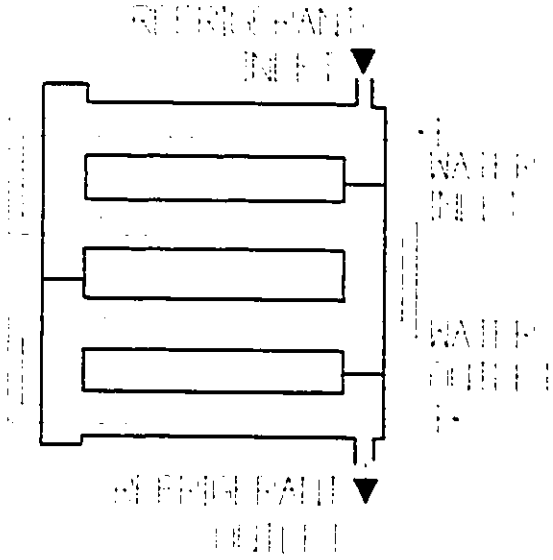

Figure 22: Concentric Tube Condenser

A. Modelling of Condenser

The following assumptions were made in modelling both types of condensers:

1) steady state conditions,
2) one dimensional radial heat transfer,
3) full condensation begins when the refrigerant side wall temperature equals the saturation temperature,
4) the refrigerant leaves the condenser as a saturated liquid

when a receiver is located at the condenser outlet.

The condenser is modelled as three portions: the dry portion, where no condensation takes place and the refrigerant is a superheated vapour; the wet portion, where condensation takes place; and the liquid portion, in which the refrigerant is subcooled.

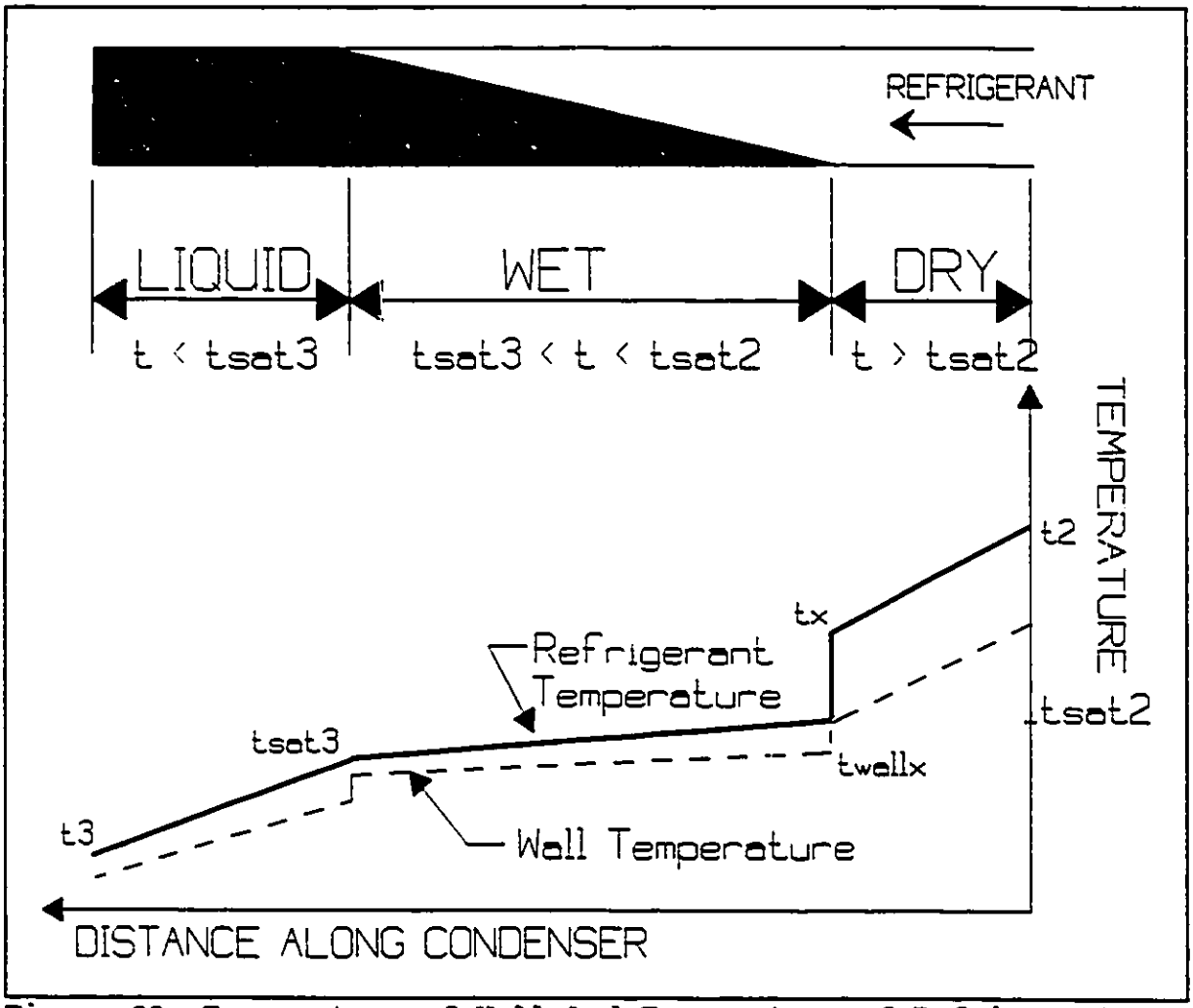

Figure 23: Temperature of Wall And Temperature of Refrigerant VS Distance Along Condenser

The wall and refrigerant temperature discontinuities shown in figure 23 at the end of the dry portion represent the third

modelling assumption listed previously: that full condensation starts to occur when the wall temperature equals the refrigerant saturation temperature (tsat2). In reality the refrigerant vapour is still superheated when condensation begins. Hence, the bulk refrigerant temperature is greater than, not equal to, the saturation temperature when condensation begins. Note that figure 23 depicts the situation in which a liquid portion exists; hence, the situation in which there is no receiver located at the condenser outlet.

The fourth assumption is that the refrigerant leaves the condenser as a saturated liquid when a receiver is located at the condenser outlet. Under steady state conditions the liquid level in the receiver is constant. The liquid in the receiver therefore "traps" vapour in the condenser. It is therefore impossible, under steady state conditions, for the refrigerant to exit the condenser as a wet mixture. It is not likely that the refrigerant would leave the condenser as a subcooled liquid because the vapour trapped inside the condenser would tend to evaporate any subcooled liquid. It was therefore assumed that the refrigerant leaves the condenser as a saturated liquid. This assumption was confirmed by the experimental data discussed in chapter X.

1. Modelling Assumptions And Equations For Coil-in-Tank Condenser

In addition to the modelling assumptions listed in section A of this chapter, the following assumptions were made in modelling coil-in-tank condensers:

1) The water temperature is uniform,

2) To calculate the water side heat transfer coefficients, the condenser can be modelled as a straight horizontal elliptical tube with a cross section that could be formed by a vertical plane, normal to the tube plane, cutting through the inclined tube (see figure 24).
3) To calculate the refrigerant side heat transfer coefficients, the condenser can be modelled as a curved circular duct,
4) The refrigerant side heat transfer coefficient has a negligible effect on the overall thermal conductance of the wet portion since the heat transfer coefficients for condensation are much larger than heat transfer coefficients for natural convection [18].

The amount of heat transferred by the refrigerant as it passes through the dry portion is given by

$$Q\_HTdry = UA\_dry' \; Lcond\_dry \; LMTD\_dry \qquad (18)$$

where UA_dry' is the overall thermal conductance per unit length for the dry portion, Lcond_dry is the length of the dry portion, and LMTD_dry is the log mean temperature difference for the dry portion. Similarly, the heat transferred in the wet portion of the condenser is given by

$$Q\_HTwet = UA\_wet' \; Lcond\_wet \; (t_{cond} - Tw) \qquad (19)$$

and the amount of heat transferred by the refrigerant as it

passes through the liquid portion is given by

$$Q\_HTliq = UA\_liq' Lcond\_liq\ LMTD\_liq \qquad (20)$$

For a more detailed discussion of the modelling equations see Appendix I.

Table 1 lists the heat transfer correlations that are used in the program to model coil in tank condensers. Note that Radius_curv is the radius of curvature of the coil. Figure 24 illustrates how C and B, which appear in correlation three of Table 1, are defined. The Nusselt numbers N_{u_t} and N_{u_t} correspond to laminar and turbulent flow, respectively, over the entire cylinder. The laminar Nusselt number is arrived at by first calculating N_u^T , the laminar Nusselt number based on the assumption of a thin boundary layer. This value is then corrected because the actual boundary layer for laminar flow is not thin. In the case of turbulent flow the boundary layer may be considered thin. Hence, N_{u_t} is calculated directly.

Table 1: Correlations Used To Model Coil In Tank Condenser

Correlation And Source	Restrictions And Use
1. $N_u = 0.836\, K^{0.5}\, P_r^{0.1}$ $K = R_e \left(\frac{Radius\_cond}{Radius\_curv}\right)^{\frac{1}{2}}$ [32]	$R_e < 2\left(\frac{Radius\_cond}{Radius\_curv}\right)^{0.32} 10^4$ *and* $\frac{Radius\_curv}{Radius\_cond} < 860$ - *Single Phase* - *Forced Convection* - *Constant Surface Temperature* - *Inside Curved Duct* - *Refrigerant Side Heat Transfer Coefficient*

Table 1 Continued

2. $N_u = 0.023\, R_e^{0.85} \left(\frac{Radius\_cond}{Radius\_curv}\right)^{0.1} P_r^{0.4}$ [32]	$R_e > 2\left(\frac{Radius\_cond}{Radius\_curv}\right)^{0.32} 10^4$ and $\frac{Radius\_curv}{Radius\_cond} < 860$ - *Single Phase* - *Forced Convection* - *Constant Surface Temperature* - *Inside Curved Duct* - *Refrigerant Side Heat Transfer Coefficient*
3. $N_u = [N_{u_L}{}^m + N_{u_t}{}^m]^{\left(\frac{1}{m}\right)}$ $m = \frac{3.5}{\sqrt{\frac{C}{B} + 0.1}}$ $N_{u_L} = \frac{C_2}{\ln\left(1 + \frac{C_2}{N_u^T}\right)}$ $N_u^T = C_1 \overline{C}_L R_a^{\left(\frac{1}{4}\right)}$ $N_{u_t} = \overline{C}_t R_a^{\left(\frac{1}{3}\right)}$ *See Appendix I for* $\overline{C}_L$, $\overline{C}_t, C_1, C_2$ [32]	- *Single Phase* - *Constant Surface Temperature* - *Natural Convection Outside Horizontal Elliptical Cylinders* - *Water Side Heat Transfer Coefficient*

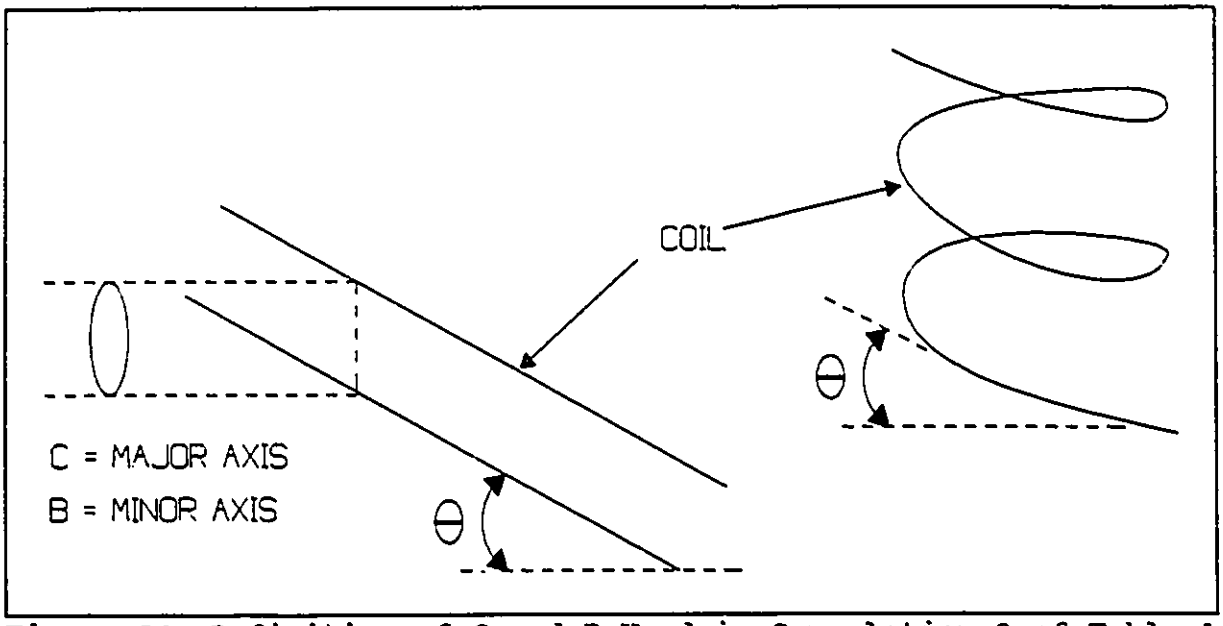

Figure 24: Definition of C and B Used in Correlation 3 of Table 1

2. Modelling Assumptions For Concentric Tube Condenser

The only modelling assumption used for concentric tube condensers, in addition to those listed in section A of this chapter, is that the effect of bends and corners is negligible.

Figures 25 and 26 define some of the nomenclature used for concentric tube condensers. Either fluid may flow in the annulus; both cases are taken into account in the program. Note that the wall temperatures shown figures 25 and 26 are the refrigerant side wall temperatures.

The amount of heat transferred by the refrigerant to the water in the dry portion is given by

$$Q\_HTdry = UA\_dry' Lcond\_dry\ LMTD\_dry \qquad (21)$$

The amount of heat transferred in the wet portion of the condenser is given by

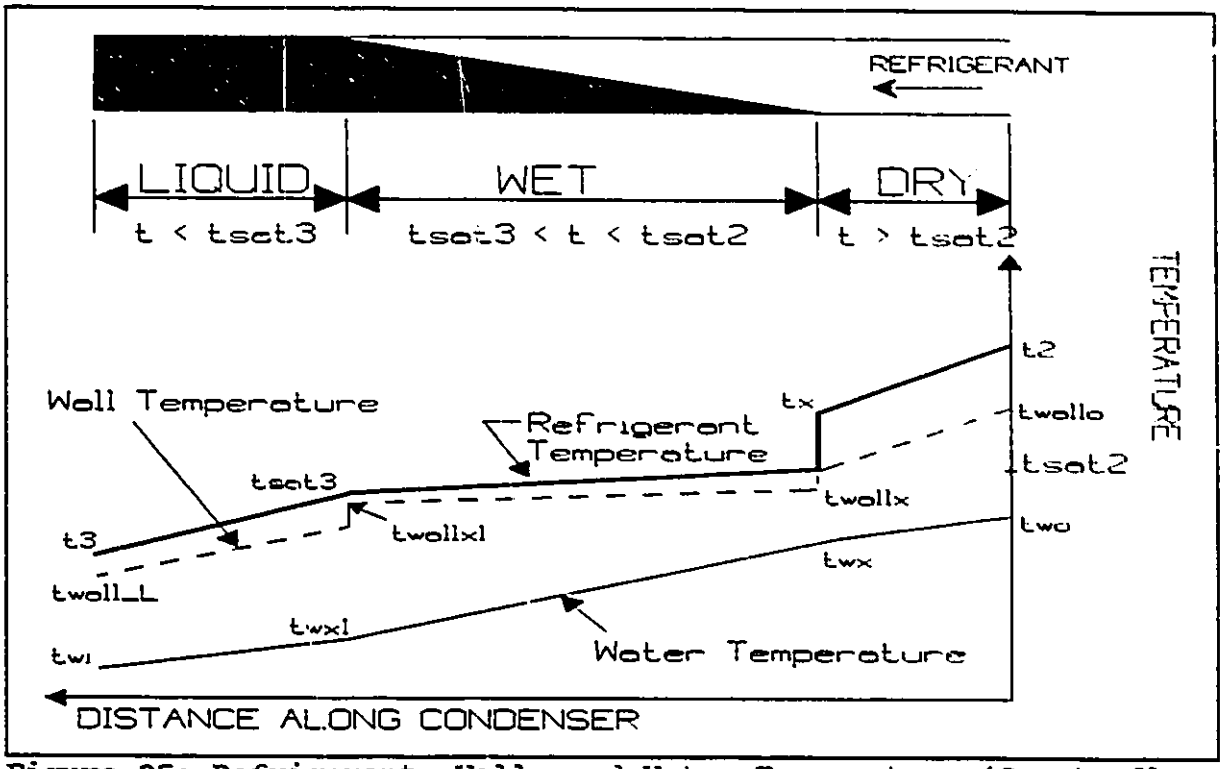

Figure 25: Refrigerant, Wall, and Water Temperature (Counterflow Concentric Tube Condenser)

$$Q\_HTwet = UA\_wet' \; Lcond\_wet \; LMTD\_wet \tag{22}$$

The heat transferred in the liquid portion of the condenser is given by

$$Q\_HTliq = Eff \; Mcp\_min \; (t_{cond} - Twx1) \tag{23}$$

where Mcp_min is the smaller of REFmdot*cpf and H2Omdot*H2Ocpf, Eff is the effectiveness, NTU is given by UA_liq/Mcp_min and Cr is given by

$$C_r = \frac{Mcp\_min}{Mcp\_max} \tag{24}$$

where Mcp_max is the larger of REFmdot*cpf and H2Omdot*H2Ocpf. UA_liq is given by

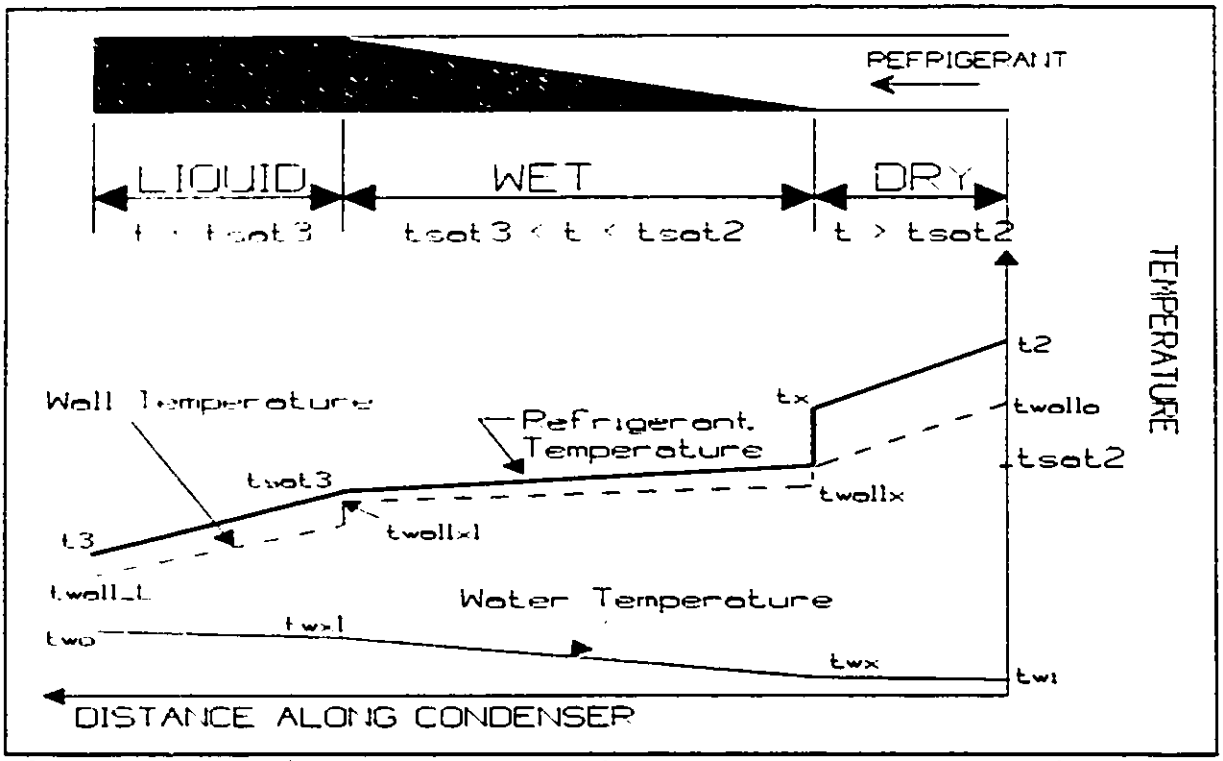

Figure 26: Refrigerant, Wall, and Water Temperature (Parallel Flow Concentric Tube Condenser)

$$UA\_liq = UA\_liq' \, Lcond\_liq \qquad (25)$$

For a more detailed discussion of the modelling equations see Appendix I.

Table 2 lists the correlations which were used in modelling concentric tube condensers. Note that D3 is the inner diameter of the outer tube, L is the length of tube, ΔT is the difference between the tube wall surface temperature and the refrigerant saturation temperature. The variable D, which appears in correlation seven, takes on the value of D1, D2 or D3 depending on which correlation is being corrected for entry

effects. The variables f and fsmooth are evaluated from

$$f = \left[\left(\frac{-2}{\ln(10)}\right)\ln\left(\frac{rough}{3.7} + \frac{2.51}{R_e\sqrt{f}}\right)\right]^{-2} \qquad (26)$$

where *rough* is the relative roughness (which is set equal to zero in the calculation of fsmooth).

The characteristic diameter that is used to calculate the Reynold's number for correlation three is equal to *D3-D2* . No data or correlations were found in the literature for the case of constant inner wall temperature. It was therefore assumed that the condition of constant inner wall heat flux yields approximately the same heat transfer coefficients as the condition of constant inner wall temperature since this is the case for flow inside a circular tube. As indicated in table 2, the data was curve fit for values of D2/D3 equal to 0.1, 0.2, 0.5, and 0.8. For diameter ratios between 0.1 and 0.8 linear interpolation is used. For ratios greater than 0.8 the values obtained for 0.8 are used. Inspection of the tabulated data reveals that error due to this approximation is about one percent (in terms of Nusselt number). For ratios less than 0.1 the values for 0.1 are used. Data for diameter ratios less than 0.1 was not available.

Correlations one and two are extrapolated to estimate heat transfer coefficients for transitional flow (Reynold's numbers between 2300 and 10 000) [32]. For transitional flow

inside circular annuli linear interpolation is used between the heat transfer coefficients obtained from correlations three and four.

If refrigerant condenses inside the inner tube then the average heat transfer coefficient is obtained from the following expression where x is the refrigerant quality [32]:

$$\frac{1}{\bar{h}_{avg}} = \int_0^1 \frac{dx}{\bar{h}_x} \tag{27}$$

The integral on the right hand side of (27) is evaluated using the approximation

$$\int_0^1 \frac{1}{\bar{h}_x} dx \doteq \sum_{j=1}^{20} \frac{\Delta x_j}{\bar{h}_{x_j}} \tag{28}$$

Upon first consideration one expects that havg should be calculated as

$$\bar{h}_{avg} = \int_0^1 \bar{h}_x dx \tag{29}$$

In Appendix I it is demonstrated why (29) is not correct.

The summation described by (28) consists of twenty terms. For each term, the local heat transfer coefficient, $\bar{h}_x$, is

Table 2: Correlations Used For Concentric Tube Condenser

Correlation And Source	Restrictions And Use
1. $N_u = 5 + 0.015\, R_e^{a}\, Pr^{b}$ $a = 0.88 - \frac{0.24}{4 + Pr}$ $b = 0.333 + 0.5\, EXP(-0.6\, Pr)$ [32]	$0.1 < Pr < 10^4$ $10^4 < R_e < 10^6$ - *Single Phase* - *Forced Convection* - *Inside Horizontal Circular Smooth Tubes* - *Independent of Thermal Boundary Condition* - *Water and Refrigerant Side Heat Transfer Coefficients*
2. $N_u = 0.021\, Pr^{0.5}\, R_e^{0.8}$ [32]	$0.6 < Pr < 0.8$ $10^4 < R_e < 10^5$ - *Single Phase* - *Forced Convection* - *Inside Horozontal Circular Tubes* - *Constant Surface Temperature* - *Refrigerant Side Heat Transfer Coefficient*

Table 2 Continued

3. $\ln(N_u) = \sum_{i=0}^{3} AA_i [\ln(R_e)]^i$ $AA_i = \sum_{j=0}^{3} a_{ij} [\ln(P_r)]^j$ for $\frac{D2}{D3}$ = $AA_i = \sum_{j=0}^{3} a_{ij} P_r^j$ for $\frac{D2}{D3} = 0.1$ *See Appendix I* [32]	$R_e > 10^4$ - *Single Phase* - *Forced Convection* - *Inside Circular Tube Annulus* - *Outer Tube Wall Insulated* - *Constant Heat Flux* - *Refrigerant and Water Side Heat Transfer Coefficient*
4. $N_u = 3.656$ [32]	*Re* < 2300 - *Constant Surface Temperature* - *Otherwise Same Comments As For* 1 & 2
5. $N_u = 5.74$ [32]	R_e < 2300 - *Constant Inner Surface Temperature* - *Otherwise Same Comments As For* 3.

Table 2 Continued

6. $N_u = \begin{cases} N_u \left(\frac{f}{f_{smooth}}\right)^{0.5}, & \frac{f}{f_{smooth}} \le 4 \\ 2N_u, & \frac{f}{f_{smooth}} > 4 \end{cases}$ [18]	- *Corrects 1,2,3,4,5 For Surface Roughness Effects*
7. $N_u = N_u\left[1 + \frac{a}{\left(\frac{L}{D}\right)^b}\right]$ $a = \frac{23.99}{R_e^{0.23}}$ $b = \frac{-2.08}{10^{0.6}} R_e + 0.815$ [26]	- *Corrects 1,2,3,4,5 For Entry Region Effects*
8. $\bar{h}_{avg} = 0.553\left[\frac{g\rho_f(\rho_f-\rho_g)\,k_f^3\,h'_{fg}}{\mu_f\,\Delta T\,D_1}\right]^{\frac{1}{4}}$ $h'_{fg} = h_{fg} + \frac{3}{8} C_{p_f}\Delta T$ [32]	- *Forced Convection Condensation* - *Inside Staight Horizontal Circular Tube* - *Refrigerant Side Heat Transfer Coefficient*

Table 2 Continued

9. $\bar{h}_{avg} = 0.728\left[\frac{g\rho_f(\rho_f-\rho_g)k_f^3 h'_{fg}}{\mu_f \Delta T D_2}\right]^{\frac{1}{4}}$ $h'_{fg} = hfg + \frac{3}{8} C_{p_f} \Delta T$ [32]	- *Natural Convection Condensation* - *Ouside Horizontal Tube* - *Refrigerant Side Heat Transfer Coefficient*
10. $N_u = 0.15 \frac{Pr_f R_{e_f}^{0.9}}{F2}\left[\frac{1}{X}+\frac{2.85}{X^{0.476}}\right]$ $F2 = 5Pr_f + 5\ln(1+5Pr_f) + 2.5\ln(0.0031R_{e_f}^{0.812})$, $R_{e_f} > 1125$ $F2 = 5Pr_f + 5ln[1+Pr_f(0.0964R_{e_f}^{0.585}-1)]$, $50 \le R_{e_f} \le 1125$ $F2 = 0.707Pr_f R_{e_f}^{0.5}$, $R_{e_f} < 50$ $X = \left(\frac{\mu_f}{\mu_g}\right)^{0.1}\left(\frac{(1-x)}{x}\right)^{0.9}\left(\frac{\rho_g}{\rho_f}\right)^{0.5}$ [37]	- *Forced Convection Condensation* - *Inside Staight Horizontal Circular Tube* - *Refrigerant Side Heat Transfer Coefficient*

Table 2 Continued

11. $\bar{h}_{avg} = \left[1 + 0.004\left(\frac{Vel_g^2 \rho_g h_{avg}}{g \rho_f k_f}\right)^{0.4}\right]$ [32]	- *Correction of 9 For Effect of Vapour Velocity*

calculated from correlations 8 and 10; the larger value for $\bar{h}_z$ is used. For qualities greater than 0.20 correlation 10 usually yields the larger value of hz.

If the refrigerant condenses inside the annulus then correlations 9 and 11 are used. It is appropriate to use these correlations when the refrigerant flows in the annulus because the refrigerant then condenses on the outside of the inner tube. Correlation 9 was developed assuming zero vapour velocity. When refrigerant condenses in the annulus the vapour velocity is not zero until the end of the condenser's wet portion. The correction for the effect of vapour inlet velocity is provided by correlation 11. The inlet vapour velocity, Vel_g, is given by

$$Vel_g = \frac{refmdot}{\rho_{g7}\frac{\pi (D_3^2 - D_2^2)}{4}} \qquad (30)$$

B. The Condenser Module

The function that the condenser module performs in the simulation program depends on where excess refrigerant is stored in the system being simulated. Refrigerant is either stored in a receiver (located at the condenser outlet) or in an accumulator (located at the evaporator outlet).

1. Accumulator at Evaporator Outlet

For the case in which an accumulator is located downstream of the evaporator, the objective of the condenser module is to calculate the enthalpy of the refrigerant at the condenser outlet (h3) and the amount of heat transferred from the condenser to the surroundings. When the condenser module is called from within the simulation program, the known quantities are the refrigerant inlet temperature and pressure, the refrigerant outlet pressure, the refrigerant mass flow rate, the size and configuration of the condenser, and the water (sink) temperature.

a. Coil-in-Water Tank Condenser

Figure 27 outlines the solution technique. Note that Lcond is the total length of condenser tubing and hf_cond is the enthalpy of saturated liquid at p3. An iterative procedure is used to solve for tx and UA_dry'. The procedure is based on finding the refrigerant temperature "tx" that makes

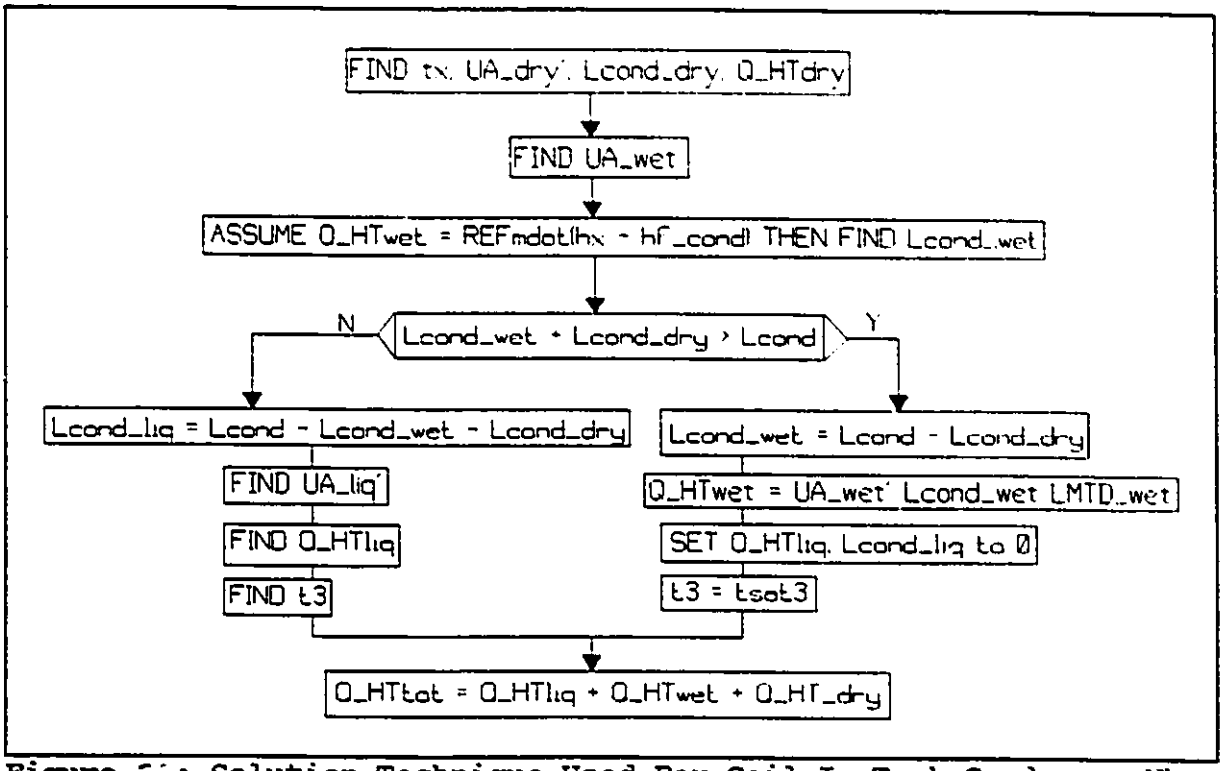

Figure 3?: Solution Technique Used For Coil In Tank Condenser When Accumulator at Evaporator Outlet

twallx equal to tsat2 (within a tolerance of 0.1 degrees Celsius).

If the overall thermal conductance of the wet portion, UA_wet, is an input to the program, then the slightly modified solution technique outlined in figure 28 is used.

b. Concentric Tube Condenser

The procedure used to find t3 and Q_HTtot is shown in figure 29. Note that hx is the enthalpy of the refrigerant as it leaves the dry portion of the condenser. Using effectiveness to calculate Q_HTliq and t3 ensures that the second law of thermodynamics is satisfied.

The iterative procedure used for the calculation of

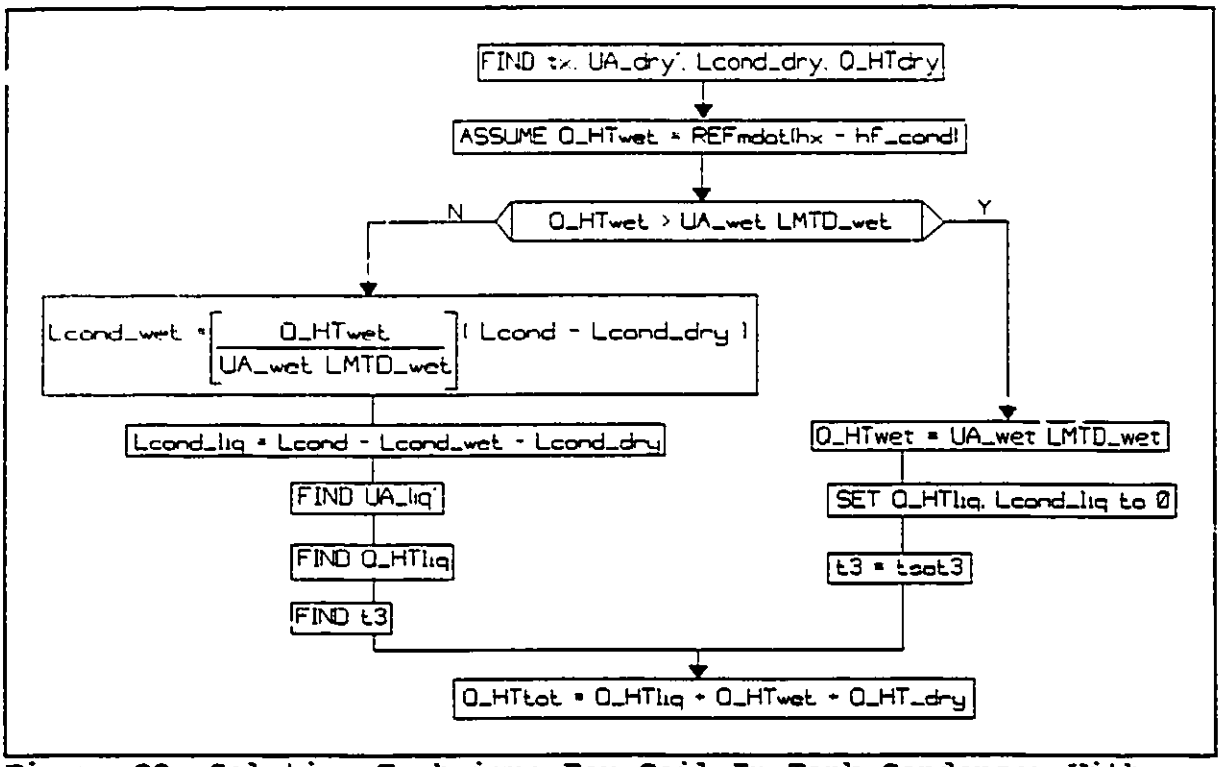

Figure 28: Solution Technique For Coil In Tank Condenser With Accumulator at Evaporator Outlet And Thermal Conductance of Wet Portion of Condenser as Input

tx, twx, and hx is illustrated in figure 30. For each estimate of tx, a corresponding value of twallx is calculated. The variable, error_Twallx, is defined as (twallx-tsat2). The best possible estimate of tx yields a value of twallx equal to tsat2, hence, makes error_Twallx go to zero. Figure 31 indicates that tx must lie between tsat2 and t2 (the refrigerant inlet temperature). Therefore tsat2 and t2 are the initial values of tx_n and tx_p respectively. The following expression shows how tx_n and tx_p are used to obtain tx:

$$tx = tx\_n + \frac{tx\_p - tx\_n}{1 + \frac{error\_Twallx\_p}{error\_Twallx\_n}} \qquad (31)$$

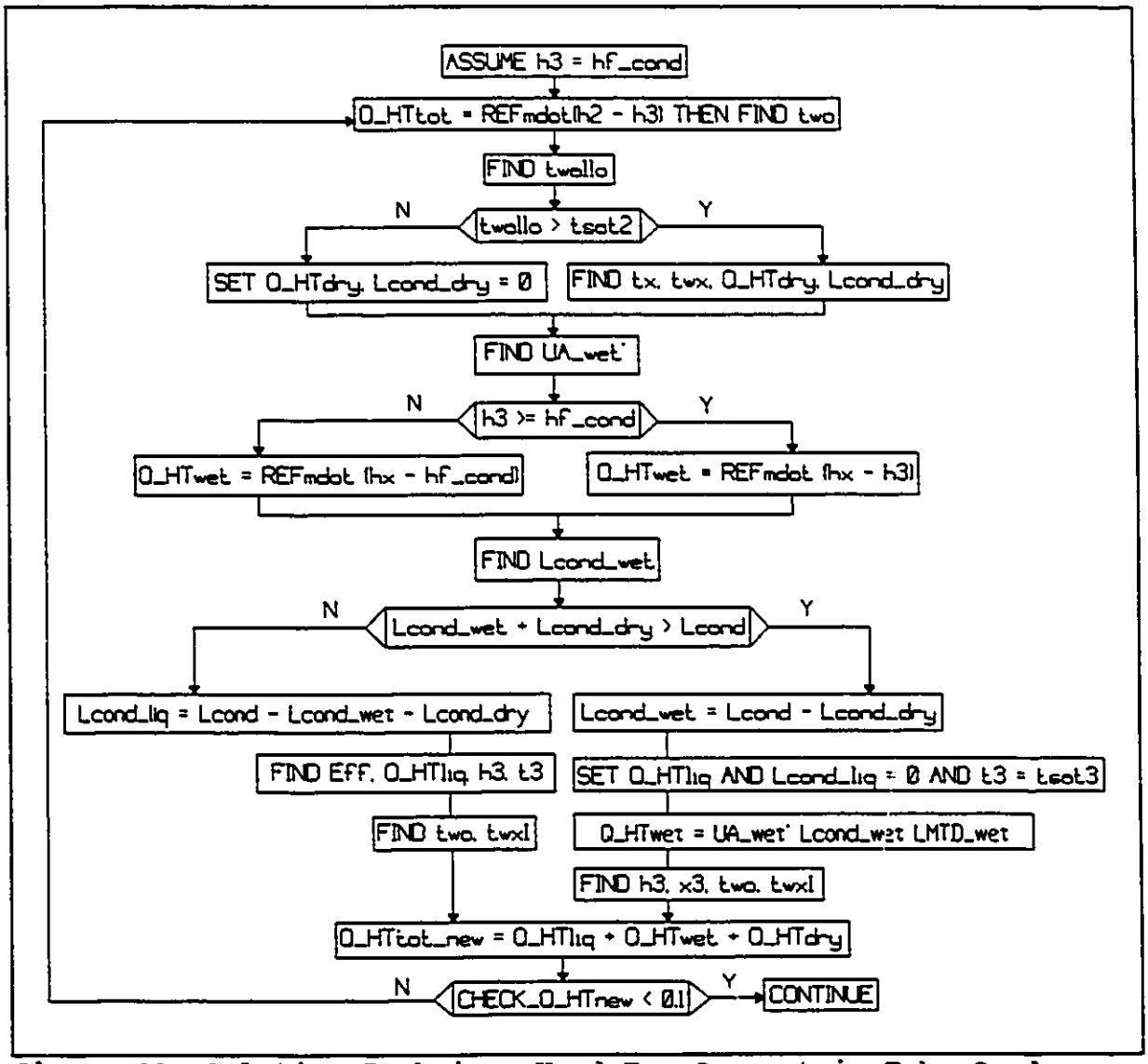

Figure 29: Solution Technique Used For Concentric Tube Condenser When Accumulator at the Evaporator Outlet

If UA_wet is input to the program then the modified solution technique is used. This technique is outlined in figure 32.

2. <u>Accumulator at Condenser Outlet</u>

For the case in which an receiver is located downstream of the condenser, the objective of the condenser module is to

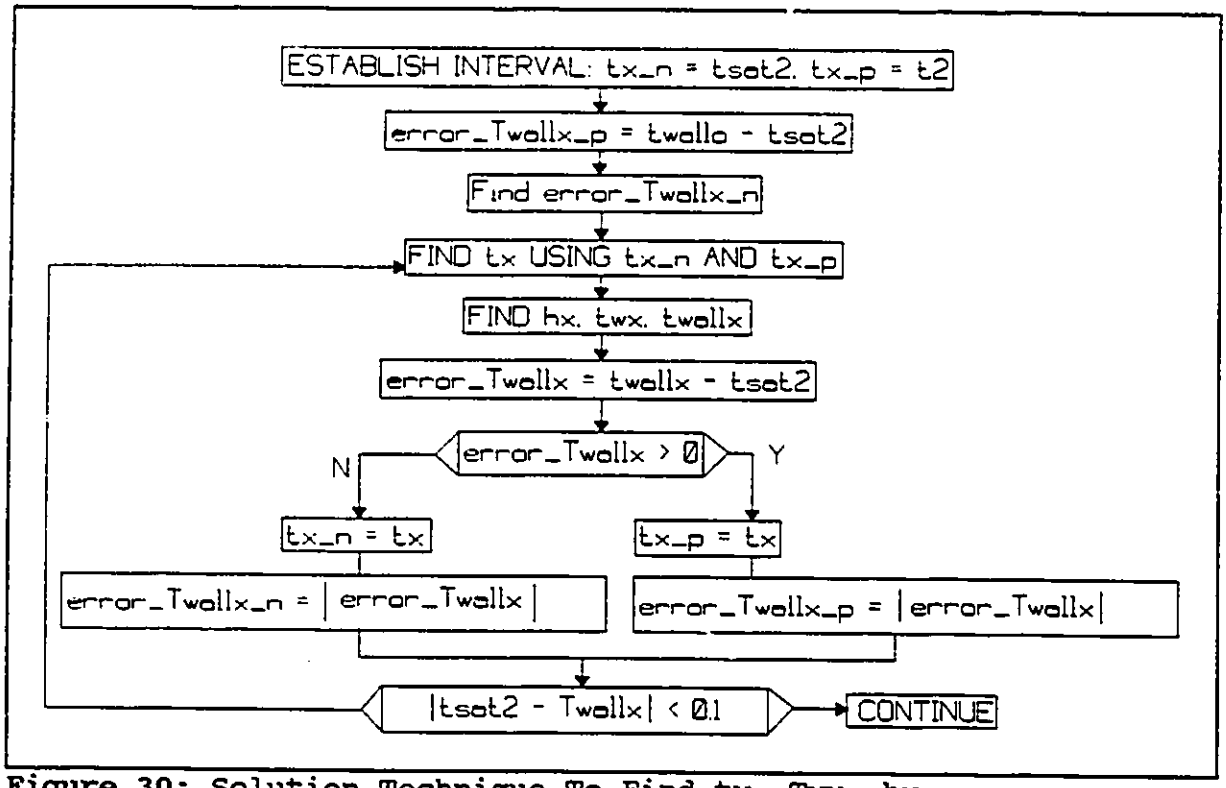

Figure 30: Solution Technique To Find tx, Twx, hx

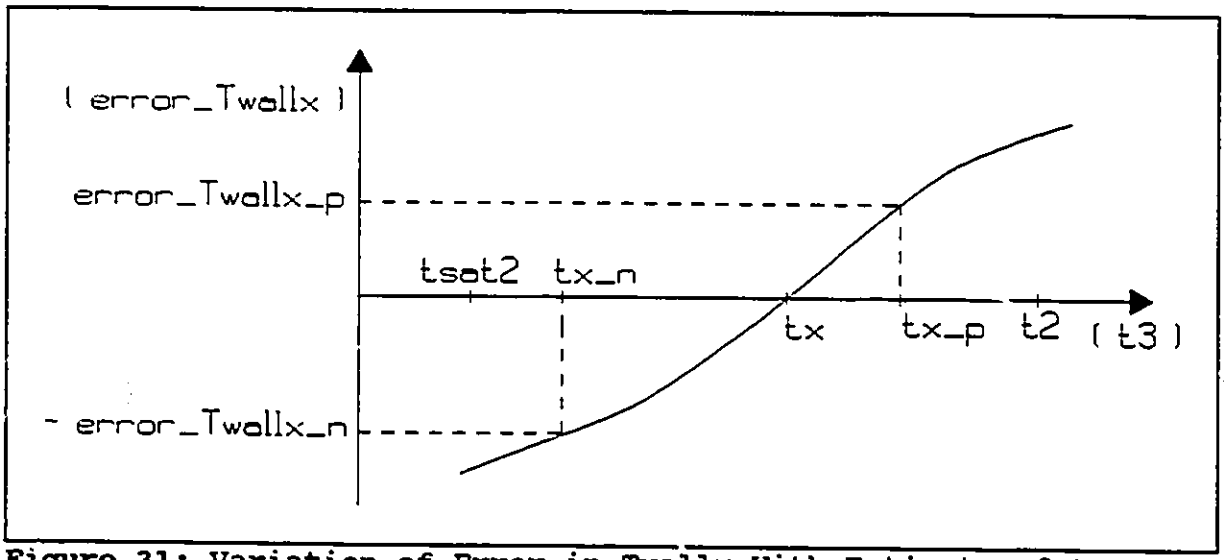

Figure 31: Variation of Error in Twallx With Estimate of tx

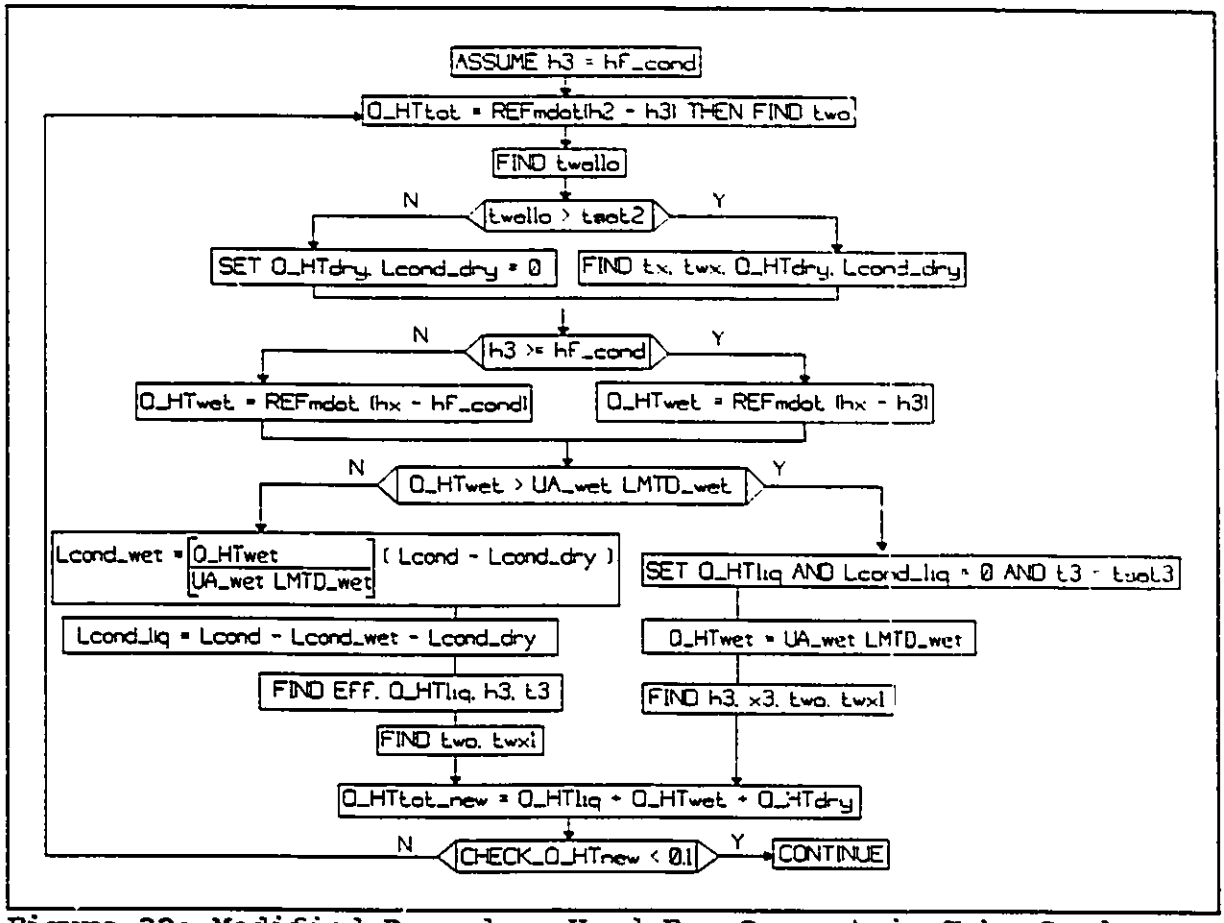

Figure 32: Modified Procedure Used For Concentric Tube Condenser When UA_wet is Input

calculate the amount of heat transferred from the condenser to the surroundings based on heat transfer relationships (Q_HTtot) and also based on the first law of thermodynamics (Q_thermo). When the condenser module is called from within the simulation program, the known quantities are the refrigerant inlet temperature and pressure, the refrigerant outlet temperature and pressure, the refrigerant mass flow rate, the size and configuration of the condenser, and the condenser cooling water temperature.

a. Coil-in-Water Tank Condenser

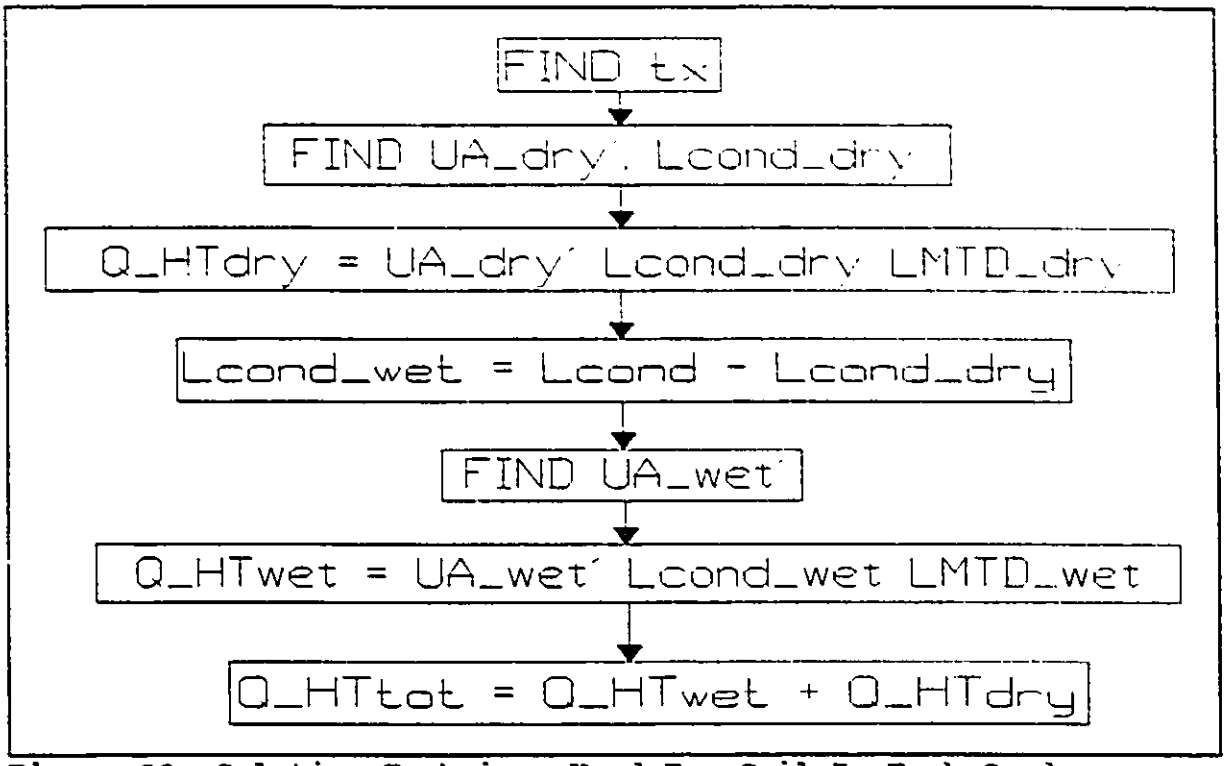

Figure 33: Solution Technique Used For Coil In Tank Condenser With Receiver Located at Condenser Outlet

Figure 33 outlines the procedure to find Q_HTtot. The same iterative method is used to find tx that was mentioned in section B.1.a of this chapter. The value of Q_thermo is easily determined from

$$Q\_thermo = REFmdot(h2 - h3) \tag{32}$$

since all quantities on the right hand side are known when the condenser module is called.

If UA_wet is input to the program then UA_wet' and Lcond_wet are not calculated, and Q_HTwet is given by

$$Q\_HTwet = UA\_wet\ LMTD\_wet \tag{33}$$

b. Concentric Tube Type Condenser

Figure 34 outlines the solution technique used to determine Q_HTtot. The water outlet temperature is determined

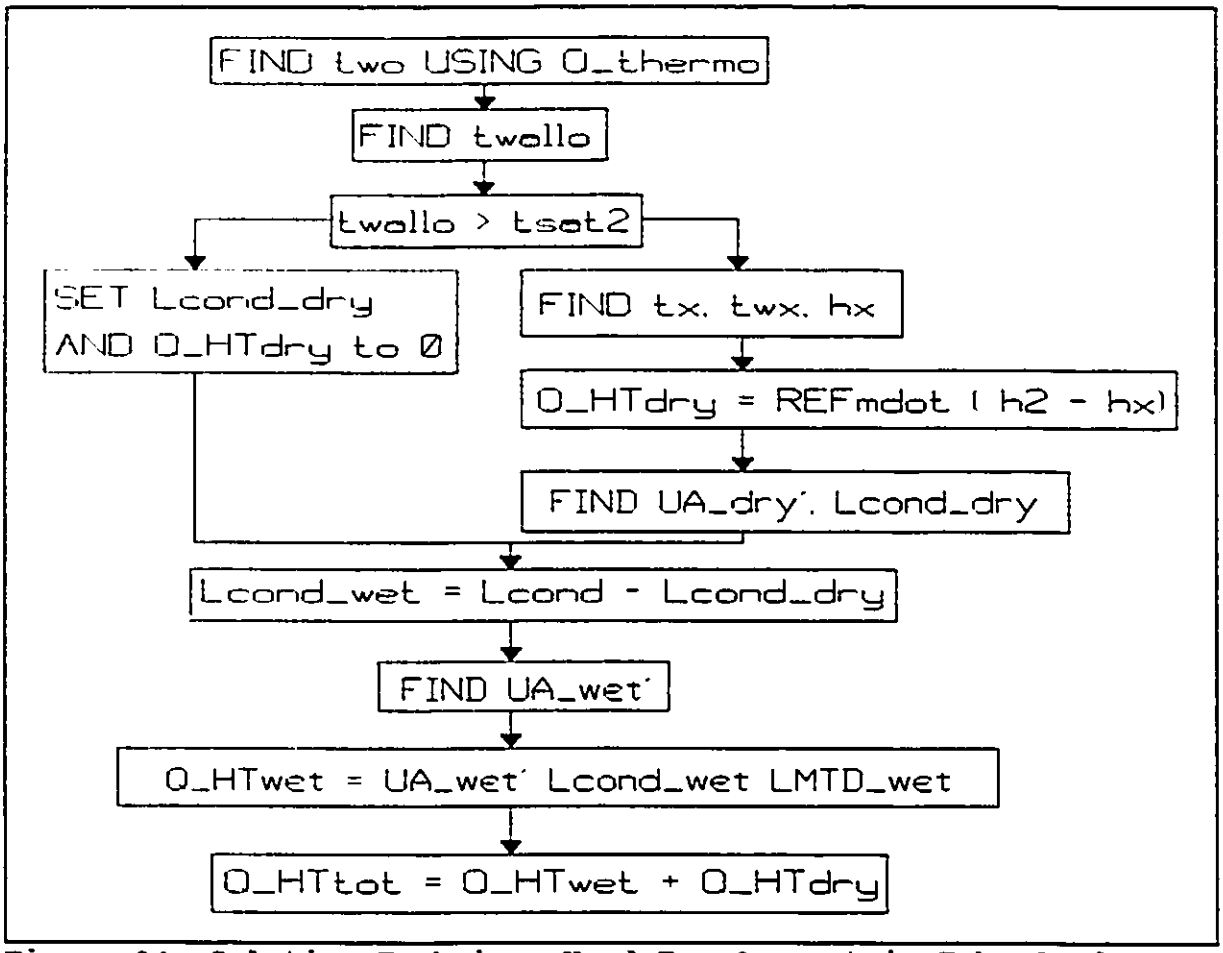

Figure 34: Solution Technique Used For Concentric Tube Condenser With Receiver Located at Condenser Outlet

from

$$Q\_thermo = H2Omdot\ H2Ocpf\ (tw_o - twi) \qquad (34)$$

where Q_thermo is easily determined by applying the first law of thermodynamics to the refrigerant. The same iterative procedure that is outlined in figure 30 is used to find tx, Twx and hx.

Again, if UA_wet is an input to the program then

Lcond_wet and UA_wet' are not calculated, and Q_HTwet is determined from (33).

V. EVAPORATOR MODELLING AND SIMULATION

The only evaporator that was modelled was a compact heat exchanger of the type shown in figure 35 in which air flows over a bundle of fined tubes.

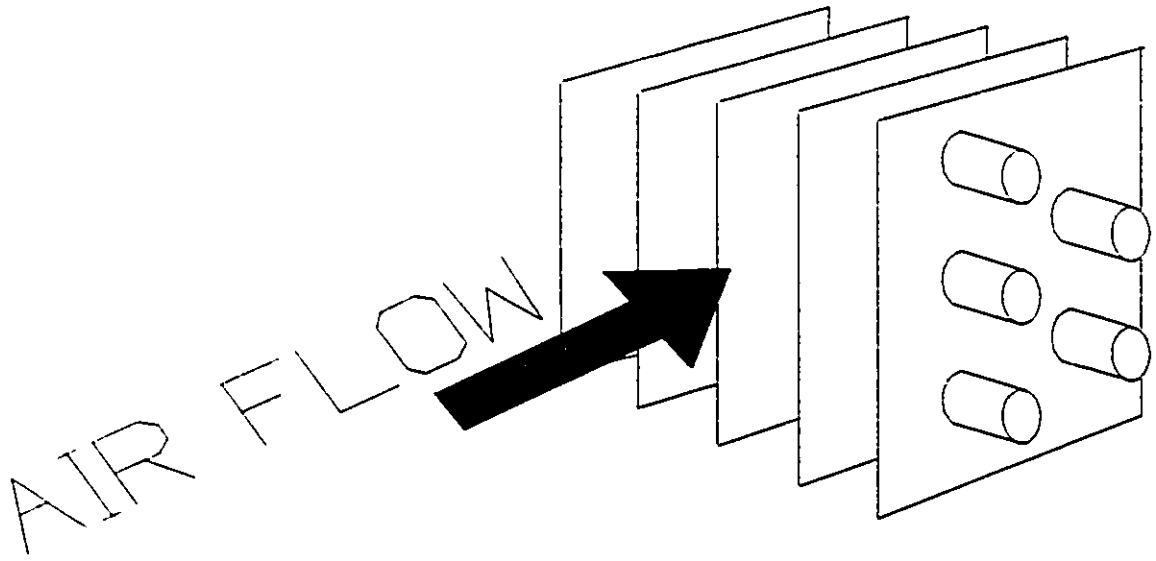

Figure 35: Evaporator That Was Modelled

A. Modelling of Evaporator

As shown in figure 36, the evaporator was modelled as two portions: the wet portion, in which *refrigerant* is a wet mixture; and the dry portion, in which *refrigerant* is superheated vapour. The following assumptions were made:

1) The dry portion of the evaporator can be modelled as a cross flow, single pass type heat exchanger in which both fluids are unmixed

2) No spacial variations in air temperature and relative humidity that are normal to the air flow.

3) The air side heat transfer coefficient is the same for both the wet and dry portions of the evaporator

4) The effect of bends on the refrigerant side heat transfer coefficient is negligible

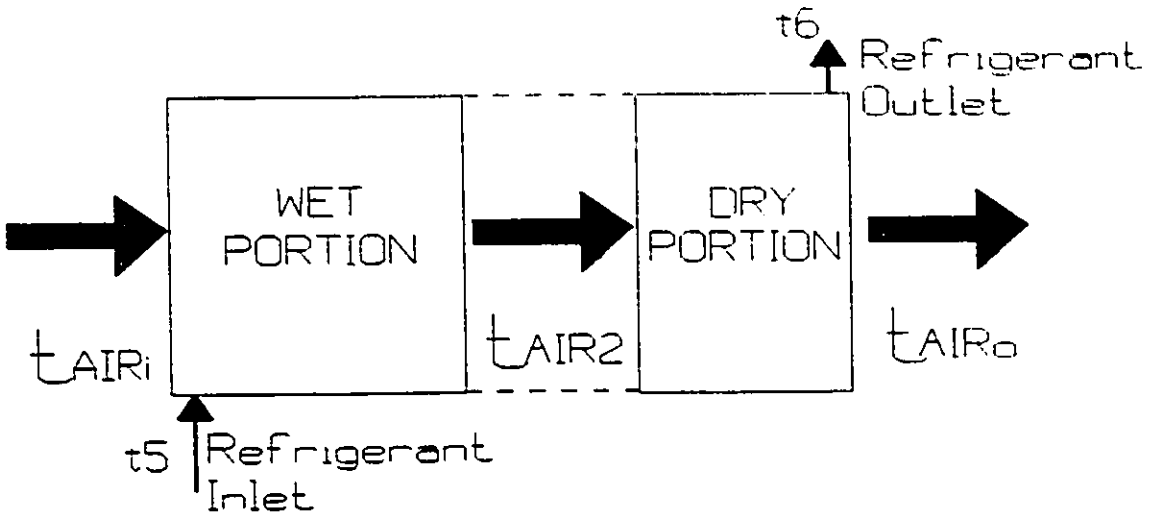

Figure 36: The Wet And Dry Portions Of Evaporator

5) The air side pressure drop is negligible

6) The refrigerant pressure at the end of the wet portion is equal to the refrigerant outlet pressure.

7) Frosting does not alter the mass flow rate of the air

8) The temperature of the frost is uniform and constant at 0 degrees Celsius

Figure 37 is a pressure versus enthalpy diagram that shows the process the refrigerant undergoes as it flows through the evaporator. The temperature of the refrigerant as it leaves the wet portion is equal to tsat6, the saturation temperature of the

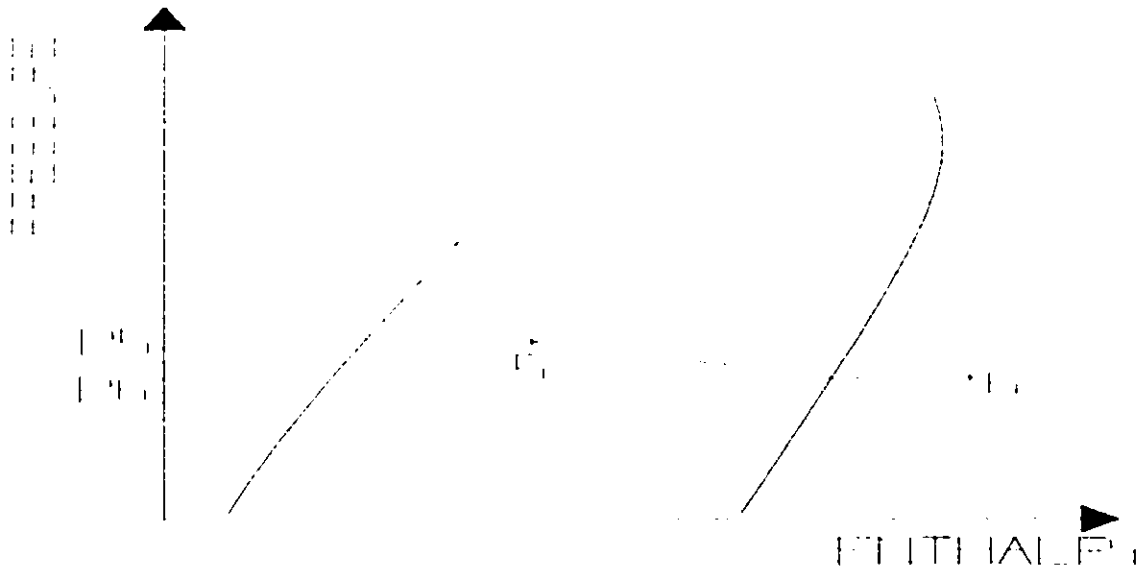

Figure 37: Process That Refrigerant Undergoes Inside Evaporator

refrigerant at p6.

Table 3 lists the correlations that are used to model the evaporator. Because of the way the evaporator was modelled, only refrigerant side heat transfer coefficients are calculated.

Correlation 4 is used to calculate local heat transfer coefficients in the wet portion of the evaporator. The average heat transfer coefficient is obtained from the following expression [32]:

$$\frac{1}{\bar{h}_{avg}} = \int_{x_5}^{1} \frac{dx}{\bar{h}_x} \qquad (35)$$

where x5 is the evaporator inlet quality. See Appendix I for the derivation of a similar expression that is used to model the condenser. The integral on the right hand side of (35) is

Table 3: Correlations Used To Model Evaporator

Correlation And Source	Restrictions And Use
1. $N_u = 0.021\, Pr^{0.5} R_e^{0.8}$ [32]	$0.6 < Pr < 0.8$ $10^4 < R_e < 10^5$ - *Single Phase* - *Forced Convection* - *Inside Horozontal Circular Tubes* - *Constant Surface Temperature* - *Refrigerant Side Heat Transfer Coefficient*

Table 3 Continued

2. $N_u = 5 + 0.015\, R_e^{a}\, Pr^{b}$ $a = 0.88 - \frac{0.24}{4 + Pr}$ $b = 0.333 + 0.5\, EXP(-0.6\, Pr)$ [32]	$0.1 < Pr < 10^4$ $10^4 < R_e < 10^5$ - *Single Phase* - *Forced Convection* - *Inside Horizontal Circular Tubes* - *Independent of Surface Boundary Condition* - *Refrigerant Side Heat Transfer Coefficient*
3. $N_u = 3.656$ [32]	$Re < 2300$ - *Otherwise Same Comments As For 1*
4. $\bar{h}_z = 0.023 \frac{FF\, k_f}{D_{evap}} \left(\frac{G\,(1-x)\, D_{evap}}{\mu_f} \right)^{}$ $FF = 2.37 \left(0.29 + \frac{1}{X}\right)^{0.85}$ $X = \left(\frac{\mu_f}{\mu_g}\right)^{0.1} \left(\frac{1-x}{x}\right)^{0.9} \left(\frac{\rho_g}{\rho_f}\right)^{0.5}$ [20]	- $x > 0.10$ - *Forced Covection Boiling* - *Inside Circular Tubes* - *Refrigerant Side Heat Transfer Coefficient*

evaluated using the approximation

$$\int_{x_1}^{1} \frac{1}{\bar{h}_x} dx = \sum_{i=1}^{20} \frac{\Delta x_i}{\bar{h}_{x_i}} \qquad (36)$$

1. Accumulator at Evaporator Outlet

When the accumulator is located at the evaporator outlet the task of the evaporator module is to calculate how much heat is transferred from the air to the refrigerant based on heat transfer relationships, Q_HTtot; how much heat is transferred from the air to the refrigerant based on the first law of thermodynamics, Q_thermo; the temperature of the air at the evaporator outlet, and the humidity ratio of the air at the evaporator outlet. When the evaporator module is called from within the simulation program, the known quantities are the evaporator's overall thermal conductance when the refrigerant process is completely inside the wet region, UA_allwet; the inlet temperature of the air, the mass flow rate and specific humidity of the air, and the refrigerant properties at the evaporator inlet and outlet.

a. The Solution Technique

Figure 38 outlines the solution technique that is used to find Q_HTtot. The log mean temperature difference, LMTD_e, is initially estimated based on the assumption that the refrigerant leaves the evaporator as a saturated vapour. Appendix II gives details on how tair_o and wo are found by applying the first law to the air space in the evaporator. The

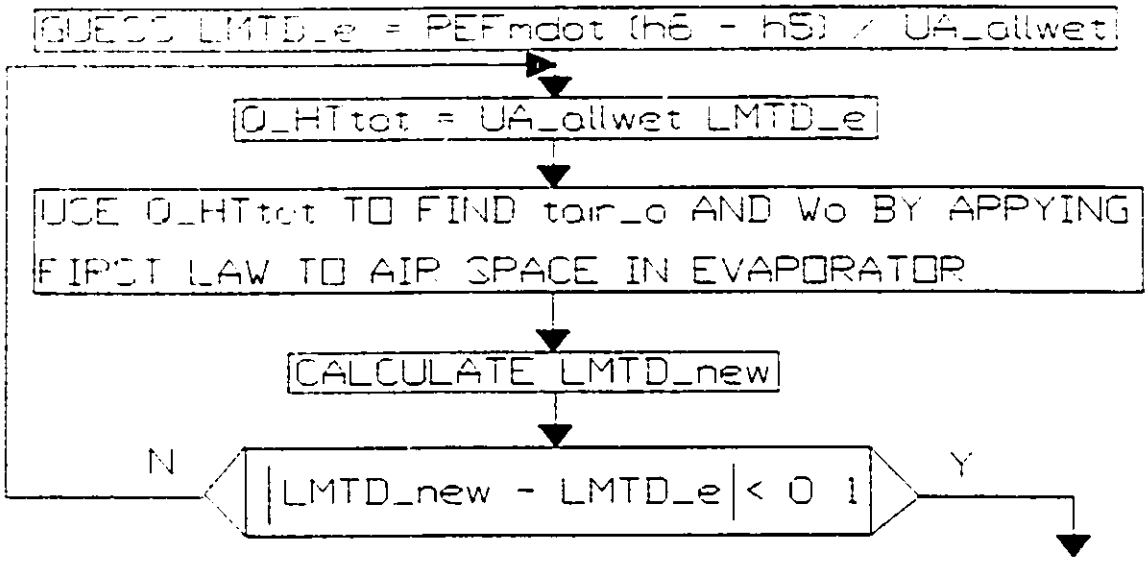

Figure 38: Solution Technique For Finding Q_HTtot When Accumulator At Evaporator Outlet

log mean temperature difference, LMTD_new, is given by

$$LMTD\_new = \frac{(tair\_i - t5) - (tair\_o - tsat6)}{\ln\left[\frac{tair\_i - t5}{tair\_o - tsat6}\right]} \qquad (37)$$

After Q_HTtot is found, Q_thermo is found by applying the first law to the refrigerant space in the evaporator.

2. Accumulator at Condenser Outlet

In the case where the accumulator is located at the condenser outlet the task of the evaporator module is to calculate the amount of heat transferred from the air to the refrigerant, Q_HTtot (in this case Q_HTtot is equal to Q_thermo); the outlet air temperature, and the properties of the refrigerant at the evaporator outlet. When the evaporator module is called from within the simulation program, the known quantities are the

evaporator's overall thermal conductance when the process the refrigerant undergoes is completely inside the wet region, UA_allwet; the inlet temperature of the air, the mass flow rate of the air, and the refrigerant properties at the evaporator inlet.

a. The Solution Technique

Figure 39 is a flow diagram of the solution technique. The value of Qmax is the maximum amount

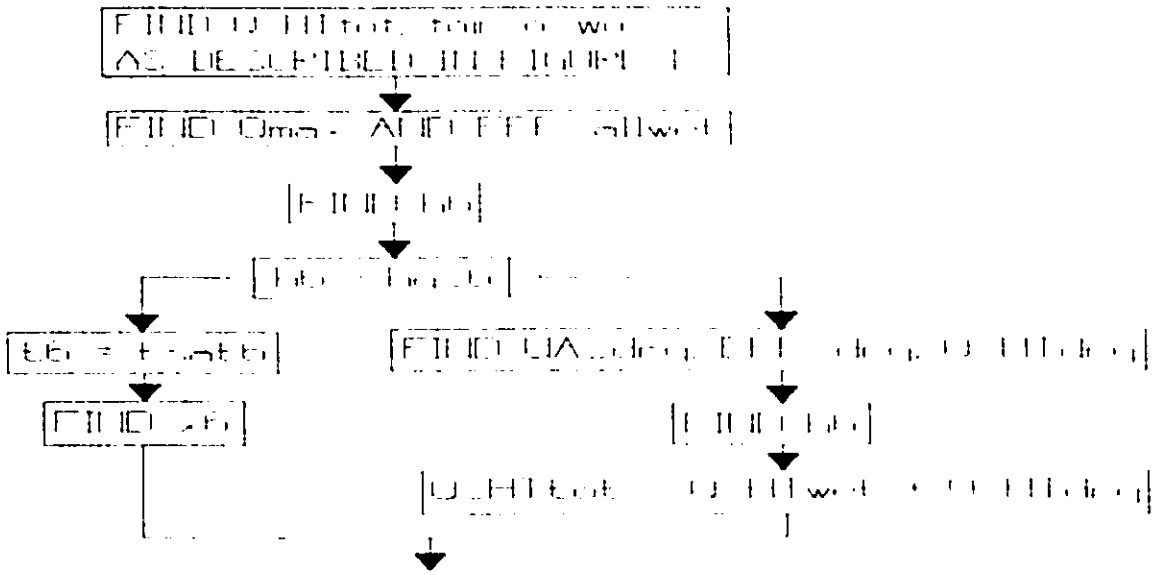

Figure 39: Solution Technique For Finding Q_HTtot When Receiver At Condenser Outlet

of heat that could possibly be transferred from the air to the refrigerant in the wet region. See Appendix II for details on how Qmax is determined. The effectiveness of the evaporator, EFF_allwet, is calculated as Q_HTtot/Qmax where Q_HTtot was calculated by assuming that the refrigerant leaves the evaporator as a saturated vapour. The value of h6 is found by applying the

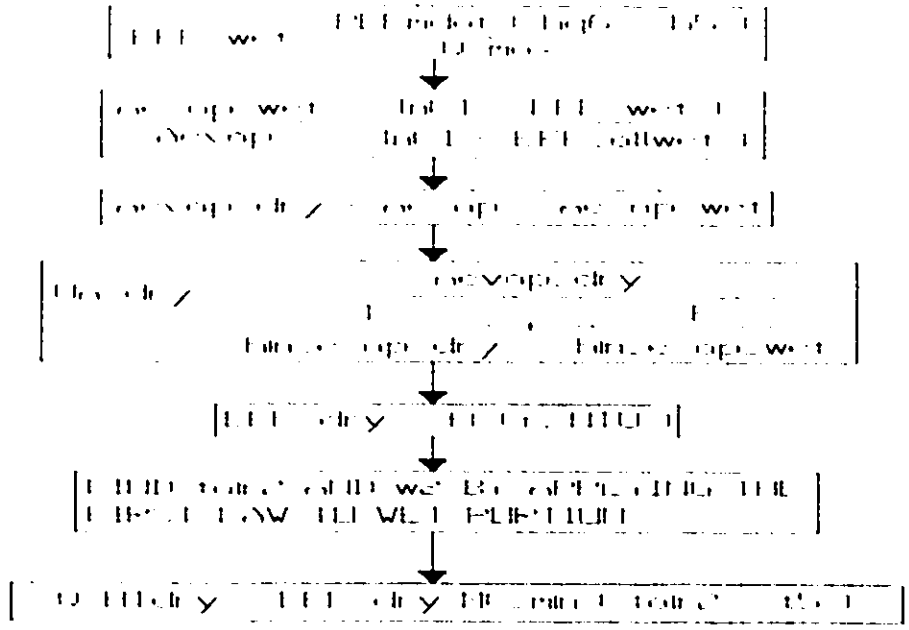

Figure 40: Procedure to Find Q_HTdry

first law to the refrigerant space inside the evaporator. If h6 is found to be greater than hg_6, the enthalpy of saturated vapour at t6, then EFF_allwet is used in the procedure to find Q_HTdry.

Figure 40 outlines the way Q_HTdry is obtained. Note that EFF_allwet is given by

$$EFF\_allwet = \frac{UA\ allwet\ LMTD\_e}{Q_{max}} \qquad (38)$$

It is important to understand the distinction between EFF_allwet and EFF_wet: EFF_allwet is the effectiveness that the *entire* evaporator would have if the refrigerant exited as a saturated vapour; EFF_wet is the effectiveness of the wet portion of the evaporator alone. The total refrigerant side area of the

evaporator, Aevap, is given by

$$A_{evap} = \pi \, D_{evap} \, L_{evap} \tag{39}$$

where Devap is the inside tube area and Levap is the total length of tubing; Aevap_wet and Aevap_dry are similarly defined for the wet and dry portions of the evaporator. The expression for the ratio of Aevap_wet to Aevap is derived in Appendix II. The quantity F, which appears in the expression for UA_dry, is defined as

$$\bar{h}in\_evap\_wet \, A_{evap\_wet} = F \, \bar{h}out\_evap\_wet \, A_{out\_wet} \tag{40}$$

where $\bar{h}in\_evap\_wet$ and $\bar{h}out\_evap\_wet$ are, respectively, the refrigerant and air side heat transfer coefficients for the wet portion, and Aout_wet is the air side area of the wet portion. The expression for UA_dry is derived in Appendix II. The effectiveness of the dry portion is calculated as [18]

$$EFF\_dry = 1 - EXP\left[\frac{NTU^{0.22}}{C_r}\{EXP[-C_r \, NTU^{0.78}] - 1\}\right] \tag{41}$$

where Cr is MCp_max/MCp_min and NTU is UA_dry/MCp_min. The value of MCp_min is the lesser of AIRmdot*AIRcp and REfmdot*Cpg; MCp_max is the larger of the two. The values of tair2 and w2 are determined by applying the first law to the air space in the wet portion of the evaporator as described in section A of Appendix II.

VI. THE COMPRESSOR MODULE

The objective of the compressor module is to determine the thermodynamic properties of the refrigerant at the compressor outlet, the mass flow rate of the refrigerant, and the amount of work done on the compressor crank shaft. The known parameters are the refrigerant's thermodynamic properties at the compressor inlet; the compressor outlet to inlet pressure ratio, PRATIO; the compressor crank shaft speed, N; the total swept volume of the compressor, Vs; the isentropic ratio, isen_ratio defined in equation 42; and the overall work ratio, ovrl_ratio.

If the process inside the compressor is assumed to be polytropic then the following are inputs to the program: the polytropic constant for the process inside the compressor, n; and the clearance fraction of the compressor, CF.

IF the process inside the compressor is not assumed to be polytropic then an experimentally determined correlation for volumetric efficiency must be specified. See section B of this chapter for details.

Only reciprocating compressors are simulated in the program. Reciprocating compressors with double acting pistons or multiple stages are not simulated.

A. State of Refrigerant at Outlet

The isentropic ratio, isen_ratio, is defined as

$$isen\_ratio = \frac{h2_s - h1}{h2 - h1} \qquad (42)$$

where h2s is the enthalpy the refrigerant would have if the process in the compressor were isentropic. The actual and isentropic processes are shown in figure 41 on a temperature versus entropy diagram. Note that if the actual process is adiabatic then isen_ratio is equal to the isentropic efficiency. In any process where heat transfer occurs isen_ratio may be greater than one and cannot therefore be considered an efficiency. Once h2s is known h2 is easily found from (42).

If the accumulator is located downstream of the evaporator then state 1 is always in the superheated vapour region. In this case h2s is given by the correlation for the enthalpy of refrigerant vapour:

$$h2_s = h(t_{2s}, v_{2s}) \qquad (43)$$

However, before this correlation can be used t2s and v2s must be found by solving the following equations simultaneously:

$$s_{2s} = s(t_{2s}, v_{2s}) \qquad (44)$$
$$p_{2s} = p(t_{2s}, v_{2s}) \qquad (45)$$

In figure 41 it can be seen that s2s equals s1 and p2s equals p2; therefore the left hand sides of the preceding equations are known.

If the accumulator is located at the condenser outlet the situations depicted in figure 42 may also occur. Neither case is a desirable operating condition since the presence of liquid in

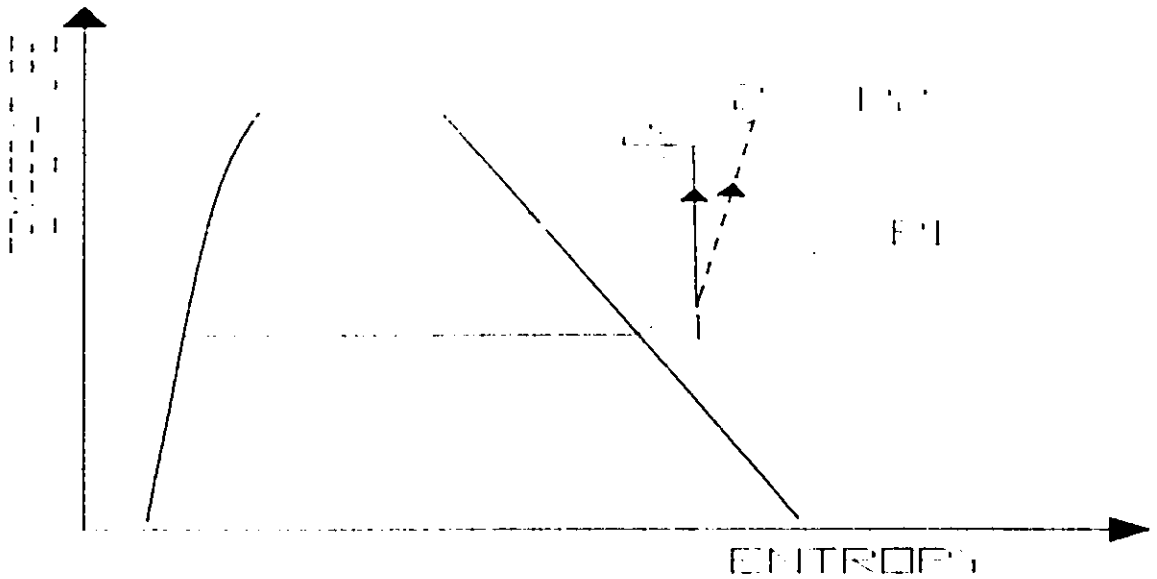

Figure 41: The Actual and Isentropic Processes

the compressor can be very destructive.

In the first case shown on figure 42, in which state 2s is in the superheated vapour region, the value of h2s is obtained in the manner previously described; in the second case, however, h2s is calculated by

$$h_{2s} = hf(t_{cond}) + x_{2s}\, h_{fg}(t_{cond}) \qquad (46)$$

where x2s is given by

$$x_{2s} = \frac{s_{2s} - s_f(t_{cond})}{s_{fg}(t_{cond})} \qquad (47)$$

B. <u>Refrigerant Mass Flow Rate</u>

The refrigerant mass flow rate is calculated as follows:

$$REFmdot = \frac{volum\_eff\ V_s\ N}{v_1} \qquad (48)$$

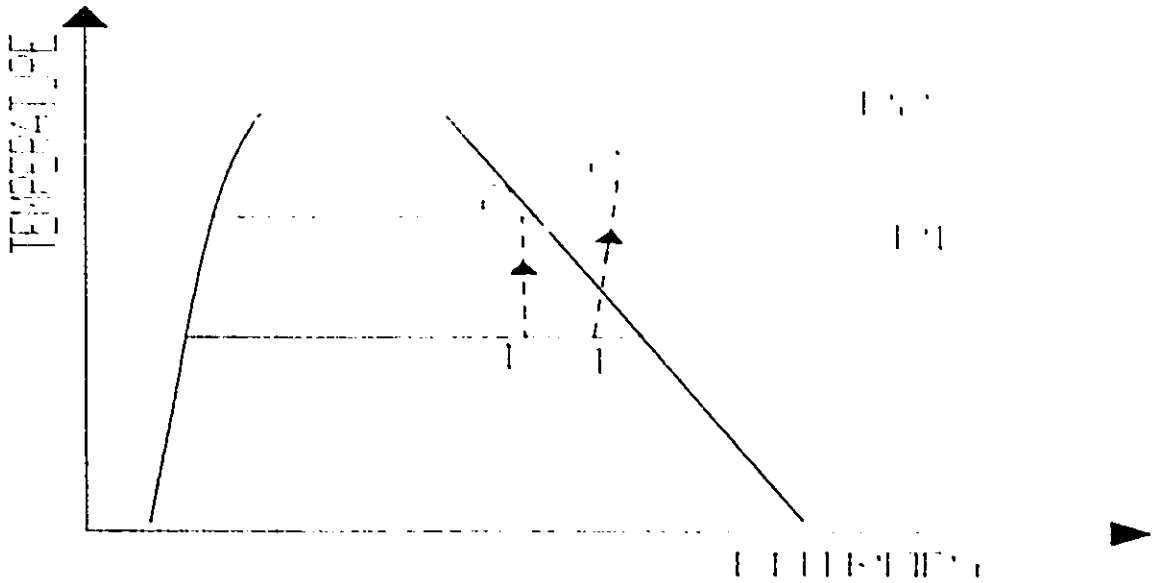

Figure 42: Possible Situations If Receiver at Condenser Outlet

The volumetric efficiency, volum_eff, can either be entered as a correlation in terms of PRATIO or calculated as follows:

$$volum\_eff = 1 + CF(1 - PRATIO^{(\frac{1}{n})}) \quad (49)$$

The derivations of the expressions for refmdot and volum_eff may be found in any applied thermodynamics text book [40]. The required assumptions are that the re-expansion of the refrigerant (process c to d on figure 43) is polytropic and that the specific volume of the refrigerant does not change during the intake stroke (process d to a on figure 43).

If volum_eff is specified as an experimentally determined correlation, then the user must specify the values of A1, A2, A3, A4, and A5 in the following equation:

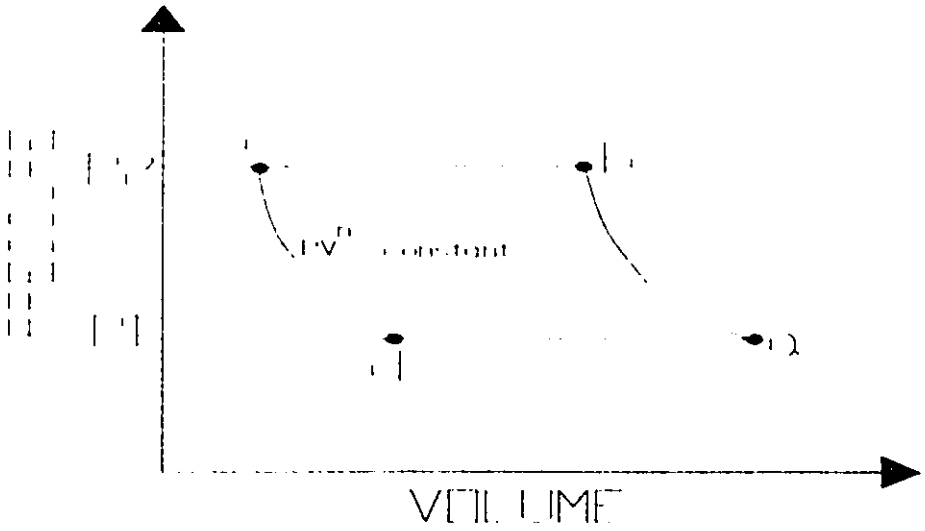

Figure 43: The Process Inside Compressor

$$volum\_eff = A1 + A2\ (PRATIO)^{A3} + A4\ (PRATIO)^{A5} \qquad (50)$$

A correlation of the form given above was found to correlate the experimental data discussed in chapter IX as well as experimental data collected by Tassou et al [36].

C. Work Done on Crank Shaft

The overall work ratio, ovrl_ratio, is defined as

$$ovrl\_ratio = \frac{Wcomp\_mec}{Ecomp} \qquad (51)$$

where Wcomp_mec is the actual work done on the compressor crank shaft and Ecomp is given by

$$Ecomp = REFmdot\ (h2-h1) \qquad (52)$$

VII. PROPERTY SIMULATION

The program makes use of correlations for the thermodynamic and thermophysical properties of R-12, R-22, water, and air. This section lists the correlations that are used. In some cases (e.g. to find the temperature of saturated liquid refrigerant given its pressure) iterative procedures are used. All iterative procedures for property evaluation are also explained in this section.

A. Properties of R-12

Table 4 lists the functional form of the property correlations which are used for R-12 and the source for each correlation.

As shown in table 4 the main sources for R-12 property correlations were ASHRAE's Thermodynamic Properties of Refrigerants [3] and ASHRAE's Thermophysical Properties of Refrigerants [2]. It was found, however, more convenient to use a correlation for the latent heat of vaporization provided by Downing [12]. In order to ensure that the correlations provided by Thermodynamic Properties of Refrigerants were properly implemented into the program they were checked against the values tabulated in 1989 ASHRAE Handbook: Fundamentals [4]. This provided a legitimate check because the correlations provided by ASHRAE [3] produced the tables in 1989 ASHRAE Handbook: Fundamentals. It was found that the values produced by the correlations of ASHRAE [3] agreed with the tabulated values in

1989 ASHRAE Handbook: Fundamentals.

Table 4: Functional Form and Source of Each Correlation For R-12

Functional Form (See Appendix III for full correlations)		Source
Gas Density	dg =dg(t)	ASHRAE [3]
Gas Thermal Conductivity	kg =kg(t)	ASHRAE [2]
Gas Viscosity	μg =μg(t)	ASHRAE [2]
Gas Specific Heat Capacity	cpg =cpg(t)	ASHRAE [2]
Liquid Density	df =df(t)	ASHRAE [3]
Liquid Thermal Conductivity	kf =kf(t)	ASHRAE [2]
Liquid Viscosity	μf=μf(t)	ASHRAE [2]
Liquid Specific Heat Capacity	cpf =cpf(t)	ASHRAE [2]
Saturation Pressure	psat =psat(t)	ASHRAE [3]
Latent Heat of Vaporization	hfg =hfg(t)	Downing [12]
Vapour Enthalpy	h =h(t,v)	ASHRAE [3]
Vapour Entropy	s =s(t,v)	ASHRAE [3]
Vapour Equation of State	p =p(t,v)	ASHRAE [3]

B. Properties of R-22

Table 5 lists the property correlations which are used for R-22 and the source for each correlation.

In the case of R-22, the correlations used for the enthalpy and entropy of superheated vapour are those provided by Downing [12] instead of the correlations provided by ASHRAE [3] because Downing's were in closer agreement with data tabulated by ASHRAE [4].

C. Refrigerant Properties Derived From Other Properties

For both R-12 and R-22 the same basic relationships are used

Table 5: Functional Form and Source of Each Correlation for R-22

Functional Form (See Appendix III for full correlations)		Source
Gas Density	dg =dg(t)	ASHRAE [3]
Gas Thermal Conductivity	kg =kg(t)	ASHRAE [2]
Gas Viscosity	μg =μg(t)	ASHRAE [2]
Gas Specific Heat Capacity	cpg =cpg(t,p)	Kletskii [22]
Liquid Density	df =df(t)	ASHRAE [2]
Liquid Thermal Conductivity	kf =kf(t)	ASHRAE [2]
Liquid Viscosity	μf=μf(t)	ASHRAE [2]
Liquid Specific Heat Capacity	cpf =cpf(t)	ASHRAE [2]
Saturation Pressure	psat =psat(t)	ASHRAE [3]
Latent Heat of Vaporization	hfg =hfg(t)	Downing [12]
Vapour Enthalpy	h =h(t,v)	Downing [12]
Vapour Entropy	s =s(t,v)	Downing [12]
Vapour Equation of State	p =p(t,v)	ASHRAE [3]

for the calculation of the Prandtl number of saturated liquid, Prf; the Prandtl number of saturated vapour, Prg; the specific volume of saturated liquid, vf; the specific volume of saturated vapour, vg; the specific entropy of vaporization, sfg; and the enthalpy of saturated liquid, hf:

$$P_{r_f} = \frac{\mu_f c_{pf}}{k_f} \qquad (53)$$

$$P_{r_g} = \frac{\mu_g c_{pg}}{k_g} \qquad (54)$$

$$v_f = \frac{1}{d_f} \qquad (55)$$

$$v_g = \frac{1}{d_g} \qquad (56)$$

$$s_{fg} = \frac{h_{fg}}{T} \qquad (57)$$

$$h_f = h_{fg} - h_g \qquad (58)$$

The value of hg is from the correlation for the enthalpy of superheated vapour.

D. Iterative Procedures For Refrigerant Properties

Iterative procedures are used only when the desired property is not defined explicitly in a correlation.

1. Determining Vapour Temperature and Specific Volume Given Enthalpy and Pressure

Inspection of tables 4 and 5 reveals that the correlation for the entropy of superheated vapour is of the form

$$h = h(t, v) \qquad (59)$$

and that the equation of state for superheated vapour is of the form

$$p = p(t, v) \qquad (60)$$

Hence, the preceding correlations must be solved simultaneously if the temperature needs to be determined with enthalpy and pressure as the known properties. This is accomplished through the use of the Newton-Raphson method.

To use the Newton-Raphson method initial estimates are

required for t and v. As mentioned in chapter III, obtaining good initial guesses for refrigerant properties that need to be evaluated using iterative procedures has a very significant effect on how fast the program converges.

Based on the ideas of Hill and Jeter [17], the procedure explained in Appendix III was developed for obtaining the required initial estimates of t and v. For R-12, the error in the initial estimate for temperature never exceeded 3.82 degrees Celsius, and the error in the initial estimate for specific volume never exceeded 2.42 percent of the actual value.

2. Determining Vapour Temperature and Specific Volume Given Entropy and Pressure

Tables 4 and 5 reveal that the correlation for the entropy of superheated vapour is of the form

$$s = s(t, v) \tag{61}$$

and that the equation of state for superheated vapour is of the form

$$p = p(t, v) \tag{62}$$

The preceding correlations must therefore be solved simultaneously if the temperature needs to be determined with entropy and pressure as the known properties. Again this is accomplished through the use of the Newton-Raphson method for which initial estimates of temperature and specific volume were required. The procedure that was used to obtain the required estimates is described in Appendix III. In the case of R-12, the error in the initial estimate for temperature never exceeded 7.5

degrees Celsius, and the error in the initial estimate for specific volume never exceeded 2.4 percent of the actual value.

3. Determining Liquid Temperature Given Enthalpy

To find the temperature of saturated liquid given enthalpy the Newton-Raphson method was used. The required initial estimate for temperature is found based on the following approximation:

$$\frac{hf-hf(t_{ref})}{t-t_{ref}} = c_{p_f}(t_{ref}) \qquad (63)$$

The value of the reference temperature, tref, was arbitrarily chosen within the range of values expected in the simulation program. This method is effective because cpf is a relatively weak function of temperature.

4. Determining Saturation Temperature Given Saturation Pressure

The Newton-Raphson method is also used to obtain saturation temperature given pressure. The initial guess required for the temperature is determined from

$$\ln(P_r) = A_1 + A_2\left(\frac{1}{T_r}-1\right) \qquad (64)$$

where Pr and Tr are defined as p/pc and t/tc respectively; A1 and A2 are constants. Hill and Jeter [17] found that for refrigerants the relationship between ln(Pr) and (1/Tr-1) is essentially linear for values of Tr which are greater than 0.5 and less than 1. The constants A1 and A2 were determined by curve fitting values obtained from tabulated data [38]. The range of values for

saturation temperature encountered in the simulation program is well within the range of values for which (64) is valid (e.g. in the case of R-12 values of Tr ranging from 0.5 to 1 correspond to values of temperature ranging from -80 to 111.8 degrees Celsius). It was found that the error in the initial estimates never exceeded 1.5 degrees Celsius (in the case of R-12).

E. Properties of Air And Water

Table 6 lists the functional form and source for each of the water property correlations that are used in the program.

Table 6: Functional Form and Source of Water Property Correlations

Functional Form (see Appendix III for full correlation)	Source
Bf = Bf(t)	Curve Fit of Data Tabulated by Incropera and Dewitt [18]
kf = kf(t)	Curve Fit of Data Tabulated by Incropera and Dewitt [18]
μf = μf(t)	Curve Fit of Data Tabulated by Incropera and Dewitt [18]
cpf = cpf(t)	Curve Fit of Data Tabulated by Incropera and Dewitt [18]
psat = psat(t)	ASHRAE [4]
Prf = Prf(t)	Curve Fit of Data Tabulated by Incropera and Dewitt [18]

The full correlations are provided in Appendix III. Table 7 lists the functional form and source for the air property correlations. The full correlations are provided in Appendix III.

Table 7: Functional Form and Source of Air Property Correlations

Functional Form (see Appendix III for full correlation)	Source
Thermal Conductivity $k = k(t)$	Curve Fit of Data Tabulated by Incropera and Dewitt [18]
Kinematic Viscosity $\nu = \nu(t)$	Curve Fit of Data Tabulated by Incropera and Dewitt [18]
Specific Heat Capacity $cp = cp(t)$	Curve Fit of Data Tabulated by Incropera and Dewitt [18]
Thermal Diffusivity $\alpha = \alpha(t)$	Curve Fit of Data Tabulated by Incropera and Dewitt [18]
Prandtl Number $Pr = Pr(t)$	Curve Fit of Data Tabulated by Incropera and Dewitt [18]

VIII. FRICTIONAL PRESSURE DROP IN CONDENSER, EVAPORATOR, AND INTERCONNECTING PIPING

A. Pressure Drop in Interconnecting Piping

With the exception of the piping connecting the throttle valve to the evaporator, the frictional pressure drops that occur in the interconnecting piping were calculated using correlations for single phase flow. The pressure drop in each tube is given by

$$\Delta P = \rho\left(\frac{f L}{D} + K\_minor\right)\frac{Vel^2}{2} \tag{65}$$

where L is the length of the tubing, D is the inside diameter of the tube, f is the friction factor. K_minor takes into account all minor losses in the tube and is determined based on experimental data tabulated by White [39] for losses in bends, elbows, entrances, exits, and tees (see Appendix V). The velocity of the refrigerant is given by

$$Vel = \frac{REFmdot}{\rho\pi\frac{D^2}{4}} \tag{66}$$

The friction factor, f, is given by

$$f = \frac{64}{Re} \tag{67}$$

for laminar flow, and from

$$f = \left[\left(\frac{-2}{\ln(10)}\right)\ln\left(\frac{rough}{3.7} + \frac{2.51}{R_e\sqrt{f}}\right)\right]^{-2} \qquad (68)$$

for turbulent flow where *rough* is the relative roughness.

In cases where the refrigerant is a wet mixture the homogeneous flow model was used i.e. the preceding single phase correlations are used but with density and viscosity evaluated as follows

$$\rho = (1-x)\rho_f + x\rho_g \qquad (69)$$

$$\mu = (1-X)\mu_f + x\mu_g \qquad (70)$$

where the subscripts "f" and "g" denote the properties of the liquid and gaseous components of the mixture respectively and x is quality.

For the piping that joins the throttle valve to the evaporator, Bo Pierre's correlation is used [6]. This correlation is discussed in section C of this chapter.

B. Pressure Drop In Condenser

The pressure drop in the wet portion of the condenser was determined by dividing the condenser into twenty portions of equal quality change. The pressure gradient for each of the twenty portions is given by

$$\frac{dp}{dz} = \left(\frac{dp}{dz}\right)_f + \left(\frac{dp}{dz}\right)_m + \left(\frac{dp}{dz}\right)_g \qquad (71)$$

the three terms on the right hand side are pressure gradients due

to friction, change in momentum, and gravity. For the concentric tube condenser the contribution of gravity is zero. For the coil in tank condenser the contribution of gravity was neglected. The remaining two pressure gradients are determined using the correlations derived by Traviss et al [37]:

$$\left(\frac{dp}{dz}\right)_f = -0.09(1 + 2.85X^{0.523})^2 \frac{\mu_g^{0.2}(Gx)^{1.8}}{\rho_g D^{1.2}} \quad (72)$$

$$\left(\frac{dp}{dz}\right)_m = -\frac{G^2}{\rho_g}\frac{dx}{dz}\left[2x + (1-2x)\left(\frac{\rho_g}{\rho_f}\right)^{\frac{1}{3}} + (1-2x)\left(\frac{\rho_g}{\rho_f}\right)^{\frac{2}{3}} - (2-2x)\left(\frac{\rho_g}{\rho_f}\right)\right] \quad (73)$$

where G is mass flux given by

$$G = \frac{REFmdot}{\pi\frac{D^2}{4}} \quad (74)$$

x is quality, and X is given by

$$X = \left(\frac{\mu_f}{\mu_g}\right)^{0.1}\left(\frac{(1-x)}{x}\right)^{0.9}\left(\frac{\rho_g}{\rho_f}\right)^{0.5} \quad (75)$$

The derivative, $\frac{dx}{dz}$,is calculated from

$$\frac{dx}{dz} = \frac{4\,h_z\,\Delta T}{DGh_{fg}} \quad (76)$$

where hfg is the latent heat of vaporization and ΔT is

equal to (tcond-Twall). The local heat transfer coefficient, hz, is calculated using both the correlations listed in table 8. The larger value is used in (76). For qualities greater than 0.20, correlation one of table 8 usually yields the larger value of hz. The pressure change for each of the twenty portions with equal quality change is given by

$$\Delta p_i = \left[\frac{\left(\frac{dp}{dz}\right)_f + \left(\frac{dp}{dz}\right)_m}{\frac{dx}{dz}} \right] \Delta x \qquad (77)$$

where the subscript "i" denotes that the pressure drop is one of the twenty portions.

The frictional pressure drops that occur in the dry and liquid portions of the condenser are calculated using the single phase correlations discussed in section A of this chapter.

C. Pressure Drop in Evaporator

The frictional pressure drop that occurs in the wet portion of the evaporator was calculated using the correlation developed by Bo Pierre [6]:

$$\Delta p = \left[\frac{f L}{D} + \frac{\Delta x}{x_m} \right] \frac{G^2}{\rho_m} \qquad (78)$$

where the subscript "m" indicates an average of the properties in the wet portion and the friction factor is given by

$$f = 0.00329 \left[\frac{R_e L g}{h_{fg} \Delta x} \right]^{0.25} \qquad (79)$$

The frictional pressure drop that occurs in the dry portion

of the evaporator is calculated using the single phase equations discussed in section A of this chapter.

Table 8: Correlations Used To Determine hz

Correlation And Source	Restrictions And Use
1. $N_u = 0.15 \frac{Pr_f R_{e_f}^{0.9}}{F2}\left[\frac{1}{X}+\frac{2.85}{X^{0.476}}\right]$ $F2 = 5\,Pr_f + 5\ln(1+5Pr_f) + 2.5\ln(0.0031 R_{e_f}^{0.812}),\ R_{e_f} > 1125$ $F2 = 5Pr_f + 5ln[1+Pr_f(0.0964 R_{e_f}^{0.585}-1)],\ 50 \le R_{e_f} \le 1125$ $F2 = 0.707 Pr_f R_{e_f}^{0.5},\ R_{e_f} < 50$ $X = \left(\frac{\mu_f}{\mu_g}\right)^{0.1}\left(\frac{(1-x)}{x}\right)^{0.9}\left(\frac{\rho_g}{\rho_f}\right)^{0.5}$ [37]	- *Forced Convection Condensation* - *Inside Staight Horizontal Circular Tube*
2. $h_{avg} = 0.553\left[\frac{g\rho_f(\rho_f-\rho_g)k_f^3\, h'_{fg}}{\mu_f\, \Delta T\, D_1}\right]^{\frac{1}{4}}$ $h'_{fg} = h_{fg} + \frac{3}{8} C_{p_f}\Delta T$ [32]	- *Forced Convection Condensation* - *Inside Staight Horizontal Circular Tube*

IX. TEST RIG

To validate the simulation program an experimental study was carried out on an air-to-water refrigeration unit charged with R-12. The objectives of the study were to obtain performance data for the system as a function of four parameters: the compressor crank shaft rotational speed, the condenser cooling water temperature, the throttle valve setting, and the condenser cooling water mass flow rate.

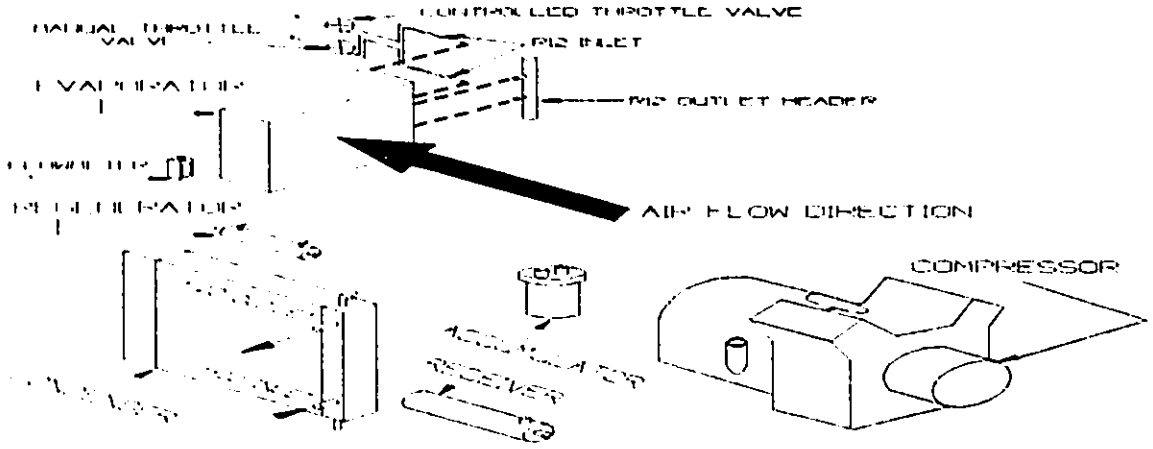

Figure 44: Three Dimensional Schematic of System

The system was built by Carrier Canada Ltd in 1959, but no documentation for the unit could be provided by Carrier. Specifications for the compressor were available from its manufacturer: Tecumseh Products of Canada. The motor specifications were available from its name plate. Figures 44 and 45 show the general appearance and configuration of the system components.

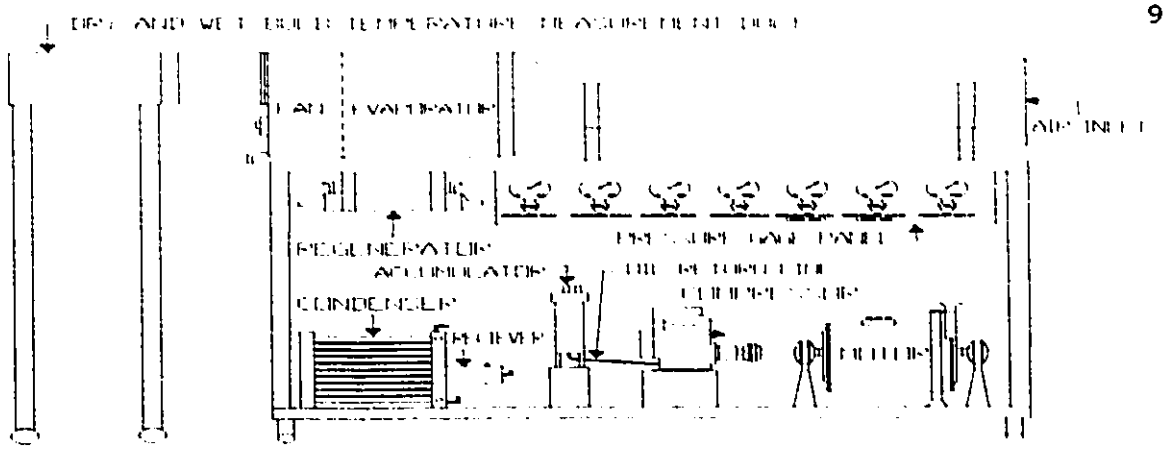

Figure 45: Two Dimensional Schematic of System

The compressor was a model CH four cylinder reciprocating type manufactured by Tecumseh Products of Canada. Each cylinder and piston had a 1.75 inch bore and 1.75 inch stroke [29].

A variable speed D.C. motor, manufactured by Bepco Canada Limited, powered the compressor. The motor was rated for 3 hp and designed to operate at drive shaft speeds ranging from 400 to 1200 RPM.

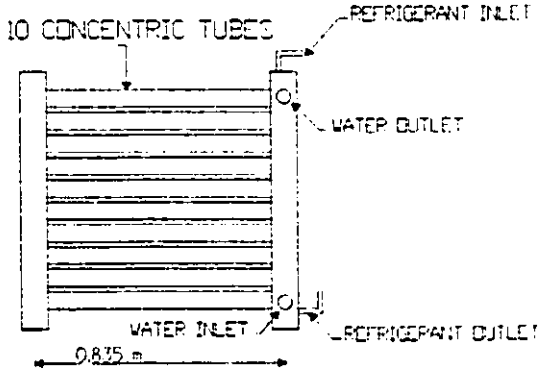

Figure 46: The Condenser

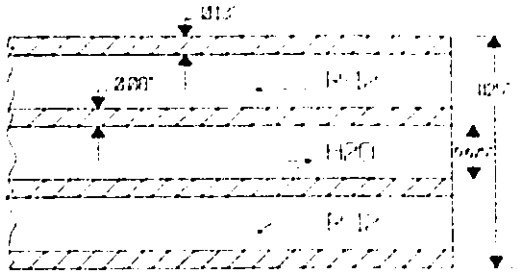

Figure 47: Concentric Tube of The Condenser

The condenser was a concentric-tube, counter-flow type with

R-12 flowing in the annulus as depicted by Figure 46. The diameters indicated on Figure 47 were determined by use of a micrometer. Tube thicknesses were then looked up in a handbook listing sizes of copper tubing [28].

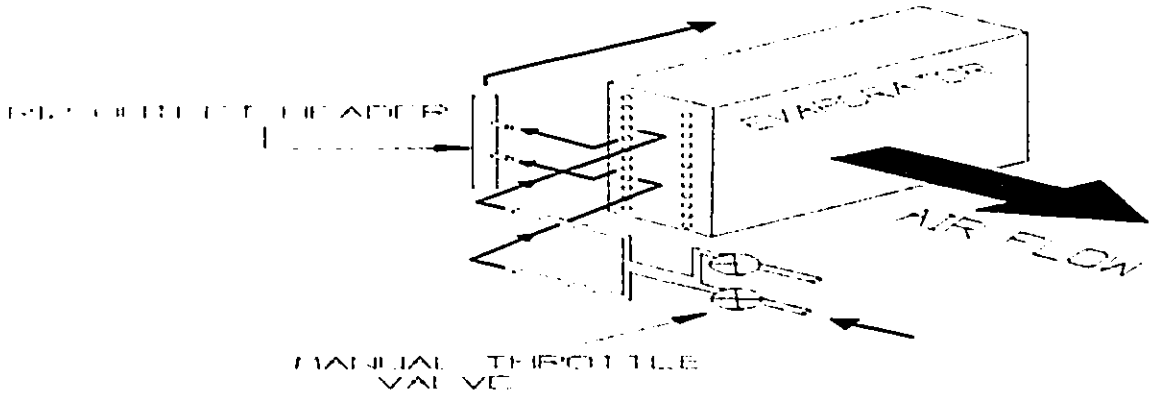

Figure 48: The Evaporator

The evaporator, shown in figure 48, consisted of two sets of twelve tubes (each set two rows deep and six rows high). Each tube had fourteen fins per inch. The fin thickness was approximately 0.2 mm, and the fin diameter was approximately 4.5 cm.

The regenerator was a counter flow concentric tube heat exchanger.

The following quantities were measured during each experimental run:

1) atmospheric pressure,
2) atmospheric temperature,
3) refrigerant volume flow rate (read directly from rotameter),
4) force applied to the dynamometer torque arm,

5) rotational speed of the compressor crank shaft,
6) average condenser cooling water mass flow rate (accumulated mass per time interval),
7) electrical power input to evaporator fan,
8) evaporator inlet air relative humidity (direct reading from hygrometer),
9) refrigerant pressure at seven locations on system,
10) refrigerant temperature at thirteen locations on system,
11) condenser cooling water inlet and outlet temperature,
12) evaporator outlet air dry bulb temperature (at nine locations on a cross sectional grid),
13) evaporator outlet air velocity (at nine locations on a cross sectional grid),
14) average evaporator outlet air wet bulb temperature.

A. Measurement of Atmospheric Pressure

The atmospheric pressure was measured with a mercury filled barometer. As illustrated in Figure 49, the mercury reservoir level could be adjusted to ensure that accurate readings were made. Through the use of a Vernier scale the barometer could be read to the nearest hundredth of an inch. By taking several readings (each time offsetting and then readjusting the mercury reservoir level) the uncertainty in the readings was found to be 0.05 inches.

B. Measurement of Atmospheric Temperature

The atmospheric temperature was measured with an Anschutz

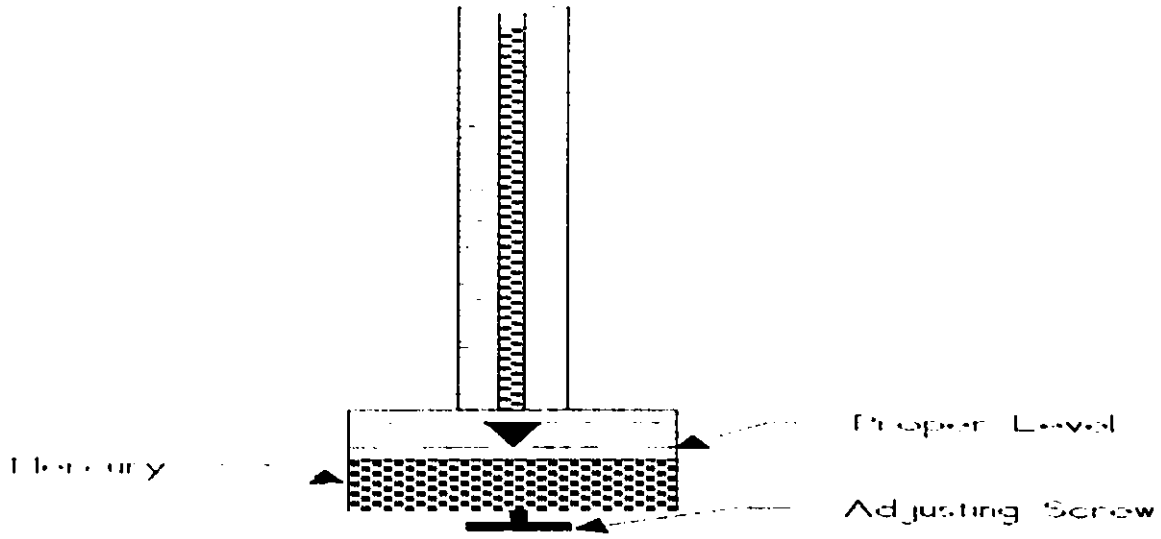

Figure 49: Barometer Adjustment

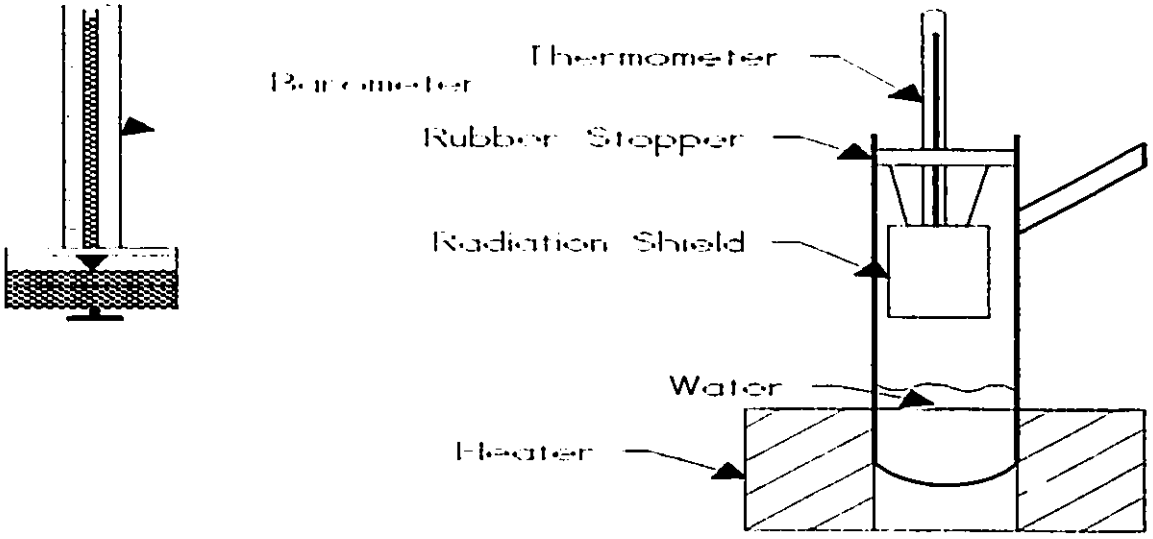

Figure 50: Calibration Apparatus

precision thermometer. The thermometer was calibrated at the steam point of water using the apparatus shown in Figure 50. The true value of the steam point was considered to be the saturation temperature of water at the pressure indicated by the mercury filled barometer. The effect of radiation was reduced by the shield shown in Figure 50. Care was taken to maintain the water

level above that of the heater to avoid superheating the steam. It was found that 0.40 degrees Celsius needed to be added to each reading. The uncertainty in the thermometer reading was equal to 0.1 degrees Celsius.

C. Measurement of Refrigerant Volume Flow Rate

The refrigerant volume flow rate was measured with a rotameter located about 0.70 meters upstream of the throttle valve. The rotameter float was calibrated by the manufacturer for saturated R-12 at 90 degrees fahrenheit. Hence, in the data acquisition program, the rotameter reading was multiplied by the ratio of the actual density of the refrigerant in the rotameter to the density of saturated refrigerant at 90 degrees fahrenheit. The uncertainty in the rotameter reading was 2.36E-07 cubic meters per second.

D. Measurement of Force Applied to Dynamometer Torque Arm

The force applied to the dynamometer torque arm was measured by the dynamometer scales. For calibration, the scales were removed and had weights hung from them (see the CALC module in Appendix IV for the calibration curves). The uncertainty in the readings of the scales was 0.27 Newtons.

E. Measurement of Rotational Speed of Compressor Crank Shaft

The rotational speed of the compressor crank shaft was measured with a Hasler-M hand tachometer. The smallest division on the tachometer was 50 RPM (since the 3000 RPM scale was used). However, the uncertainty in the readings was estimated to be 15 RPM because the needle was thin and because it held steady while

readings were being taken. Based on comparisons with other tachometers, it was concluded that the accuracy of the tachometer was within this uncertainty.

F. Condenser Cooling Water Mass Flow Rate

The condenser cooling water mass flow rate was determined by collecting water in a pail for a period of time (usually about thirty seconds) measured by a digital stopwatch . The water's mass was then measured on a balance (Toledo "honest weight" scale). The uncertainty in the readings of the balance was 0.05 lbm. The uncertainty in the period of time taken to collect the water in the pail was 0.33 seconds because the stopwatch could not be started at exactly the instant water entered the pail, or stopped at exactly the instant water no longer entered the pail.

G. Electrical Power Input to Evaporator Fan

The electrical power supplied to the fan was measured with a Weston wattmeter. The 1 kW scale was read. The uncertainty in the reading was due to reading error and was equal to 0.01 W.

H. Evaporator Inlet Air Relative Humidity

The evaporator inlet air relative humidity was measured by an analog hygrometer. The hygrometer was calibrated through the following procedure. The evaporator fan was turned on with the refrigeration unit turned off (and having been turned off for long enough so that the refrigerant inside the evaporator coil was at room temperature). The wet bulb temperature of the air was measured by a thermocouple which was covered with a moist cloth and located in the outlet air duct. The inlet air relative

humidity could then be calculated because both the dry and wet bulb temperatures of the air were known. It was found that 0.82 had to be added to the hygrometer reading. The uncertainty in the hygrometer relative humidity reading was 1.5.

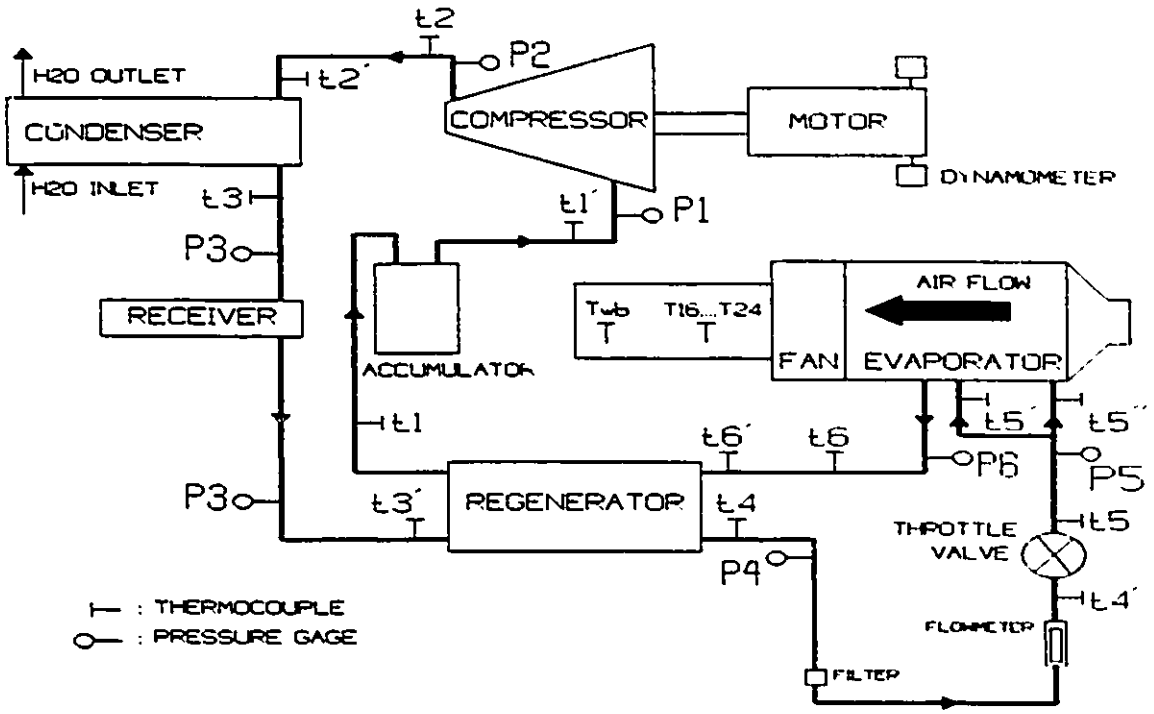

Figure 51: Refrigeration Unit Instrumentation

I. Measurement of Refrigerant Pressures

The refrigerant pressure at the locations shown in figure 51 were measured with Bourdon Tube pressure gages. Each calibrated with a dead weight gage tester (see CALC module in Appendix IV for calibration curves). Vibration of the gage needles could be attenuated by closing a small valve located just below each gage. The uncertainty in the readings for each gages was plus or minus 0.014 MPa.

J. Measurement of Refrigerant Temperatures

The refrigerant temperatures were measured with copper-constantan thermocouples. The thermocouples were positioned on the refrigeration unit as shown in figure 51. Each thermocouple had one junction on the pipe wall of the refrigeration unit and the other on the board of an Sciemetric 8082A data logger. The data logger is essentially an analog to digital converter which was interfaced with a computer (an IBM XT compatible). The analog signal each thermocouple sent to the data logger was proportional to the temperature difference between the pipe wall and the board on the data logger. A thermistor provided the temperature of the board so that the absolute temperature of the pipe wall could be determined. An aluminum bar was placed on the board to make the board's temperature more uniform.

The thermocouples were calibrated at the steam point of water using the same apparatus that was used to calibrate the precision thermometer which measured the atmospheric temperature (see section B of this chapter). The thermocouples were also calibrated at room temperature by using the precision thermometer reading as the true value. The calibration of the thermocouples can be found in the CALC module in Appendix IV.

If radial and longitudinal heat conduction through the pipe wall did not occur then the temperature of the pipe wall would be equal to the refrigerant temperature. However, radial and longitudinal conduction always occur and introduce error into the measurement of the refrigerant temperature. Half inch thick

Armstrong Armaflex insulation was placed on the piping to reduce this error.

Consider figure 52 to understand how fixed errors in the measurement of the refrigerant temperatures were accounted for in the data analysis program. The temperature of the refrigerant at point A is desired. However, to reduce the error due to longitudinal conduction, the thermocouple is installed on the pipe wall at point E, a short distance downstream of A. Let the difference in temperature between the pipe wall at point E and the refrigerant at point B due to radial conduction be (Tb-Te)rad. Let the difference in temperature between the same two points due to longitudinal conduction be (Tb-Te)lng. The difference in temperature between the refrigerant at point A and the refrigerant at point B is (Ta - Tb). All sources of fixed error were then combined as follows

$$T_a = T_e + (T_b - T_e)rad + (T_b - T_e)lng + (T_a - T_b) \qquad (80)$$

A complete discussion of how (Tb - Te)rad, (Tb - Te)lng, and (Ta - Tb) were calculated is given in Appendix V.

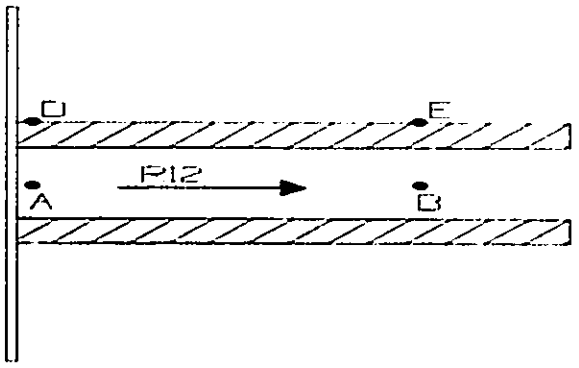

Figure 52: Positioning of Thermocouple on Pipe Wall

K. Condenser Cooling Water Temperatures

The condenser cooling water temperatures were measured by thermocouples in the same manner as were the refrigerant temperatures. One thermocouple measured the water inlet temperature and another measured the water outlet temperature. The same sources of error considered in the measurement of the refrigerant temperatures were taken into account in the measurement of the water temperatures.

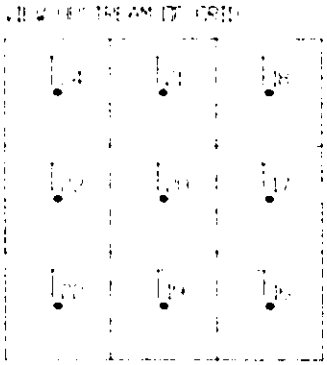

Figure 53: Thermocouple Grid

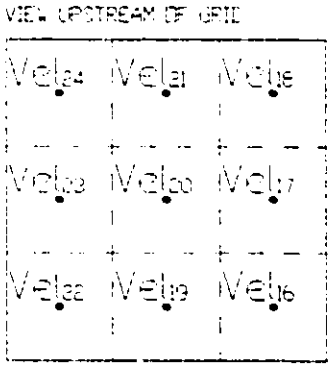

Figure 54: Air Velocity Grid

L. Measurement of Evaporator Outlet Air Dry Bulb Temperature

The evaporator outlet air temperature was measured by a grid of nine thermocouples shown in figure 53. The numbering of the thermocouples corresponds to those indicated in figure 51. The outlet air duct was divided into nine rectangular sections of equal area with one thermocouple positioned in the centre of each area. The thermocouples were all calibrated as discussed in the section dealing with refrigerant temperature measurement.

M. Measurement of Evaporator Outlet Air Velocity

The evaporator outlet air velocity was measured downstream of both the evaporator and the fan. The outlet air duct was divided

into nine equal areas. Velocity readings were taken by placing a Kurz series 440 air velocity meter (hot film anemometer) at the centre of each of the nine areas. The readings were numbered as shown in figure 54. The six meter per second scale was used. About one minute was required for the indicating needle to stabilize. The uncertainty of the velocity readings was 0.1 meters per second based on the stability of the needle and readability of the scale.

N. Measurement of Evaporator Outlet Air Wet Bulb Temperature

A thermocouple covered by a moist cloth measured the wet bulb temperature. This thermocouple was located downstream of the grid used to measure the outlet air dry bulb temperature. The portion of cloth covering the thermocouple remained moist because part of the cloth was kept in a small jar filled with water. The thermocouple was calibrated the same way the thermocouples measuring the refrigerant temperatures were calibrated.

O. Test Procedure

The following experimental procedure was carried out:

1) the evaporator outlet air duct was connected to the frame of the refrigeration unit,
2) the cloth covering the thermocouple that was to measure the evaporator outlet air wet bulb temperature was moistened and the reservoir (a small jar containing part of the cloth) was filled with water,
3) the valve upstream of the manual expansion valve was fully opened, and the valve upstream of the thermostatically

controlled valve was fully closed so that all refrigerant flowed through the manual expansion valve during the tests,

4) the evaporator air fan was then turned on and set to the desired speed (high, medium or low),
5) the velocity probe battery charger was then turned on (the guard was left on the probe),
6) the computer and data logger were then turned on,
7) the thermocouple wires were connected to the data logger using connectors as shown in figure 55,
8) the condensing cooling water tap was then adjusted to produce the desired flow rate (a pail and stopwatch were used to determine the flowrate),
9) the condenser cooling water temperature was set to the desired level,
10) the compressor was then started by turning on its DC power supply and closing two switches located next to the compressor speed control,
11) the speed control knob was adjusted to obtain the desired speed,
12) the manual expansion valve was adjusted as indicated in figure 56 (two and a quarter turns from the fully open position was the maximum amount the valve could be closed),
13) after the system attained quasi-steady state conditions (usually within fifteen minutes), the data acquisition

program was run by typing "refrig",

14) the channels on the data logger which were to be scanned were entered into the program (channels 2 to 36),

15) the data logger channel where the reference thermistor was located was inputed to the program,

16) the program was told that each channel was to be scanned 25 times,

17) the barometric pressure and ambient air temperature were inputed to the program

18) the pressure gage readings were inputed to the program in order from left to right as they appear when facing the gage panel,

19) after the program requested the evaporator outlet air velocities the evaporator outlet air duct was disconnected from the frame of the refrigeration unit,

20) the velocity probe guard was then removed and velocity readings were taken,

21) the readings were entered into the program in the order corresponding to the labelling in figure 54,

22) the distance between the lines of action of the forces exerted on the dynamometer scales was inputed (24 inches as shown in figure 57),

23) the compressor was turned off and the dynamometer scale readings were taken and entered into the program,

24) the results of the data analysis were then stored on paper and on floppy disk

The average time required to carry out the tasks listed above was twenty-five minutes.

After inputting the readings of the dynamometer scales with the compressor operating, the readings of the scales before the compressor was turned on is requested by the program. At this point the compressor was turned off and the dynamometer scale readings were taken and entered into the program. It was found that this procedure provided more reliable results than recording the readings of the scales before the compressor was turned on. The reason for this was that the high compressor start up torque disturbed the dynamometer scale needles.

Table 9 indicates how the channels corresponded to the thermocouples shown in figure 51.

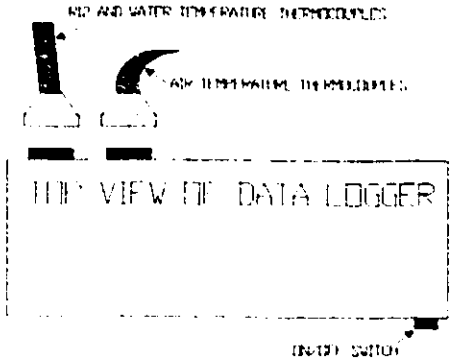

Figure 55: Connection of Thermocouples to Data Logger

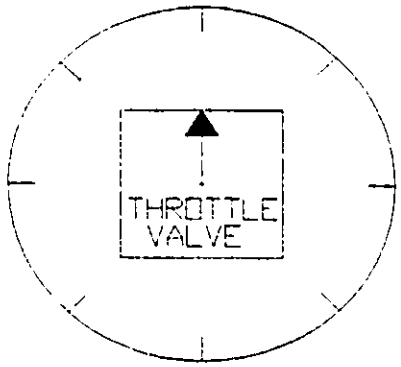

Figure 56: Manual Expansion Valve

P. Data Acquisition Program

A listing of the program is given in Appendix IV. The program incorporates the calibration constants for Sciemetric data logger with serial number 311083. The program calculated thirty-six

Table 9: Correspondence of Thermocouple Numbers With Channel Numbers on Data Logger 106

Temperature	Channel	Temperature	Channel
t1′	2	t1	11
t2	3	twi	12
t2′	4	two	13
t3	5	T16	27
t3′	6	T17	28
t4	7	T18	29
t4′	8	T19	30
t5	9	T20	31
t5′	14	T21	32
t5′′	15	T22	33
t6	16	T23	34
t6′	10	T24	35
		Twb	36

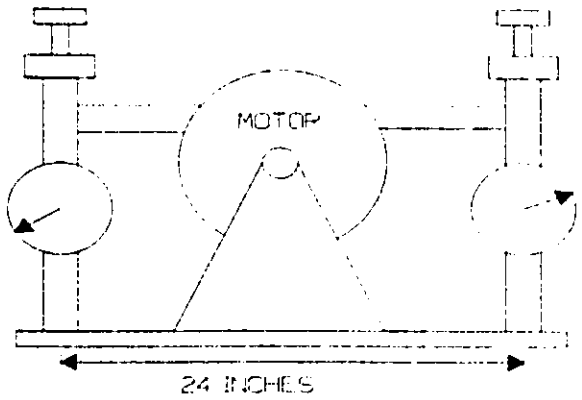

Figure 57: Distance Between Lines of Action of Forces on Scales

quantities using the raw data (see CALC module in Appendix IV). For each quantity which the data acquisition program calculated, an uncertainty analysis was carried out using the Kline-McKlintock method, this method is described in any engineering

instrumentation text book [34]. The data acquisition program therefore needed to evaluate a great many partial derivatives (see UNANAL module in Appendix IV).

The mass flow rate of the refrigerant based on the rotameter reading was given by

$$REFmdot\_f = (voldot*\rho_{4'}) \left(\frac{\rho_{ref}}{\rho_{4'}}\right) \tag{81}$$

where $\rho_{4'}$ is the density of the refrigerant at state 4', and ρ_{ref} is the density of saturated R12 at 90 degrees Fahrenheit, the state at which the flowmeter was calibrated by the manufacturer.

The thermal conductance for the portion of the condenser where the refrigerant was condensing was given by

$$UA_{cond} = -H2Omdot*H2Ocpf*\ln(1-EFF_{cond}) \tag{82}$$

where EFFcond was given by

$$EFF_{cond} = \frac{(t_{wo}-t_{wi})}{(t3-t_{wi})} \tag{83}$$

Note that t3 was always equal to the saturation temperature of the refrigerant at the condenser outlet temperature.

The average of the temperature of the refrigerant in the evaporator which was evaporating was calculated as

$$t_{evap} = \frac{(t5' + t5'' + t_{sat6})}{3} \tag{84}$$

where tsat6 is the saturation temperature of the refrigerant at

the evaporator outlet pressure as shown in figure 51.

The heat absorbed by the air passing through the evaporator was given by

$$Q_{evap\_a} = \sum_{j=16}^{24} [\ (1.005(T_{atm}-T_j) + Wi(2501+1.82T_{atm}) - Wo(2501+1.82T_j) + 4.186(Wo-Wi)T_j)\ AIRmdot_j\ ] + W_{fan} \quad (85)$$

The symbol Qmax denotes the most heat that the refrigerant in the wet portion of the evaporator can absorb without violating the second law. EFF_wet, was calculated by

$$EFF\_wet = \frac{Q_{evap\_wet}}{Q_{max}} \quad (86)$$

The thermal conductance for the portion of the evaporator where refrigerant boiled was calculated as

$$UA\_wet = -MC_p\_mix \ln(1-EFF\_wet) \quad (87)$$

where the air's mass flow rate was given by

$$AIRmdot = \sum_{j=16}^{24} \left(\frac{P_{atm}}{R_{air} T_j}\ Vel_j\ A_j \right) \quad (88)$$

and MCp_mix was given by

$$MC_p\_mix = \frac{Q_{max}}{Tatm - T_{evap}} \quad (89)$$

The log mean temperature difference for the portion of the evaporator where the refrigerant boiled was calculated as

$$LMTD\_e = \frac{Q_{evap\_wet}}{UA\_wet} \tag{90}$$

X. EXPERIMENTAL RESULTS

A. Experimental Data

The following tables list the experimental data which is referred to in section B of this chapter. In all the tables in this section, the small numbers underneath the larger ones are absolute uncertainties. The labelling of the data is such that data set 1-3, for example, corresponds to the data obtained from the third run on the first day that tests were carried out.

Table 10A: The Effect of Compressor Crank Shaft Speed

Data	RPM	Valve setting	H2Omdot kg/s	Twi °C	AIRmdot kg/s	Tair_i °C	Qreg (liq) kW	Qreg (vap) kW	EFFreg
1-6	501 15	675° 10°	0.385 9E-05	46.63 0.32	0.382 0.0037	27.6 0.1	0.21 0.03	0.36 0.05	0.33 0.01
1-7	606 15	675° 10°	0.389 9E-05	47 0.32	0.383 0.0037	27.59 0.1	0.16 0.02	0.24 0.03	0.31 0.01
1-8	702 15	675° 10°	0.401 0.0001	47.15 0.32	0.372 0.00368	27.59 0.1	0.16 0.02	0.24 0.03	0.31 0.01
1-9	800 15	675° 10°	0.399 9E-05	47.27 0.32	0.385 0.00369	27.6 0.1	0.15 0.02	0.23 0.03	0.31 0.01
1-10	925 15	675° 10°	0.379 8E-05	47.16 0.32	0.371 0.00367	27.46 0.1	0.15 0.02	0.23 0.03	0.3 0.01
3-1	525 15	450° 10	0.38196 8E-05	14.98 0.32	0.374 0.00368	26.28 0.1	0.05 0.01	-0.03 0.01	0.03 0.02
3-2	650 15	450° 10°	0.383 8E-05	14.89 0.32	0.375 0.00369	26.4 0.1	0.11 0.02	-0.04 0.01	0.1 0.02
3-3	750 15	450° 10°	0.389 9E-05	15 0.32	0.376 0.0037	26.23 0.1	0.23 0.03	-0.05 0.01	0.18 0.01
3-4	850 15	450° 10°	0.389 9E-05	15.02 0.32	0.377 0.00371	26.29 0.1	0.31 0.03	-0.06 0.01	0.21 0.01
3-5	950 15	450° 10°	0.395 9E-05	15.01 0.32	0.377 0.00371	26.44 0.1	0.01 0.01	0.05 0.01	0.22 0.05
3-6	950 15	450° 10°	0.389 9E-05	15.02 0.32	0.382 0.00375	25.89 0.1	0.37 0.04	-0.07 0.01	0.22 0.01
3-7	950 15	450° 10°	0.180 1E-05	15.18 0.32	0.386 0.0038	24.47 0.1	0.22 0.02	-0.05 0.01	0.12 0.01
3-8	855 15	450° 10°	0.188 1E-05	15.27 0.32	0.386 0.00379	24.19 0.1	0.14 0.01	-0.04 0.01	0.08 0.01
3-9	753 15	450° 10°	0.185 1E-05	15.27 0.32	0.385 0.00379	24 0.1	0.09 0.01	-0.04 0.01	0.05 0.01
3-10	652 15	450° 10°	0.188 1E-05	15.26 0.32	0.384 0.00378	23.91 0.1	0.07 0.01	-0.03 0.01	0.04 0.01
4-5	520 15	720° 10°	0.424 0.00011	39.41 0.32	0.378 0.00372	23.75 0.1	0.09 0.02	0.09 0.02	0.4 0.01
4-6	380 15	720° 10°	0.424 0.00011	39.87 0.32	0.379 0.00372	23.69 0.1	0.09 0.03	0.09 0.03	0.4 0.01

Table 10B

Data	RPM	Valve setting	H2Omdot kg/s	Twi °C	AIRmdot kg/s	Tair_i °C	Torque kN*m	Wcomp (mec) kW	Wcomp (rev) kW	Ecomp kW
1-6	501 15	675° 10°	0.385 5E-05	46.63 0.32	0.382 0.0037	27.6 0.1	0.021 0.0005	1.083 0.011	0.85 0.02	0.93 0.01
1-7	606 15	675° 10°	0.389 5E-05	47 0.32	0.383 0.0037	27.59 0.1	0.020 0.0005	1.277 0.011	1 0.02	1.16 0.01
1-8	702 15	675° 10°	0.401 0.0001	47.15 0.32	0.372 0.00368	27.59 0.1	0.020 0.0005	1.442 0.0463	1.11 0.02	1.24 0.01
1-9	800 15	675° 10°	0.399 5E-05	47.27 0.32	0.385 0.00369	27.6 0.1	0.019 0.0005	1.594 0.049	1.19 0.03	1.37 0.01
1-10	925 15	675° 10°	0.379 5E-05	47.16 0.32	0.371 0.00367	27.46 0.1	0.018 0.0005	1.785 0.0525	1.29 0.03	1.51 0.01
3-1	525 15	450° 10	0.38196 5E-05	14.98 0.32	0.37395 0.00368	26.28 0.1	0.0109 0.0003	0.599 0.025	0.43 0.02	0.34 0.01
3-2	650 15	450° 10°	0.383 5E-05	14.89 0.32	0.375 0.00369	26.4 0.1	0.0116 0.0003	0.788 0.0291	0.51 0.02	0.41 0.01
3-3	750 15	450° 10°	0.389 5E-05	15 0.32	0.376 0.0037	26.23 0.1	0.014 0.0004	1.102 0.037	0.75 0.03	0.64 0.02
3-4	850 15	450° 10°	0.389 5E-05	15.02 0.32	0.377 0.00371	26.29 0.1	0.0133 0.0004	1.18 0.0386	0.84 0.03	1.05 0.02
3-5	950 15	450° 10°	0.395 5E-05	15.01 0.32	0.377 0.00371	26.44 0.1	0.0132 0.0004	1.312 0.0418	0.84 0.03	1.12 0.11
3-6	950 15	450° 10°	0.389 5E-05	15.02 0.32	0.382 0.00375	25.89 0.1	0.0139 0.0004	1.38 0.0432	0.95 0.03	1.07 0.02
3-7	950 15	450° 10°	0.180 1E-05	15.18 0.32	0.386 0.0038	24.47 0.1	0.0148 0.0004	1.472 0.0453	1.02 0.03	0.89 0.02
3-8	855 15	450° 10°	0.188 1E-05	15.27 0.32	0.386 0.00379	24.19 0.1	0.014 0.0004	1.257 0.0401	0.95 0.02	0.8 0.02
3-9	753 15	450° 10°	0.185 1E-05	15.27 0.32	0.385 0.00379	24 0.1	0.0138 0.0004	1.087 0.0366	0.77 0.03	0.65 0.01
3-10	652 15	450° 10°	0.188 1E-05	15.26 0.32	0.384 0.00378	23.91 0.1	0.0127 0.0004	0.867 0.0315	0.63 0.02	0.52 0.01
4-5	520 15	720° 10°	0.424 0.00011	39.41 0.32	0.378 0.00372	23.75 0.1	0.0142 0.0004	0.774 0.0305	0.49 0.02	0.46 0.01
4-6	380 15	720° 10°	0.424 0.00011	39.87 0.32	0.379 0.00372	23.69 0.1	0.0157 0.0004	0.623 0.0294	0.41 0.01	0.41 0.01

Table 10C

Data	RPM	Valve setting	H2Omdot kg/s	Twi °C	ASmdot kg/s	Tair_i °C	PRATIO	rstmdot_f kg/s	volum_eff	poly_index	isen_ratio	CF	COPhp
1-6	501	675°	0.385	46.63	0.382	27.6	3.38	0.0358	0.78	1.06	0.92	0.102	5.36
	15	15°	5E-05	0.32	0.0007	0.1	0.05	0.00028	0.01	0.02	0.02	0.002	0.07
1-7	606	675°	0.389	47	0.383	27.59	3.94	0.03528	0.76	1.08	0.86	0.095	4.56
	15	15°	5E-05	0.32	0.0007	0.1	0.06	0.00028	0.02	0.02	0.02	0.008	0.06
1-8	702	675°	0.401	47.15	0.372	27.59	4.47	0.03517	0.74	1.08	0.89	0.086	4.33
	15	15°	0.0011	0.32	0.00068	0.1	0.07	0.00028	0.02	0.02	0.03	0.007	0.05
1-9	800	675°	0.399	47.27	0.385	27.6	4.9	0.03515	0.72	1.09	0.86	0.086	4.02
	15	15°	5E-05	0.32	0.00063	0.1	0.08	0.00028	0.02	0.02	0.03	0.006	0.05
1-10	925	675°	0.379	47.16	0.371	27.46	5.48	0.03512	0.69	1.09	0.85	0.082	3.75
	15	15°	5E-05	0.32	0.00057	0.1	0.1	0.00028	0.02	0.02	0.04	0.005	0.04
3-1	525	450°	0.38196	14.98	0.37395	26.28	1.65	0.04802	0.93	1.03	1.27	0.11812	20.29
	15	10	5E-05	0.32	0.00068	0.1	0.04	0.00033	0.03	0.03	0.08	0.00772	0.73
3-2	650	450°	0.383	14.89	0.375	26.4	1.82	0.04833	0.80	1.03	1.26	0.25919	16.76
	15	15°	5E-05	0.32	0.00063	0.1	0.04	0.00033	0.02	0.06	0.07	0.00456	0.51
3-3	750	450°	0.389	15	0.376	26.23	1.99	0.06169	0.93	1.04	1.17	0.07536	13.68
	15	15°	5E-05	0.32	0.0007	0.1	0.05	0.00033	0.02	0.06	0.06	0.02442	0.33
3-4	850	450°	0.389	15.02	0.377	26.29	2.12	0.06178	0.85	1.10	0.78	0.15206	8.62
	15	15°	5E-05	0.32	0.00071	0.1	0.05	0.00033	0.02	0.05	0.04	0.02258	0.13
3-5	950	450°	0.395	15.01	0.377	26.44	2.75	0.0475	0.76	1.13	0.74	0.16773	6.22
	15	10°	5E-05	0.32	0.00071	0.1	0.07	0.00032	0.02	0.05	0.05	0.05366	0.14
3-6	950	450°	0.389	15.02	0.382	25.89	2.35	0.06213	0.84	1.09	0.88	0.13187	8.45
	15	15°	5E-05	0.32	0.00075	0.1	0.05	0.00033	0.02	0.05	0.04	0.0179	0.13
3-7	950	450°	0.180	15.18	0.386	24.47	2.58	0.06086	0.84	1.04	1.15	0.11024	9.55
	15	15°	5E-05	0.32	0.0008	0.1	0.06	0.00033	0.02	0.04	0.05	0.01403	0.7
3-8	855	450°	0.188	15.27	0.386	24.19	2.43	0.0606	0.90	1.04	1.2	0.07503	10.65
	15	15°	5E-05	0.32	0.00079	0.1	0.05	0.00033	0.02	0.04	0.06	0.01576	0.21
3-9	753	450°	0.185	15.27	0.385	24	2.25	0.05386	0.88	1.04	1.21	0.10397	11.71
	15	10°	5E-05	0.32	0.00079	0.1	0.05	0.00032	0.02	0.05	0.06	0.01932	0.26
3-10	652	450°	0.188	15.26	0.384	23.91	2.11	0.04745	0.87	1.04	1.21	0.12113	12.8
	15	15°	5E-05	0.32	0.00078	0.1	0.05	0.00032	0.02	0.05	0.06	0.02426	0.31
4-5	520	720°	0.424	39.41	0.378	23.75	5.04	0.0143	0.61	1.07	1.06	0.1108	4.92
	15	15°	0.00011	0.32	0.00072	0.1	0.11	0.0003	0.02	0.02	0.03	0.00083	0.15
4-6	380	720°	0.424	39.87	0.379	23.69	3.98	0.01434	0.64	1.07	1.01	0.1353	5.45
	15	15°	0.00011	0.32	0.00072	0.1	0.08	0.0003	0.01	0.02	0.05	0.01311	0.16

Table 10D

Data	RPM	Valve setting	H2Omdot kg/s	Twi °C	Alfmdot kg/s	Tair_i °C	Qevap_r kW	Qevap_a kW	Qevap_wat kW	UAevap kW/K	LMTDevap °C	Tao °C	Wi	Wo
1-6	501	675°	0.385	46.63	0.382	27.6	3.97	4.34	3.96	0.27	13.81	17.06	0.0103	0.0102
	15	1P	5E-05	0.32	0.0037	0.1	0.03	0.43	0.03	0.006	2.11	0.03	0.0004	0.0001
1-7	606	675°	0.389	47	0.383	27.59	4.15	4.52	3.76	0.201	18.02	16.93	0.0096	0.0093
	15	1P	5E-05	0.32	0.0037	0.1	0.03	0.43	0.03	0.004	2.55	0.03	0.0004	0.0001
1-8	702	675°	0.401	47.15	0.372	27.59	4.18	4.48	3.68	0.178	20.9	17.7	0.0103	0.0096
	15	1P	0.0001	0.32	0.0036	0.1	0.03	0.42	0.03	0.003	2.86	0.03	0.0004	0.0001
1-9	800	675°	0.399	47.27	0.385	27.6	4.19	4.35	3.63	0.146	23.91	18.19	0.0106	0.0101
	15	1P	5E-05	0.32	0.0036	0.1	0.03	0.56	0.03	0.002	3.33	0.03	0.0004	0.0001
1-10	925	675°	0.379	47.16	0.371	27.46	4.19	2.96	3.58	0.132	26.12	18.34	0.0098	0.0103
	15	1P	4E-05	0.32	0.0037	0.1	0.03	0.51	0.03	0.002	3.38	0.03	0.0004	0.0001
3-1	525	450°	0.38196	14.98	0.37395	26.28	6.52	5.432	6.52	0.57	9.23	17.11	0.013728	0.011709
	15	1D	4E-05	0.32	0.0036	0.1	0.05	0.423	0.05	0.018	1.24	0.03	0.00004	8.5E-05
3-2	650	450°	0.383	14.89	0.375	26.4	6.6	6.348	6.59	0.728	8.53	16.19	0.013717	0.011157
	15	1P	4E-05	0.32	0.0036	0.1	0.05	0.497	0.05	0.009	1.01	0.03	0.00042	8.5E-05
3-3	750	450°	0.389	15	0.376	26.23	8.44	6.854	8.43	0.9	7.72	15.52	0.013572	0.010633
	15	1P	5E-05	0.32	0.0037	0.1	0.05	0.428	0.05	0.009	0.87	0.03	0.00039	8.3E-05
3-4	850	450°	0.389	15.02	0.377	26.29	8.44	7.6	8.43	0.947	7.77	14.9	0.013622	0.01024
	15	1P	5E-05	0.32	0.0037	0.1	0.05	0.432	0.05	0.053	0.84	0.03	0.00004	8.1E-05
3-5	950	450°	0.395	15.01	0.377	26.44	5.84	7.392	5.24	0.237	22.14	15.02	0.012735	0.010027
	15	1P	5E-05	0.32	0.00371	0.1	0.58	0.55	0.5	0.004	2.38	0.03	0.00034	8E-05
3-6	950	450°	0.389	15.02	0.382	25.89	8.48	8.36	8.47	0.729	10.31	11.66	0.011147	0.008223
	15	1P	5E-05	0.32	0.0035	0.1	0.05	0.431	0.05	0.007	1.01	0.03	0.00026	7.1E-05
3-7	950	450°	0.188	15.18	0.386	24.47	8.07	7.258	8.05	0.568	11.59	9.73	0.008532	0.007063
	15	1P	2E-05	0.32	0.0038	0.1	0.04	0.418	0.05	0.007	0.65	0.03	0.00029	6.5E-05
3-8	855	450°	0.188	15.27	0.386	24.19	8	6.729	7.99	0.53	11.61	10.09	0.008388	0.007197
	15	1P	2E-05	0.32	0.0039	0.1	0.04	0.415	0.05	0.005	0.71	0.03	0.00028	6.6E-05
3-9	753	450°	0.185	15.27	0.385	24	7.08	5.794	7.06	0.472	11.86	10.69	0.008292	0.00713
	15	1P	2E-05	0.32	0.0039	0.1	0.04	0.411	0.04	0.002	0.76	0.03	0.00026	6.7E-05
3-10	652	450°	0.188	15.26	0.384	23.91	6.24	5.424	6.23	0.388	12.81	11.61	0.00823	0.007647
	15	1P	2E-05	0.32	0.0039	0.1	0.04	0.408	0.04	0.008	0.9	0.03	0.00024	6.5E-05
4-5	520	720°	0.424	39.41	0.378	23.75	1.9	1.504	1.5	0.064	32.35	18.06	0.00719	0.00778
	15	1P	0.00011	0.32	0.0037	0.1	0.04	0.403	0.03	0.001	1.65	0.03	0.00078	7.4E-05
4-6	380	720°	0.424	39.87	0.379	23.69	1.88	1.553	1.65	0.084	25.3	17.41	0.00717	0.00793
	15	1P	0.00011	0.32	0.0037	0.1	0.04	0.402	0.03	0.001	6.9	0.03	0.00027	7.6E-05

Table 10E

Data	RPM	Valve setting	H2Omdot kg/s	Twi °C	AIRmdot kg/s	Tair_i °C	Qcond kW	UAcond kW/K	LMTDcond °C	Two °C	t4-tsat_4 °C
1-6	501	675°	0.385	46.63	0.382	27.6	4.98	1.19	4.17	49.63	0.72
	15	10°	9E-05	0.32	0.0037	0.1	0.04	0.18	0.65	0.26	0.52
1-7	606	675°	0.389	47	0.383	27.59	5.29	1.25	4.25	50.23	0.79
	15	10°	9E-05	0.32	0.0037	0.1	0.04	0.18	0.62	0.26	0.51
1-8	702	675°	0.401	47.15	0.372	27.59	5.39	1.3	4.14	50.48	0.73
	15	10°	0.0001	0.32	0.00368	0.1	0.04	0.18	0.59	0.26	0.51
1-9	800	675°	0.399	47.27	0.385	27.6	5.52	1.28	4.32	50.55	0.56
	15	10°	9E-05	0.32	0.00369	0.1	0.04	0.18	0.62	0.26	0.51
1-10	925	675°	0.379	47.16	0.371	27.46	5.65	1.27	4.46	50.69	0.74
	15	10°	8E-05	0.32	0.00367	0.1	0.05	0.17	0.61	0.26	0.51
3-1	525	450°	0.38196	14.98	0.37395	26.28	6.82	1.17	5.82	18.45	1.04
	15	10	8E-05	0.32	0.00369	0.1	0.05	0.16	0.78	0.26	0.67
3-2	650	450°	0.383	14.89	0.375	26.4	6.86	1.24	5.54	18.97	1.2
	15	10°	9E-05	0.32	0.00369	0.1	0.05	0.14	0.64	0.26	0.86
3-3	750	450°	0.389	15	0.376	26.23	8.82	1.27	6.96	19.51	1.02
	15	10°	9E-05	0.32	0.0037	0.1	0.05	0.13	0.73	0.26	0.85
3-4	850	450°	0.389	15.02	0.377	26.29	9.08	1.3	6.98	19.93	0.6
	15	10°	9E-05	0.32	0.00371	0.1	0.05	0.13	0.68	0.26	0.83
3-5	950	450°	0.395	15.01	0.377	26.44	6.96	1.26	5.54	19.26	0.28
	15	10°	9E-05	0.32	0.00377	0.1	0.66	0.14	0.81	0.26	0.84
3-6	950	450°	0.389	15.02	0.382	25.89	9.07	1.31	6.93	20.02	0.91
	15	10°	9E-05	0.32	0.00375	0.1	0.05	0.13	0.66	0.26	0.83
3-7	950	450°	0.180	15.18	0.386	24.47	8.54	1.13	7.53	24.55	2.06
	15	10°	1E-05	0.32	0.0038	0.1	0.05	0.09	0.58	0.26	0.8
3-8	855	450°	0.188	15.27	0.386	24.19	8.5	1.14	7.46	23.69	1.9
	15	10°	1E-05	0.32	0.00379	0.1	0.05	0.09	0.61	0.26	0.81
3-9	753	450°	0.185	15.27	0.385	24	7.57	1.11	6.83	23.07	1.57
	15	10°	1E-05	0.32	0.00379	0.1	0.05	0.1	0.6	0.26	0.82
3-10	652	450°	0.188	15.26	0.384	23.91	6.67	1.03	6.45	22.1	1.43
	15	10°	1E-05	0.32	0.00378	0.1	0.05	0.1	0.6	0.26	0.83
4-5	520	720°	0.424	39.41	0.378	23.75	2.27	1.86	1.22	41.1	1.22
	15	10°	0.00011	0.32	0.0037	0.1	0.05	0.6	0.1	0.26	0.61
4-6	380	720°	0.424	39.87	0.379	23.69	2.22	1.79	1.24	41.53	1.69
	15	10°	0.00011	0.32	0.0037	0.1	0.05	0.58	0.1	0.26	0.61

Table 11A: The Effect of Condenser Cooling Water Temperature

Data	RPM	Valve setting	H2Omdot kg/s	Twi °C	AIRmdot kg/s	Tair_i °C	Qreg (liq) kW	Qreg (vap) kW	EFFreg
5-1	650	585°	0.396	15.24	0.388	22.89	0.22	-0.04	0.2
	15	10°	9E-05	0.32	0.00372	0.1	0.03	0.01	0.01
5-2	650	585°	0.396	24.56	0.385	23.04	0.19	-0.03	0.15
	15	10°	9E-05	0.32	0.00372	0.1	0.03	0.01	0.01
5-3	650	585°	0.396	27.67	0.385	23.66	0.17	-0.03	0.13
	15	10°	9E-05	0.32	0.00372	0.1	0.03	0.01	0.01
5-4	650	585°	0.396	30.79	0.384	23.55	0.16	-0.03	0.11
	15	10°	9E-05	0.32	0.00372	0.1	0.03	0.01	0.01
5-5	650	585°	0.396	45.59	0.381	23.87	0.11	-0.03	0.05
	15	10°	9E-05	0.32	0.00372	0.1	0.02	0.01	0.01
5-6	690	615°	0.396	28.65	0.386	23.83	0.28	-0.04	0.18
	15	10°	9E-05	0.32	0.00372	0.1	0.04	0.01	0.01
5-7	675	615°	0.396	36.01	0.384	23.57	0.22	-0.03	0.13
	15	10°	9E-05	0.32	0.00372	0.1	0.03	0.01	0.01

Table 11B

Data	RPM	Valve setting	H2Omdot kg/s	Twi °C	AIRmdot kg/s	Tair_i °C	Torque kN*m	Wcomp (mec) kW	Wcomp (rev) kW	Ecomp kW
5-1	650	585°	0.396	15.24	0.388	22.89	0.0112	0.76	0.56	0.44
	15	10°	9E-05	0.32	0.00372	0.1	0.0003	0.0287	0.02	0.01
5-2	650	585°	0.396	24.56	0.385	23.04	0.0138	0.938	0.72	0.61
	15	10°	9E-05	0.32	0.00372	0.1	0.0004	0.0334	0.02	0.01
5-3	650	585°	0.396	27.67	0.385	23.66	0.0144	0.979	0.74	0.62
	15	10°	9E-05	0.32	0.00372	0.1	0.0004	0.0345	0.02	0.01
5-4	650	585°	0.396	30.79	0.384	23.55	0.0155	1.054	0.75	0.64
	15	10°	9E-05	0.32	0.00372	0.1	0.0004	0.0366	0.02	0.01
5-5	650	585°	0.396	45.59	0.381	23.87	0.02	1.36	0.94	0.82
	15	10°	9E-05	0.32	0.00372	0.1	0.0005	0.0453	0.02	0.01
5-6	690	615°	0.396	28.65	0.386	23.83	0.0153	1.106	0.78	0.67
	15	10°	9E-05	0.32	0.00372	0.1	0.0004	0.0375	0.02	0.01
5-7	675	615°	0.396	36.01	0.384	23.57	0.0176	1.244	0.92	0.83
	15	10°	9E-05	0.32	0.00372	0.1	0.0004	0.0415	0.02	0.01

Table 11C

Data	RPM	Valve setting	H2Omdot kg/s	Twi °C	ARmdot kg/s	Tair_1 °C	PRATIO	refmdot_1 kg/s	volum_eff	poly_index	isen_ratio	CF	COPhp
5-1	650	585°	0.396	15.24	0.388	22.89	2.11	0.04255	0.85	1.04	1.28	0.14047	13.69
5-2	650	585°	0.396	24.56	0.385	23.04	2.37	0.04709	0.87	1.04	1.2	0.10072	10.6
5-3	650	585°	0.396	27.67	0.385	23.66	2.47	0.04635	0.82	1.03	1.22	0.1292	10.13
5-4	650	585°	0.396	30.79	0.384	23.55	2.55	0.04543	0.77	1.03	1.19	0.15399	9.41
5-5	650	585°	0.396	45.59	0.381	23.87	3.15	0.04619	0.70	1.01	1.17	0.13984	6.97
5-6	630	615°	0.396	28.65	0.386	23.83	2.6	0.04638	0.79	1.03	1.19	[illegible]873	9.27
5-7	675	615°	0.396	36.01	0.384	23.57	2.78	0.05048	0.82	1.03	1.12	0.1073	7.89

Table 11D

Data	RPM	Valve setting	H2Omdot kg/s	Twi °C	ARmdot kg/s	Tair_1 °C	Qevap_r kW	Qevap_a kW	Qevap_wei kW	UAevap kW/K	LMTDevap °C	Tao °C	Wi	Wo
5-1	650	585°	0.396	15.24	0.388	22.89	5.83	5.301	5.83	0.362	14.23	10.89	0.007513	0.006974
5-2	650	585°	0.396	24.56	0.385	23.04	6.14	4.753	6.12	0.383	12.11	11.78	0.007762	0.007459
5-3	650	585°	0.396	27.67	0.385	23.66	5.94	4.972	5.92	0.374	11.83	12.44	0.008062	0.00752
5-4	650	585°	0.396	30.79	0.384	23.55	5.68	4.392	5.67	0.396	10.82	12.93	0.007833	0.007641
5-5	650	585°	0.396	45.59	0.381	23.87	5.04	3.191	5.02	0.582	6.94	15.39	0.008264	0.008433
5-6	630	615°	0.396	28.65	0.386	23.83	5.93	5.098	5.92	0.424	11.73	11.93	0.00751	0.007114
5-7	675	615°	0.396	36.01	0.384	23.57	6.17	4.394	6.05	0.41	10.95	13.05	0.007301	0.007052

Data	RPM	Valve setting	H2Omdot kg/s	Twi °C	AIRmdot kg/s	Tair_i °C	Qcond kW	UAcond kW/K	LMTDcond °C	Two °C	t4-tsat_4 °C
5-1	650	585°	0.396	15.24	0.388	22.89	6.04	1.16	5.2	18.49	1.41
	15	10°	9E-05	0.32	0.00372	0.1	0.05	0.16	0.73	0.26	0.88
5-2	650	585°	0.396	24.56	0.385	23.04	6.44	1.16	5.55	27.54	-1.1
	15	10°	9E-05	0.32	0.00372	0.1	0.05	0.18	0.85	0.26	0.71
5-3	650	585°	0.396	27.67	0.385	23.66	6.25	1.19	5.24	30.52	1.82
	15	10°	9E-05	0.32	0.00372	0.1	0.04	0.19	0.85	0.26	0.71
5-4	650	585°	0.396	30.79	0.384	23.55	6.05	1.24	4.87	33.62	1.71
	15	10°	9E-05	0.32	0.00372	0.1	0.04	0.2	0.8	0.26	0.68
5-5	650	585°	0.396	45.59	0.381	23.87	5.7	1.48	3.85	48.44	1.22
	15	10°	9E-05	0.32	0.00372	0.1	0.04	0.26	0.68	0.26	0.53
5-6	690	615°	0.396	28.65	0.386	23.83	6.21	1.18	5.28	31.84	2.49
	15	10°	9E-05	0.32	0.00372	0.1	0.04	0.17	0.76	0.26	0.7
5-7	675	615°	0.396	36.01	0.384	23.57	6.56	1.31	5.01	39.04	2.71
	15	10°	9E-05	0.32	0.00372	0.1	0.04	0.21	0.79	0.26	0.63

Table 12A: Effect of Throttle Valve Setting

Data	RPM	Valve setting	H2Omdot kg/s	Twi °C	AIRmdot kg/s	Tair_i °C	Qreg (liq) kW	Qreg (vap) kW	EFFreg
1-1	540	653°	0.381	48.12	0.396	26.8	0.38	-0.03	0.19
	15	10°	8E-05	0.32	0.00371	0.1	0.06	0.01	0.01
1-2	549	675°	0.384	48.13	0.383	26.92	0.16	0.27	0.3
	15	10°	9E-05	0.32	0.00369	0.1	0.03	0.04	0.01
1-3	550	698°	0.366	46.92	0.384	27.21	0.13	0.17	0.34
	15	10°	8E-05	0.32	0.00367	0.1	0.02	0.03	0.01
1-4	556	720°	0.377	48.71	0.376	27.69	0.12	0.11	0.4
	15	10°	8E-05	0.32	0.00364	0.1	0.03	0.03	0.01
1-5	556	731°	0.375	49.29	0.377	27.75	0.08	0.07	0.43
	15	10°	8E-05	0.32	0.00362	0.1	0.03	0.02	0.01
2-3	540	0°	0.376	14.92	0.37198	27.21	0.03	-0.03	0
	15	0°	9E-05	0.32	0.00369	0.1	0.01	0.01	0.02
2-4	540	450°	0.365	14.91	0.37198	27.11	0.05	-0.03	0.03
	15	10°	7E-05	0.32	0.00369	0.1	0.01	0.01	0.02
2-5	540	630°	0.366	14.75	0.372	27.1	0	-0.02	-0.21
	15	10°	8E-05	0.32	0.00368	0.1	0.01	0	0.09
2-6	540	540°	0.373	14.92	0.368	27.21	0.14	-0.04	0.15
	15	10°	8E-05	0.32	0.00364	0.1	0.02	0.01	0.02
2-7	530	540°	0.384	14.71	0.375	27.74	0	-0.01	-0.11
	15	10°	9E-05	0.32	0.00368	0.1	0.01	0	0.23
2-8	530	563°	0.377	14.73	0.372	27.8	0	-0.01	-0.15
	15	10°	8E-05	0.32	0.00365	0.1	0.01	0	0.2
2-9	540	585°	0.383	14.73	0.37297	27.64	0	-0.02	-0.17
	15	10°	9E-05	0.32	0.00365	0.1	0.01	0	0.11
2-10	540	608°	0.379	14.75	0.368	27.39	0	-0.02	-0.18
	15	10°	9E-05	0.32	0.00364	0.1	0.01	0	0.08
4-1	502	495°	0.424	38.32	0.382	23.81	0.06	-0.02	0.03
	15	10°	0.00011	0.32	0.00375	0.1	0.01	0.01	0.01
4-2	502	585°	0.424	38.39	0.382	23.83	0.07	-0.02	0.04
	15	10°	0.00011	0.32	0.00376	0.1	0.02	0.01	0.01
4-3	502	630°	0.424	39.02	0.382	23.93	0.11	-0.02	0.07
	15	10°	0.00011	0.32	0.00376	0.1	0.02	0.01	0.01
4-4	512	675°	0.424	38.99	0.38196	25.14	0.38	-0.03	0.23
	15	10°	0.00011	0.32	0.00377	0.1	0.07	0.01	0.01
4-5	520	720°	0.424	39.41	0.378	23.75	0.09	0.09	0.4
	15	10°	0.00011	0.32	0.00372	0.1	0.02	0.02	0.01

Data	RPM	Valve setting	H2Omdot kg/s	Twi °C	AIRmdot kg/s	Tair_i °C	Torque kN*m	Wcomp (mec) kW	Wcomp (rev) kW	Ecomp kW
1-1	540	653°	0.381	48.12	0.396	26.8	0.022	1.2331	0.85	0.87
	15	10°	8E-05	0.32	0.00371	0.1	0.0005	0.0449	0.02	0.01
1-2	549	675°	0.384	48.13	0.383	26.92	0.022	1.2445	0.89	0.84
	15	10°	9E-05	0.32	0.00369	0.1	0.0005	0.0449	0.02	0.01
1-3	550	698°	0.366	46.92	0.384	27.21	0.019	1.1057	0.76	0.78
	15	10°	8E-05	0.32	0.00367	0.1	0.0005	0.0401	0.02	0.01
1-4	556	720°	0.377	48.71	0.376	27.69	0.021	1.2214	0.52	0.49
	15	10°	8E-05	0.32	0.00364	0.1	0.0005	0.0439	0.02	0.01
1-5	556	731°	0.375	49.29	0.377	27.75	0.013	0.7829	0.62	0.53
	15	10°	8E-05	0.32	0.00362	0.1	0.0004	0.0301	0.03	0.01
2-3	540	0°	0.376	14.92	0.37198	27.21	0.0113	0.641	0.34	0.27
	15	0°	9E-05	0.32	0.00369	0.1	0.0003	0.0261	0.04	0.03
2-4	540	450°	0.365	14.91	0.37198	27.11	0.0109	0.6188	0.36	0.28
	15	10°	7E-05	0.32	0.00369	0.1	0.0003	0.0254	0.04	0.03
2-5	540	630°	0.366	14.75	0.372	27.1	0.0106	0.5974	0.4	0.39
	15	10°	8E-05	0.32	0.00368	0.1	0.0003	0.0248	0.07	0.07
2-6	540	540°	0.373	14.92	0.368	27.21	0.0111	0.6257	0.48	0.37
	15	10°	8E-05	0.32	0.00364	0.1	0.0003	0.0256	0.02	0.01
2-7	530	540°	0.384	14.71	0.375	27.74	0.0111	0.6186	0.42	0.48
	15	10°	9E-05	0.32	0.00368	0.1	0.0003	0.0255	0.06	0.07
2-8	530	563°	0.377	14.73	0.372	27.8	0.0111	0.6141	0.43	0.55
	15	10°	8E-05	0.32	0.00365	0.1	0.0003	0.0254	0.06	0.08
2-9	540	585°	0.383	14.73	0.37297	27.64	0.0107	0.6074	0.43	0.54
	15	10°	9E-05	0.32	0.00365	0.1	0.0003	0.0251	0.06	0.08
2-10	540	608°	0.379	14.75	0.368	27.39	0.0108	0.6119	0.44	0.53
	15	10°	8E-05	0.32	0.00364	0.1	0.0003	0.0252	0.07	0.08
4-1	502	495°	0.424	38.32	0.382	23.81	0.0188	0.9873	0.51	0.43
	15	10°	0.00011	0.32	0.00375	0.1	0.0005	0.0391	0.09	0.08
4-2	502	585°	0.424	38.39	0.382	23.83	0.0189	0.996	0.49	0.45
	15	10°	0.00011	0.32	0.00376	0.1	0.0005	0.0394	0.09	0.08
4-3	502	630°	0.424	39.02	0.382	23.93	0.0182	0.956	0.73	0.62
	15	10°	0.00011	0.32	0.00376	0.1	0.0004	0.037	0.02	0.01
4-4	512	675°	0.424	38.99	0.38196	25.14	0.0175	0.939	0.76	0.61
	15	10°	0.00011	0.32	0.00377	0.1	0.0004	0.0361	0.02	0.01
4-5	520	720°	0.424	39.41	0.378	23.75	0.0142	0.774	0.49	0.46
	15	10°	0.00011	0.32	0.00372	0.1	0.0004	0.0305	0.02	0.01

Table 12C

Data	RPM	Valve setting	H2Omdot kg/s	Twi °C	AFmdot kg/s	Tdir_1 °C	PRATIO	refmdot_1 kg/s	volum_eff	poly_index	isen_ratio	CF	COPhp
1-1	540	653°	0.381	48.12	0.356	26.8	3.08	0.04201	0.70	1.03	0.98	0.152	5.57
1-2	549	675°	0.384	48.13	0.383	26.92	3.58	0.03501	0.72	1.04	1.07	0.115	5.81
1-3	550	698°	0.366	46.92	0.384	27.21	4.41	0.02456	0.67	1.07	0.98	0.110	4.76
1-4	556	720°	0.377	48.71	0.376	27.69	5.91	0.01366	0.52	1.07	1.07	0.113	4.31
1-5	556	731°	0.375	49.29	0.377	27.75	7.99	0.01388	0.73	1.06	1.22	0.044	4.13
2-3	540	0°	0.376	14.92	0.37198	27.21	1.66	0.0617	0.71	1.03	1.26	0.450	19.78
2-4	540	450°	0.365	14.91	0.37198	27.11	1.7	0.04806	0.73	1.03	1.3	0.396	19.51
2-5	540	630°	0.366	14.75	0.372	27.1	2.55	0.02879	0.76	1.08	1.05	0.177	9.2
2-6	540	540°	0.373	14.92	0.368	27.21	1.74	0.04855	0.95	1.03	1.3	0.064	18.6
2-7	530	540°	0.384	14.71	0.375	27.74	2.09	0.03513	0.80	1.10	0.86	0.214	9.62
2-8	530	563°	0.377	14.73	0.372	27.8	2.17	0.03513	0.80	1.12	0.77	0.197	8.39
2-9	540	585°	0.383	14.73	0.37297	27.64	2.24	0.03519	0.78	1.12	0.78	0.212	8.16
2-10	540	608°	0.379	14.75	0.368	27.39	2.45	0.02872	0.81	1.12	0.82	0.151	7.67
4-1	502	495°	0.424	38.32	0.382	23.81	2.54	0.04859	0.57	1.01	1.2	0.285	9.22
4-2	502	585°	0.424	38.39	0.382	23.83	2.47	0.04269	0.58	1.03	1.1	0.297	8.71
4-3	502	630°	0.424	39.02	0.382	23.93	2.61	0.04295	0.82	1.01	1.2	0.116	8.87
4-4	512	675°	0.424	38.99	0.38196	25.14	3.03	0.03877	0.81	1.01	1.28	0.097	8.18
4-5	520	720°	0.424	39.41	0.378	23.75	5.04	0.0143	0.61	1.07	1.06	0.111	4.92

Table 12D

Data	RPM	Valve setting	H2Omdot kg/s	Twi °C	ARmdot kg/s	Tair_i °C	Qevap_r kW	Qevap_a kW	Qevap_wal kW	UAevap kW/K	LMTDevap °C	Tao °C	Wi	Wo
1-1	540	653°	0.381	48.12	0.396	26.8	4.83	3.90	4.82	0.59	7.46	18.23	0.0129	0.0125
	IS	EP	9E-05	0.12	0.00071	0.1	0.03	0.03	0.03	0.08	1.03	0.03	0.0003	0.0001
1-2	549	675°	0.384	48.13	0.383	26.92	4.03	4.53	3.75	0.223	13.39	18.04	0.0127	0.0117
	IS	EP	9E-05	0.12	0.00068	0.1	0.03	0.03	0.03	0.003	1.03	0.03	0.0003	0.0001
1-3	550	698°	0.366	46.92	0.384	27.21	3	3.15	2.62	0.103	23.68	20.05	0.0128	0.0126
	IS	EP	9E-05	0.12	0.00069	0.1	0.03	0.56	0.03	0.005	1.05	0.03	0.0004	0.0001
1-4	556	720°	0.377	48.71	0.376	27.69	1.74	0.99	1.44	0.043	34.66	22.37	0.0119	0.0129
	IS	EP	9E-05	0.12	0.00134	0.1	0.04	0.56	0.03	0.002	0.5	0.03	0.0004	0.0001
1-5	556	731°	0.375	49.28	0.377	27.75	1.82	0.92	1.45	0.034	42.94	24.24	0.0128	0.0133
	IS	EP	9E-05	0.12	0.00136	0.1	0.04	0.56	0.03	0.001	14.14	0.03	0.0004	0.0001
2-3	540	0°	0.376	14.92	0.37198	27.21	5.18	5.484	5.18	0.492	10.55	16.47	0.012413	0.010956
	IS	EP	9E-05	0.12	0.00369	0.1	0.03	0.027	0.03	0.014	1.02	0.03	0.000254	8.5E-05
2-4	540	450°	0.365	14.91	0.37198	27.11	5.16	5.204	5.15	0.467	11.07	16.82	0.012573	0.01123
	IS	EP	7E-05	0.12	0.00369	0.1	0.03	0.024	0.03	0.013	1.03	0.03	0.000253	8.4E-05
2-5	540	630°	0.366	14.75	0.372	27.1	3.22	2.835	2.8	0.091	30.75	19.82	0.012574	0.012268
	IS	EP	9E-05	0.12	0.00368	0.1	0.03	0.502	0.03	0.003	3.05	0.03	0.000253	9.1E-05
2-6	540	540°	0.373	14.92	0.368	27.21	6.67	5.412	6.66	0.462	11.66	16.78	0.012425	0.010954
	IS	EP	9E-05	0.12	0.00364	0.1	0.05	0.026	0.05	0.012	1.5	0.03	0.000253	8.4E-05
2-7	530	540°	0.384	14.71	0.375	27.74	4.19	4.73	3.77	0.166	22.78	18.7	0.012377	0.011226
	IS	EP	9E-05	0.12	0.00369	0.1	0.03	0.56	0.03	0.003	2.56	0.03	0.000246	8.5E-05
2-8	530	563°	0.377	14.73	0.372	27.8	4.1	4.635	3.66	0.152	24.12	19.18	0.012661	0.011471
	IS	EP	9E-05	0.12	0.00365	0.1	0.03	0.503	0.03	0.003	2.72	0.03	0.000268	8.6E-05
2-9	540	585°	0.383	14.73	0.37297	27.64	3.9	3.93	3.46	0.136	25.58	19.96	0.013004	0.01209
	IS	EP	9E-05	0.12	0.00365	0.1	0.03	0.054	0.03	0.002	4.2	0.03	0.000265	8.6E-05
2-10	540	608°	0.379	14.75	0.368	27.39	3.61	3.198	3.16	0.112	28.17	20.72	0.013472	0.012832
	IS	EP	9E-05	0.12	0.00364	0.1	0.03	0.548	0.03	0.002	4.9	0.03	0.000263	8.6E-05
4-1	502	495°	0.424	38.32	0.382	23.81	3.62	3.375	3.62	0.48	7.56	15.42	0.00776	0.00769
	IS	EP	0.00011	0.12	0.00375	0.1	0.03	0.1	0.04	0.005	1.5	0.03	0.000079	7.3E-05
4-2	502	585°	0.424	38.39	0.382	23.83	3.55	3.349	3.55	0.437	8.14	15.25	0.0075	0.00754
	IS	EP	0.00011	0.12	0.00376	0.1	0.03	0.1	0.03	0.003	1.63	0.03	0.000079	7.2E-05
4-3	502	630°	0.424	39.02	0.382	23.93	5.04	3.514	5.04	0.484	7.88	15.17	0.00745	0.00739
	IS	EP	0.00011	0.12	0.00376	0.1	0.04	0.107	0.04	0.005	1.5	0.03	0.000081	7.2E-05
4-4	512	675°	0.424	38.99	0.38196	25.14	4.76	5.041	4.75	0.358	11.87	14.17	0.00782	0.00705
	IS	EP	0.00011	0.12	0.00377	0.1	0.04	0.10	0.04	0.003	2.1	0.03	0.000082	7E-05
4-5	520	720°	0.424	39.41	0.378	23.75	1.9	1.604	1.6	0.064	32.35	18.06	0.00719	0.00778
	IS	EP	0.00011	0.12	0.00372	0.1	0.04	0.103	0.03	0.001	0.6	0.03	0.000078	7.6E-05

Table 12E

Data	RPM	Valve setting	H2Omdot kg/s	Twi °C	AIRmdot kg/s	Tair_i °C	Qcond kW	UAcond kW/K	LMTDcond °C	Two °C	t4-tsat_4 °C
1-1	540	653°	0.381	48.12	0.396	26.8	5.22	1.23	4.25	51.18	1.22
	15	10°	8E-05	0.32	0.00371	0.1	0.04	0.19	0.66	0.26	0.51
1-2	549	675°	0.384	48.13	0.383	26.92	4.86	1.22	4	51.3	0.57
	15	10°	9E-05	0.32	0.00369	0.1	0.04	0.18	0.59	0.26	0.5
1-3	550	698°	0.366	46.92	0.384	27.21	3.71	1.24	2.99	49.58	-0.39
	15	10°	8E-05	0.32	0.00367	0.1	0.04	0.23	0.54	0.26	0.51
1-4	556	720°	0.377	48.71	0.376	27.69	2.12	1.62	1.31	50.26	0.99
	15	10°	8E-05	0.32	0.00364	0.1	0.04	0.47	0.38	0.26	0.52
1-5	556	731°	0.375	49.29	0.377	27.75	2.18	3.68	0.59	50.64	1.21
	15	10°	8E-05	0.32	0.00362	0.1	0.05	3.6	0.58	0.26	0.53
2-3	540	0°	0.376	14.92	0.37198	27.21	5.35	1.26	4.24	18.37	0.97
	15	0°	9E-05	0.32	0.00369	0.1	0.63	0.17	0.77	0.26	0.86
2-4	540	450°	0.365	14.91	0.37198	27.11	5.4	1.18	4.58	18.48	0.93
	15	10°	7E-05	0.32	0.00369	0.1	0.61	0.16	0.8	0.26	0.87
2-5	540	630°	0.366	14.75	0.372	27.1	3.56	1.14	3.12	17.1	0.59
	15	10°	9E-05	0.32	0.00368	0.1	0.61	0.23	0.82	0.26	0.91
2-6	540	540°	0.373	14.92	0.368	27.21	6.89	1.16	5.93	18.53	0.69
	15	10°	8E-05	0.32	0.00364	0.1	0.05	0.15	0.77	0.26	0.87
2-7	530	540°	0.384	14.71	0.375	27.74	4.65	1.14	4.07	17.63	0.29
	15	10°	9E-05	0.32	0.00368	0.1	0.65	0.18	0.85	0.26	0.88
2-8	530	563°	0.377	14.73	0.372	27.8	4.61	1.15	4.01	17.69	0.27
	15	10°	8E-05	0.32	0.00365	0.1	0.63	0.18	0.83	0.26	0.88
2-9	540	585°	0.383	14.73	0.37297	27.64	4.4	1.16	3.78	17.5	0.36
	15	10°	9E-05	0.32	0.00365	0.1	0.64	0.19	0.84	0.26	0.89
2-10	540	608°	0.379	14.75	0.368	27.39	4.1	1.16	3.55	17.36	0.5
	15	10°	8E-05	0.32	0.00364	0.1	0.64	0.2	0.83	0.26	0.9
4-1	502	495°	0.424	38.32	0.382	23.81	3.97	1.48	2.68	40.63	0.41
	15	10°	0.00011	0.32	0.00375	0.1	0.7	0.31	0.79	0.26	0.6
4-2	502	585°	0.424	38.39	0.382	23.83	3.93	1.46	2.7	40.68	2.78
	15	10°	0.00011	0.32	0.00376	0.1	0.7	0.31	0.75	0.26	0.62
4-3	502	630°	0.424	39.02	0.382	23.93	5.49	1.51	3.65	41.43	1.25
	15	10°	0.00011	0.32	0.00376	0.1	0.04	0.31	0.74	0.26	0.6
4-4	512	675°	0.424	38.99	0.38196	25.14	4.95	1.17	4.22	41.57	0.06
	15	10°	0.00011	0.32	0.00377	0.1	0.04	0.21	0.74	0.26	0.58
4-5	520	720°	0.424	39.41	0.378	23.75	2.27	1.86	1.22	41.1	1.22
	15	10°	0.00011	0.32	0.00372	0.1	0.05	0.6	0.4	0.26	0.61

Table 13A: The Effect of Condenser Cooling Water Mass Flow Rate

Data	RPM	Valve setting	H2Omdot kg/s	Twi °C	AIRmdot kg/s	Tair_i °C	Qreg (liq) kW	Qreg (vap) kW	EFFreg
2-1	503 15	675° 10°	0.367 8E-05	45.51 0.32	0.373 0.00367	26.78 0.1	0.16 0.02	0.24 0.03	0.32 0.01
2-2	501 15	675° 10°	0.183 2E-05	47.82 0.32	0.369 0.00366	27.31 0.1	0.2 0.02	0.33 0.02	0.31 0.01
3-6	950 15	450° 10°	0.389 9E-05	15.02 0.32	0.382 0.00375	25.89 0.1	0.37 0.04	-0.07 0.01	0.22 0.01
3-7	950 15	450° 10°	0.180 1E-05	15.18 0.32	0.386 0.0038	24.47 0.1	0.22 0.02	-0.05 0.01	0.12 0.01

Table 13B

Data	RPM	Valve setting	H2Omdot kg/s	Twi °C	AIRmdot kg/s	Tair_i °C	Torque kN*m	Wcomp (mec) kW	Wcomp (rev) kW	Ecomp kW
2-1	503 15	675° 10°	0.367 8E-05	45.51 0.32	0.373 0.00367	26.78 0.1	0.0212 0.0005	1.118 0.0426	0.88 0.02	0.93 0.01
2-2	501 15	675° 10°	0.183 2E-05	47.82 0.32	0.369 0.00366	27.31 0.1	0.0226 0.0005	1.184 0.045	0.86 0.02	0.97 0.01
3-6	950 15	450° 10°	0.389 9E-05	15.02 0.32	0.382 0.00375	25.89 0.1	0.0139 0.0004	1.38 0.0432	0.95 0.03	1.07 0.02
3-7	950 15	450° 10°	0.180 1E-05	15.18 0.32	0.386 0.0038	24.47 0.1	0.0148 0.0004	1.472 0.0453	1.02 0.03	0.89 0.02

Table 13C

Data	RPM	Valve setting	H2Omdot kg/s	Twi °C	Altmdot kg/s	Tair_i °C	PRATIO	refrmdot_i kg/s	volum_eff	poly_index	isen_ratio	CF	COPhp
2-1	5103	675°	0.367	45.51	0.373	26.78	3.42	0.03567	0.80	1.06	0.94	0.08956	5.49
	6	IP	8E-05	0.32	0.00367	0.1	0.05	0.00028	0.03	0.02	0.02	0.00224	0.07
2-2	5101	675°	0.183	47.82	0.369	27.31	3.49	0.03475	0.72	1.06	0.88	0.1238	4.55
	6	IP	2E-05	0.32	0.00366	0.1	0.05	0.00027	0.02	0.02	0.01	0.01026	0.07
3-6	950	450°	0.389	15.02	0.382	25.89	2.35	0.06213	0.84	1.09	0.88	0.13187	8.45
	6	IP	5E-05	0.32	0.00375	0.1	0.05	0.00033	0.02	0.05	0.04	0.01079	0.13
3-7	950	450°	0.180	15.18	0.386	24.47	2.58	0.06086	0.84	1.04	1.15	0.11024	9.55
	6	IP	4E-05	0.32	0.0038	0.1	0.06	0.00033	0.02	0.04	0.05	0.01403	0.17

Table 13D

Data	RPM	Valve setting	H2Omdot kg/s	Twi °C	Altmdot kg/s	Tair_i °C	Qevap_r kW	Qevap_a kW	Qevap_wet kW	UAevap kW/K	DLMTDevap °C	Too °C	Wi	Wo
2-1	5103	675°	0.367	45.51	0.373	26.78	4.21	2.906	3.92	0.272	13.59	18.28	0.011281	0.011711
	6	IP	8E-05	0.32	0.00367	0.1	0.03	0.415	0.03	0.006	1.92	0.03	0.000283	5E-05
2-2	5101	675°	0.183	47.82	0.369	27.31	3.74	4.134	3.72	0.302	11.85	18.42	0.012943	0.012163
	6	IP	2E-05	0.32	0.00366	0.1	0.03	0.423	0.03	0.007	0.9	0.03	0.000357	9.2E-05
3-6	950	450°	0.389	15.02	0.382	25.89	8.48	8.36	8.47	0.729	10.31	11.65	0.011147	0.008223
	6	IP	5E-05	0.32	0.00375	0.1	0.05	0.431	0.05	0.007	1.01	0.03	0.000326	7.1E-05
3-7	950	450°	0.180	15.18	0.386	24.47	8.07	7.258	8.05	0.568	11.53	9.73	0.008532	0.007063
	6	IP	4E-05	0.32	0.0038	0.1	0.04	0.418	0.05	0.007	0.66	0.03	0.000324	6.5E-05

Table 13E

Data	RPM	Valve setting	H2Omdot kg/s	Twi °C	AIRmdot kg/s	Tair_i °C	Qcond kW	UAcond kW/K	LMTDcond °C	Two °C	t4-tsat_4 °C
2-1	503 15	675° 10°	0.367 8E-05	45.51 0.32	0.373 0.00367	26.78 0.1	5.12 0.04	1.23 0.18	4.17 0.62	48.75 0.26	-0.24 0.52
2-2	501 15	675° 10°	0.183 2E-05	47.82 0.32	0.369 0.00366	27.31 0.1	4.82 0.04	1.01 0.1	4.78 0.48	52.07 0.26	0.91 0.48
3-6	950 15	450° 10°	0.389 9E-05	15.02 0.32	0.382 0.00375	25.89 0.1	9.07 0.05	1.31 0.13	6.93 0.66	20.02 0.26	0.91 0.83
3-7	950 15	450° 10°	0.180 1E-05	15.18 0.32	0.386 0.0038	24.47 0.1	8.54 0.05	1.13 0.08	7.53 0.58	24.55 0.26	2.06 0.8

B. The Effects of Compressor Crank Shaft Speed, Condenser Cooling Water Temperature, Throttle Valve Setting, and Condenser Cooling Water Mass Flow Rate on System Performance

Of the forty-six tests that were run, seventeen were run to study the effect of compressor crank shaft speed, seven were run to study the effect of condenser cooling water temperature, eighteen were run to study the effect of throttle valve setting, and four were run to study the effect of condenser cooling water mass flow rate.

1. Compressor Crank Shaft Speed

The tests to study the effect of crank shaft speed on system performance were divided into two categories: those tests in which superheated refrigerant vapour left the evaporator and those in which a wet mixture left the evaporator.

a. Superheated Vapour Leaves Evaporator

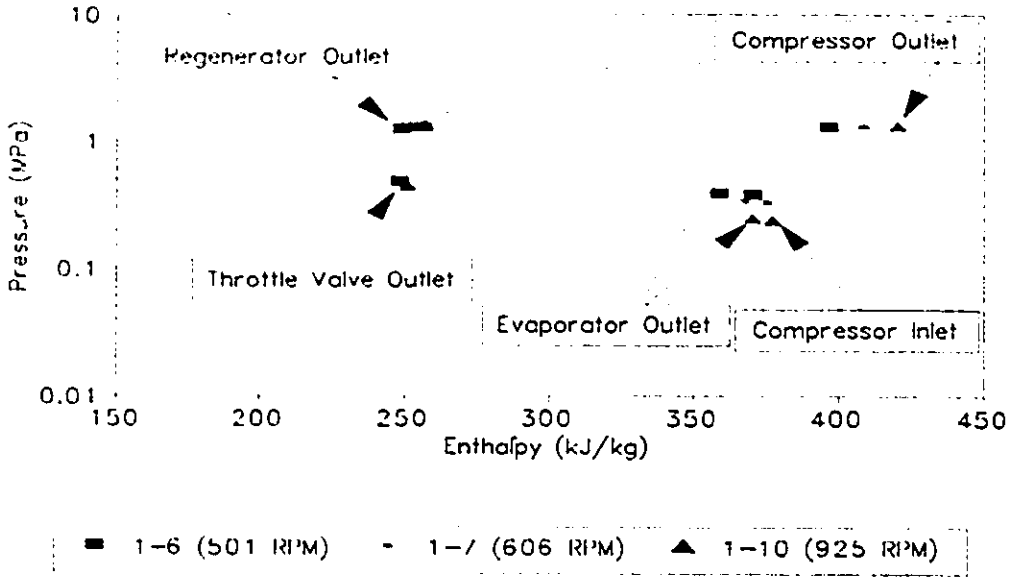

Figure 58: Effect on Thermodynamic Cycle of Crank Shaft Speed When Superheated Refrigerant Leaves Evaporator

The effect on the thermodynamic cycle of varying the compressor crank shaft speed when superheated vapour leaves the evaporator is depicted in figure 58. The following quantities increased when the speed was increased: the compressor outlet to inlet pressure ratio, the refrigerant specific enthalpy rise through the compressor, the refrigerant enthalpy drop through the condenser, the amount of refrigerant superheat at the compressor inlet, and the evaporator inlet quality. The compressor inlet pressure decreased as the crank shaft speed was increased. The refrigerant enthalpy rise through the evaporator remained constant within the range of experimental error.

The refrigerant mass flow rate remained constant within the range of experimental error. The refrigerant mass flow rate was determined three different ways: by using the flowmeter reading, by applying the first law to the condenser, and by applying the first law to the evaporator. Each method confirmed this observation.

The torque applied to compressor crank shaft by the motor decreased slightly when the crank shaft speed was increased. The work rates, Wcomp_mec and Wcomp_rev, on the other hand, increased when the speed was increased.

The heat rate, Qevap, remained constant within the range of experimental error while the evaporator's overall heat conductance, UAevap, decreased and it's log mean temperature difference, LMTDevap, increased when the crank shaft speed was increased. The heat transfer rate, Qevap_wet, decreased when the speed was increased.

The heat rate, Qcond, increased when the speed increased while the condenser's overall heat conductance, UAcond, and log mean temperature difference, LMTDcond, both remained constant within the range of experimental error when the crank shaft speed was increased.

b. Wet Mixture Leaves Evaporator

The effect on the thermodynamic cycle of varying the compressor crank shaft speed when wet mixture leaves the evaporator is depicted in figure 59. The following quantities increased when the speed was increased: the compressor inlet to

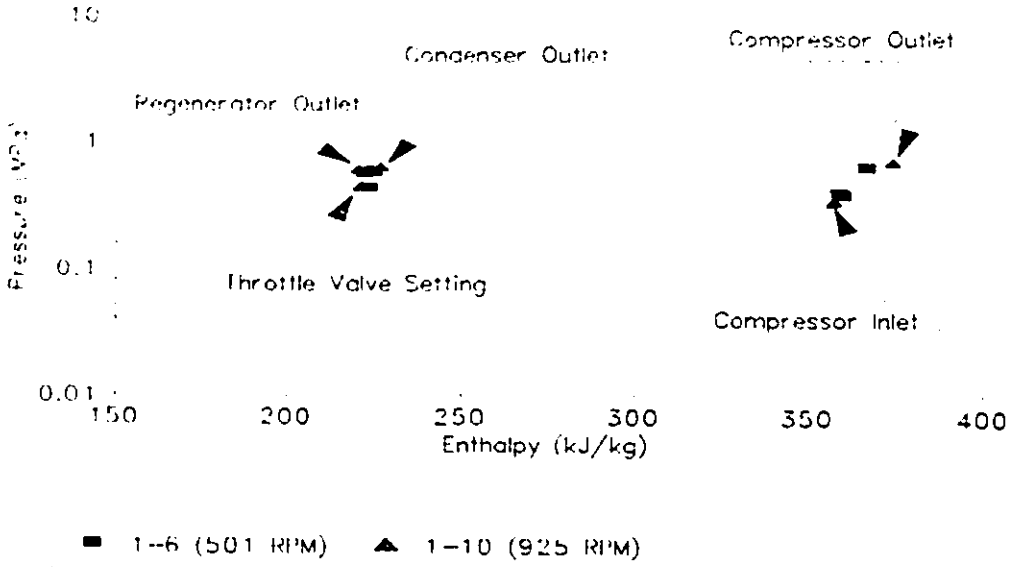

Figure 59: Effect on Thermodynamic Cycle of Crank Shaft Speed When Wet Mixture Leaves Evaporator

outlet pressure ratio, the refrigerant enthalpy rise through the compressor, the compressor outlet pressure, the refrigerant enthalpy drop through the condenser, and the refrigerant specific enthalpy rise through the evaporator. The compressor inlet pressure and evaporator inlet quality decreased as the crank shaft speed was increased. No simple trend was observed for the amount of compressor inlet superheat; sometimes the amount of superheat increased and sometimes it decreased as the crank shaft speed was increased.

The refrigerant mass flow rate increased slightly as the crank shaft speed increased.

No simple trend was found for the torque applied to

the compressor crank shaft by the motor. The work rates, Wcomp_mec and Wcomp_rev, on the other hand, increased when the speed was increased.

The heat rates, Qevap and Qevap_wet, increased as the compressor's crank shaft speed was increased. No simple trend could be found for the evaporator's overall heat conductance, UAevap, and it's log mean temperature difference, LMTDevap.

The heat rate, Qcond, increased slightly when the speed increased while the condenser's overall heat conductance, UAcond, and log mean temperature difference, LMTDcond, both remained constant within the range of experimental error.

2. Condenser Cooling Water Temperature

In all seven tests that were run to study the effect of condenser cooling water temperature, a wet mixture left the evaporator. Tests were run with temperatures ranging from 15 to 45 degrees Celsius. The effect on the thermodynamic cycle of varying the water temperature is shown in figure 60. The following quantities increased when the water temperature was increased: the compressor inlet to outlet pressure ratio, the evaporator inlet quality, the compressor outlet pressure, the compressor inlet pressure, and the refrigerant enthalpy rise through the compressor. The following quantities decreased when the water temperature increased: the refrigerant enthalpy rise through the evaporator and the refrigerant enthalpy drop through the condenser.

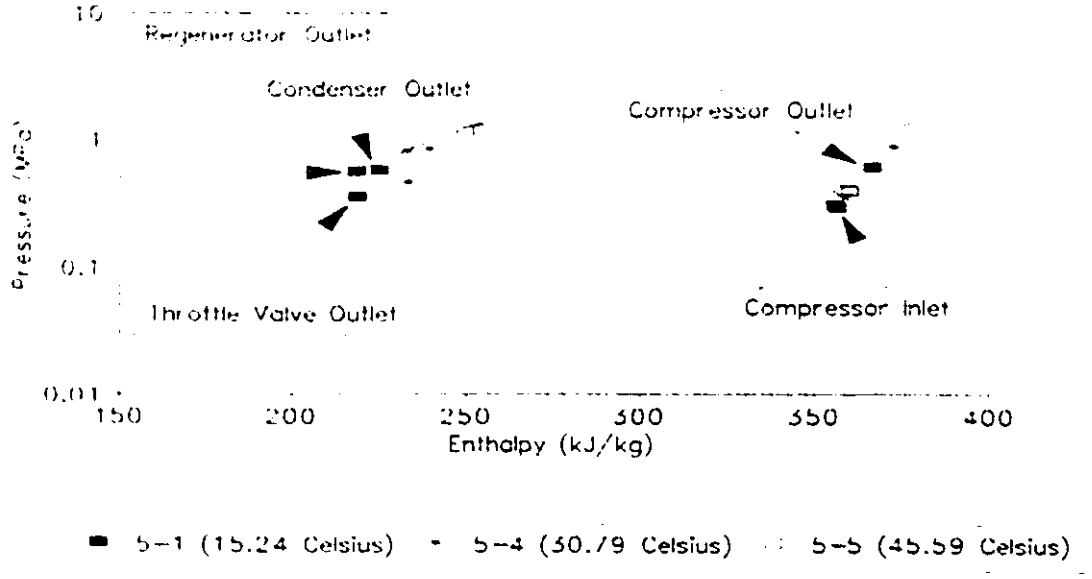

Figure 60: Effect on The Thermodynamic Cycle of Condenser Cooling Water Temperature

No simple trend could be found for the refrigerant mass flow rate or the compressor inlet superheat.

The torque applied to compressor crank shaft increased when the water temperature increased. The work rates, Wcomp_mec and Wcomp_rev, also increased.

No simple trends were found for the heat transfer rates Qevap and Qevap_wet or for the evaporator overall conductance, UAevap. The evaporator's log mean temperature difference, LMTDevap, remained constant within the range of experimental error.

No simple trend was found for Qcond. The condenser's overall heat conductance, UAcond, and its log mean temperature

difference, LMTDcond, both remained constant within the range of experimental error.

3. Throttle Valve Setting

The tests to study the effect of throttle valve setting on system performance were divided into two categories: those tests in which superheated refrigerant vapour left the evaporator and those in which a wet mixture left the evaporator. Tests were run at throttle valve settings ranging from fully open to 730 degrees from fully open.

a. Superheated Vapour Leaves Evaporator

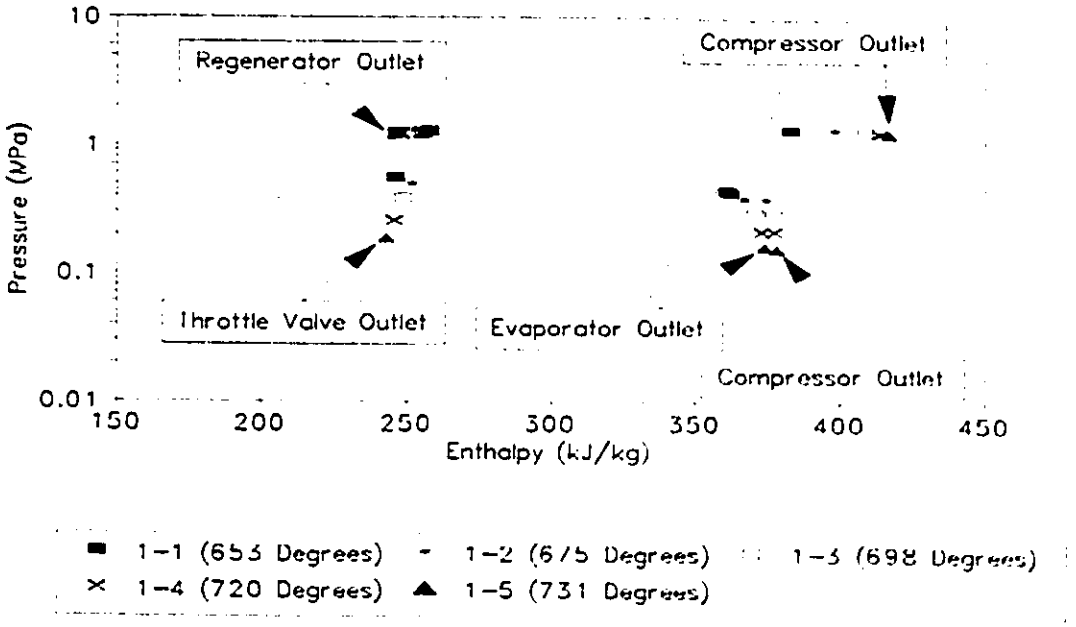

Figure 61: Effect on Thermodynamic Cycle of Throttle Valve Setting When Superheated Refrigerant Leaves Evaporator

The effect on the thermodynamic cycle of varying the throttle valve setting when superheated vapour leaves the

evaporator is depicted in figure 61. The following quantities increased as the throttle valve was closed: the compressor inlet to outlet pressure ratio, the refrigerant enthalpy rise through the compressor, the refrigerant enthalpy drop through the condenser, the amount of refrigerant superheat at the compressor inlet, the refrigerant enthalpy rise through the evaporator. The following quantities decreased as the throttle valve was closed: the compressor inlet pressure, the compressor outlet pressure, and the evaporator inlet quality.

The refrigerant mass flow rate decreased as the valve was closed.

No simple trends were observed for the torque applied to compressor crank shaft by the motor or the work rates, Wcomp_mec and Wcomp_rev.

The heat transfer rates, Qevap and Qevap_wet, and the evaporator's overall heat conductance, UAevap, decreased as the valve was closed while the log mean temperature difference, LMTDevap, increased.

The heat rate, Qcond, and the log mean temperature difference, LMTDcond, decreased as the throttle valve was closed while the condenser's overall heat conductance, UAcond, remained constant within the range of experimental error.

b. Wet Mixture Leaves Evaporator

The effect on the thermodynamic cycle of varying the throttle valve setting when wet mixture leaves the evaporator is depicted in figure 62. The following quantities increased when

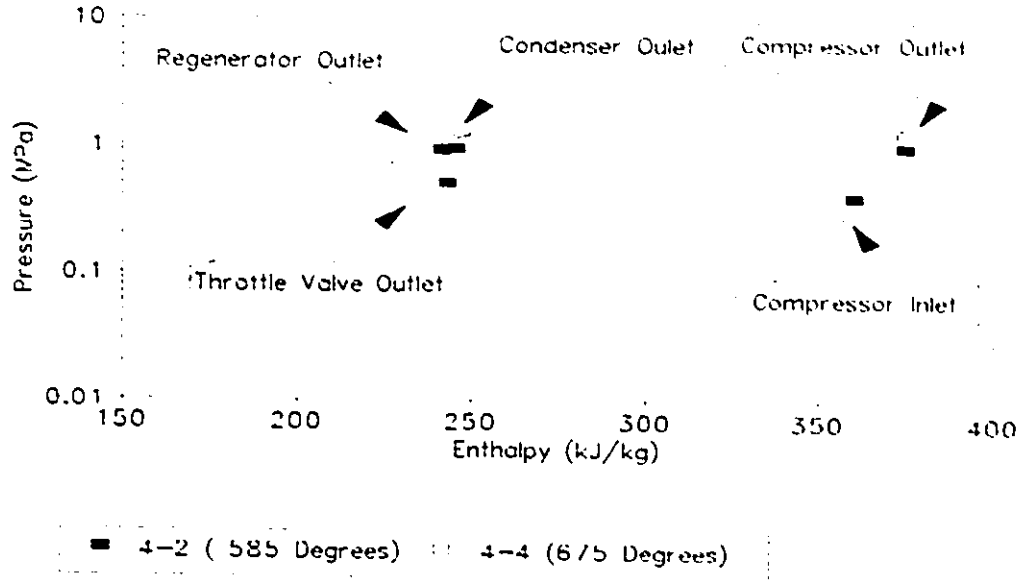

Figure 62: Effect on Thermodynamic Cycle of Throttle Valve Setting When Wet Mixture Leaves Evaporator

the valve was closed: the compressor inlet to outlet pressure ratio, and the compressor outlet pressure. The compressor inlet pressure decreased as the throttle valve was closed.

No simple trend was observed for the refrigerant mass flow rate.

The torque applied to compressor crank shaft by the motor remained constant within the range of experimental error as did the work rate Wcomp_mec. The work rate, Wcomp_rev, on the other hand, increased as the throttle valve was closed.

All other quantities remained constant within the range of experimental error.

4. Condenser Cooling Water Mass Flow Rate

Tests were run for water mass flow rates ranging from 0.180 to 0.389 kg/s. The tests could be divided into two categories: those tests in which superheated vapour left the evaporator and those tests in which wet mixture left the evaporator.

a. Superheated Vapour Leaves Evaporator

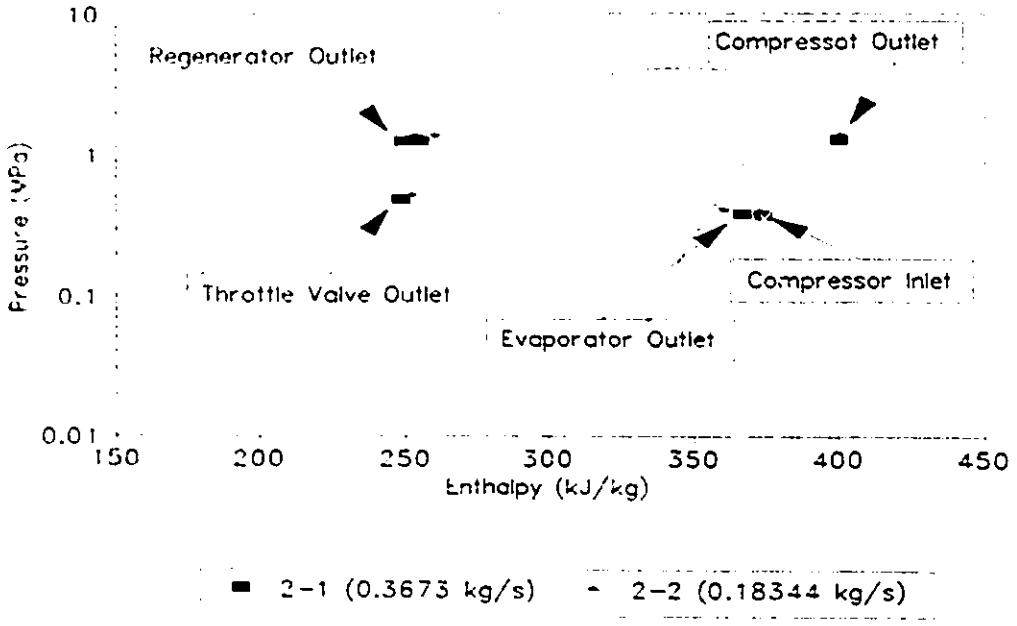

Figure 63: Effect on The Thermodynamic Cycle of Condenser Cooling Water Mass Flow Rate When Superheated Vapour Leaves Evaporator

Figure 63 shows the effect on the thermodynamic cycle of varying the water mass flow rate when superheated vapour leaves the evaporator. As the water mass flow rate decreased the following quantities increased: the compressor inlet to outlet pressure ratio, the compressor outlet pressure, the compressor

inlet pressure, the quality at the evaporator inlet, the enthalpy rise through the compressor. The following quantities decreased when the water mass flow rate was decreased: the enthalpy drop through the condenser, the enthalpy rise in the evaporator, and the amount of superheat at the compressor inlet.

The refrigerant mass flow rate decreased when the water mass flow rate decreased.

The torque applied and mechanical work done on the compressor crank shaft increased as the water mass flow rate decreased. The work rate, Wcomp_rev, remained constant within the range of experimental uncertainty.

The rate of heat transfer in the condenser and the condenser's overall heat conductance decreased when the water mass flow rate decreased. The condenser's log mean temperature difference remained constant within the range of experimental uncertainty.

The total rate of heat transfer in the evaporator, its overall heat conductance, and the rate of heat transfer in the portion of the evaporator where refrigerant boiled, all decreased when the water mass flow rate decreased. The evaporator's log mean temperature difference remained constant within the range of experimental uncertainty.

b. Wet Mixture Leaves Evaporator

Figure 64 shows the effect on the thermodynamic cycle of varying the water mass flow rate when a wet mixture leaves the evaporator. As the water mass flow rate decreased the

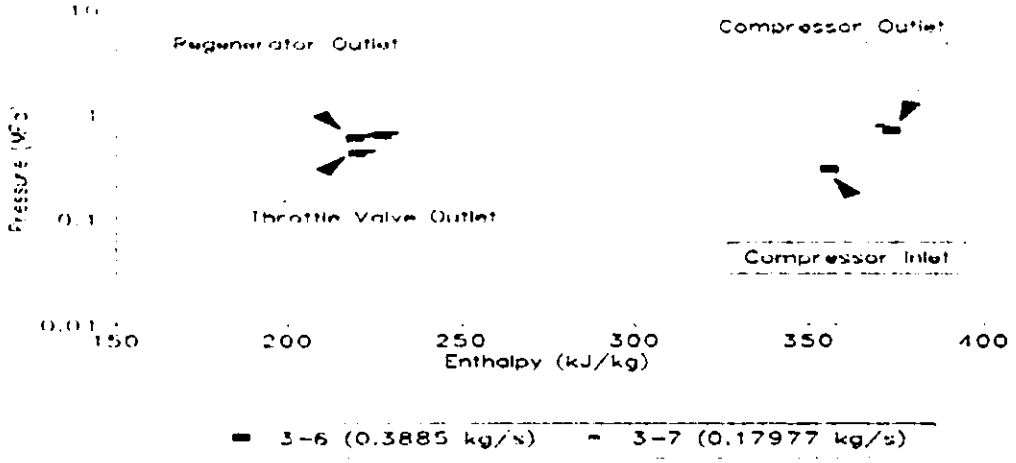

Figure 64: Effect on Thermodynamic Cycle of Water Mass Flow Rate When Wet Mixture Leaves Evaporator

following quantities increased: the compressor inlet to outlet pressure ratio, the compressor outlet pressure, and the quality at the evaporator inlet. The following quantities decreased when the water mass flow rate was decreased: the enthalpy drop through the condenser, the enthalpy rise in the evaporator, and the enthalpy rise in the compressor.

The refrigerant mass flow rate decreased when the water mass flow rate decreased.

The torque applied and mechanical work done on the compressor crank shaft increased as the water mass flow rate decreased. The work rate, Wcomp_rev, increased as the water mass flow rate decreased.

The rate of heat transfer in the condenser and the condenser's overall heat conductance decreased when the water mass flow rate decreased. The condenser's log mean temperature

difference remained constant within the range of experimental uncertainty.

The total rate of heat transfer in the evaporator, and the rate of heat transfer in the portion of the evaporator where refrigerant boiled decreased when the water mass flow rate decreased. The evaporator's overall heat conductance increased when the water mass flow rate was increased. The evaporator's log mean temperature difference remained constant within the range of experimental uncertainty.

C. Accounting for Unsteadiness

The process inside a reciprocating compressor is inherently unsteady (i.e. at any given instant the time derivatives of the refrigerant properties are not zero). For this reason steady state conditions could not (even in theory) be achieved with the system that was run. At best, quasi-steady state conditions could be achieved, meaning that the properties of the refrigerant fluctuated slightly and about essentially fixed average values. It will be shown that neglecting unsteadiness made a negligible contribution to error in the results by considering how REFmdot_c was calculated.

Equation (93) is the first law written for the control volume defined by the water space inside the condenser; (94) is the first law written for the control volume defined by the refrigerant inside the condenser. In each equation unsteady terms are included on the right hand side.

$$Q_{cond} + H2Omdot H2Ocp\,(t_{wi}-t_{wo}) = \left(mC_p\frac{dT}{d\tau}\right)_{H2O} \quad (93)$$

$$-Q_{cond} + refmdot\_c\,(h_2-h_3) = \left(mC_p\frac{dT}{d\tau}\right)_{R12gas} + \left(mC_p\frac{dT}{d\tau}\right)_{R12liq} \quad (94)$$

In equation 94 it is assumed that fluctuation in the mass of R12 liquid and vapour inside the condenser can be neglected. Adding (93) and (94) we obtain

$$H2Omdot H2Ocp\,(t_{wi}-t_{wo}) + refmdot\_c\,(h_2-h_3) = \left(mC_p\frac{dT}{d\tau}\right)_{H2O} + \left(mC_p\frac{dT}{d\tau}\right)_{R12gas} + \left(mC_p\frac{dT}{d\tau}\right)_{R12liq} \quad (95)$$

The data acquisition program scanned the thermocouple channels twenty-five times. The average value of the readings for each channel were then used in calculations. Hence the values used in the data acquisition program are more applicable to (95) if it is time averaged over the time period of the scans (approximately seven minutes). The time averaged version of (95) can be solved for refmdot_c provided that the derivatives on the right hand side of (95) are the average values of the derivatives over the period of the scans. These derivatives were approximated in the data acquisition program as the temperature change between two successive scans divided by the time interval between the scans. The average of the derivatives over the scanning period for the channels corresponding to twi, two and t3 were used to evaluate the terms on the right hand side of (95) for all the tests that were run. It was found that these terms contributed less than one percent error to the calculation of refmdot_c, far

less than the uncertainty in the calculation of refmdot_c which was usually about ten percent.

D. Flashing in the Flowmeter

Flashing in the flowmeter occurred in nine of the forty-five tests that were run. Before tests were run it was expected that flashing would occur when the compressor outlet to inlet pressure ratios were lowest. It was expected that under such conditions the flowmeter might provide some of the necessary throttling. However, it was found that at some low pressure ratios flashing did not occur while at some of the higher pressure ratios it did.

E. Both Sides of Regenerator Decreasing in Temperature

When the refrigerant exited the evaporator as wet mixture the thermocouple readings often indicated that what appeared to be slightly superheated refrigerant vapour in the low pressure side of the regenerator decreased in temperature while the liquid in the other side also decreased in temperature. It was concluded that the low pressure side of the regenerator actually contained refrigerant which was still boiling, not superheated vapour. Uncertainty in the calculation of the refrigerant superheat resulted from uncertainty in the thermocouple readings and uncertainty in the pressure gage readings.

F. Regenerator Desuperheating Refrigerant Entering Compressor

In four tests superheated vapour entered the regenerator at a temperature higher than the temperature with which liquid exited the regenerator. In these tests the vapour was cooled in the regenerator, and the liquid side was heated.

XI. COMPARISONS BETWEEN SIMULATION RESULTS AND EXPERIMENTAL DATA

The tables and figures in this chapter compare the experimental data to results produces by the simulation program. On the left side of the tables the operating conditions are listed (which is also input to the program). On the right side of the tables, the experimental data are placed above the simulation results.

A. The Effect of Compressor Crank Shaft Speed

The program was successful in predicting the trends in system performance when the compressor speed was varied. The trends indicated in table 14 and in figure 65 are in agreement with the trends that were observed in the experimental apparatus.

B. The Effect of Throttle Valve Setting

The trends in system performance that occur when the throttle valve setting is varied were also successfully predicted by the program. Figure 66 and table 15 indicate the trends.

C. The Effect of Water Mass Flow Rate

Figure 67 and table 16 show the trends in system performance predicted by the simulation program for varying water flow rate. The trends shown in the table 16 and in the figure 67, with the exception of the trend indicated for REFmdot, are in agreement with experimentally observed trends. In the experimental system, REFmdot decreased by an amount that was negligible when uncertainty was taken into account.

D. The Effect of Condenser Cooling Water Temperature

The program successfully predicted the trends in performance when the water inlet temperature was varied. Table 17 and figure 68 show the trends.

Table 14: Trends in Performance When Compressor Speed Varied

Data	INPUT TO THE PROGRAM										PROGRAM OUTPUT AND EXPERIMENTAL RESULTS (experimental results are italic)								
	RPM	$\dot{m}_{fuel}$ kg/s	T_{air} °C	$\dot{m}_{air}$ kg/s	T_{amb} °C	RH %	η_{comp}	PR$_{HOT}$	C_{pHOT} kJ/kg°C	γ_{HOT}	Q_{comp} kW	$\dot{Q}_{comp}$ kW	$C_{pHOT}\dot{m}_{air}\Delta T$ kW	$C_{pCOLD}\dot{m}_{air}\Delta T$ kW	$\dot{m}_{fuel}$ kg/s	η_{th}	T_{exh} °C	η_{ex}	T_{exh} °C
1-6	5011	0.1385	46.63	1.938	27.6	44	0.72	3.38	0.2531	0.92	0.71	0.655	2.97	4.38	0.03558	5.36	17.06	0.0102	45.63
											0.45	0.506	3.07	4.783	0.04068	5.22	17.54	0.0101	45.7
1-7	4866	0.1395	47	1.938	27.55	41	0.71	3.24	0.2531	0.92	0.6	1.15	4.15	5.25	0.03552	4.56	16.93	0.0093	51.23
											0.24	1.45	4.11	5.25	0.03741	4.55	16.9	0.0094	51.24
1-8	7012	0.1401	47.5	1.938	27.59	47.5	0.71	4.47	0.2531	0.93	0.6	1.24	4.12	5.35	0.03567	4.33	17.7	0.0096	51.42
											0.23	1.231	4.12	5.34	0.03701	4.43	16.88	0.0101	51.44
1-9	8000	0.1399	47.27	1.938	27.6	45.1	0.71	4.9	0.2531	0.96	0.6	1.37	4.19	5.52	0.03565	4.02	18.19	0.0101	51.55
											0.23	1.365	4.13	5.49	0.03695	4	16.65	0.0104	51.67
1-10	9026	0.1395	47.16	1.938	27.46	47.16	0.7	5.46	0.2531	0.95	0.6	1.51	4.15	5.65	0.03562	3.75	18.34	0.0103	51.69
											0.21	1.455	4.12	5.607	0.03675	3.75	16.73	0.0106	51.82

Table 15: Trends Predicted by Simulation Program When Throttle Valve is Closed

Data	INPUT TO THE PROGRAM										PROGRAM OUTPUT AND EXPERIMENTAL RESULTS (experimental results are italic)								
	RPM	$\dot{m}_{fuel}$ kg/s	T_{air} °C	$\dot{m}_{air}$ kg/s	T_{amb} °C	RH %	η_{comp}	PR$_{HOT}$	C_{pHOT} kJ/kg°C	γ_{HOT}	Q_{comp} kW	$\dot{Q}_{comp}$ kW	$C_{pHOT}\dot{m}_{air}\Delta T$ kW	$C_{pCOLD}\dot{m}_{air}\Delta T$ kW	$\dot{m}_{fuel}$ kg/s	η_{th}	T_{exh} °C	η_{ex}	T_{exh} °C
1-2	5498	0.1384	46.13	2.001	26.92	48	0.7	3.58	0.2531	1.07	0.6	0.84	4.03	4.86	0.03501	5.61	18.04	0.0107	51.3
											0.3	0.807	3.98	4.75	0.03624	5.78	18.08	0.0109	51.21
1-3	5500	0.1366	45.92	2.001	27.21	48	0.7	4.41	0.2531	0.98	0.53	0.78	3	3.71	0.02456	4.76	20.05	0.0106	49.58
											0.15	0.768	2.92	3.669	0.0248	4.78	20.04	0.0106	49.4
1-4	5516	0.1377	45.71	2.001	27.65	48	0.7	5.91	0.2531	1.07	0.47	0.49	1.74	2.12	0.01366	4.31	22.37	0.0109	50.26
											0.07	0.502	1.71	2.191	0.01465	4.38	22.49	0.0108	50.15

Table 16: Trends in Performance Predicted by Simulation Program For Varying Water Mass Flow Rate

Data no	INPUT TO THE PROGRAM										PROGRAM OUTPUT AND EXPERIMENTAL RESULTS (experimental results in italics)								
	RPM	$\dot{m}_w$ kg/s	T_{wi} °C	$\dot{m}_a$ kg/s	T_{ai} °C	RH %	Effreg	PR HUD	$C_{pa}(1+\omega_i)$ kW/K	Conv ratio	Q_{reg} kW	E_{comp} kW	$E_{wi}-Q_{reg}$ kW	$E_{wi}-E_{comp}$ kW	$\dot{m}_{wc}$ kg/s	COP$_{hp}$	T_{wo} °C	ω_o	T_{wo} °C
5-1	950	0.347	45.51	2.00	26.78	45.51	0.72	3.42	0.77	0.94	0.16	0.59	4.21	5.12	0.035620	5.46	38.28	0.010711	40.75
											0.07	0.568	4.11	5.02	0.03572	5.46	37.78	0.00773	40.88
5-2	950	0.333	47.02	2	27.31	47.02	0.71	3.49	0.77	0.98	0.2	0.59	3.74	4.92	0.03475	4.55	38.42	0.012163	42.07
											0.12	0.567	3.75	4.783	0.03576	4.57	38.58	0.013503	41.16

Table 17: Trends in Performance Predicted by The Simulation Program For Varying Water Inlet Temperature

Data no	INPUT TO THE PROGRAM										PROGRAM OUTPUT AND EXPERIMENTAL RESULTS (experimental results in italics)								
	RPM	$\dot{m}_w$ kg/s	T_{wi} °C	$\dot{m}_a$ kg/s	T_{ai} °C	RH %	Effreg	PR HUD	$C_{pa}(1+\omega_i)$ kW/K	Conv ratio	Q_{reg} kW	E_{comp} kW	$E_{wi}-Q_{reg}$ kW	$E_{wi}-E_{comp}$ kW	$\dot{m}_{wc}$ kg/s	COP$_{hp}$	T_{wo} °C	ω_o	T_{wo} °C
5-1	950	0.33584	45.24	1.98	22.88	49	0.7	2.11	0.791	1.28	0.22	0.44	5.83	6.04	0.04525	13.49	38.88	0.008874	38.49
											0.07	0.412	5.23	5.68	0.03936	13.56	9.79	0.007488	38.7
5-2	950	0.33584	24.56	1.98	23.04	49	0.6	2.37	0.95	1.2	0.19	0.61	6.14	6.44	0.04498	10.6	11.78	0.007488	27.54
											0.08	0.604	5.82	6.46	0.04537	10.57	5.26	0.007722	28.51
5-3	950	0.33584	27.69	1.98	23.66	49	0.63	2.49	0.85	1.22	0.17	0.62	5.94	6.25	0.04455	10.13	12.44	0.00752	30.52
											0.08	0.608	5.56	6.19	0.04434	10.08	10.07	0.007703	31.46
5-4	950	0.33568	30.79	1.98	23.55	49	0.61	2.55	0.837	1.19	0.16	0.64	5.68	6.05	0.04548	9.41	12.53	0.007641	33.62
											0.08	0.638	5.38	6.04	0.04586	9.38	10.15	0.007741	34.55

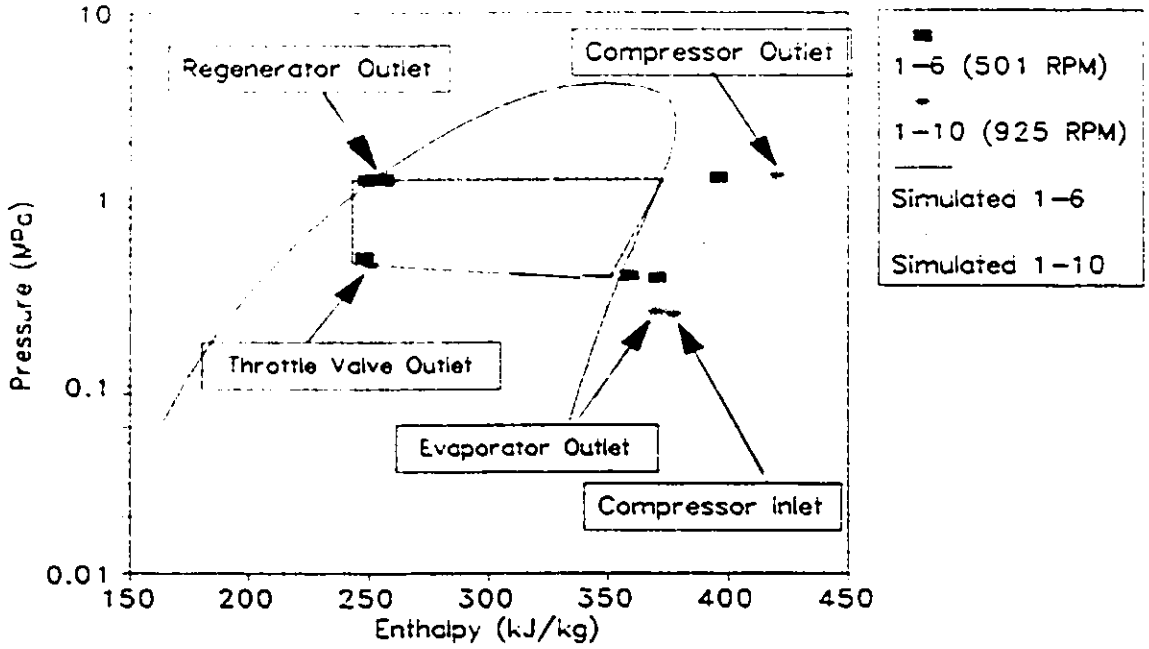

Figure 65: Trends in The Thermodynamic Cycle Predicted By The Simulation Program For Varying Compressor Speed

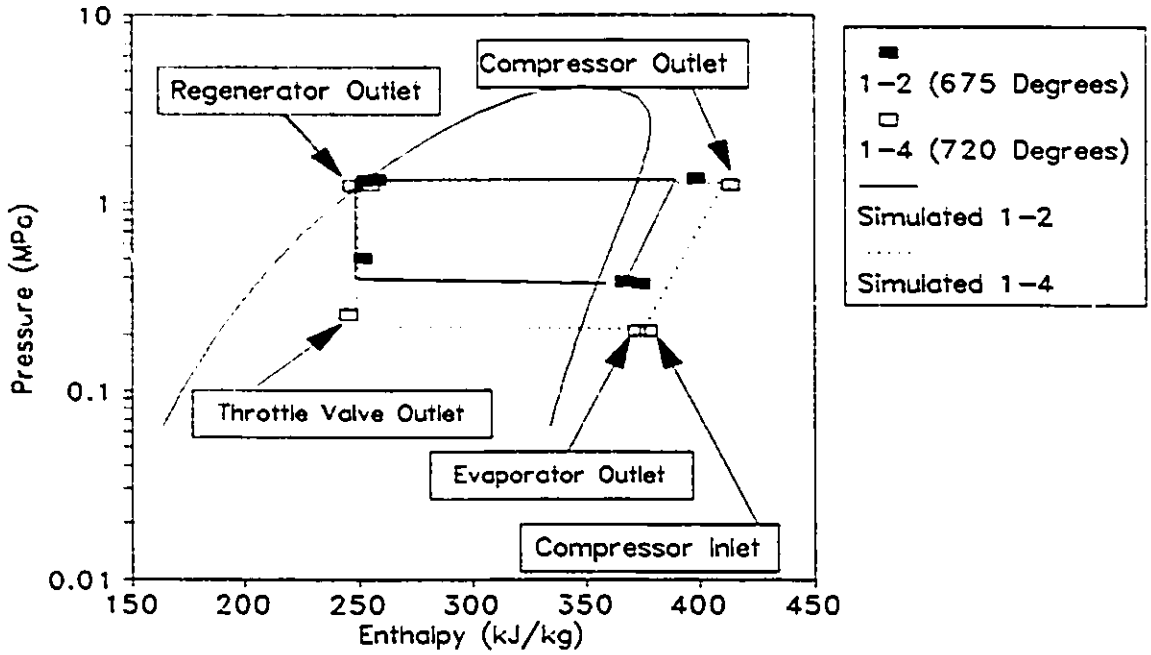

Figure 66: Trends in The Thermodynamic Cycle Predicted By Simulation Program For Varying Throttle Valve Setting

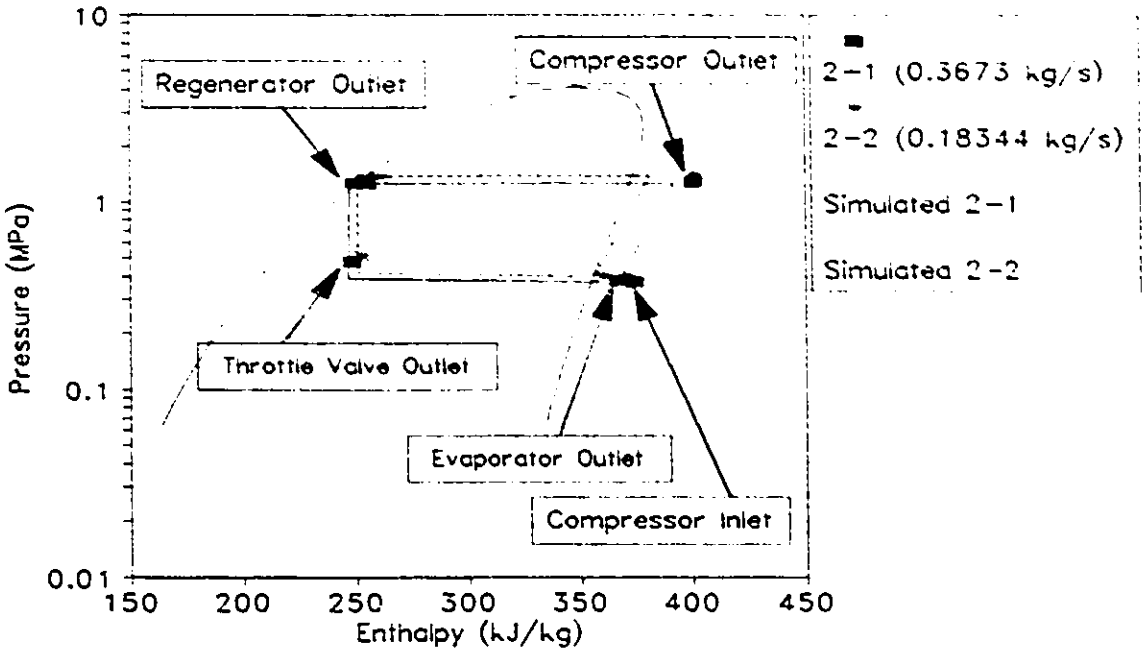

Figure 67: Trends In Thermodynamic Cycle Predicted By Simulation Program When Water Mass Flow Rate is Varied

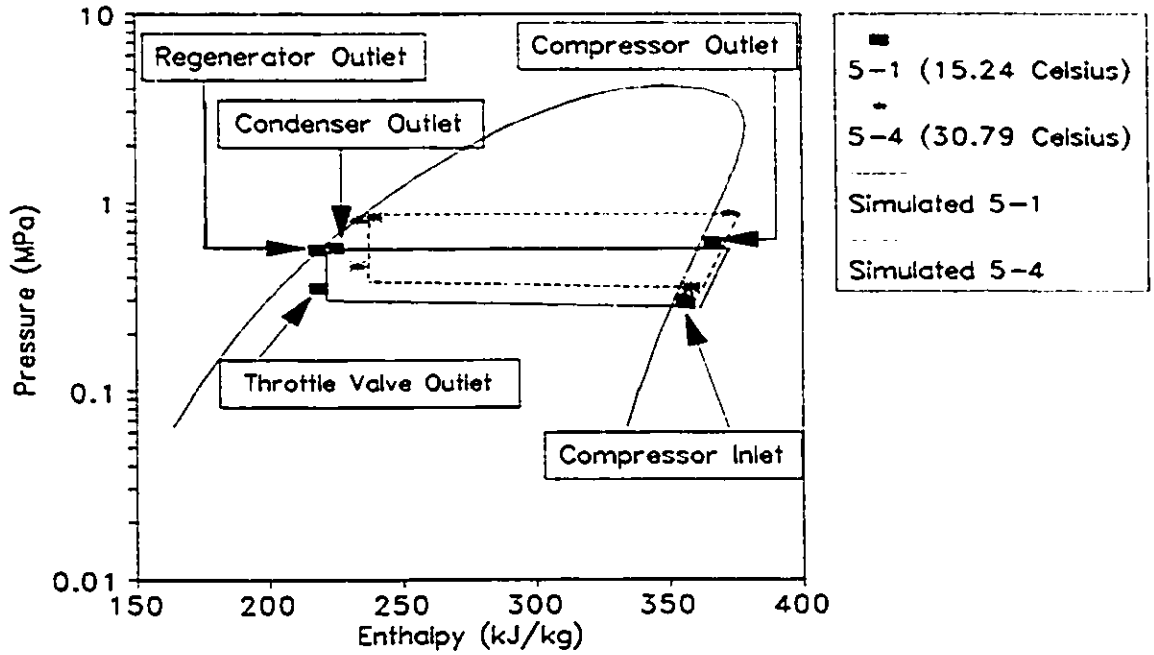

Figure 68: Trends In Thermodynamic Cycle Predicted By Simulation Program For Varying Water Inlet Temperature

XII. CONCLUSIONS AND RECOMMENDATIONS

The computer program was capable of predicting the system performance trends when the compressor crank shaft speed, throttle valve setting, condenser cooling water mass flow rate, and condenser cooling water temperature were each independently varied.

The condenser capacity, CnD.Q_thermo, evaporator capacity, EvP.Q_thermo, and Ecomp were always predicted within 10 percent. The refrigerant pressures at the compressor outlet and inlet differed by as much as 0.03 MPa from the experimental values (the corresponding saturation temperatures differed as much as 2 degrees Celsius). This is not very significant because the maximum pressure differences in the cycle were between 0.3 and 0.9 MPa. The predictions of refrigerant temperature at the compressor inlet, compressor outlet and evaporator outlet, however, differed by as much as 20 degrees Celsius from the actual values.

There are two general ways in which the simulation program can be improved. One way is to increase the number of system types that can be simulated (for example, by adding the capability for water to water system simulation). The other way is to make the simulation of air to water systems more detailed (for example, by altering the evaporator module so that fin

spacing and thickness become inputs to the program so that their effect on system performance can be studied directly).

The easiest improvement to make to the simulation program would be to add property subroutines that would allow the simulation of systems that operate with refrigerants other than R12 and R22. It would be especially appropriate for the program to simulate systems working with R134a, the proposed alternative to R12 after the phase out of R12 [20].

REFERENCES

1. Armstrong, Specifications-Installation of Armstrong Armaflex Insulations, p 5, Armstrong World Industries, Inc., (1991).

2. ASHRAE, Thermophysical Properties of Refrigerants, American Society of Heating, Refrigerating and Air-Conditioning Engineers, Inc, New York, (1976).

3. ASHRAE, Thermodynamic Properties of Refrigerants, American Society of Heating, Refrigerating and Air-Conditioning Engineers, Inc, Atlanta, GA, (1986).

4. ASHRAE, ASHRAE Handbook: Fundamentals, American Society of Heating, Refrigerating and Air-Conditioning Engineers, Inc, Atlanta, GA, (1985).

5. Berghmans,J., Domestic Heat Pump Applications, Proceedings of the NATO Advanced Study Institute on Heat Pump Fundamentals, Espinho, Spain, (September 1-12, 1980).

6. Bo Pierre, V. The Coefficient of Heat Transfer for Boiling Freon 12 in Horizontal Tubes, S.F. Review, 2, n 1, (English), pp. 55-68,(Published by A.B. Svenska Flaktfabriken, Stockholm, Sweden), (1955).

7. Chen, J.C., Correlation for Boiling Heat Transfer to Saturated Fluids in Convective Flows, Ind. Eng. Chem. Process Design Develop., 5, n 3, (1966).

8. Damasceno, G.S., and Goldschmidt, V.W. An Update of the August 1986 User's Guide of the Heat Pump Performance Model HN, Ray W. Herrick Laboratories Report No. Hl 87-37p, Purdue University, West Lafayette, IN, (1987).

9. Damasceno, G.S., and Goldschmidt, V.W., Rooke, S.P., Comparison of Three Steady-State Heat Pump Computer Models, ASHRAE Transactions, 96, Pt 2, (1990).

10. Davis, G.L., Chianese, F., Scott, T.C., Computer Simulation of Automotive Air Conditioning-Components,System, and Vehicle, SAE paper 720073, (1972).

11. Domanski, P., and Didion, D., Computer Modelling of the Vapor Compression Cycle with Constant Flow Area Expansion Device, Report No.NBS BSS 155, NBS, (1983).

12. Downing, R.C., Refrigerant Equations, ASHRAE Transactions, 80, Pt 2, (1974).

13. D'Valentine, M., and Goldschmidt, V.W. Apple (Personal Computer) Program for Modelling The Steady State Performance of Air Conditioners, Proceedings of XVIIth International Congress of Refrigeration, E, Wieh, (1987).

14. Fischer, S.K., and Rice, C.K., The Oak Ridge Heat Pump Models: A Steady-State Computer Design Model for Air-to-Air Heat Pumps, Report No. ORNLICON-80/R1, Oak Ridge, TN: Oak Ridge National Laboratory, (1983).

15. Fischer, S.K., Rice, C.K., Jackson, W.L, The Oak Ridge Heat Pump Design Model: Mark III version program documentation. Report No. ORNL/TM-10192, Oak Ridge, TN: Oak Ridge National Laboratory. (1988).

16. Hamilton, J.F, and Miller, J.L, A Simulation Program For Modelling An Air-Conditioning System, ASHRAE Transactions, 96, Pt. 1, (1990).

17. Hill, J.M., Jeter, S.M., Techniques For Obtaining Improved Initial Estimates of Explicit State Variables For Computer-Based Thermodynamic Property Routines, ASHRAE Transactions, 96, Pt. 1, (1990).

18. Incropera, F.P. and Dewitt, D.P., Fundamentals of Heat and Mass Transfer, pp 8, 504-525, John Wiley & Sons, Inc., Toronto, (1985).

19. Jeter, S.M., Wepfer, W.J., Fadel, G.M., Cowden, N.E., Dymek, A.A., Analysis and Simulation of Variable Speed Drive Heat Pumps, A.A. Energy (Oxford), 12, n 12, pp. 1289-1298, (1987).

20. Jung, D.S., Radermacher, R., Prediction of Heat Transfer Coefficient of Various Refrigerants During Evaporation, ASHRAE Transactions, 97, Pt. 2, (1991).

21. Kew, P.A., The Industrial Applications of Heat Pumps, Proceedings of the NATO Advanced Study Institute on Heat Pump Fundamentals, Espinho, Spain, (September 1-12, 1980).

22. Kletskii, A.V., Thermophysical properties of Freon-22, pp. 10-23, Israel Program for Scientific Transactions Ltd., Jerusalem, (1971).

23. MacArthur, J.W., Theoretical Analysis of the Dynamic Interactions of Vapor Compression Heat Pumps, Energy Convers Mgmt, 24, n 1, pp. 49-66, (1984).

24. McMullan, J.T., Morgan, R., Hughes, D.W., The Discrepancy Between Heat Pump Field and Test Performance: A Simulation Study, Int. J. Energy Res., 5, pp. 83-94, (1981).

25. Ministry of Energy, Ontario., Ministry of Tourism and Recreation, Ontario., Energy Encyclopedia for Arenas and Swimming Pools: Energy Conservation Measures for Recreation Facilities, Ice Skating Arenas and Indoor Pools, Toronto, pp. 123,124, (1987)

26. Molki, M., Sparrow, E.M., An Empirical Correlation for the Average Heat Transfer Coefficient in Circular Tubes, ASME Transactions, 108, (May, 1986).

27. Moran, M.J., Shapiro, H.N., Fundamentals of Engineering Thermodynamics, John Wiley & Sons, Inc., Toronto, (1988).

28. Mueller Brass Co., Refrigeration and Air Conditioning Products, Catalog R-182, Port Huron, (1989).

29. Newman, Steve, of Tecumseh Products of Canada Limited, Personal Communication, (September 21, 1991).

30. Parise, J.A.R., Simulation of Vapor Compression Heat Pumps, Simulation, 71, (February, 1986).

31. Petersen, Stephen R., Advanced Heat Pumps For The 1990s, ASHRAE J., 31, n 9, (September, 1989).

32. Rohsenow, W.M., Hartnett, J.P., Ganic, E.N., Handbook of Heat Transfer Fundamentals, McGraw-Hill Inc., New York, (1985).

33. Rosell, J., Morgan, R., McMullan, J.T., The Performance of Heat Pumps In Service: A Simulation Study, Int. J. Energy Res, 6, pp. 83-99, (1982).

34. Schenck, Hilbert, Jr., Theories of Engineering Experimentation, McGraw-Hill Book Company, Toronto, (1968).

35. Sauer, H.J., Howell, R.H, Heat Pump Systems, John Wiley & Sons, Toronto, (1983).

36. Tassou, S.A., Marquand, C.J., Wilson, D.R., Modelling of Variable Speed Air-to-Water Heat Pump Systems, J. Inst. Energy, 55, pp. 59-64, (June, 1982).

37. Traviss, D.P., Rohsenhow, W.M., Baron, A.B., Forced Convection Condensation Inside Tubes: A Heat Transfer Equation for Condenser Design, ASHRAE Transactions, 79, Pt. 1, (1973).

38. Vargaftik, N.B. 1975. Tables on the Thermophysical Properties of Liquids and Gases, pp. 369-372, 381-390, Hemisphere Publishing Co., Washington D.C., (1975).

39. White, F.M., Fluid Mechanics, pp. 332-359, McGraw-Hill Inc., New York, (1979).

40. Wood, B.D., Applications of Thermodynamics, p 151-158, Addison-Wesley Publishing Company, Inc., Reading, Massachusetts, (1982).

APPENDIX I

Condenser Modelling

APPENDIX I

A. Modelling Equations For Coil in Tank Condenser

The amount of heat transferred by the refrigerant as it passes through the dry portion is given by

$$Q\_HTdry = UA\_dry' \; Lcond\_dry \; LMTD\_dry \tag{96}$$

where UA_dry' is the overall thermal conductance per unit length for the dry portion, Lcond_dry is the length of the dry portion, and LMTD_dry is given by

$$LMTD\_dry = \frac{t_2 - t_x}{\ln\left(\frac{t_2 - t_w}{t_x - t_w}\right)} \tag{97}$$

where t2 is the refrigerant inlet temperature, tw is the water temperature, and tx is the temperature of the refrigerant at the end of the dry portion. The overall thermal conductance (on a per unit length basis) is given by

$$UA\_dry' = \frac{1}{R'_{in} + R'_{out} + R'_{wall}} \tag{98}$$

where Rin', Rout', and Rwall' are thermal resistances; Rin' is given by

$$R'_{in} = \frac{1}{\bar{h}_{in\_cond\_dry} \; (2 \pi \, Radius\_cond)} \tag{99}$$

Rout' is given by

$$R'_{out} \quad \frac{1}{\bar{h}_{out\_cond\_dry}\,(2\,\pi\,(Radius\_cond+2\,thick))} \qquad (100)$$

and Rwall is given by

$$R'_{wall} = \frac{\ln\left(\frac{Radius\_cond+2\,thick}{Radius\_cond}\right)}{2\pi k_{pipe}} \qquad (101)$$

$\bar{h}in\_cond\_dry$ and $\bar{h}out\_cond\_dry$ are the inside and outside convection heat transfer coefficients for the condenser's dry portion respectively. Radius_cond is the inner radius of the condenser coil, and *thick* is the thickness of the condenser coil.

By combining (96) with the first law of thermodynamics, the following expression for Lcond_dry may be derived:

$$Lcond\_dry = \frac{-REFmdot\,C_{p_g}}{UA\_dry'}\ln\left(\frac{tx-Tw}{t2-Tw}\right) \qquad (102)$$

The refrigerant side wall temperature at the point where condensation begins, twallx, is given by

$$\frac{tx - twallx}{R'_{in}} = \frac{tx - t_w}{R'_{in} + R'_{wall} + R'_{out}} \qquad (103)$$

where Rin' and Rout' are determined using local heat transfer coefficients. Recall that a discontinuity in the wall temperature was assumed to occur immediately downstream of this point. The value of twallx equals tsat2 if the local value

of $\bar{h}in\_cond\_dry$ is used to determine Rin'.

The heat transferred in the wet portion of the condenser is given by

$$Q\_HTwet = UA\_wet' \; Lcond\_wet \; (t_{cond}-Tw) \tag{104}$$

where tcond is (tsat2+tsat3)/2 and UA_wet' is given by

$$UA\_wet' = \frac{1}{R'_{wall} + R'_{out}} \tag{105}$$

where $\bar{h}out\_cond\_wet$, the outside heat transfer coefficient for the wet portion, is used to evaluate Rout'. The value of Rin' is neglected.

The amount of heat transferred by the refrigerant as it passes through the liquid portion is given by

$$Q\_HTliq = UA\_liq' \; Lcond\_liq \; LMTD\_liq \tag{106}$$

where UA_liq' is the overall thermal conductance per unit length of the liquid portion, Lcond_liq is the length of the liquid portion, and LMTD_liq is given by

$$LMTD\_liq = \frac{t_{sat3}-t_3}{\ln\left(\frac{t_{sat3}-t_w}{t_3-t_w}\right)} \tag{107}$$

where t3 is the refrigerant outlet temperature, tw is the water temperature, and tsat3 is the refrigerant saturation temperature at the outlet pressure. The overall thermal conductance (on a per

unit length basis) is given by (98) with $\bar{h}in\_cond\_liq$ and $\bar{h}out\_cond\_liq$, the inside and outside convection heat transfer coefficients for the condenser's liquid portion respectively, used to calculate the Rin' and Rout'.

By combining (106) with the first law of thermodynamics, the following expression for Lcond_liq may be derived:

$$Lcond\_liq = \frac{-REFmdot\, C_{Pf}}{UA\_liq'} \ln\left(\frac{t3-Tw}{t_{sat3}-Tw}\right) \qquad (108)$$

When (108) is solved for t3, the exponential nature of the equation ensures that the second law of thermodynamics is not violated.

B. Constants Required For Use of Correlation For Natural Convection on Outside of Horizontal Elliptical Cylinder

The following quantities appear in correlation three of table 1: $\bar{C}_L$, $\bar{C}_t$, $C1$, $C2$. The following equations were obtained by curve fitting tabular data [32]:

$$C1 = AC1 + BC1\left(\frac{C}{B}\right) + CC1\left(\frac{C}{B}\right)^2 + DC1\left(\frac{C}{B}\right)^3 + EC1\left(\frac{C}{B}\right)^4 \qquad (109)$$

where

AC1 = 1.00008145658;

BC1 =-0.0404670767534;

CC1 =-0.585564486528;

DC1 = 0.616704402384;

EC1 =-0.218773936526;

$$C2 = \left[AC2 + BC2\left(\frac{C}{B}\right) + CC2\left(\frac{C}{B}\right)^2 + DC2\left(\frac{C}{B}\right)^3 + EC2\left(\frac{C}{B}\right)^4\right]^{\frac{1}{4}} \qquad (110)$$

where

AC2 = 70.12907661590;

BC2 = -74.1517893003;

CC2 = 140.592145799;

DC2 =-320.462301052;

EC2 = 194.346040535;

$$\overline{C}_L = Acl + Bcl \ln(P_r) + Ccl [\ln(P_r)]^2 \qquad (111)$$

where

Acl = 0.533885099378;

Bcl = 0.0519665203960;

Ccl =-0.00570411048084;

$$\begin{aligned}\overline{C}_t &= Act + Bct\left(\frac{C}{B}\right) \\ &+ \left[Cct + Dct\left(\frac{C}{B}\right) + Ect\left(\frac{C}{B}\right)^2 + Fct\left(\frac{C}{B}\right)^3 + Gct\left(\frac{C}{B}\right)^4\right]\ln(P_r) \\ &+ \left[Hct + Ict\left(\frac{C}{B}\right) + Jct\left(\frac{C}{B}\right)^2 + Kct\left(\frac{C}{B}\right)^3 + Lct\left(\frac{C}{B}\right)^4\right][\ln(P_r)]^2\end{aligned} \qquad (112)$$

where

Act = 0.106417471100;

Bct =-0.00140960955369;

Cct = 0.00792657837602;

Dct = 0.00548641724353;

Ect =-0.0312646623618;

Fct = 0.0361650917618;

Gct =-0.0130581394917;

Hct =-0.00266422274173;

Ict =-0.00122692647805;

Jct = 0.00991883857844;

Kct =-0.0126651236192;

Lct = 0.00496259193808;

C. Modelling Assumptions For Concentric Tube Condenser

The amount of heat transferred by the refrigerant to the water in the dry portion is given by

$$Q\_HTdry = UA\_dry' \; Lcond\_dry \; LMTD\_dry \tag{113}$$

where UA_dry' is given by

$$UA\_dry' = \frac{1}{R'_{in} + R'_{out} + R'_{wall}} \tag{114}$$

where Rin' is given by

$$R'_{in} = \frac{1}{\bar{h}in\_cond\_dry \, \pi \, D1} \tag{115}$$

Rout' is given by

$$R'_{out} = \frac{1}{\bar{h}out\_cond\_dry \, \pi \, D2} \tag{116}$$

and Rwall' is given by

$$R'_{wall} = \frac{\ln\left(\frac{D2}{D1}\right)}{2\,\pi\,k_{pipe}} \tag{117}$$

where D1 and D2 are the inner and outer diameters of the inner tube respectively and $\bar{h}in\_cond\_dry$ and $\bar{h}out\_cond\_dry$ are the inside and outside heat transfer coefficients for the dry portion. LMTD_dry is given by

$$LMTD\_dry = \frac{(t2-tw_o) - (tx-twx)}{\ln\left(\frac{t2-tw_o}{tx-twx}\right)} \tag{118}$$

for counter flow and by

$$LMTD\_dry = \frac{(t2-twi) - (tx-twx)}{\ln\left(\frac{t2-twi}{tx-twx}\right)} \tag{119}$$

for parallel flow.

The amount of heat transferred in the wet portion of the condenser is given by

$$Q\_HTwet = UA\_wet'\ Lcond\_wet\ LMTD\_wet \tag{120}$$

where UA_wet' is given by

$$UA\_wet' = \frac{1}{R'_{in} + R'_{out} + R'_{wall}} \tag{121}$$

where Rin' and Rout' are determined using $\bar{h}in\_cond\_wet$ and $\bar{h}out\_cond\_wet$ respectively; LMTD_wet

is given by

$$LMTD\_wet = \frac{(t_{cond}-twx)-(t_{cond}-twx1)}{\ln\left(\frac{t_{cond}-twx}{t_{cond}-twx1}\right)} \qquad (122)$$

where tcond is (tsat2+tsat3)/2.

The heat transferred in the liquid portion of the condenser is given by

$$Q\_HTliq = Eff\ Mcp\_min\ (t_{cond}-twx1) \qquad (123)$$

where Mcp_min is the smaller of REFmdot*cpf and H2Omdot*H2Ocpf. The effectiveness, Eff, is given by

$$Eff = \frac{1 - EXP[-NTU(1-C_r)]}{1-C_r EXP[-NTU(1-C_r)]} \qquad (124)$$

for counterflow and by

$$0Eff = \frac{1 - EXP[-NTU(1+C_r)]}{1 + C_r} \qquad (125)$$

for parallel flow; NTU is given by UA_liq/Mcp_min and Cr is given by

$$C_r = \frac{Mcp\ min}{Mcp\_max} \qquad (126)$$

where Mcp_max is the larger of REFmdot*cpf and H2Omdot*H2Ocpf. UA_liq is given by

$$UA\_liq = \frac{Lcond\ liq}{R'_{in} + R'_{out} + R'_{wall}} \qquad (127)$$

For parallel flow, the temperature of the wall at the refrigerant inlet can be found from

$$\frac{t2 - twallo}{R'_{in}} = \frac{t2 - twi}{R'_{in} + R'_{wall} + R'_{out}} \tag{128}$$

where Rin' and Rout' are determined using local heat transfer coefficients. For counter flow, twi is replaced with two in the preceding expression. The preceding equation assumes that refrigerant flows inside the inner tube. If this is not the case then Rin' and Rout' must be interchanged.

Similar expressions are used to determine the other wall temperatures:

$$\frac{t_{sat3} - twallx1}{R'_{in}} = \frac{t_{sat3} - twx1}{R'_{in} + R'_{wall} + R'_{out}} \tag{129}$$

$$\frac{t3 - twall\ L}{R'_{in}} = \frac{t3 - twi}{R'_{in} + R'_{wall} + R'_{out}}\ (CounterFlow) \tag{130}$$

$$\frac{t3 - twall\ L}{R'_{in}} = \frac{t3 - tw_o}{R'_{in} + R'_{wall} + R'_{out}}\ (Parallel\ Flow) \tag{131}$$

In each case Rin' and Rout' are determined using the appropriate local heat transfer coefficients. Again, if refrigerant flows in the outer tube then Rin' and Rout' must be interchanged.

twallx is set equal to tsat2 so that tx can be found from

$$\frac{tx - twallx}{R'_{in}} = \frac{tx - twx}{R'_{in} + R'_{wall} + R'_{out}} \tag{132}$$

where Rin' is calculated using a single phase heat transfer correlation. Because of the discontinuity in the wall temperature which was assumed to exist at the end of the dry portion, twallx is found from

$$\frac{t_{sat2} - twallx}{R'_{in}} = \frac{t_{sat2} - twx}{R'_{in} + R'_{wall} + R'_{out}} \qquad (133)$$

where Rin is determined using a condensation heat transfer correlation. If refrigerant flows in the outer tube then Rin' and Rout' must be interchanged in (132) and (133).

D. <u>The Constants in the Correlation For Single Phase Forced Convection Inside a Circular Annulus</u>

Curve fits of tabulated data for Nuselt number [32] results in a correlation of the following form

$$\ln(N_u) = AA0 + AA1 \ln(R_e) + AA2 [\ln(R_e)]^2 + AA3 [\ln(R_e)]^3 \qquad (134)$$

For inner to outer diameter ratios (D2/D3) of 0.2, 0.5, and 0.8, the values of AA0, AA1, AA2, and AA3 are related to Prandtl number, Pr, as follows

$$AA0 = a0 + a1 \ln(P_r) + a2 [\ln(P_r)]^2 + a3 [\ln(P_r)]^3 \qquad (135)$$

$$AA1 = b0 + b1 \ln(P_r) + b2 [\ln(P_r)]^2 + b3 [\ln(P_r)]^3 \qquad (136)$$

$$AA2 = c0 + c1 \ln(P_r) + c2 [\ln(P_r)]^2 + c3 [\ln(P_r)]^3 \qquad (137)$$

$$AA4 = d0 + d1 \ln(P_r) + d2 [\ln(P_r)]^2 + d3 [\ln(P_r)]^3 \qquad (138)$$

For a diameter ratio of 0.1 the values of AA0, AA1, AA2, and AA3 are related to Pr as follows

$$AA0 = a0 + a1\,P_r + a2\,P_r^2 + a3\,P_r^3 \quad (139)$$

$$AA1 = b0 + b1\,P_r + b2\,P_r^2 + b3\,P_r^3 \quad (140)$$

$$AA2 = c0 + c1\,P_r + c2\,P_r^2 + c3\,P_r^3 \quad (141)$$

$$AA3 = d0 + d1\,P_r + d2\,P_r^2 + d3\,P_r^3 \quad (142)$$

For a ratio of 0.8 the constants are

a0 = 1.95653;

a1 = -0.78983;

a2 = 0.535249;

a3 = -0.17814;

b0 = -0.55089;

b1 = 0.361541;

b2 = -0.21566;

b3 = 0.060355;

c0 = 0.10168;

c1 = -0.03206;

c2 = 0.023629;

c3 = -0.00626;

d0 = -0.00248;

d1 = 0.000994064889374;

d2 = -0.000808068534355;

d3 = 0.000206042209747;

For a ratio of 0.5 the constants are

a0 = 2.33360295243;

a1 = 7.10734519691;

a2 = -6.53028476912;

a3 = 1.13142256110;

b0 = -0.600229843578;

b1 = -1.81875243453;

b2 = 1.70934149506;

b3 = -0.294252923828;

c0 = 0.103244906522;

c1 = 0.166870147870;

c2 = -0.149989870496;

c3 = 0.0255281984874;

d0 = -0.00245835033759;

d1 = -0.00501560184824;

d2 = 0.00438119497035;

d3 = -0.000738687062978;

For a ratio of 0.2 the constants are

a0 = 4.12443;

a1 = -1.32416;

a2 = -1.13126;

a3 = 0.312337;

b0 = -0.96663;

b1 = 0.360112;

b2 = 0.303265;

b3 = -0.08244;

c0 = 0.13072;

c1 = -0.02096;

c2 = -0.02847;

c3 = 0.007391;

d0 = -0.00315;

d1 = 0.000377297489018;

d2 = 0.000886119765576;

d3 = -0.000221728409166;

For a ratio of 0.1 the constants are

a0 = 7.73035897327;

a1 = -3.42550329091;

a2 = 0.376158092501;

a3 = -0.00904377531472;

b0 = -1.80741263547;

b1 = 0.917247348933;

b2 = -0.100644880679;

b3 = 0.002420167214;

c0 = 0.193050539135;

c1 = -0.0738009156176;

c2 = 0.00827044207261;

c3 = -0.00020006559022;

d0 = -0.004728782156;

d1 = 0.002011682996;

d2 = -0.000228447546;

d3 = 5.54670680532e-06;

E. Use of Integration to Find Average Heat Transfer Coefficient For Condensation Inside a Circular Tube

If refrigerant condenses inside the inner tube then the average heat transfer coefficient is obtained from the following

expression [32]:

$$\frac{1}{\bar{h}_{avg}} = \int_0^1 \frac{dx}{\bar{h}_z(x)} \tag{143}$$

By definition havg is

$$\bar{h}_{avg} = \frac{\int_{z=0}^{z=L} \bar{h}_z(z)\, dz}{L} \tag{144}$$

Making the change of variable from distance along the tube to quality, the following is obtained

$$\bar{h}_{avg} = \frac{\int_{x=1}^{x=0} \bar{h}_z(x) \frac{dz}{dx} dx}{L} \tag{145}$$

By applying the first law to a portion of the condenser of length Δz the following is obtained:

$$\pi D \bar{h}_z(x) \Delta T \Delta z = -REFmdot\ h_{fg}\ \Delta x \tag{146}$$

from which it is easily seen that

$$\frac{dz}{dx} = -\frac{REFmdot\ h_{fg}}{\pi D \bar{h}_z(x) \Delta T} \tag{147}$$

where D is the diameter of the tube and ΔT is the difference between the refrigerant saturation temperature and the wall temperature. If ΔT is assumed constant then integration of (147)

yields

$$L = -\frac{REPmdot}{\pi D \Delta T} h_{sg} \int_{x=1}^{x=0} \frac{1}{\bar{h}_z(x)} dx \qquad (148)$$

Substitution of (147) and (148) into (144) yields

$$h_{avg} = \frac{-1}{\int_{x=1}^{x=0} \frac{1}{h_z(x)} dx} \qquad (149)$$

from which it is easily seen that

$$\frac{1}{\bar{h}_{avg}} = \int_{x=0}^{x=1} \frac{1}{\bar{h}_z(x)} dx \qquad (150)$$

APPENDIX II

Evaporator Modelling

APPENDIX II

A. Finding Outlet Air Temperature And Relative Humidity

The amount of heat transferred by the air to the refrigerant is given by

$$Q\_air = AIRmdot\,[\,(h_{AIR_i} + w_i h_{g_i}) - (h_{AIR_o} + w_o h_{g_o}) - (w_i - w_o) * hf_o\,] \qquad (151)$$

where wi and wo are the humidity ratios of the air at the evaporator inlet and outlet respectively, h_{AIR_i} and h_{AIR_o} are the enthalpies of the inlet and outlet air respectively, hgi and hgo are enthalpies of water vapour at the inlet and outlet respectively, and hfo is the enthalpy of water condensate that leaves the condenser. If frosting accumulates on the evaporator coil then Q_air is given by

$$Q\_air = AIRmdot\,[\,(h_{AIR_i} + w_i h_{g_i}) - (h_{AIR_o} + w_o h_{g_o}) - (w_i - w_o)\ u\_ice\,] \qquad (152)$$

where u_ice is the specific internal energy of the frost at zero degrees Celsius. The following expression results from substitution into (151) of linear regression formulae for the enthalpies of water liquid and water vapour [27] along with the approximation that the enthalpy change of dry air is equal to its specific heat capacity multiplied by the temperature change:

$$Q\_air = AIRmdot\,[\,AIRcp\,(t_{AIR_i} - t_{AIR_o}) + w_i\,(2501.1 + 1.82\,t_{AIR_i}) - w_o\,(2501.1 + 1.82\,t_{AIR_o}) - 4.186\,(w_i - w_o)\,t_{AIR_o}\,] \quad (153)$$

where t_{AIR_i} and t_{AIR_o} must be in degrees Celsius. A similar expression can be derived using (152). t_{AIR_o} and wo can be found for known values of Q_air, t_{AIR_i}, and wi by solving (153) iteratively since wo is either equal to wi or a function only of t_{AIR_o}.

Figure 69 is a psychometric chart on which the three possible types of processes that the air can undergo are identified. After process a to b the water vapour in the air remains superheated. After process a to b the water vapour in the air is saturated vapour. The temperature of the air after this process is tdew, the dew point temperature. After process a to d the water vapour that remains in the air is saturated but some vapour has condensed out of the moist air. In processes a to b and in process a to c the value of wi equals wo. In process a to d the value of wo is less than that of wi. However, the water vapour in the air at state d is saturated. The value of wo is therefore given by

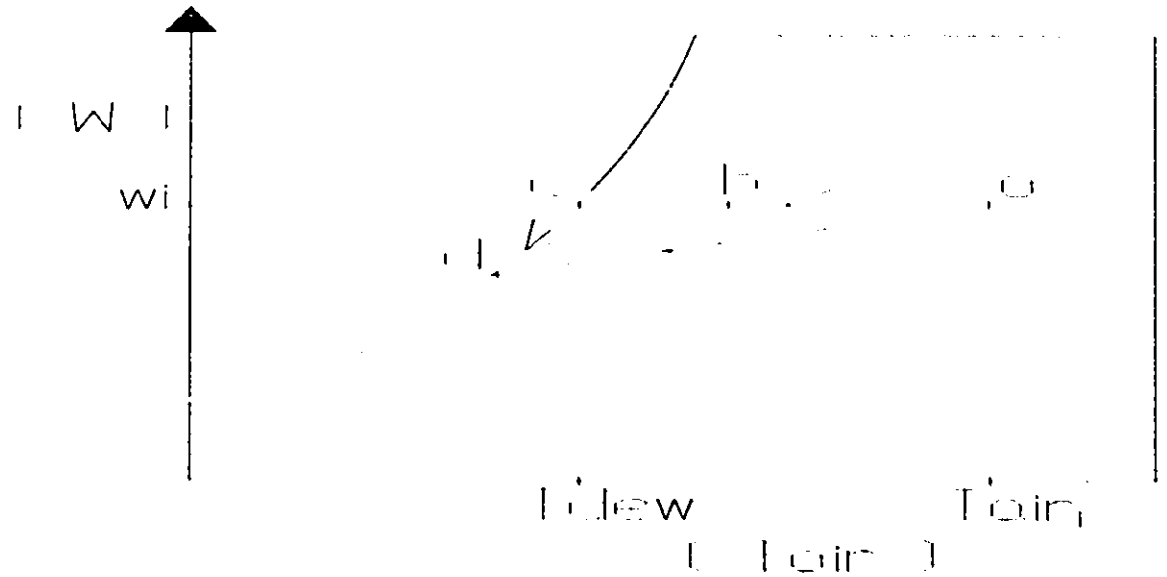

Figure 69: Processes Air May Undergo In Evaporator

$$w_o = \frac{0.622\ psat(T_{air_o})}{P - psat(T_{air_o})} \qquad (154)$$

where $psat(T_{air_o})$ is the saturation pressure of water vapour at t_{AIR_i} and p is the pressure of the moist air mixture (assumed not to change during the process). Note that wo is a function of t_{AIR_i} alone.

To decide if wi is equal to or less than wo the value of Q_air is compared with that of Qac, the amount of heat that is transferred in process a to c. The value of Qac is determined from (153) with t_{AIR_i} set equal to tdew and wo set equal to wi. If

Q_air is less than or equal to Qac, then wo is equal to wi; otherwise, (154) must be used to find wo.

B. Calculation of The Maximum Amount of Heat That Can Be Transferred in The Wet Portion

If, in the wet portion, the maximum amount of heat were extracted from the air, then the air would leave the wet portion as saturated air at a temperature of tsat6. The maximum amount of heat transfer possible in the wet portion is therefore given by

$$Q\_air = AIRmdot\,[\,AIRcp\,(t_{AIR_i} - tsat6) + w_i\,(2501.1 + 1.82\,t_{AIR_i}) - w_m\,(2501.1 + 1.82\,tsat6) - 4.186\,(w_i - w_m)\,tsat6\,] \quad (155)$$

where all temperatures are in Celsius.

C. Calculation of The Ratio of The Area of The Wet Portion To The Area of The Entire Evaporator

The effectiveness of the wet portion of the evaporator is given by

$$EFF\_wet = 1 - EXP\left(\frac{-UA\_wet}{MC\_min}\right) \quad (156)$$

where UA_wet is the thermal conductance of the wet portion and MC_min is given by

$$MC\_min = \frac{Q_{max}}{T_{air_i} - t_{sat6}} \quad (157)$$

The effectiveness that the *entire* evaporator would have if the refrigerant exited as a saturated vapour is given by

$$EFF\_allwet = 1 - EXP\left(\frac{-UA\_allwet}{MC\_min}\right) \quad (158)$$

By isolating the thermal conductances in (156) and (158) the

following are obtained:

$$UA\_wet = -MC\_min\ \ln(1-EFF\_wet) \tag{159}$$

$$UA\_allwet = -MC\_min\ \ln(1-EFF\_allwet) \tag{160}$$

Division of (159) by (160) yields

$$\frac{UA\ wet}{UA\_allwet} = \frac{\ln(1-EFF\ wet)}{\ln(1-EFF\_allwet)} \tag{161}$$

The desired expression is then obtained by assuming that the overall heat transfer coefficients are equal:

$$\frac{Aevap\ wet}{Aevap} = \frac{\ln(1-EFF\ wet)}{\ln(1-EFF\_allwet)} \tag{162}$$

D. The Thermal Conductance of The Dry Portion

Recall the definition of F as

$$\bar{h}in\_evap\_wet\ A_{evap\_wet} = F\ \bar{h}out\_evap\_wet\ A_{out\_wet} \tag{163}$$

Since it is assumed the air side heat transfer coefficient is the same for the dry and wet portions of the evaporator, it follows that

$$\bar{h}in\_evap\_wet\ A_{evap\_dry} = F\ \bar{h}out\_evap\_dry\ A_{out\_dry} \tag{164}$$

where Aout_dry is the air side area of the dry portion.

The thermal conductance, UA_wet, is given by

$$\frac{1}{UA\_wet} = \frac{1}{\bar{h}in\_evap\_dry\ A_{evap\_dry}} + \frac{1}{\bar{h}out\_evap\_dry\ A_{out\_dry}} \tag{165}$$

By substitution of (163) into (165) and rearranging, the

following expression is obtained:

$$UA\_dry = \frac{Aevap\_dry}{\frac{1}{\bar{h}in\_evap\_dry} + \frac{F}{\bar{h}in\_evap\_wet}} \qquad (168)$$

It should be pointed out that the value of F is obtained from

$$\frac{1}{UA\_allwet} = \frac{1}{\bar{h}in\_evap\_wet\, A_{evap}} + \frac{F}{\bar{h}in\_evap\_wet\, A_{evap}} \qquad (167)$$

which after isolating F becomes

$$F = \frac{\bar{h}in\_evap\_wet\ A_{evap}}{UA\_allwet} - 1 \qquad (168)$$

APPENDIX III

Property Correlations And Approximation

APPENDIX III

A. Determining Vapour Temperature and Specific Volume Given Enthalpy and Pressure

1. First Approximation For Temperature

The first approximation for temperature is given by

$$t^{1rst} = \frac{-\bar{E1} + [\ \bar{E1}^2 - 2\bar{E1}(A_q + h_q - h)\ ]^{1/2}}{E2} \qquad (170)$$

where Aq is given by

$$A_q = -\left(\frac{E2\,t_q^2}{2} + \bar{E1}\,t_q\right) \qquad (171)$$

Equation (170) was derived based on the assumptions that the vapour behaves as an ideal gas and that the specific heat of the vapour varied linearly with temperature. The properties tq, vq, hq are all properties of superheated vapour corresponding to a reference state at very low pressure, pq, so that, for all practical purposes, the vapour behaves as an ideal gas. Therefore, at the reference pressure, the specific heat capacity at constant volume of superheated vapour can be considered as being a function of temperature alone. It was additionally assumed that the specific heat capacity at constant volume was related to temperature as

$$C_v^o = E1 + E2t \qquad (172)$$

where E1 and E2 are constants (E2 also appears in (170)) and

$$\bar{E1} = E1 + R \qquad (173)$$

where R is the ideal gas constant for the refrigerant (not the universal value). The constants E1 and E2 were determined by curve fitting tabulated data [38]. The choice of reference state ensures that the values of hq and Aq are such that the quantity inside the square brackets in (170) is always positive.

3. First Approximation For Specific Volume

After a first approximation of temperature is obtained from (170), a first approximation of specific volume is obtained. The basis for the approximation was the Redlich-Kwong equation:

$$p = \frac{Rt}{(v-b_{rk})} - \frac{a_{rk}}{[t^{0.5}v(v+b_{rk})]} \tag{174}$$

where a_{rk} is given by

$$a_{rk} = \frac{0.4275\,R^2 t_c^{2.5}}{p_c} \tag{175}$$

and b_[rk} is given by

$$b_{rk} = 0.0867\,Rt_c/p_c \tag{176}$$

tc and pc being, respectively, the critical temperature and pressure of the refrigerant. Rearranging the Redlich-Kwong equation the following cubic equation for specific volume is obtained:

$$v^3 + \alpha_2 v^2 + \alpha_1 v + \alpha_0 = 0 \tag{177}$$

where the constants are given by

$$\alpha_2 = -R\frac{t}{p}$$
$$\alpha_1 = -b_{rk}^2 - \frac{R\,t\,b_{rk}}{p} + \frac{a_{rk}}{p\sqrt{t}} \qquad (178)$$
$$\alpha_0 = -\frac{a_{rk}\,b_{rk}}{p\sqrt{t}}$$

In the program, one root of (177), Vrn, is found by using the Newton-Raphson method (the ideal gas law provides the initial guess). The other two roots are found using the quadratic formula to solve the following equation:

$$v^2 + (\alpha_2 + Vrn)\,v + [\alpha_1 + Vrn(\alpha_2 + \alpha_1)] = 0 \qquad (179)$$

Hill and Jeter [17] have found that the root of interest is always the largest of the real roots of (177).

3. Second Approximations of Temperature And Specific Volume

The first approximations for temperature and specific volume are then used to calculate enthalpy using the correlation for the enthalpy of superheated refrigerant vapour. The second approximation for temperature is then obtained from

$$t^{2nd} = t^{1rst} + C_{pg}\,(h - h^{1rst}) \qquad (180)$$

where Cpg is obtained at t^{1rst} . The second order approximation for specific volume is then made using the same method described in section A.2.. The second approximations are then used as the initial estimates required for the execution of the Newton-Raphson method.

B. Determining Vapour Temperature and Specific Volume Given Entropy and Pressure

1. First Approximation For Temperature

The following expression was derived based on the assumption that the refrigerant behaved as an ideal gas with constant specific heats (for details see Appendix X):

$$t^{1rst} = \left[\left(\frac{P v_y}{R}\right)^R t_y^{c_{v_y}} EXP(s - s_y)\right]^{\frac{1}{(c_{p_y} + R)}} \qquad (181)$$

where all the properties denoted with a "y" subscript are evaluated at an arbitrarily chosen reference state that is within the range of state points likely to be encountered in the simulation program.

2. First Approximation For Specific Volume

The first approximation for specific volume is then made based on the first approximation for temperature. The Redlich-Kwong equation of state was solved in order to obtain specific volume as described previously.

3. Second Approximations For Temperature And Specific Volume

The first approximations for temperature and specific volume are then used to determine entropy and specific heat at constant pressure; these values are then used in place of the properties with the "y" subscript in (181) so that the second approximation for temperature is obtained and used to generate the second approximation for specific volume (again the Redlich-Kwong equation is used). The second approximations are used as

the initial guesses required for the execution of the Newton-Raphson method.

C. R12 Property Correlations

1. Gas Density

The volume of saturated vapour in kilograms per cubic meter is given by [3]

$$\frac{dg}{ROWI} = [E6\ TOU^{-\frac{5}{3}} + E11 + E13\ TOU^{\frac{2}{3}} + E22\ TOU^{\frac{11}{3}} + E23\ TOU^{\frac{12}{3}} + E24\ TOU^{\frac{13}{3}}]\ M \quad (182)$$

where TOU is (1-t/TI), M is molecular mass (120.914 kg/kmol), and TI and ROWI are equal to 385.2 and 4.616 respectively. Temperature, t, is in Kelvin. The constant on the right hand side are

E6 = 0.788904825e-05

E11 = -0.1900330949

E13 = -0.5947813469*10

E22 = -0.5126536438e+03

E23 = 0.1142994928e+04

E24 = -0.6905751515e+03

2. Gas Thermal Conductivity

The following equation is used to calculate the thermal conductivity of R12 in kW/(m k) (temperature is in Kelvin):

$$k_g = \frac{\sqrt{1.8\ t}}{\left(A + \frac{B}{1.8\ t} + \frac{C}{(1.8\ t)^2}\right) 1000}$$

The constants on the right hand side are:

A = 420.391

B = 7.167492e+05

C = 1.886802e+08

3. Gas Viscosity

The following equation is used to calculate the absolute viscosity of R12 gas (in Pascal seconds) at temperatures between 250 and 470 Kelvin [2]:

$$\mu_g = \frac{\sqrt{t}}{(A + B\,t + C\,t^2)\ 1e{+}06} \tag{183}$$

The constants on the right hand side are

A = 0.75309

B = 188.969

C = -803.786

4. Gas Specific Heat Capacity

The following equation is used to calculate the specific heat capacity of R12 saturated vapour in kJ/(kg*K) (t is in Kelvin) [2]:

$$C_{p_g} = A + B\,t + C\,t^2 + D\,t^3 \tag{184}$$

For values of t less than or equal to 600 Kelvin, the constants on the right hand side are

A = 0.116661

B = 2.37994e-03

C = -2.94788e-06

D = 1.37282e-09

For temperatures greater than 600 Kelvin the constants are

A = 0.427182

B = 9.38152e-04

C = -6.89715e-07

D = 1.78066e-10

5. Liquid Density

The following correlation is used to calculate the density of saturated liquid in kilograms per cubic meter [3]:

$$d_f = [AL + BL\ TOU^{\frac{1}{3}} + dll\ TOU + FL\ TOU^{\frac{1}{2}} + GL\ TOU^2]\ 16.01891 \quad (185)$$

where TOU is (1-t/tc), t is temperature in Kelvin, tc is 384.95 Kelvin. The constants on the right hand side are:

AL = 34.84

BL = 53.341187

dll = 18.69137

FL = 21.98396

GL = -3.150994

6. Liquid Thermal Conductivity

The following equation is used to calculate the thermal conductivity of saturated liquid in kW/(mK) for temperatures between 144 to 344 Kelvin (t is in Kelvin) [2]:

$$k_f = \frac{A + B\ (t\text{-}273.15)}{1000} \quad (186)$$

The constants on the right hand side are

A = 0.07830

B = -0.000366

7. Liquid Viscosity

The viscosity of saturated liquid (in Pascal seconds) is calculated by the following equation for temperatures between 170 and 340 Kelvin [2] (t is in Kelvin):

$$\mu_f = \frac{EXP[\, A + \frac{B}{t}\,]}{1000} \qquad (187)$$

The constants on the right hand side are

A = -3.81728

B = 681.713

For temperatures between 340 and 380 Kelvin the viscosity is given by

$$\mu_f = \frac{A + B\,t + C\,t^2}{1000} \qquad (188)$$

The constants on the right hand side are

A = -2.36010

B = 0.01591

C = -0.000025

8. Liquid Specific Heat Capacity

This correlation calculates the specific heat capacity of R12 liquid in kJ/(kg K) [2] (t is in Kelvin):

$$C_{p_f} = A + B\,t + C\,t^2 + D\,t^3 \qquad (190)$$

For temperatures less than or equal to 300 Kelvin, the constants on the right hand side are

A = 4.02967e-02

B = 9.71208e-03

C = -4.07078e-05

D = 6.25641e-08

For temperatures greater than 300 Kelvin, the constants are

A = -16.7169

B = 1.83132e-01

C = -6.37959e-04

D = 7.47156e-07

9. Saturation Pressure

The following correlation is used to calculate saturation pressure in MPa [3]:

$$\frac{psat}{p_c} = EXP\left[\frac{t_c}{t}(B1\ TOU + B2\ TOU^{1.5} + B3\ TOU^3 + B4\ TOU^4 + B5\ TOU^5)\right] \quad (191)$$

where TOU is 1-t/tc, and tc and pc are the critical temperature and pressure respectively (tc is 384.95 Kelvin and pc is 4.125 MPa). The constants on the right hand side are

B1 = -6.9670659

B2 = 1.6788237

B3 = -4.079537026

B4 = 4.482102063

B5 = -5.064659805

10. Latent Heat of Vaporization

The following equation os used to calculate the latent heat of vaporization [12] in kJ/kg:

where t is in Rankine, p is in psia, and dg and df are in pounds

$$h_{tg} = 2.33 \ln(10) \left(- \frac{B}{t^2} + \frac{C}{t \ln(10)} + D \right) J p t \left(\frac{1}{dg} - \frac{1}{df} \right)$$

per square foot. The constants on the right hand side are

J = 0.185053

B = -3436.632228

C = -12.47152228

D = 4.73044244e-03

11. Vapour Enthalpy

The vapour enthalpy in kJ/kg is given by [3]

$$\frac{b}{R\,t_c} = \Bigg[1 + d_r \left(A1 + 2\frac{A2}{t_r} + 3\frac{A3}{t_r^2} + 4\frac{A4}{t_r^3} \right) + \frac{d_r^2}{2}\left(2A5 + 3\frac{A6}{t_r} + 4\frac{A7}{t_r^2} \right) + \frac{d_r^3}{3}\left(3A8 + 4\frac{A9}{t_r} + 5\frac{A10}{t_r^2} \right) + \frac{d_r^4}{4}\left(4A11 + 5\frac{A12}{t_r} \right) + \frac{d_r^6}{6}\left(6A13 + 7\frac{A14}{t_r} \right) + A15\, d_r^8 \Bigg] t_r + \frac{1}{R}\left[\frac{C1}{t_c} \ln\left(\frac{t_r}{t_0} \right) + (C2-R)(t_r - t_0) + \frac{C3\, t_c}{2}(t_r^2 - t_0^2) + \frac{C4\, t_c^2}{3}(t_r^3 - t_0^3) + \frac{C5\, t_c^3}{4}(t_r^4 - t_0^4) + \frac{C6\, t_c^4}{5}(t_r^5 - t_0^5) \right] + \frac{X}{R\,t_c} \qquad (192)$$

where tr is t/tc, and dr is $\frac{\rho}{\rho_c}$. The value of tc is 384.95

Kelvin; ρ_c is 557.9993724 $\frac{kg}{m^3}$; t0 is 0.691606532e-01; R is

6.876308781e-02 kJ/(kg K). The other constants are

A1 = 2.337370817

A2 = -6.41240639

A3 = 4.830185249

A4 = -1.965519089

A5 = -3.00798019

A6 = 6.836347882

A7 = -3.379592003

A8 = 3.12596727

A9 = -7.177260909

A10 = 4.136982393

A11 = 0.4704538125e-02

A12 = -0.1573667708e-01

A13 = 0.139844784

A14 = -0.18631037131

A15 = 0.1221380142e-01

C1 = 0.85309*10

C2 = -0.58573e-01

C3 = 0.36561e-02

C4 = -0.71739e-05

C5 = 0.77377e-08

C6 = -0.35804e-11

x = 339.11

12. Vapour Entropy

The vapour entropy is given by

$$\frac{S}{R} = -\Bigg[\ln(d_r) + d_r \left(A1 - 3\frac{A3}{t_r^2} - 2\frac{A4}{t_r^3} \right) + \frac{d_r^2}{2}\left(A5 - \frac{A7}{t_r^2} \right) + \frac{d_r^3}{3}\left(A8 - \frac{A10}{t_r^2} \right) + A11\,\frac{d_r^4}{4} + A13\,\frac{d_r^6}{6} + A15\,\frac{d_r^8}{8} \Bigg] + \frac{1}{R}\Bigg[\frac{C1}{t_c}\left(\frac{1}{t_0} - \frac{1}{t_r} \right) + (C2-R)\ln\left(\frac{t_r}{t_0} \right) + C3\,t_c\,(t_r - t_0) + \frac{C4\,t_c^2}{2}(t_r^2 - t_0^2) + \frac{C5\,t_c^3}{3}(t_r^3 - t_0^3) + \frac{C6\,t_c^4}{4}(t_r^4 - t_0^4) \Bigg] + \frac{Y}{R} \tag{193}$$

where the value of y is 1.33018. The values of all the other constants are listed in section C.11 of this appendix.

13. Equation of State

The equation of state for R12 vapour is [3]

$$\frac{p}{\rho RT} = 1 + d_r\left(A1 + \frac{A2}{t_r} + \frac{A3}{t_r^2} + \frac{A4}{t_r^3}\right) + d_r^2\left(A5 + \frac{A6}{t_r} + \frac{A7}{t_r^2}\right) + d_r^3\left(A8 + \frac{A9}{t_r} + \frac{A10}{t_r^2}\right) + d_r^4\left(A11 + \frac{A12}{t_r}\right) + d_r^6\left(A13 + \frac{A14}{t_r}\right) + A15\, d_r^8 \qquad (194)$$

The definitions of tr and dr and the values of all constants are given in section C.11 of this appendix.

D. R22 Property Correlations

1. Gas Density

The following correlation was used to calculate the density of saturated vapour coefficients for saturated vapor in kilograms per cubic meter [3]:

$$\frac{dg}{ROWI} = [\, E1 + E5\, TOU^{\frac{4}{3}} + E6\, TOU^{\frac{5}{3}} + E7\, TOU^{\frac{6}{3}} + E8\, TOU^{\frac{7}{3}} + E9\, TOU^{\frac{8}{3}} + E10\, TOU^{\frac{9}{3}} + E12\, TOU^{-\frac{2}{3}} + E15\, TOU^{-\frac{5}{3}} + E17\, TOU^{-\frac{7}{3}} + E18\, TOU^{-\frac{8}{3}} + E20 \ln\left(\frac{t}{TI}\right)]\, M \qquad (195)$$

where TOU is 1 - t/TI, TI is 369.3, ROWI is 5.9328, and M is 86.469. The other constants on the right hand side are

E1 = -0.1125494951

E5 = 489.2280363

E6 = -1227.271507

E7 = 1629.238081

E8 = -859.194511

E9 = -144.0371655

E10 = 292.5609255

E12 = -0.002447993522

E15 = 0.00001815569814

E17 = -0.0000004028006124

E18 = 2.289562605e-08

E20 = 94.65371017

2. Gas Thermal Conductivity

The thermal conductivity of saturated vapour in kW/(m K) is calculated using the following correlation [2] (t is in Kelvin):

$$k_g = \frac{(A + B\,t)}{1e{+}06} \tag{196}$$

The constants on the right hand side are

A = -3.038488

B = 0.048685

3. Gas Viscosity

The viscosity of saturated vapour (in Pascal seconds) is calculated by the following equation [2]:

$$\mu_g = \frac{EXP[\,A + \frac{B}{t}\,]}{1e{+}06} \tag{197}$$

A = 5.804344

B = -279.8194

4. Gas Specific Heat Capacity

The specific heat capacity of refrigerant vapour is given by [38]

$$C_{p_g} = \left[8 v_r^7 \left(\frac{H0}{t_r} + H1 + \frac{H2}{t_r^4} \right) + 7 v_r^6 \left(\frac{G0}{t_r} + G1 + \frac{G2}{t_r^4} \right) + 6 v_r^5 \left(\frac{F0}{t_r} + F1 + \frac{F2}{t_r^4} \right) + 5 v_r^4 \left(\frac{E0}{t_r} + E1 + \frac{E2}{t_r^4} \right) + 4 v_r^3 \left(\frac{D0}{t_r} + D1 + \frac{D2}{t_r^4} \right) + 3 v_r^2 \left(\frac{C0}{t_r} + C2 + \frac{C2}{t_r^4} \right) + 2 v_r \left(\frac{B0}{t_r} + B1 + \frac{B2}{t_r^4} \right) + 1 \right]^{-1} \left(\alpha_1 - \frac{3\beta}{t_r} \right)^2 R + C_v \quad (198)$$

where Cv is given by

$$C_v = a_1 + b\,t + c\,t^2 + d\,t^3 - \frac{12\,R}{t_r^4} \left(B2\,v_r + \frac{C2}{2} v_r^2 + \frac{D2}{3} v_r^3 + \frac{E2}{4} v_r^4 + \frac{F2}{5} v_r^5 + \frac{G2}{6} v_r^6 + \frac{H2}{7} v_r^7 \right) \quad (199)$$

where tr is t/tc and vr is vc/v. α_1 is given by

$$\alpha_1 = 1 + B1\,v_r + C1\,v_r^2 + D1\,v_r^3 + E1\,v_r^4 + F1\,v_r^5 + G1\,v_r^6 + H1\,v_r^7 \quad (200)$$

β is given by

$$\beta = B2\,v_r + C2\,v_r^2 + D2\,v_r^3 + E2\,v_r^4 + F2\,v_r^5 + G2\,v_r^6 + H2\,v_r^7 \quad (201)$$

The value of tc is 369.28 Kelvin; vc is 1.95e-03 cubic meters per kilogram; R is 0.096144.

The other constants are

a1 = 0.16146

b = 0.001394

c = -4.85e-08

d = -7.27e-10

B0 = -1.842726

B1 = 0.874986

B2 = -0.308738

C0 = 1.661300

C1 = -0.938097

C2 = -0.155737

D0 = -1.711909

D1 = 1.334412

D2 = 0.581155

E0 = 3.221985

E1 = -2.520731

E2 = -1.353292

F0 = -1.086343

F1 = 0.405841

F2 = 1.556336

G0 = -4.287381

G1 = 3.700215

G2 = -0.010270

H0 = 2.406900

H1 = -1.945130

H2 = -0.308876

5. Liquid Density

The following equation is used to calculate the liquid density in kilograms per cubic meter [3] (t is in Kelvin):

$$df = [AL + BL\ TOU^{\frac{1}{3}} + CL\ TOU^{\frac{2}{3}} + dll\ TOU + EL\ TOU^{\frac{4}{3}}]\ 16.01819 \quad (202)$$

where TOU is 1 - t/tc, and tc is 369.3 Kelvin. The constants on the right hand side are

AL = 32.76

BL = 54.6344093

CL = 36.74892

dll = -22.2925657

EL = 20.47328862

6. Liquid Thermal Conductivity

The following correlation is used to determine the thermal conductivity of saturated liquid in kW/(m K) [2] (t is in Kelvin):

$$k_f = \frac{(A + B\ t + C\ t^2)}{1e{+}07} \quad (203)$$

The constants on the right hand side are

A = 1990.179111

B = -2.110145

C = -0.005789

7. Liquid Viscosity

The viscosity (in Pascal seconds) of saturated liquid is determined from the following equation [2] (t is in Kelvin):

$$\mu_\ell = \frac{EXP[\,A + \frac{B}{t} + C\ln(t) + D\,t + E\,t^2]}{1e{+}07} \qquad (204)$$

The constants on the right hand side are

A = -157.383131

B = 3204.489487

C = 32.393116

D = -0.124985

E = 0.000080

8. Liquid Specific Heat Capacity

The following correlation is used to calculate the specific heat capacity of saturated liquid [2] (t is in Kelvin):

$$C_{p_\ell} = EXP[\,A + \frac{B}{t} + C\ln(t) + D\,t + E\,t^2] \qquad (205)$$

For temperatures less than or equal to 263.15 Kelvin the constants on the right hand side are

A = -1.17099

B = -142.559065

C = 0.900297

D = -0.020317

E = 0.000031

For temperatures greater than 263.15 Kelvin the constants are

A = -6218.919893

B = 112405.883410

C = 1212.655529

D = -4.358195

E = 0.002613

9. Saturation Pressure

The saturation pressure in MPa is given by

$$\frac{psat}{p_c} = EXP\left[\frac{t_c}{t}(B1\ TOU + B2\ TOU^{1.5} + B3\ TOU^3 + B4\ TOU^4 + B5\ TOU^5)\right] \tag{206}$$

where TOU is 1 - t/tc, tc is 369.3 Kelvin, and pc is 4.988 MPa. The constants on the right hand side are

B1 = -7.0340913

B2 = 1.4030736

B3 = -4.960588

B4 = 8.88280890000

B5 = -10.600638

10. Latent Heat of Vaporization

The following equation os used to calculate the latent heat of vaporization [12] in kJ/kg:

$$h_{fg} = 2.33\ln(10)\left[-\frac{B}{t^2} + \frac{C}{t\ln(10)} + D - \frac{E}{\ln(10)}\left(\frac{1}{t} + F\frac{\ln(F-t)}{t^2}\right)\right] J\,p\,t\left(\frac{1}{dg} - \frac{1}{df}\right) \tag{207}$$

where t is in Rankine, p is in psia, and dg and df are in pounds per square foot. The constants on the right hand side are

J = 0.185053

B = -3845.193152

C = -7.86103122

D = 0.002190939

E = 0.445746703

F = 686.1

11. Vapour Enthalpy

The vapour enthalpy in BTU/lbm is given by

$$h = AA\,t + \frac{BBB}{2}\,t^2 + \frac{CC}{3}\,t^3 - \frac{FF}{t} + J\,p\,v + J\left[\frac{AA2}{v-BB} + \frac{AA3}{2(v-BB)^2} + \frac{AA4}{3(v-BB)^3} + \frac{AA5}{4(v-BB)^4}\right] + J\,EXP\left[\frac{-KK\,t}{t_c}\right]\left(1 + \frac{KK\,t}{t_c}\right)\left[\frac{C2}{v-BB} + \frac{C3}{2(v-BB)^2} + \frac{C5}{4(v-BB)^4}\right] + X \qquad (208)$$

where t is in Rankine, p is in psia, and v is in cubic feet per pound mass. The value of tc is 664.74 Rankine. The values of enthalpy obtained from the preceding equation are then converted to kJ/kg and the datum is made the same as that used by ASHRAE for S.I. units [12] by the following equation

$$h(in\ kJ/kg) = 2.33\,[h(in\ BTU/lbm) - 19.318] + 200 \qquad (209)$$

The values of the constants are

J = 0.185053

AA = 2.812836E-02

BBB = 0.0002255408

BB = 0.002

CC = -6.509607e-08

FF = 257.341

AA2 = -4.353547

AA3 = -0.017464

AA4 = 0.002310142

AA5 = -0.00003724044

KK = 4.2

CC2 = -44.066868

CC3 = 1.483763

CC5 = -1.845051e-04

X = 62.4009

12. Vapour Entropy

The vapour entropy in BTU/(lbm R) is given by

$$s = AA\ln(t) + BBB\,t + \frac{CC}{2}t^2 - \frac{FF}{2t^2} + JR\ln(v-BB) - J\left[\frac{B2}{(v-BB)} + \frac{B3}{2(v-BB)^2} + \frac{B4}{3(v-BB)^3} + \frac{B5}{4(v-BB)^4}\right] + \frac{JKK\,EXP\left[\frac{-KK\,t}{t_c}\right]}{t_c}\left[\frac{C2}{v-BB} + \frac{C3}{2(v-BB)^2} + \frac{C5}{4(v-BB)^4}\right] + Y \quad (210)$$

The values of entropy obtained from the preceding equation are then converted to kJ/(kg K) and the datum is made the same as that used by ASHRAE for S.I. units [12] by the following equation

$$s\ (in\ kJ/(kg\,K)) = 4.1868\,[\,s(in\ BTU/(lbm\,R)) - 4.52343023E\text{-}02] + 1 \quad (211)$$

With the exception of the constants listed below, all other constants are listed in section D.11 of this appendix.

R = 0.124098

BB2 = 0.002407252

BB3 = 0.0000762789

BB4 = -0.000003605723

BB5 = 0.00000005355465

Y = -0.0453335

13. Equation of State

The following equation of state is used for R22 vapour [3]:

$$\begin{aligned}\frac{p}{\rho R t} = 1 &+ d_r\left(A1 + \frac{A2}{t_r} + \frac{A3}{t_r^4} + \frac{A4}{t_r^6}\right) \\ &+ d_r^2\left(A5 + \frac{A6}{t_r} + \frac{A7}{t_r^4}\right) \\ &+ d_r^3\left(A8 + \frac{A9}{t_r} + \frac{A10}{t_r^2} + \frac{A11}{t_r^4}\right) \\ &+ d_r^4\left(\frac{A12}{t_r} + \frac{A13}{t_r^4}\right) \\ &+ d_r^5\left(\frac{A14}{t_r^2} + \frac{A15}{t_r^3} + \frac{A16}{t_r^4} + \frac{A17}{t_r^6}\right) \\ &+ A18\, dr_6 + d_r^7\left(\frac{A19}{t_r^2} + \frac{A20}{t_r^6}\right) + \frac{A21}{t_r}\, dr^8 \\ &+ d_r^9\left(\frac{A22}{t_r^2} + \frac{A23}{t_r^6}\right) + d_r^{10}\left(\frac{A24}{t_r} + \frac{A25}{t_r^6}\right) \\ &+ d_r^{11}\left(\frac{A26}{t_r} + \frac{A27}{t_r^2} + \frac{A28}{t_r^6}\right)\end{aligned} \qquad (212)$$

where tr is t/tc and dr is $\frac{\rho}{\rho_c}$; t is in Kelvin,. ρ is in kilograms per cubic meter, and p is in MPa. The value of tc is 369.3 Kelvin; ρ_c is 512.999 kilograms per cubic meter; R is 8.314E-03. The other constants are

A1 = 0.545762

A2 = -1.39198

A3 = -0.432562

A4 = 0.02214

A5 = -0.1307418

A6 = 0.79211

A7 = -0.167024

A8 = 0.56743874000

A9 = -1.35071

A10 = -0.115487

A11 = 1.024567

A12 = 0.34435035

A13 = -0.4082677

A14 = 0.0830099

A15 = -0.1899033

A16 = 0.08821727

A17 = 0.0190595

A18 = -0.0376347

A19 = 0.03329212

A20 = -0.03794234

A21 = 0.00786909

A22 = -0.004626965

A23 = 0.02336405

A24 = -0.002066556

A25 = -0.01050183

A26 = 0.0005276995

A27 = 0.000209547

A28 = 0.001346363

E. Liquid Water Property Correlations

1. Volumetric Thermal Expansion Coefficient

The following equation calculates the expansion coefficient for saturated liquid water at temperatures between 280 and 370 Kelvin (t is in Kelvin):

$$B_f = \frac{(A + B\,t + C\,t^2)}{1e{+}06} \tag{213}$$

The correlation was obtained by curve fitting tabulated data [18]. The constants on the right hand side are

A = -6555.122706

B = 36.043197

C = -0.044297

2. Thermal Conductivity

The following equation calculates the thermal conductivity of liquid water in kW/(m K) (t is the temperature in Kelvin):

$$k_f = \frac{A + B\,t + C\,t^2}{1e{+}06} \tag{214}$$

The correlation is a curve fit of tabulated data [18]. The constants on the right hand side are

A = -480.588001

B = 5.836573

C = -0.007298

3. Viscosity

The following equation calculates the absolute viscosity

of saturated liquid water in Pascal seconds at temperatures between 280 and 370 Kelvin (t is in Kelvin):

$$\mu = \frac{EXP[\,A + \frac{B}{t}]}{1e{+}06} \qquad (215)$$

The equation is a curve fit of tabulated data [18]. The constants on the right hand side are

A = 0.632273

B = 1841.695823

4. Specific Heat Capacity

The following equation calculates the specific heat capacity of saturated liquid water in kJ/(kg K) at temperatures between 280 and 370 Kelvin (t is in Kelvin):

$$C_{p_f} = EXP[\,A + \frac{B}{t} + C\ln(t) + D\,t + E\,t^2] \qquad (216)$$

The equation is a curve fit of tabulated data [18]. For temperatures less than or equal to 305 Kelvin, the constants are

A = -23.856069

B = 2452.396491

C = 0.222509

D = 0.07917

E = -0.000088

For temperatures greater than 305 Kelvin, the constants are

A = 8.681538

B = -33.905663

C = -1.55847

D = 0.006943

E = -0.000004

5. Saturation Pressure

The following equation calculates the saturation pressure of water vapour in MPa at temperatures between greater than or equal to 273.15 Kelvin [4] (t is in Kelvin):

$$psat = \frac{EXP[\frac{A}{t} + B + C\,t + D\,t^2 + E\,t^3 + F\ln(t)]}{1e+06} \quad (217)$$

The constants are

A = -5.8002206e3

B = 1.3914993

C = -4.8640239e-2

D = 4.1764768e-5

E = -1.4452093e-8

F = 6.5459673

For temperatures less than 273.15 Kelvin, the saturation pressure is given by

$$psat = \frac{EXP[\frac{G}{t} + H + I\,t + J\,t^2 + K\,t^3 + L\ln(t)]}{1e+06} \quad (218)$$

The constants are

G = -5.6745359e3

H = 6.3925247

I = -9.677843e-3

J = 6.22115701e-7

K = 2.0747825e-9

L = -9.484024e-13

M = 4.1635019

6. Prandtl Number

The following equation calculates the Prandtl number of saturated liquid water in kJ/(kg K) at temperatures between 280 and 370 Kelvin (t is in Kelvin):

$$P_r = EXP[\, A + B\ln(t) + C\,[\ln(t)]^2 + D\,[\ln(t)]^3] \qquad (219)$$

The equation is a curve fit of tabulated data [18]. The constants are

A = 1767.89475511

B = -854.846129581

C = 138.194620406

D = -7.47016383964

F. Air Property Correlations

In all the following correlations t is the temperature in Kelvin. All of following correlations are curve fits of data tabulated by Incropera and Dewit [18], and all the correlations are valid for temperatures between 250.15 and 399.15 Kelvin.

1. Thermal conductivity

The thermal conductivity in kW/(m K) is given by

The constants are

$$k = \frac{A + B\,t + C\,t^2}{1e{+}06} \qquad (220)$$

A = 1.22

B = 0.089399999999

C = -1.999999999e-05

2. Kinematic Viscosity

The kinematic viscosity in square meters per second is given by

$$\nu = \frac{A + B\,t + C\,t^2}{1e{+}06} \qquad (221)$$

The constants are

A = -3.135999999999

B = 0.032279999999

C = 0.000104

3. Specific Heat Capacity

The specific heat capacity of the air in kJ/(kg K) is given by

$$C_p = A + B\,t + C\,t^2 \qquad (222)$$

The constants are

A = 1.0331

B = -0.000208

C = 4e-07

4. Thermal Diffusivity

The thermal diffusivity in square meters per second is given by

$$\alpha = \frac{A + B\,t + C\,t^2}{1e{+}06} \qquad (223)$$

The constants are

A = -3.39

B = 0.0322

C = 0.000179999999999

5. Prandtl Number

The Prandtl number is given by

$$P_r = A + \frac{B}{t} + C \ln(t) \qquad (224)$$

The constants are

A = 0.993413737197

B = 3.17898154393

C = -0.0518750317069

APPENDIX IV

The Data Acquisition Program

APPENDIX V

Accounting For Error In Thermocouple Temperature Measurement

APPENDIX V

A. Accounting For Radial Conduction

Figure 70 shows the heat transfer circuit for a tube carrying refrigerant assuming one dimensional steady state heat conduction in the radial direction. The four thermal resistances which must be taken into account are the following: R1, the resistance due to the refrigerant convection boundary layer; R2, the resistance of the copper tubing; R3, the resistance of the insulation; and R4, the resistance of the outside air boundary layer. The temperature Te is the temperature that the thermocouple measures. Because one dimensional steady state conduction was assumed the following expression relating Tb, Te, and Tair is valid

$$\frac{(T_b-T_e)_{rad}}{T_e-T_{air}} = \frac{R_1+R_2}{R_3+R_4} \qquad (225)$$

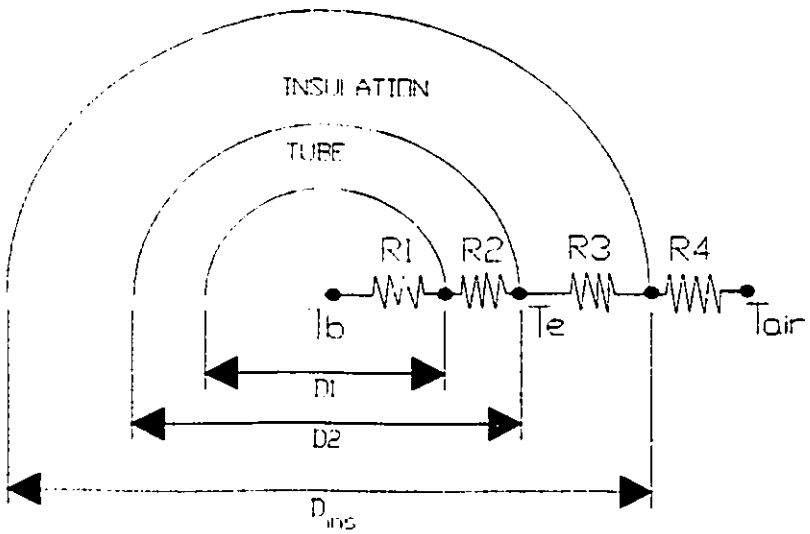

Figure 70: The Heat Transfer Circuit For Radial Conduction

The error due to radial conduction, (Tb-Te)rad, was obtained from

the preceding expression.

The resistance R1 was calculated as follows:

$$R_1 = \frac{1}{\bar{h}_{in}\pi D_1} \qquad (226)$$

The refrigerant side heat transfer coefficient, $\bar{h}_{in}$, was calculated from the following correlation for forced convection inside horizontal tubes[32]:

$$\begin{aligned} N_u &= 5 + 0.015 R_e^a P_r^b \\ a &= 0.88 - \frac{0.24}{4 + P_r} \\ b &= 0.333 + 0.5 e^{-0.6 P_r} \end{aligned} \qquad (227)$$

For the case where the refrigerant was boiling (at the outlet of the throttle valve and inlet to the evaporator) a value of 2 $kW/(m^2K)$ was used for $\bar{h}_{in}$. The value was chosen based on the results given by the heat transfer correlation used in the simulation program to model the wet portion of the evaporator.

The resistance R2 was calculated as

$$R_2 = \frac{\ln\left(\frac{D_2}{D_1}\right)}{2\pi K_{tube}} \qquad (228)$$

The value of Ktube, the thermal conductivity of copper, was 0.401 kW/(mK). The tube diameters and thicknesses for the fifteen locations on the refrigeration system where the thermocouples were installed on tube walls are given in Table 18.

Table 18: Tube Diameters And Thicknesses at Locations of Thermocouple Placement

Temperature	Tube Diameter (m)	Tube thickness (m)
t1	0.022	0.0011
t2	0.016	0.00089
t3	0.016	0.00089
t4	0.0095	0.00081
t5	0.0095	0.00081
t6	0.0095	0.00081
t7	0.0095	0.00081
t8	0.019	0.0011
t9	0.0064	0.00076
t10	0.0064	0.00076
t11	0.22	0.0011
t12	0.22	0.0011
t13	0.22	0.0011
t14	0.013	0.00081
t15	0.013	0.00081

The resistance R3 was calculated as

$$R_3 = \frac{\ln\left(\frac{D_{ins}}{D_2}\right)}{2\pi K_{ins}} \tag{229}$$

The value of Kins, the thermal conductivity of the Armstrong Armalflex insulation, was 0.0389E-03 kW/(mK) [1].

The resistance R4 was calculated as

$$R_4 = \frac{1}{\bar{h}_{air}\pi D_{ins}} \tag{230}$$

The air side heat transfer coefficient, $\bar{h}_{air}$, was calculated using the following correlation for natural convection on the outside of horizontal tubes[18]:

$$N_u = \left[0.60 + \frac{0.387\, R_a^{1/6}}{[1 + (0.559/P_r)^{9/16}]^{8/27}}\right]^2 \qquad (231)$$

where the Rayleigh number was given by

$$R_a = \frac{g\beta\,(T_{air} - T_{ins})\, D_3^3}{\nu\,\alpha} \qquad (232)$$

B. Accounting For Longitudinal Conduction

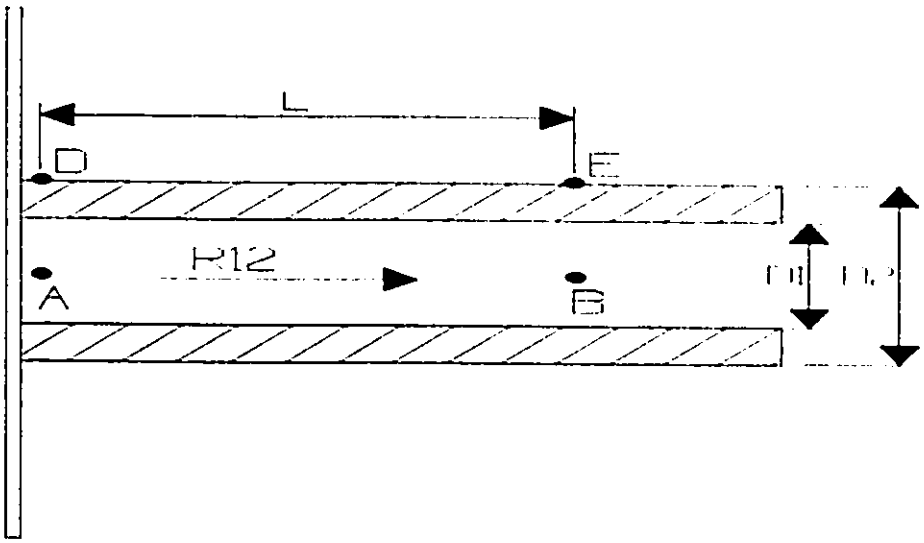

Figure 71: Effect of Longitudinal Conduction

Figures 71 and 72 illustrate how longitudinal heat conduction along the length of the tube where the thermocouple was installed can affect the accuracy of the refrigerant temperature measurement. The temperature of the refrigerant at point A is desired. However,

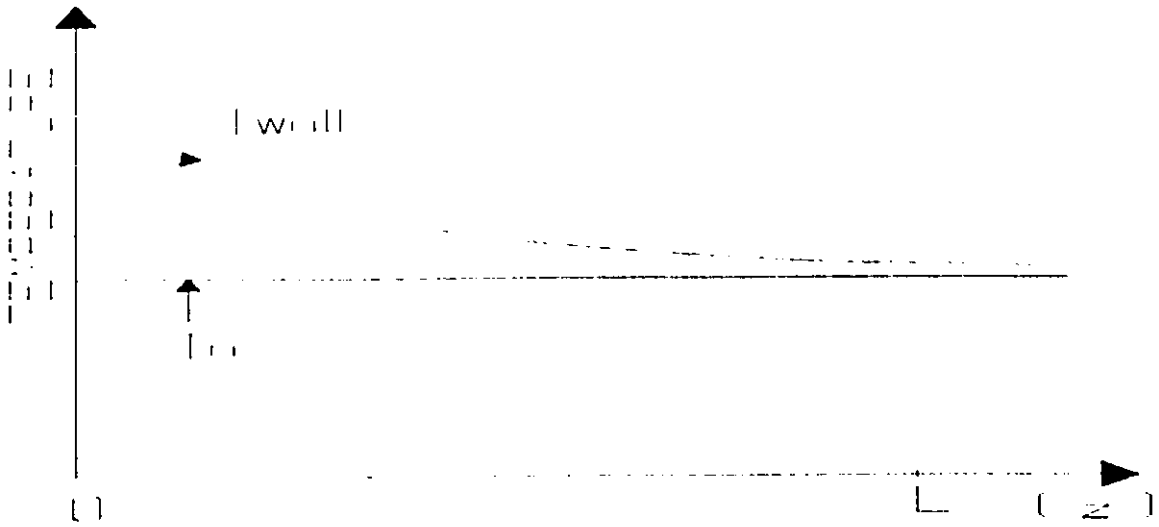

Figure 72: Temperature of Wall and Refrigerant

the wall temperature at point D is significantly higher than the wall temperature at point A. Point D would therefore be a poor location to install the thermocouple. Instead, the thermocouple is installed at point E where, as shown in figure 72, the wall temperature is much closer to that of the refrigerant at point A. By assuming one dimensional steady state conduction along the length of the tube and neglecting the fact that the refrigerant temperature changes between points A and B, the following differential equation governing the temperature distribution of the tube wall can be derived:

$$K_{tube} A_c \frac{d^2\theta}{dz^2} - \bar{h}_{in} \pi D1 \theta = 0 \qquad (233)$$

where $\theta = T_{wall(z)} - T_a$, Ac is the cross sectional area of the tube given by $\pi\, thick\, D_m$, "thick" is the tube thickness

and $D_m = (D2+D1)/2$. The solution of the differential equation yields the following temperature distribution:

$$\theta(z) = \theta(0)\, e^{-\sqrt{B}z} \tag{234}$$

where $B = \dfrac{\bar{h}_{in} D1}{k_{tube}\, thick\, D_m}$ and $\theta(0)$ is Td-Ta. Point E is located a distance L from point B; the error due to longitudinal conduction for installing the thermocouple at point E is therefore given by

$$(T_b - T_e)_{lng} = -\theta(0)\, e^{-\sqrt{B}L} \tag{235}$$

In the data acquisition program $\theta(0)$ was assumed to equal $0.5\,(T_{air}-T_e)$. This assumption resulted in an over estimate of the error due to axial conduction since

$$\theta(0) = \frac{R1+R2}{R3+R4}\,(T_{air}-T_d) \tag{236}$$

and typically

$$|\,T_{air}-T_e\,| > |\,T_{air}-T_d\,| \tag{237}$$

and

$$0.5 > \frac{R1+R2}{R3+R4} \tag{238}$$

Table 19: Distances From Point of Thermocouple Installation To216 Point Where Temperature Was Desired

Temperature	Distance (m)
t1	0.19
t2	0.20
t3	0.20
t4	0.20
t5	0.11
t6	0.09
t7	0.30
t8	0.09
t9	0.095
t10	0.095
t11	0.45
t12	0.21
t13	0.17
t14	0.13
t15	0.12

Equation (236) is for radial conduction between points A and D on figure 72. Equation (238) is based on typical values of R1, R2, R3, and R4 that were calculated in the data analysis program. Even if R3 is neglected, equation (238) is valid.

The distances required for the calculation of error due to longitudinal conduction (i.e. the distances that correspond to L in the preceding equation) are given in Table 19.

C. Accounting For Temperature Change of The Refrigerant Between The Point Where The Thermocouple Was Installed and The Point Where The Temperature Was Desired

Due to both axial and radial conduction, the temperature of the refrigerant at point B (shown in figure 73) is different than it is at point A. This temperature difference was estimated in the data acquisition program by separately considering the contributions of both radial and axial conduction to heat loss.

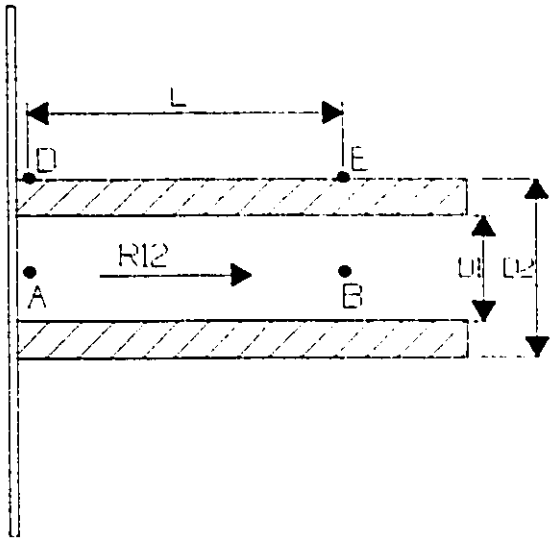

Figure 73: Positioning of Thermocouple on Tube Wall For Refrigerant Temperature Measurement

If only radial heat conduction through the pipe wall occurred then the amount of heat lost by the refrigerant between points A and B could be calculated by

$$q_{loss} = \frac{(T_o - T_{air})\, L}{R_1 + R_2 + R_3 + R_4} \qquad (239)$$

where R1, R2, R3, R4 are the resistances defined in equations (226), (228), (229), and (230).

If only longitudinal heat conduction along the wall occurred then the amount of heat lost by the refrigerant between points A and B could be determined by evaluating the following integral:

$$q_{loss} = -\int_{z=0}^{z=L} \bar{h}_{in}\theta(z)\,\pi D1\,dz \qquad (240)$$

Substitution of (234) for $\theta(z$ allows evaluation of the integral to obtain the following expression:

$$q_{loss} = \frac{\theta(0)}{\sqrt{B}}\left[e^{-\sqrt{B}L} - 1\right] \qquad (241)$$

In the data acquisition program $\theta(0$ was estimated as $0.5\,(T_{air}-T_e)$ for reasons explained in section b of this appendix.

Since both radial and longitudinal heat occurred the heat loss by the refrigerant was estimated by combining (239) and (241) as follows:

$$q_{loss} = \frac{(T_e-T_{air})\,L}{R_1+R_2+R_3+R_4} + \frac{\theta(0)}{\sqrt{B}}\left[e^{-\sqrt{B}L} - 1\right] \qquad (242)$$

The first law first law requires that for cases where the thermocouple was positioned downstream of where the temperature was desired (i.e. downstream of an outlet to one of the system components)

$$REFmdot\_f\ C_p\ (T_a-T_b) = q_{loss} \qquad (243)$$

where Cp is evaluated at Te. Therefore, the error due to

temperature change between the point where the thermocouple was installed and the point where the temperature was desired was calculated as

$$Ta-Tb = \frac{q_{loss}}{REFmdot\_f\ C_p} \qquad (244)$$

where (242) was used to determine $q_{los.}$. For cases where the thermocouple was positioned upstream of where the temperature was desired the following expression was used:

$$Ta-Tb = \frac{-q_{loss}}{REFmdot\_f\ C_p} \qquad (245)$$

where (242) was used to determine q_{loss}.

In cases where flashing occurred in the flowmeter, REFmdot_c rather than REFmdot_f was used in (244) and (245).

A similar analysis of error was carried out for the measurement of water temperature.

D. Uncertainty Analysis

For each quantity which the data acquisition program calculated, an uncertainty analysis was carried out using the Kline-McKlintock method [34].

APPENDIX VI

The Simulation Program

APPENDIX VII

The User Interface of RHEsim92

APPENDIX VII

Figure 74 is first menu screen to appear after the user runs RHEsim92. Figures 75, 76, and 77 show the menu screens that appear before a data entry screen appears to accept input for a concentric tube counter flow condenser. The "View Input" screen gives the user an overview what has been entered into the program. Note that the "Run" and "Output" screens are protected until are the required information is provided to the program. The "Known Parameter" screen is where the user must specify the compressor outlet to inlet pressure ratio. The user can exit any screen, except for the main menu screen, by pressing the escape key.

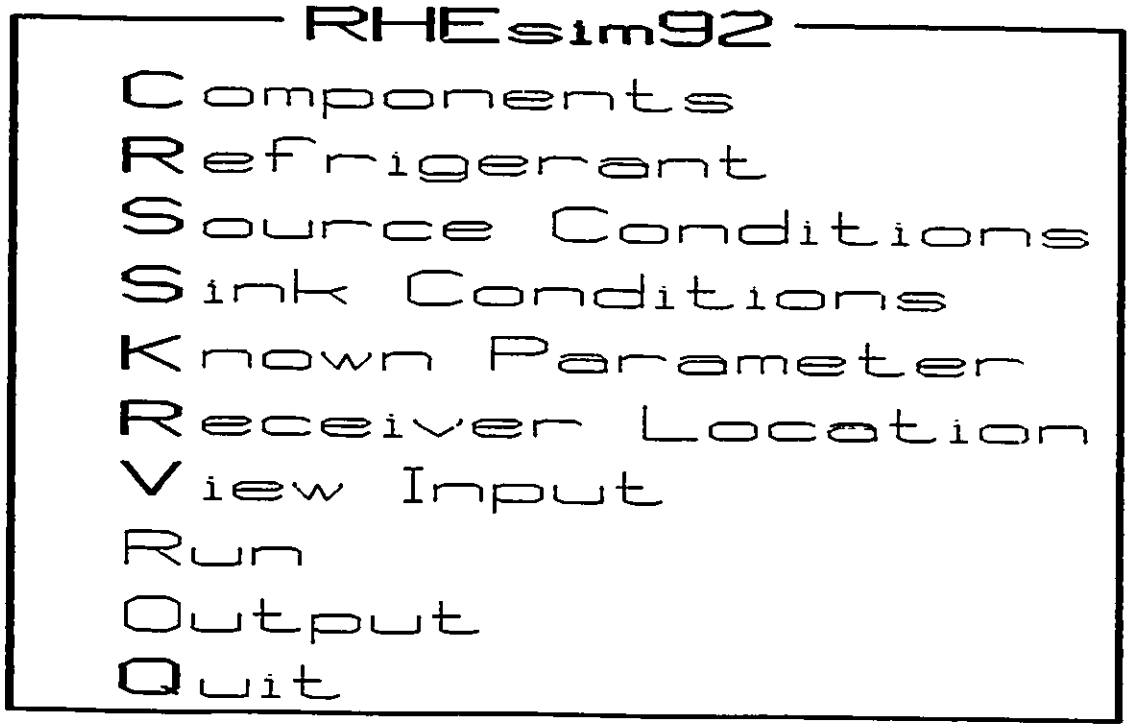

Figure 74: The Main Menu Screen of RHEsim92

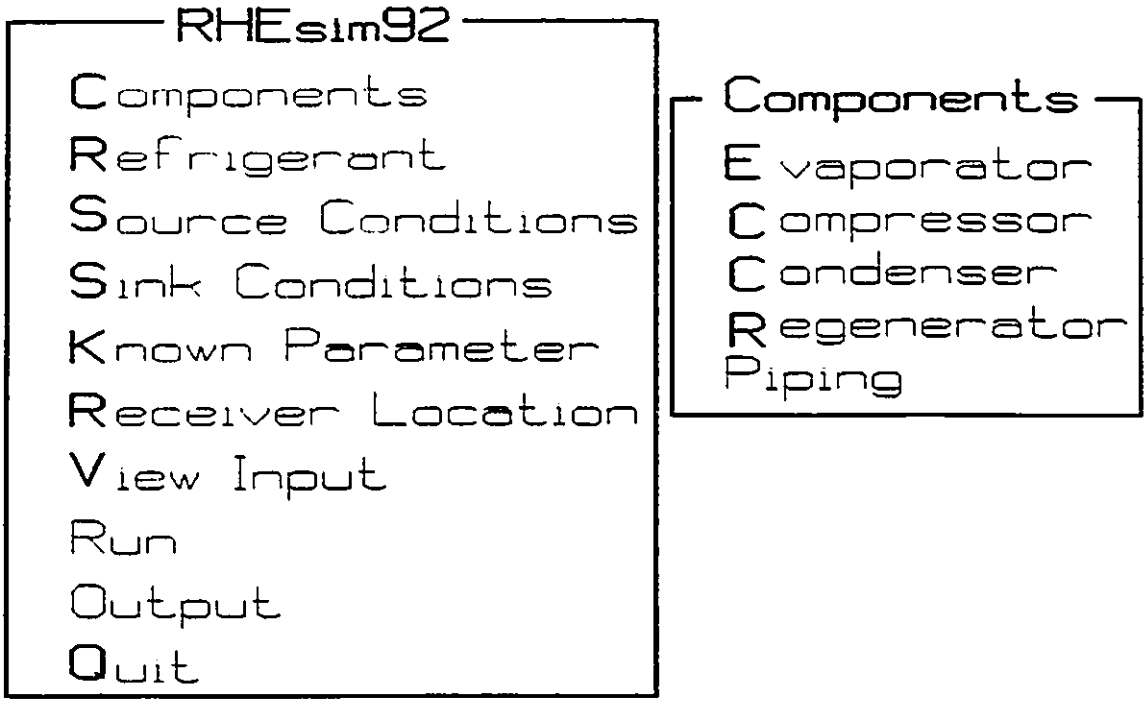

Figure 75: After "Components" Is Selected From Main Menu

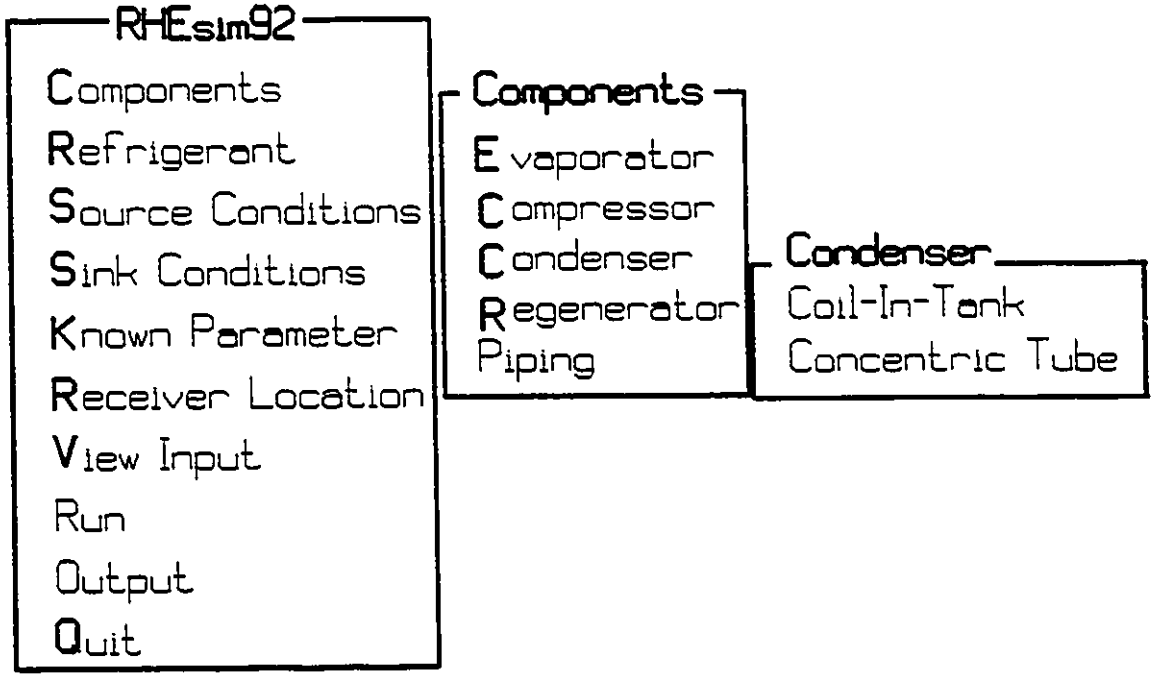

Figure 76: "Condenser" Selected From "Components" Screen

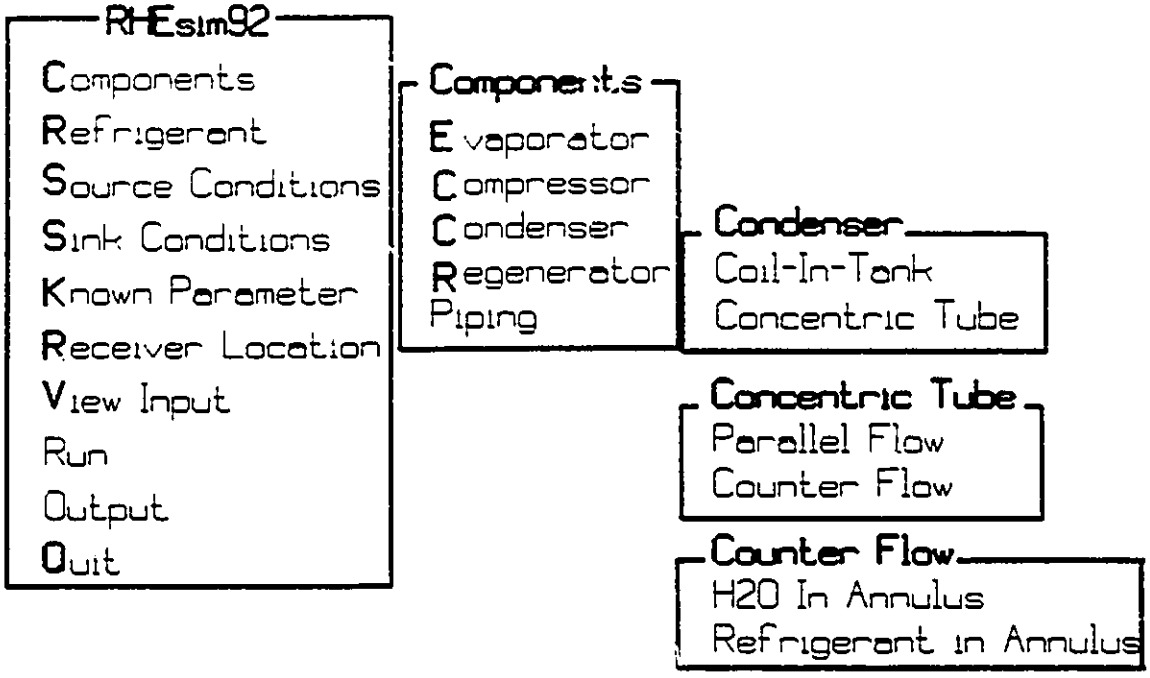

Figure 77: After "Concentric Tube" and "Counter Flow" Are Selected

Vita Autoris

1966 Born in Windsor, Ontario, Canada on July 16

1985 Completed secondary school at Walkerville Collegiate

1989 Received Bachelor of Applied Science in Mechanical Engineering at the University of Windsor

1992 Currently a candidate for the degree of Master of Applied Science in Mechanical Engineering